Approaching Neanderthal behavior through the geoarchaeological study of combustion structures: Investigations in soil micromorphology and lipid biomarkers

Doctoral Thesis

LUCIA LEIERER

Supervisor:

Carolina Mallol

Universidad de La Laguna

2021

Approaching Neanderthal behavior through the geoarchaeological study of combustion structures: Investigations in soil micromorphology and lipid biomarkers

LUCIA LEIERER

I. Table of Contents

II. Abstract

This dissertation seeks to illuminate Neanderthal behavioral variation based on a geoarchaeological approach to analyzing Neanderthal combustion features at the Middle Paleolithic site of El Salt, Spain. This approach involves investigations of Neanderthal combustion features, emphasizing their synchronic and diachronic relationships, in search of clues about pyrotechnology, environmental context, settlement and mobility patterns, and mobility.

The investigations are carried out focusing on the organic sedimentary record of combustion structures and using geoarchaeological, microcontextual methodologies at microscopic and molecular scales of analysis. The main techniques applied are micromorphology and lipid biomarker analysis, which were conducted jointly on a comprehensive archaeological and experimental sample set.

The findings of this research reveal variability in Neanderthal pyrotechnological behavior. Two major types of combustion structures were documented: Simple, flat combustion structures and complex, pit hearths. They also provide information on specific aspects of pyrotechnology, such as fuel acquisition, which was shown to have been done away from the site while the local trees surrounding the site were not used as fuel. Finally, touching on Neanderthal settlement patterns, the results indicate that human occupation had little impact on the surroundings and that the time intervals between occupations were relatively long. The study also furnished new reference data to advance micromorphology and lipid biomarker research on the topic of fire, including the burning of Weissia moss.

This work contributes evidence of high Neanderthal mobility and pyrotechnological variation relevant to advancing our knowledge of Neanderthal behavioral variability. Furthermore, it demonstrates the effectiveness of high-resolution archaeological science approaches to help us build an objective, detailed picture of Neanderthal behavior.

III. Resumen

Esta tesis doctoral pretende arrojar luz sobre la variabilidad del comportamiento neandertal a través de un enfoque geoarqueológico, utilizando como ejemplo el análisis de un conjunto de estructuras de combustión neandertales procedentes del yacimiento de Paleolítico medio de El Salt, Alcoy, España. Dicho enfoque consiste en investigar las estructuras de combustión con énfasis en las relaciones de sincronía y diacronía entre ellas, en aspectos pirotecnológicos y ambientales, y en los patrones de asentamiento y movilidad grupal.

Las investigaciones geoarqueológicas se centraron en el registro sedimentario orgánico de las estructuras de combustión a través de métodos y técnicas microcontextuales a escalas de observación microscópicas y moleculares. Se utilizaron la micromorfología de suelos y el análisis de biomarcadores lipídicos como técnicas principales, implementándose en paralelo en un conjunto amplio de muestras arqueológicas y experimentales.

Los resultados de la investigación revelaron indicadores de variabilidad en el comportamiento pirotecnológico neandertal. En primer lugar, se documentaron dos tipos de estructura de combustion: simples planas y complejas en cubeta. En segundo lugar, el estudio de las estructuras aportó información sobre diferentes aspectos pirotecnológicos, tales como la adquisición de combustible, llevada a cabo fuera del lugar de habitación mientras que la madera de las inmediaciones no era utilizada. En tercer lugar, los resultados proporcionaron datos relativos a los patrones de asentamiento de los grupos neandertales en cuestión; las ocupaciones humanas tuvieron un bajo impacto en el medio natural inmediato y los periodos de abandono del lugar eran relativamente largos. Por último, este estudio contribuye al exiguo corpus de datos referenciales micromorfológicos y lipídicos para la investigación en pirotecnología prehistórica.

Esta tesis aporta evidencia de que los neandertales de El Salt tenían una alta movilidad grupal y variabilidad pirotecnológica, todo ello de relevancia para avanzar en nuestro conocimiento sobre el comportamiento neandertal. Además, demuestra la eficacia de los enfoques de arqueología científica de alta resolución hacia una aproximación al pasado prehistórico objetiva y detallada.

IV. Keywords

Geoarchaeology
Micromorphology
Lipid biomarker analysis
Middle Paleolithic
Combustion structures
Neanderthal behavior

V. Acknowledgments

Throughout the writing and work on this dissertation, I have received a great deal of support and assistance. This research was supported by the ERC Consolidator Grant project PALEOCHAR – 648871https://erc.europa.eu/funding/consolidator-grants. Archaeological research at El Salt is funded by Spanish I+D Project HAR2008-06117/HIST, HAR2015-68321-P (MINECO-FEDER/UE), and the Cultural Heritage Department of the Valencia Government and the Archaeological Museum Camil Visedo of Alcoy, under the direction of Professor Bertila Galván of Universidad de La Laguna. The archaeomagnetic and zooarchaeological research was funded by Junta de Castilla y León (project BU235P18), the European Fund for Economic and Regional Development (EFRD), and the project PID2019-105796 GB-I00 of the Agencia Estatal de Investigación (AEI/10.13039/501100011033).

Foremost, I would first like to thank my supervisor, Dr. Carolina Mallol, for her guidance and feedback along the way, without which this dissertation would not have been possible. Besides my supervisor, I would like to extend thanks to my colleagues from AMBI Lab, especially Dr. Antonio V. Herrera-Herrera, for helping me with every single chemistry-related problem I had and for contributing with his knowledge to make this thesis a better work. I'm grateful to my coauthors, for contributing to the articles I wrote. I would also like to thank Thomas Beckmann, Dr. Caterina Rodríguez, and Panagiotis Kritikakis for the manufacture of the thin sections used, as well as the lab personnel at IPE-SCIC for Total Organic Carbon measurements. I would like to extend my sincere thanks to David Friesem and Charlie French for allowing me to do a research stay in Cambridge, which significantly contributed to my scientific development. Additional thanks go to the members of the El Salt archaeological excavation team. Special thanks go to my Ph.D. colleague Rory Connolly for hours of stimulating archaeological and non-archaeological discussions and for being a good friend.

I would also like to extend my gratitude to my friends, especially Annie, Emily, and Melania, for their support, for proofreading my thesis and all the invaluable comments they provided me with. The warmest thanks go to my husband for giving me comfort, encouragement, emotional and technical support. Thank you for being there for me. I want to thank my parents for supporting me, for having my back, and for giving me the chance to study and become an archaeologist. Thank you also for my families on both sides, the German and the Montenegrin one. Special thanks to Bugi and Lady for the companionship and comfort they provided during the writing of my thesis, as well as to Lea and Ophelia for all the peaceful walks they accompanied me on.

VI. List of Abbreviations

AMBI	Archaeological Micromorphology and Biomarker
a.s.l.	Above sea level
BL	Black Layer
BM	Biomarker
BP	Before Present
BSTFA	N,O-Bis(trimethylsilyl)trifluoroacetamide
CNRS	Centre national de la recherche scientifique
CPI	Carbon Preference Index
CSIA	Compound Specific Isotope Analysis
DCM	Dichloromethane
EtOAc	Ethyl Acetate
FAME	Fatty Acid Methyl Ester
FTIR	Fourier Transform Infrared
GC	Gas Chromatography
gdp	grams of dry plant
gdbp	grams of dry burnt plant
gd(b)p	grams of dry (burnt) plant
gds	grams of dry sediment
H2SO4	Sulfuric Acid
IS	Internal Standard
kA	Kiloannum, 1000 years
MeOH	Methanol
MFT	Microfacies Type
MFU	Microfacies Unit
MIS	Marine Isotope Stage
MM	Micromorphology
MS	Mass Spectrography
NIST	National Institute of Standards and Technology
PPL	Plane Polarized Light
RL	Red Layer
SPE	Solid Phase Extraction
SU	Stratigraphic Unit
TC	Total Carbon
TCMS	Trimethylchlorosilane
TIC	Total Inorganic Carbon
TL	Total Lipid
TLE	Total Lipid Extract
TMS	Trimethylsilyl group
TOC	Total Organic Carbon
WL	White Layer
XPL	Cross Polarized Light

VII. List of Figures

VIII. List of Tables

Introduction

1. Introduction

> "We have only indirect means of knowing the courage and activity of the Neanderthals in the chase, through the bones of animals hunted for food which are found intermingled with the flints around their ancient hearths." (Osborn, 1914 p. 211)
> *- Henry Fairfield Osborn, 1914 in Men of the Old Stone Age, their Environment, Life and Art, 211.*

Studying Neanderthals today does not seem to differ much from that described by Osborn. This was written 58 years after finding the Neanderthal namesake in the Neander valley, which was confirmed to belong to a different human species around eight years after its discovery (Klein, 2009). In the last decade predating this quotation, numerous other Neanderthal fossils were uncovered in La Chapelle-aux-Saints, Le Moustier, La Ferrassie, La Quina, and Krapina Rockshelter (Klein, 2009). Currently, over a century later, the overall aim of studying Neanderthals remains the same and still focuses on revealing how Neanderthals lived their lives, while the methods of excavating and investigating have vastly improved.

Today we know a lot about Neanderthals in certain aspects, elucidated from material findings. The vast number of Neanderthal skeletal remains provided information on their body shape and adaptation for colder climates (Churchill, 2014) and provided enough material for a total reconstruction of the Neanderthal genome (Green et al., 2010). We know about their geographical and temporal range by having excavated numerous Neanderthal sites, their material culture by studying mainly lithic remains and parts of their diet according to faunal remains (Churchill, 2014). Other aspects of Neanderthal life, like their behavior, are less sufficiently studied yet. Neanderthal behavior is a vast but also slightly abstract topic that can include settlement patterns, diet, pyrotechnology, burial practices, language, art, and adornment. Consequently, studying Neanderthal behavior can go beyond the classical study of the material remains towards increasingly using scientific methods on all kinds of anthropogenic remains, which is done to a greater extent in recent years.

The study of Neanderthal combustion features offers possible insight into Neanderthal behavior, especially in terms of pyrotechnology and settlement patterns. In modern-day hunter-gatherer groups, the hearth is the main focus and central element around which activities are carried out (Binford, 1978; Binford, 1998; Fisher and Strickland, 1991; Jones, 1993; O'Connell, 1987; Yellen, 1977), from which the assumption can be drawn that the hearth was equally crucial for Neanderthal activities as well. Combustion structures can therefore be treated as archives of Neanderthal activities and behavior.

Likewise, combustion structures are proxies for occupations since the spatial location of the hearth indicates the level of the occupation horizon during which the fire was burnt, making a combustion structure a basic element of a single occupation episode (Henry, 2012; Machado et al., 2013; Vallverdú et al., 2005b; Vaquero and Pastó, 2001). Furthermore, combustion structures can also act as markers to dissect palimpsests. A palimpsest is a complex superimposition of successive activities, occupation episodes of an unknown number, and numerous natural processes, representing long periods of time within an archaeological unit (see Chapter 3.1) (Bailey, 2007; Lucas, 2005). Combustion structures point out isolated occupation episodes from which a minimum number of occupations within a palimpsest can be deduced (Vaquero and Pastó, 2001). Isolating single human occupations and dissecting the palimpsest is a premise for further analyzing human activities and human behavior within its temporal context (Mallol and Hernández, 2016). Furthermore, charring can preserve organic material, making combustion structures archives for organic material (Weiner, 2010). These qualities reinforce the necessity of studying combustion structures.

The study of combustion structures can be approached by studying fire as an artifact (Stahlschmidt et al., 2020). Since combustion structures mainly consist of anthropic sediment, where humans contributed to depositional and postdepositional processes, they should be given similar significance as other recoverable artifacts. Through the sedimentary nature of combustion structures, geoarchaeological techniques need to be applied to obtain relevant information (Miller, 2011). Different methodologies have been used in the last decade to study combustion structures as artifacts (Mallol et al., 2017; Mallol and Henry, 2017; Mentzer, 2012; Mentzer, 2017; Miller, 2011). Some methods are suitable to study fire remains, including micromorphology (Mallol et al., 2017) and lipid biomarker analysis (Allué et al., in prep). Micromorphological studies on combustion structures can provide a detailed understanding of the depositional and post-depositional formation processes through the study under high-resolution and in their undisturbed state (see Chapter 2.2). Besides that, micromorphology is crucial for the contextualization and integrity of the lipid biomarker results. The lipid biomarker approach focuses on recovering organic materials, specifically lipid molecules, from the sediment (see Chapter 2.3). This approach is useful for recreating organic input into the fire or the sediment. Both methods combined aid in extracting microscopic and molecular information, which contextualizes data on Neanderthal fire features.

The Middle Paleolithic fire record has been extensively investigated (Allué et al., 2012; Cabanes et al., 2010; Courty et al., 2012; Heyes et al., 2016; Koller et al., 2001; Pastó et al., 2000; Picornell-Gelabert et al., 2017; Sandgathe, 2017; Théry-Parisot, 2002b; Vidal-Matutano, 2016; Vidal-Matutano et al., 2017; Vidal-Matutano et al., 2018; Yravedra and Uzquiano, 2013), yet there are still no standardized excavation and investigation strategies in place. In many instances, the documentation of combustion structures does not exceed the description of shape and size and the removal of charcoal, bones, and lithic objects (Roebroeks and Villa, 2011). Likewise, investigations from a geoarchaeological, microcontextual perspective are not sufficiently applied. Publications on Neanderthal use of fire and associated behavior involving fire are similarly limited, making comparisons challenging, if not impossible. This impedes our evaluation of Neanderthal settlement strategies, pyrotechnology, and ultimately Neanderthal behavior.

This thesis seeks to expand on the knowledge of Neanderthal behavior by studying combustion structures from a geoarchaeological, microcontextual perspective using exhaustive and comprehensive investigation and excavation strategies. The investigations will be concentrated at the Middle Paleolithic site of El Salt, Spain, covering combustion structures from two stratigraphic units (SUs). The investigation will be addressed through a novel approach within prehistoric archaeology: the study of the organic sedimentary record using microscopic and molecular methods. This approach will result in a better understanding of Neanderthal behavior restricted to one group of Neanderthals in this specific region and timeframe. Furthermore, this thesis and its consequent case studies will motivate other archaeologists to adapt this research strategy to their sites and combustion structures and thus contribute to a comprehensive knowledge of Neanderthal pyrotechnology and settlement strategies across regions and timeframes.

This thesis is split into three independent case studies, which contribute to this dissertation's overall aim. The topic of Case Study I was chosen because of the abundance of combustion features in the Middle Paleolithic site of El Salt, of which only a few were previously studied. This Case Study was sought out to be a comprehensive study of a large number of combustion structures from the same stratigraphic unit (SU) to gain exhaustive knowledge on Neanderthal settlement strategies. Short-term occupations and resulting group mobility seem generally accepted as the model in which Neanderthals occupied sites, yet their timing and intensity remain unresolved. The detailed study of Middle Paleolithic anthropogenic combustion structures can reveal information on timing, intensity, and natural setting of Neanderthal occupations and contribute to a better understanding of Neanderthal settlement strategies. Eleven flat, simple combustion structures from SU Xb of the Middle Paleolithic site of El Salt, Spain, were investigated using a geoarchaeological approach combining micromorphology, lipid biomarker analysis, and compound-specific isotope analysis.

Case Study II was motivated through the results of Case Study I. A combustion structure with a peculiar pit shape unlike any of the combustion structures studied in Case Study I was uncovered. This combustion structure was standing out to the flat, simple combustion structures indicating low impact short-term occupations studied before, for having a pit-like depression filled with a white ashy substance overlying a reddened substrate. Combustion structures not only record information on settlement strategies but also preserve information on the pyrotechnology used by their makers. Studying this pit hearth microcontextually, using micromorphology, lipid biomarker analysis, archaeomagnetism, and zooarchaeology will validate the combustion structure's integrity as a pit hearth and point out pyrotechnological variation, ultimately leading to a variation in Neanderthal behavior.

The need for Case Study III became apparent after encountering an unidentified plant in the ash layer of the combustion structure in Case Study II. Moss was identified as plausible source material and was sampled and investigated geoarchaeologically. This was done to clarify possible additions to the pit hearth and observe any possible addition of mosses in other combustion structures. This Case Study was undertaken as experimental work, where moss was combusted at different temperatures and analyzed with the main methods used for this thesis: micromorphology and lipid biomarker analysis.

This thesis aims to advance our understanding of Neanderthal behavior, especially connected with their use of fire and associated synchronic and diachronic variability. This includes the understanding of Neanderthal pyrotechnology and their natural environmental context as well as Neanderthal settlement patterns. The organic sedimentary archaeological record of fire is investigated to explore the potential of the microscopic and molecular sedimentary record using micromorphology and lipid biomarker analysis. This will be achieved by completing the following objectives:

1. Identifying isolated single occupation episodes.
2. Obtaining high temporal and spatial resolution data at the level of singular human occupation events related to fire use.
3. Determining anthropogenic and natural input into the Neanderthal fires.
4. Exploring objects in question using experiments.

In the following pages, I will first provide background information on the materials and methods used in this dissertation. The Middle Paleolithic Site of El Salt will be introduced, focusing on its publication history and its stratigraphy, and in particular, the stratigraphic units of interest for the case studies. The methods section will comprise and introduce the methods used in the case studies, namely micromorphology and lipid biomarker analysis, in addition to a short literature review. Subsequently, three case studies will be presented, each containing an introduction, result, discussion, and conclusion. The chapter of Case Study I includes the study of a combustion structure assemblage in El Salt and their significance to Neanderthal mobility. The chapter of Case Study II focuses on a pit shaped hearth being studied using a multidisciplinary approach to investigate Neanderthal pyrotechnology and behavioral variability. Case Study III is an experimental component related to the pit hearth of Case Study II in which one kind of moss is investigated after finding indications of the presence of moss in combustion structures. The general discussion will link the results and discussion of the three case studies, with special sections on mobility and settlement patterns and Neanderthal pyrotechnology. The general discussion will also comment on the applicability of the methods used in this discussion and give insights into future studies. The general conclusion will comment on fulfilling this thesis's objectives and summarize the results of this dissertation.

Materials and Methods

2. Materials and methods

2.1 The Middle Paleolithic site El Salt

El Salt is a Middle Paleolithic, open-air site located in Alcoy (Alicante, Spain) in Eastern Iberia (38º41'14" N, 0º30'32" W, 680 m a.s.l.) (Fig. 1a) (Galván et al., 2014a). The site has been dated by thermoluminescence and optically stimulated luminescence between 60.7 ± 8.9 and 45.2 ± 3.4 kA (Galván et al., 2014b; Garralda et al., 2014), which places it in the marine isotope stage (MIS) 3.

El Salt is situated on the foot of the Mariola mountain range at the height of 680 m above sea level (Galván et al., 2014a), close to the confluence of the Polop and Barchell rivers, two tributaries to the Serpis river (Fig. 1b) (Garralda et al., 2014). Located in the Alcoy valley, the site is in close vicinity to the following Middle Paleolithic sites: Abric del Pastor (ca. 3 km) (Mallol et al., 2019), Cova Beneito (ca. 12 km) (Iturbe et al., 1997) and Coves d'Estroig (approx. 6 km) (Faus Terol, 2000). Furthermore, over one hundred open-air sites related to flint exploitation have been identified in the surrounding valleys (Molina Hernández, 2016).

Delimiting the site to the south is a 38 m high Paleocene limestone wall covered with tufa and travertine (Fig. 1c) (Galván et al., 2014a; Galván et al., 2014b). To the north, the site is delimited by a travertine ramp at around 13 m distance to the wall, connecting the site's level with the valley bottom, possibly indicating flowing water (Garralda et al., 2014). The site is resting on a horizontal travertine platform and expands over 300 m² as a relatively flat occupation surface with 6.3 m thick deposits (Galván et al., 2014a).

An accumulation of weathered fallen blocks located at an eight- to ten-meter distance from the wall is concentrated on top of the travertine platform and is in correlation with the first archaeological layers, indicating that roof fall events might have taken place during the first occupation of the site (Galván et al., 2014a). Galván et al. (2014a) state that a travertine overhang covered parts of the site, which might have covered the entire excavated surface at the time of the overhang's maximum development. Despite that, El Salt is typically referred to as a site in an open-air setting (Fumanal García, 1994; Galván et al., 2014b; Machado and Pérez, 2015).

According to the stratigraphy and dating of the site (see 2.1.2), the site's occupations can generally be divided into two broader segments: before and after 50 kA.

Occupations older than 50 kA (Stratigraphic unit XII – IX) correspond to frequent short-term occupations. The sediment is characterized by abundant combustion structures in a geogenic and biogenic soil material (detrital sand, humified organic matter, and animal excrements) (Galván et al., 2014a).

Anthropogenic material comprises lithic tools and faunal remains with traces of thermal alteration and combustion-related material (Machado et al., 2016; Machado and Pérez, 2015; Pérez et al., 2015; Pérez, 2019; Pérez et al., 2020). Lithic raw material (flint) was sourced in the Alcoy valleys within a radius of up to 20 km (Machado and Pérez, 2015; Molina Hernández et al., 2010). Flint tools were either knapped on-site or brought to the site configured or collected and reused in the settlement itself. The majority of the tools were manufactured using the Levallois technique. Activities of butchering and vegetable processing, as well as leather and woodworking, have been detected on the flint tools (Rodriguez Rodriguez et al., 2002) closely associated with limestone pebbles (hammers, anvils) with traces of human manipulation (Galván et al., 2014a).

The faunal remains reflect similar patterns to other deposits of Iberian Mediterranean sites from MIS 3, including goats, deer, and horses and small prey like European rabbit and lagomorphs, as well as bovine, turtles, and carnivores (Pérez, 2019). Nevertheless, the majority of Leporidae, though, relates to the contribution of raptors. Human faunal exploitation has been detected on bones as traces of defleshing and intense fracturing. After use, bones were discarded throughout the excavation area, especially near the travertine wall (Pérez, 2019).

Occupations younger than 50 kA (SU VIII-$V_{superior}$ (V_{sup})) correspond to a progressive decrease of human impact compared to an increase of geogenic material (Galván et al., 2014a; Galván et al., 2014b). Materials such as lithics and faunal remains as well as combustion structures gradually diminished from SU VIII to VI. On top of SU VI, a second roof fall event marks the change of sediment dynamics and anthropogenic contribution, possibly coinciding with Heinrich event 5. Here fire activities are only represented by charcoal and thermally altered lithic and faunal remains. SU V exhibits an abrupt change in sedimentation to a high sedimentation rate of freshly broken off sands and calcite derived from the breakdown of rocky beds. This is accompanied by the presence of six dental remains at the base of SU $V_{sup,}$ which were identified as a Neanderthal right hemimaxilla of a young individual.

Subsequent to the Middle Paleolithic deposits in El Salt, Gravettian, Solutrean, Magdalenian, Epipaleolithic and Mesolithic materials were uncovered. Ceramic remains dating to an occupation between the Neolithic 1A and the Bell-Beaker horizon transition were obtained, providing the *terminus post quem* for the deposition of gravels.

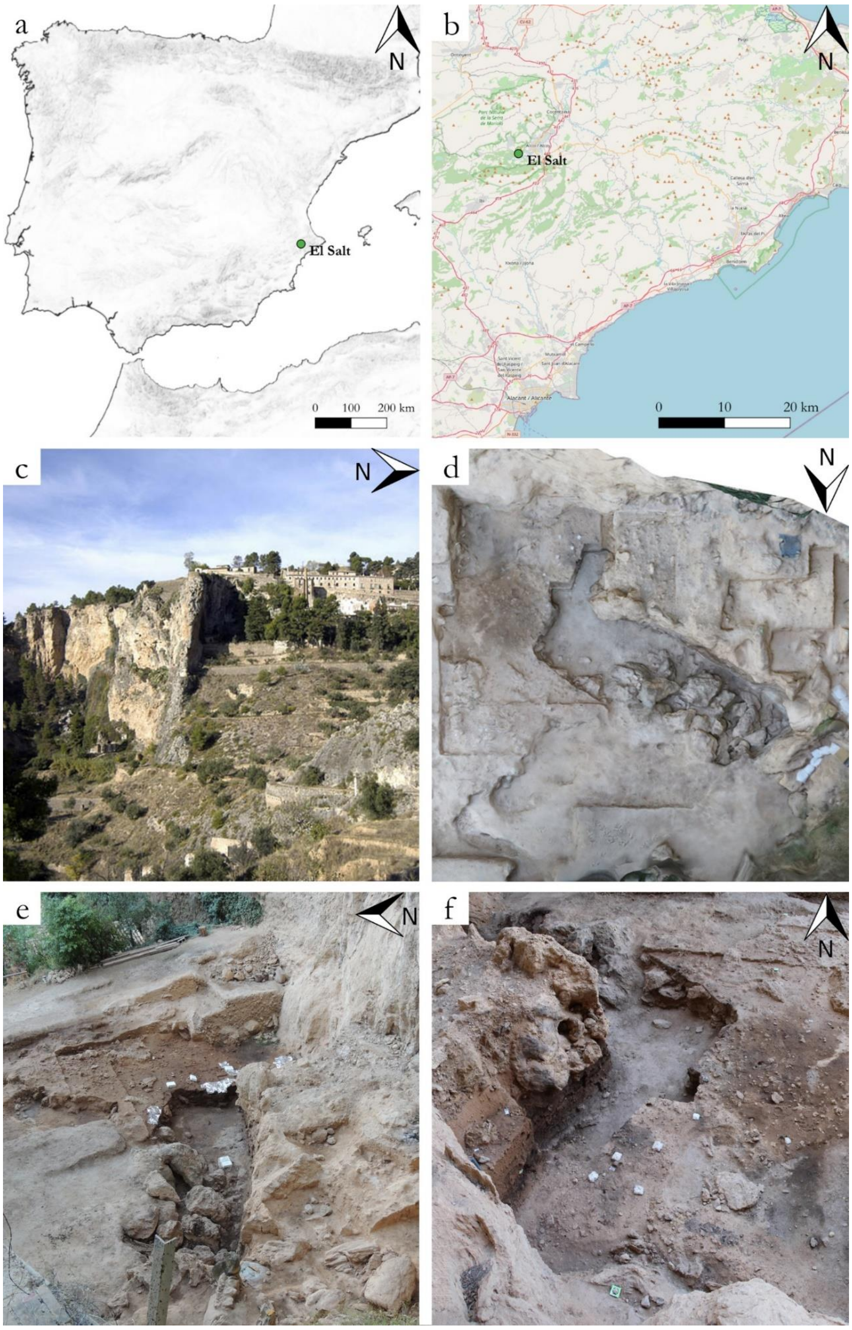

Fig. 1: Overview pictures of the Middle Paleolithic site of El Salt. a) Location of El Salt within the Iberian Peninsula, b) Location of El Salt within the closer geographical area, c) El Salt situated to the right of the limestone wall, d) orthophotograph of excavation surface created from photogrammetric model during the excavation year of 2017, e) view over excavation surface (year 2017) from west, f) view from south over excavation surface (year 2017) focusing on stratigraphic unit Xb.

2.1.1 Excavation and publication history

Excavations in El Salt began in the 1960s with an initial trench excavation covering a surface of about 30 m^2, which was dug until an archaeologically sterile travertine platform was reached. Subsequently, systematic excavation and research began in 1986 by a team of researchers from the University of La Laguna, Tenerife, Spain, and is ongoing today.

The site's basic description has been communicated in 3 publications: (1) Fumanal García (1994) describes the general geological and sedimentological characteristics of the site and creates the classification of the stratigraphic units. (2) A book chapter describes the current state of investigations and gives general information on the site (Galván et al., 2014a), and (3) the third paper is reports thermoluminescence and optically stimulated luminescence dates, which form the foundation for the overall frame of dates used for the site (Galván et al., 2014b).

Studies on faunal assemblages produced information on past climates. A micro-mammal study of SU Xb suggests a colder and more humid climate than the present day (Fagoaga et al., 2017). In contrast, in SU $V_{sup,}$ dryer conditions predominated, supporting the hypothesis that aridification played a part in the Neanderthal disappearance (Fagoaga et al., 2019). A study of a macro mammal bone assemblage generated by human activities containing ibex, deer, and horse shows characteristics of Mediterranean macroclimate (Pérez et al., 2017a).

A highly discussed topic for publication in El Salt is the dissection of palimpsests. Especially in SU X, sedimentation is slow and anthropogenic material is abundant. To extract behavioral information from these remains and to get as close as possible to single occupational events, these accumulations needed to be dissected. This has been done using lithic analysis of raw material units (Machado et al., 2016; Machado Gutiérrez et al., 2011; Mayor et al., 2019; Mayor et al., 2020) as well as a combination of faunal and lithic analysis (Machado and Pérez, 2015; Pérez et al., 2015; Pérez et al., 2020) and anthracological analysis (Vidal-Matutano, 2016).

The study of combustion structures is another topic that has been and still is extensively investigated. In particular, the combustion structures of stratigraphic unit X, which researchers have been excavating since 2000, were investigated using various methods and tools. Micromorphological studies on combustion structures investigated the black layer (BL) and compared it with a set of experimental combustion structures to determine that the origin of the BL is fire altered topsoil, thus a remainder of an occupation surface (Mallol et al., 2013a). From the same set of experimental combustion structures, a study on human actions involving combustion structures, like the input of wood and meat, sweeping, trampling, and relighting, was performed (Mallol et al., 2013b). This study concluded that sweeping is the process that can most likely be recognized through micromorphology, and relighting is the process that might be least recognizable (Mallol et al., 2013b). Another experimental combustion structure study focused on the direct and indirect thermal alteration of modern faunal remains in order to better understand archaeological faunal remains (Pérez et al., 2017b). In the case of El Salt, bones trampled into the occupational surface were indirectly burned by overlying combustion structures (Pérez et al., 2017b). Studies of combustion structures without a link to experimental samples have been done using FTIR analysis and phytolith analysis in which combustion structures exhibited thermally altered clay and a phytolith input deposited by natural agents (Rodríguez-Cintas and Cabanes, 2015). In an anthracological study, charcoal with features of fungal decay prior to charring was recovered in two combustion structures from El Salt, possibly indicating dead wood gathering and combustion structures with smoking-related functions (Vidal-Matutano et al., 2017). Another study investigating lipid biomarkers from fireplaces was able to estimate if fireplaces served as a heat source or as a cooking fire and, in the case of cooking fires, whether input in the fire was of vegetal or animal origin (Sistiaga Gutiérrez et al., 2011).

Other studies include a functional analysis of the lithic industry (Rodriguez Rodriguez et al., 2002), a bioanthropological study of dental remains that can be attributed to Neanderthals (Garralda et al., 2014), a study of fecal biomarkers (Coprostanol and 5β-Stigmastanol), which presence can be argued in favor of a mixed meat and vegetable diet of the inhabitants of El Salt (Sistiaga et al., 2014) and an anthracological and carpological study over multiple stratigraphic units which concludes that firewood was gathered from nearby and seeds from trees contributed to the sediment which wood is not represented in the charcoal record (Vidal-Matutano et al., 2018). A very recent study was published encompassing the investigation of Neanderthal gut microbiota in El Salt (Rampelli et al., 2021).

2.1.2 Site stratigraphy and dating

The site comprises a 6.3 m thick stratified deposit, which is divided into 13 lithostratigraphic units and can be grouped into five distinct segments (see Table 1) (Galván et al., 2014b; Garralda et al., 2014). The deposit is dated to between 60.7 ± 8.9 and 45.2 ± 3.4 kA (Galván et al., 2014b). The Middle Paleolithic sequence includes stratigraphic units from V_{sup} until XII (Galván et al., 2014b). This sequence is described as horizontally bedded geogenic sands containing archaeological remains and combustion residues (Fumanal García, 1994; Galván et al., 2014b). The anthropogenic input is more abundant in stratigraphic units IX to XII than in the overlying stratigraphic units (Galván et al., 2014b). SU XIII is an archaeologically sterile horizontal travertine platform and has been dated to 81.5 ± 2.7 kA and 80.1 ± 4 kA (Fumanal García, 1994; Galván et al., 2014b).

Segment	SU	Description
5	I - IV	Irregular beds of gravel and cobbles in a silty clayey matrix, combined remains of late Upper Paleolithic, Epipaleolithic, Mesolithic, and Neolithic
4	$V_{inferior}$	Massive gravel in the top 20 cm and massive sandy silt, almost archaeologically sterile
3	V_{sup} - VIII	Horizontally bedded geogenic sand and decreasing evidence of human input
2	IX - XII	Horizontally bedded fine sands with abundant archaeological remains and combustion residues
1	XIII	Sterile horizontal travertine platform

Table 1: Summary of site stratigraphy after Galván et al. (2014b)

2.1.3 Stratigraphic units of interest

2.1.3.1 Stratigraphic unit X

SU X is dated to 52.3 ± 4.6 kA by thermoluminescence on burnt flint objects (Galván et al., 2014b). The stratigraphic unit has different characteristics depending on the position within the excavation surface and can be broadly divided into an area closer to the travertine wall and farther away from the travertine wall. The stratigraphic unit is about 15-20 cm thick along the travertine wall and extends up to a thickness of 35 cm farther away from the wall (Fumanal García, 1994). The sediment is sandy-silty, calcareous, and yellowish-brown (Galván et al., 2014b), containing rare clasts towards the wall and more frequent clasts farther away from the wall (Fumanal García, 1994). It is rich in archaeological material such as faunal remains, flint flakes, and anthropogenically modified cobbles (Galván et al., 2014b). The stratigraphic unit has a massive appearance farther away from the wall, and a laminar appearance caused by combustion features closer to the wall (Fumanal García, 1994).

These combustion structures are numerous and clustered towards the site's back wall. They are flat and of variable dimensions (between 0.2 and 1.0 m in diameter) (Galván et al., 2014b; Machado et al., 2016; Mallol et al., 2013a; Sistiaga Gutiérrez et al., 2011). These structures often overlap, generating a combustion structure palimpsest. Individual combustion structures seem well preserved in the field and yield a stratigraphic succession of WL, BL, and RL typical for flat, *in situ* combustion structures (Mallol and Henry, 2017). Selected combustion structures have been observed micromorphologically as simple, flat, open, *in situ* hearths whose BL's consist of natural topsoils described as animal excrements and plant remains in a bioturbated matrix of sediment (Mallol et al., 2013a), and some might even contain human excrements (Sistiaga Gutiérrez et al., 2011).

SU X has been subdivided into two parts, SU Xa and Xb. This separation was done based on field observations of texture and color. The upper part, Xa, is roughly 10 cm thick, sandier, and lighter (brownish yellow) colored, and the lower part, Xb, is between 10 and 14 cm thick, and more clayey and darker (brown). So far, in SU Xa, 44 combustion structures were recovered, and in SU Xb 46.

2.1.3.2 Stratigraphic unit Xb

SU Xb will be the focus of Case Study I but will also play a minor role in Case Study II. It is exposed on 36 m² out of 300 m² of the whole site due to being cut by the old excavation trench and the Holocene erosion, but it is still preserved at the unexcavated part of the site (Galván et al., 2014a; Machado et al., 2016).

SU Xb has been studied using microfaunal and anthracological analysis as well as phytolith and FTIR analysis. A recent study of small mammals yielded data on rodents, insectivores, and a lagomorph from SU Xb (Fagoaga et al., 2017). In a paleoecological context, this implies that SU Xb was slightly colder and slightly more humid than today and that the environment was composed of open woodlands and dry and humid meadows (Fagoaga et al., 2017). This hypothesis is further supported by anthracological data from SU Xb, which with the presence of *Acer* sp. and *Buxus sempervirens,* is described as more humid than all other stratigraphic units and the sequence from stratigraphic units XIII to Xb as generally colder than today (Vidal-Matutano et al., 2018). With a focus on SU Xb's combustion structures, the firewood present was identified as predominantly scots pine and maple, and some charcoal fragments surrounding combustion structures could be attributed to their source hearth (Vidal-Matutano, 2016). Fungal analysis on charcoal recovered in one of the combustion structures in Xb, H57, indicated dead wood gathering as fuel, hinting towards the hearth being used as a smoking fire (Vidal-Matutano et al., 2017). A majority of the combustion structures studied by Case Study I have been subjected to comprehensive FTIR and phytolith studies, where the presence of ashes, altered clay, and phosphate minerals was detected together with principally natural sedimentation of phytoliths into the combustion structures, most probably through bird guano (Rodríguez-Cintas and Cabanes, 2015).

2.1.3.3 Stratigraphic unit XI

SU XI has not been excavated. Nevertheless, its surface is exposed in nearly the entire excavation surface of former SU X. The boundary between stratigraphic units X and XI is slightly undulating, but sharp. Likewise, this SU is exposed in the profile of the old excavations and has been described geomorphologically and sedimentologically. The stratigraphic unit appears to have a diffuse contact with SU XII and a varying thickness of 15 to 30 cm (Fumanal García, 1994). It extends throughout the exposed profiles, but its shape is disrupted by big underlying boulders from the roof collapse event of SU XII farther away from the travertine wall (Fumanal García, 1994). It exhibits a large number of combustion structures visible through irregular bands of black layers and grey ashy layers (Fumanal García, 1994). The stratigraphic unit's overall texture is silty clay interspersed with charred rocks that appear predominantly farther away from the travertine wall (Fumanal García, 1994).

2.2 Micromorphology

Archaeological soil micromorphology is the study of soil or sediment and their components in an undisturbed state on the microscopic level (Stoops, 2003). It aims to determine the composition of the constituents and their spatial relationship and to deduce their genetic and chronological relationships (Stoops and Nicosia, 2017). This ultimately leads to the understanding of each constituent's function within the soil or sediment as a whole (Stoops, 2003).

Micromorphology has its roots in pedology and was introduced in 1938 by Walter Kubiena (Kubiena, 1938). It was and is a crucial method for understanding the formation and function of the soil and how it was constructed, apart from chemical and physical analyses that defined basic soil components but not the function of the soil (Stoops, 2003). Using micromorphology, one examines soil in its undisturbed state and as an oriented sample with the aid of microscopic techniques (Nicosia and Stoops, 2017; Stoops, 2003). This can be achieved by extracting a block of undisturbed sediment, indurating it with resin, and cutting and grinding it to a thickness that enables examination under the microscope (see 2.2.3 - 2.2.5). Since the 1960s, micromorphology has been applied to archaeological sediments and gained traction so that archaeologists are currently one of the most frequent users of soil micromorphology (Stoops, 2014; Stoops and Nicosia, 2017). As a result, the mere study of soil extended to include regoliths and thus archaeological sediments (Stoops, 2003, 2010).

2.2.1 Significance

The microcontextual approach provides information about the integrity of components, their origin, deposition history, and their relation with human activities (Goldberg and Berna, 2010). The significance of micromorphology in soil science and archaeology is manifold. Generally, it is beneficial to see soil or sediment under such high-resolution. What was once performed using a magnifying glass in the field (Stoops, 2003) can now be done with a microscope in the laboratory with magnifications up to 200x. Furthermore, by using undisturbed sediment samples, one can see not only the components in high-resolution but also their context. This implies the stratigraphic, genetic, and chronological relationship of the components.

Comparing it to physical analysis where the amount of clay, for example, is measured, micromorphology can additionally study the geometrical distribution within the sample (Courty et al., 1989). Also, primary minerals can be identified and differentiated from secondarily precipitated minerals (Courty et al., 1989). Moreover, minerals and sedimentary products, as well as biogenic and anthropogenic components, can be identified and contextualized. This makes it possible to detect archaeological components such as bone, mortar, organic matter, rock fragments, or soil aggregates, which would not be detectable using chemical analyses (Courty et al., 1989). Archaeological deposits with a low sedimentation rate, frequent human activity, or both are primarily benefiting from the use of micromorphology since even microscopically thin layers can be identified and adequately examined.

All of these points allow micromorphology to stand out from other methods used in the field of soil science because these usually rely on bulk samples and analyses that require mixing, grinding, solubilization, or fractionation, which inevitably present average data (Stoops, 2003).

2.2.2 Micromorphology in the context of Middle Paleolithic fires

Archaeological soil micromorphology has been increasingly used for the last 60 years (Macphail, 2014) and has been applied to many different sites and periods in a wide geographical range. In accordance with this thesis, a short literature review will focus on micromorphological work conducted on combustion structures in the Middle Paleolithic. An overview of the literature and published material is vital to study combustion structures in the Middle Paleolithic and compare results between sites to infer similarities and differences of Neanderthal behavior and pyrotechnology across sites. This review will be divided into brief dialogues on general literature about micromorphology on combustion features, experimental work on combustion features using micromorphology, and micromorphological studies on combustion structures of Middle Paleolithic sites.

Combustion structures have always been one of the key focus areas of micromorphology. Miller (2011) emphasizes studying anthropogenic deposits (such as combustion structures) as artifacts, thus using similar diligence as it is done, for instance, for stone tools. This, and much more, can be achieved by using micromorphology (Miller, 2011; Stahlschmidt et al., 2020). Mentzer (2012) authored a journal article about various microarchaeological approaches for identifying combustion features in prehistoric archaeological sites, including the method of micromorphology. Along a similar line follows the entry on hearths and combustion features in the encyclopedia of geoarchaeology (Mentzer, 2017). Mallol and Henry (2017) demonstrate methodological techniques for studying paleolithic combustion structures with ethnoarchaeological hearths, including micromorphological analysis. Subsequently, the most comprehensive chapter about the analysis of combustion structures using micromorphology is from Mallol et al. (2017) in Nicosia and Stoops (2017). In that chapter, the most critical aspects for the study of combustion structures are the classification of combustion structures, the analytical strategy, the common microscopic products of combustion, the stratigraphy, and the intact and physically reworked combustion structures and their chemical diagenesis. The use of micromorphology in particular in combustion structure research is suitable for identifying calcitic ashes, phytoliths and microscopic charcoal, and the contextual integrity of ash and charcoal layers, as well as identifying the mechanism and degree of postdepositional alteration (Arpin et al., 2002; Courty et al., 1989; Goldberg et al., 2009b; Mentzer, 2012). These chapters and articles establish a solid basis for the treatment, analysis, and description of the study, interpretation, and comparison of combustion structures.

Apart from this, the interpretation of combustion structures can be aided by experimental research. To correctly identify and interpret combustion structures, the micromorphologist needs information about the circumstances and conditions under which specific features or traces can be produced and preserved in the archaeological record (Aldeias, 2017). Despite having numerous experimental, micromorphological studies on combustion structures, the discipline permanently relies on experiments trying to recreate similar conditions and processes to the archaeological dataset. Aldeias (2017) published a review article on experimental analyses performed on combustion features, limited not only to micromorphology, which highlighted experiments on the identification of anthropic fire, fuel use, hearth location and artifact alteration, alteration of underlying deposits, reworking, and the role of anthropogenic actions. The essential experimental studies from the viewpoint of Middle Paleolithic combustion structures using micromorphology are discussed below.

Intact combustion structures are the most common structures studied experimentally using micromorphology (Briz Godino et al., 2011; Mallol et al., 2007; Mallol et al., 2013a; Mallol et al., 2013b; Miller et al., 2009; Miller and Sievers, 2012; Shahack-Gross et al., 2004; Villagran et al., 2011a; Wattez, 1988). Contrary to this, anthropogenically reworked combustion features have received much less attention in experimental studies (for exceptions, see Mallol et al., 2013a; Mallol et al., 2013b; Miller et al., 2009). Relighting events could go unnoticed, as shown in a study where fireplaces were reused after a short duration (up to 15 days), and the resulting fire features showed no distinct stratigraphic features (Mallol et al., 2013b). The sediment underlying combustion features was also experimentally studied using micromorphology to see the extent of heat transfer and the sediment's resulting color change (Aldeias et al., 2016; Canti and Linford, 2000).

As crucial as experimental studies are, other studies on similar sites from the same time span are essential to facilitate a comparison between sites. This part of the review is limited to the Middle Paleolithic to ascertain comparable similarities and differences among combustion structures, ultimately leading to a comparison of Neanderthal behavior and pyrotechnology across sites. Field descriptions of combustion features alone are not sufficient for reliable inter-site comparisons. A detailed microcontextual description is necessary to define individual components, the connection and context of the separate combustion layers, and postdepositional processes. Micromorphological studies on Middle Paleolithic sites are still infrequent, even though it is one of the most studied periods in archaeological micromorphology. Therefore, I will present a list of Middle Paleolithic sites in which micromorphology has been carried out on *in situ* combustion features, alongside a description of the combustion features and their references. *In situ*, hereby, refers to combustion features in which an internal stratification is still observable and whose position is most likely the original location of the fire. Sites with evidence for combustion but without combustion structures and combustion deposits stemming from rake out and dumping processes were disregarded. Table 2 is based on Mentzer (2012)'s literature research and has been extended to include detailed descriptions of combustion features examined and to comprise additional publications from 2012 to 2020.

Site	Hearth description	References
Abric del Pastor (rockshelter), Spain	**General:** 18 combustion features in 3 stratigraphic units (II, IV, VI), no ash layers in the field (except one), 0.3-1cm thick lenses of dark gray or reddish-brown sediment, diameters between 0.5 and 1m, microscopic combustion residues (charcoal, wood ash and burned bone) **WL:** grey layer of H17: aggregated, calcite-rich matrix with frequent unidentified black particles and coatings around clasts, some fissured and rubified	(Mallol et al., 2019)
Abric Romani (rockshelter), Spain	**General:** evidence for multi-phase combustion, mostly *in situ* combustion structures, small and large combustion structures, numerous structures in levels H, I, J, K, L and O, apparent thermal alteration on travertine surfaces **WL:** well-preserved ashes from conifer wood, rare charcoal, and calcined bone fragments, complete combustion	(Courty et al., 2012; Pastó et al., 2000)
Cova del Gegant (cave), Spain	**General:** one *in situ* combustion structure containing charcoal, ashes, and burnt bones **RL:** sediment affected by heat, but no reddening observed **BL:** massive dark organic burnt material, chaotic internal organization (sediment, wood charcoal fragments, fibrous vegetal remains, and cracked bone fragments), clay is dark red and mixed with coprolite fragments **Postdeposition:** reworked by biological agents (carnivores)	(Sanz et al., 2017)
Cova Gran de Santa Linya (cave), Spain	**General:** *in situ* combustion structures, overlapping combustion structures consisting of ash residues on top and partially burned sediments at the bottom **BL:** organo-mineral groundmass, randomly distributed coarse fraction, burnt sediment aggregates, partially burnt bone fragments, charcoal, recrystallization of groundmass **WL:** fissure on top, calcitic recrystallization of groundmass, subrounded reddish sediment aggregates, sharp lower boundary **Postdeposition:** slight dissolution and recrystallization of groundmasses	(Polo-Díaz et al., 2016)
Cueva Antón (cave), Spain	**General**: at least eight fire features, sequence of whitish silty layer, blackish-brown sandy layer gradually changing into a reddened band with diffuse lower margins **RL:** concave shape deriving from thermal alteration, reddened lens indicative of thermal alteration of sands, coatings, and impregnations of iron oxides with decreasing frequency downwards **BL:** burnt bone fragments and teeth, fragments of debitage and clay with traces of rubefaction, carbonate particles with darker color, likely represents surface of anthropogenic occupation **WL:** upper part calcium carbonate and lower part micrite and microsparite, locally calcitic plant residues and channel porosity recognizable, fragments of fine sediment, burnt bone fragments, upper part likely to be deposited through biological mechanisms aided by floodwater **Postdeposition:** relatively good conservation through a quick accumulation of low-energy water-laid sediment	(Anesin, 2016; Angelucci et al., 2018)
El Salt (open-air), Spain	**General:** abundant combustion structures in El Salt, focus on unit X, *in situ* layered hearths ((RL)-BL-WL), charcoal fragments >1cm found in sediment outside of combustion features **RL:** in a few cases, thermally altered clay with calcitic ash inclusions, calcined bone, tufa grains, and rare organic punctuations **BL:** sandy sediment composed of carbonized plant litter (leaf, stem and root fragments, coprolitic residue) and unsorted detrital mineral components, scarce bone fragments (microfauna) **WL:** microcrystalline calcium carbonate aggregates and amorphous ash domains, burnt clay, moss-like morphologies in one case **Postdeposition:** BL channeled with bio galleries, bioturbation	(Mallol et al., 2013a)

Site	Hearth description	References
Gorham's Cave, Spain	**General:** Combustion zones consist of mainly a rubified base, sometimes with overlying charcoal accumulations; combustion zones are not well defined (postdepositional alteration) **RL:** containing charred guano, organic matter (coarse wood charcoal fragments and charred fine organic matter), phosphate, and burnt bone. **BL:** Present in some cases, consisting of charcoal accumulations **WL:** Ash is not preserved because of decalcification and aeolian reworking **Postdeposition:** Some combustion zones are reworked by bioturbation, aeolian, and water processes	(Macphail and Goldberg, 2000a)
Grotte XVI (cave), France	**General:** lenses of black, whitish, and reddish color. **BL:** charcoal rich **WL:** presence of ash derived from wood with contribution of grass (up to 10-15 wt%), concentration of phytoliths and burnt flint artifacts	(Karkanas et al., 2002)
Hayonim Cave, Israel	***Entrance section*** **General:** 30-40 cm across, brown circular features, without ashy components, eroded, dissolved, or transformed into phosphates ***Center section*** **General:** anthropogenic accumulations of bedded, lenticular, or tabular hearths, in mass of homogenous brown, yellow or reddish silty clay, ash, fragments of charcoal, and bones mixed in a chaotic arrangement, hearths from lower layers more massive (>110 cm across, 10-12 cm thick) intact but slightly cemented ashes **WL:** intact but slightly cemented ashes, upper units more diagenetically altered **Postdeposition:** anthropogenic trampling or bioturbation, diagenetic alteration	(Goldberg and Bar-Yosef, 1998; Schiegl et al., 1996)
Kebara Cave, Israel	**General:** lenticular in cross-section on a flat or concave surface, sometimes multiple superimposed layers of charcoal and ash **RL:** geogenic substrate (if present) burned and rubified **BL:** charcoal rich but mixed with ash (3-5 cm thick) at the base of each hearth **WL:** ash-rich layer (5-15 cm thick), present on top, composed of rhombic micrite and phytoliths (various states of preservation), some CS contain up to 45 cm thick ash layers (evidence for multiple burning events within one feature) **Postdeposition:** some altered by secondary phosphatization, reworked by humans, ash dumps	(Albert et al., 2000; Albert et al., 2012; Bar-Yosef et al., 1992; Berna and Goldberg, 2008; Goldberg, 2001; Goldberg and Bar-Yosef, 1998; Meignen et al., 1989; Meignen et al., 2000; Meignen et al., 2007; Schiegl et al., 1996)
Klisoura Cave, Greece	**General:** Open hearths consist of undisturbed sequences of superimposed thin white ash and grey and black charcoal-rich layers	(Karkanas et al., 2004)
Lakonis Cave, Greece	**General:** *in situ* or reworked hearths, rich in ashes, charcoal, and burnt bones, these accumulations have overprinted any natural sedimentation, superimposed hearth complexes, gray, thin white and brownish layer (1 cm each) alternate, undisturbed nature **WL:** Charcoal fragments and burnt bones embedded in partly recrystallized wood ashes	(Elefanti P. et al., 2008; Karkanas, 2002)
Nesher Ramla (open-air), Israel	**General:** anthropogenic combustion activity (thin ash accumulations and black sediments) located in a calcitic-clay matrix with quartz grains, interpreted as *in situ* hearth **BL:** 20% abundance of burnt bones, abundant charcoal, occasional well-preserved charred plant tissues, ash pseudomorphs, burnt flint **WL:** pure ash, ash pseudomorphs **Postdeposition:** one case of an ash dump of 20 cm thickness associated with hearth rake-out	(Friesem et al., 2014a)

Site	Hearth description	References
Misliya Cave, Israel	**General:** well-preserved hearths (unit III), blackened and calcined bones, variability in function and location of hearths, WL-BL-RL succession **RL:** burnt clayey terra rossa **BL:** black lenses of mainly charred grass tissues **WL:** grey lenses composed of micritic and sparitic calcite, calcium oxalate crystals pseudomorphs, cemented, also contains ash pseudomorphs, charred vegetal matter, carbonized and calcined bones, heated clay aggregates **Postdeposition:** rapid burial, partial dissolution, and reprecipitation of calcitic wood ash	(Weinstein-Evron et al., 2012)
Pech de l'Azé IV (cave), France	**General:** most frequent combustion features in basal layer 8, distributed along former dripline, repeated burning events in the same spot, discrete, individual lenses of ash, charcoal/organic matter and burned bone, intact features not reworked, domestic fire features lying in dark brown organic-rich sandy deposits, some erosional contacts between hearths, frequent charred bone fragments, rare calcined bone fragments, and charcoal, charred elements contributing to dark color of layer 8 **WL:** intact layers locally present, wood as fuel but also addition of bone **Postdeposition:** trampling and rake out of hearths, displacement of ashes and sediment, redistribution of combustion material as preparation for next fire	(Dibble et al., 2009; Goldberg et al., 2012; Goldberg and Berna, 2010; Turq et al., 2011)
Qafzeh (cave), Israel	**General:** numerous intact and diffuse combustion zones in exterior talus, within bedded silty calcareous rubble, cm thick hearths interbedded with sequence of inclined fine éboulis and silt **WL:** coarse-grained gray ashes mixed with sand-sized charcoal and stones, burned bone, and terra rossa aggregates	(Berna and Goldberg, 2008)
Roc de Marsal (cave), France	**General:** rubified sediment in layers 10 and 11, hearths in earliest layers (5,7,9) discrete, isolated charcoal and ash units, burnt bone, lithics and rubified sediment, stacked hearths, repeated construction in same location, 50-100 cm in diameter, spatial distribution across area especially inside of dripline and 2-3 m inside the cave mouth **RL:** rubified layer at the base **BL:** organic-rich lens **WL:** some 2 cm thick lenses of ashes, some lack ashes, some composed of small <2cm burned bone **Postdeposition:** trampling and local degree of diagenesis (calcite → dahllite)	(Aldeias et al., 2012; Goldberg et al., 2012)
Üçağızlı II Cave, Turkey	**General: anthropogenic combustion features,** wood ashes more abundant than charcoal, indicative of complete combustion in well-ventilated environment, presence of bone, rare charcoal, pseudocarbonized wood structures (state between wood and ash), wood ash and chert fragments, thin units of alternating ash and charcoal, more charcoal in lower layers (variability?) **WL:** Thick layers of ash, bone accidentally or intentionally burnt, located within 2-3 cm of intact ash layers, ashes most abundant fine component, unaltered composed of calcium carbonate, rhombic to triangular morphologies, ashes frequently surrounding coarser materials and discrete, laminated, dens bands, preservation is variable **Postdeposition:** bioturbation by insects, rodents, and plants, secondary carbonate precipitation, decalcification, and cementation.	(Mentzer, 2011)
Vanguard Cave, Spain	**General:** intact combustion features atop a variety of burned substrates, ash layers or charcoal rich layers on top of rubified sediments, rubified sediments either sandy or silty, repeated use of same locality as fireplace, heating levels low (<550 °C, phosphate analysis) **RL:** reddish-brown guano deposit, rubification by heating, phosphatized remains of earlier ash layer, contains sand, fine charcoal, charred organic matter, burned bone, and ash crystals **WL:** barely disturbed ash, 10-20 mm thick ash layer composed of micritic remains of wood ash **Postdeposition:** reuse of hearth features, thin burrows, excrements, weathering through exposure of combustion zone	(Macphail and Goldberg, 2000a)

Table 2: Summary of Middle Paleolithic intact combustion structures that underwent micromorphological examinations. The site, site type, and location are described in the first column. In the second column, combustion structures are described by dividing the description into general aspects of the feature (General), and then into the most common stratification of the combustion structure red(dish) layer (RL), black(ish) layer (BL), and white(ish) layer or ash layer (WL). The third column displays accompanying references.

Table 2 presents 19 sites with combustion features that were micromorphologically studied and confirmed to be *in situ*, intact combustion structures. Fifteen of those sites are cave sites, two are rockshelters, and two are open-air sites. eight of these 19 sites are located in Spain. The combustion structures are most commonly composed of a BL-WL transition. In a few instances, a RL is underlying the BL. The most common components detected in BL and WL are charred and calcined bone, charred organic components, charcoal, and wood ashes. The most common postdepositional agents altering the features, especially in cave sites, are decalcification and recrystallization of the ashes.

All combustion structures recovered in Middle Paleolithic sites should be studied by micromorphology, amongst other methods, to gain an understanding of context and insight in high-resolution. For adequate comparability, micromorphology aids in depicting the descriptions in a uniform and standardized manner throughout sites and combustion structures. Ideally, the comparison of different sites' combustion structures would be through an open-access database including thin section scans, microphotographs, and descriptions of combustion features from numerous sites.

So far, only a small percentage of sites containing combustion features have been examined micromorphologically. Likewise, not all combustion structures have been studied to the same extent and depth (see Table 2). This thesis will contribute to the small number of micromorphologically-studied combustion structures in the Middle Paleolithic and enrich the micromorphological record.

To conclude, the micromorphological studies, guidelines, and experiments are of great help to study combustion structures and to enrich the Middle Paleolithic record of well-documented combustion structures. The chapters and articles about the general approach for micromorphological fire analysis are crucial and helpful for a uniform description of assemblages of combustion features. Much remains to be investigated with experimental studies, but what has been explored to date has greatly increased our understanding of specific processes and circumstances. Moreover, the archaeological data finally provides insights into combustion structures from different Middle Paleolithic sites and regions, enabling inter-site comparisons of combustion features.

2.2.3 Sampling

Micromorphological samples can be collected in two ways, from the surface or an already existing profile. During the removal of the samples from the surface, parts of the sediment from an area of interest (combustion structure or control sediment) are left *in situ* while excavating, creating a block of undisturbed sediment. From the profile, an area of interest is delimited as well, and the sediment around that area is cut away using a knife.

Once either block is carved, the block is stabilized using plaster of Paris bandages on the exposed sides. After drying, the block can be extracted from the sediment using knives and chisels and by carefully separating them from the remaining sediment. The block is then wrapped in packaging tape before noting its orientation and direction and is then stored until shipment and sample preparation.

For the described case studies, 13 blocks from ten combustion structures and a block from control sediment were extracted for Case Study I, and three blocks from one combustion structure and one control block were extracted for Case Study II.

For experimental samples (Case Study III), two samples of moss were heated at 350 °C and 550 °C respectively in a rectangle-shaped aluminum container and left undisturbed until sample preparation.

2.2.4 Sample preparation

A majority of the samples were processed at the Archaeological Micromorphology and Biomarker Research Lab (AMBI Lab), Universidad de La Laguna, Tenerife, Spain. Samples were oven-dried at 60 °C for 48 hours before impregnating them using a 7:3:0.1 ratio of a mixture of polyester resin (Palatal strained resin UN1866, TNK composites), styrene (Styrene monomer (CAS: 100-42-5) UN2055, TNK composites), and a catalyzer (Methyl-ethyl-ketone (Luperox, CAS: 78-93-3), TNK composites). During the impregnation process, the air in the sediment's pores is replaced by the resin until the sediment is saturated with resin. After the hardening of the resin, the sedimentary matrix and components are immobilized and thus reflect the field's original undisturbed state. Hardened blocks were cut into slabs of 1 cm thickness using a Euro-Shatal M31100 radial saw, and selected slabs were glued onto 9 x 6 cm glass slides. These were trimmed to 1 mm thickness using a Uniprec ATA Brilliant-220 precision cutting machine and ground to 30 μm thickness using a G&N MPS-RC-Geology grinding machine.

Samples that were not processed in the AMBI Lab were either impregnated and cut into slabs using the methods mentioned above and shipped to Spectrum Petrographics Inc. (Vancouver, WA, USA) to produce 51 mm x 76 mm thin sections, or extracted blocks were entirely processed by Thomas Beckmann (Schwülper-Lagesbüttel, Germany) into 9 cm x 6 cm thin sections.

2.2.5 Analysis

Thin sections were observed and analyzed using a Nikon Eclipse E200 polarizing microscope with magnifications ranging between 20 and 100. Thin section descriptions were done following the guidelines of Stoops (2003) and Nicosia and Stoops (2017).

2.2.6 Microfacies approach

To facilitate the interpretation and understanding of micromorphological features, the microfacies approach was applied to all archaeological micromorphological samples (Courty, 2001). The concept of microfacies applied to archaeological soil micromorphology was adapted from the field of geology. There, facies defined as stratigraphic units distinguished by lithological, structural, and organic aspects are detected in the field (Boggs, 2006). Within the field of micromorphology, microfacies, or smaller-scaled facies, are identified on polished blocks or thin sections on the microscale (Courty, 2001; Flügel, 1982).

A microfacies approach is reasonable when dealing with a numerous and diverse set of deposits. These deposits that can be isolated into individual discrete stratigraphic units and distinguished by their microscopic characteristics are called microfacies units (MFU). Consequently, these MFU's can be classified into groups with identical characteristics (microstructures, porosities, components), forming microfacies types (MFT). This standardizes the analysis of the deposits themselves and helps the micromorphologist to observe patterns, thus facilitating the understanding and the interpretation of the sample set, especially regarding depositional and post-depositional processes (Courty, 2001).

Despite being a young concept used in archaeological micromorphology (Courty, 2001), it has been applied successfully in several archaeological sites and settings: Most prominently, it has been used at cave and rockshelter sites ranging from the Paleolithic to the Neolithic (Angelucci, 2003; Arriolabengoa et al., 2018; Arteaga et al., 2000; Égüez et al., 2016; Goldberg et al., 2009b; Karkanas, 2010; Karkanas et al., 2015; Karkanas and Goldberg, 2010b; Leierer et al., 2019; Patania et al., 2019; Rellini et al., 2020; Schiegl and Conard, 2006; Vannieuwenhuyse, 2017; Vannieuwenhuyse et al., 2017; Ward et al., 2017). Additionally, also shell middens (Villagran et al., 2009; Villagran et al., 2011b; Villagran, 2019), open-air sites (Karkanas et al., 2011; Macphail and McAvoy, 2008; Mallol, 2006) sites in urban settings (Karkanas and van de Moortel, 2014; Lisá et al., 2013; Macphail et al., 2007; Matarazzo et al., 2010) and mounds (Suarez Villagran and Gianotti, 2013; Villagran et al., 2019) have been investigated micromorphologically using the microfacies approach. Likewise, experimental and ethnoarchaeological research have applied the microfacies approach in their micromorphological interpretation as well (Friesem et al., 2014b; Macphail et al., 2004; Miller and Sievers, 2012).

For these studies, the microfacies approach is reasonable to initially split the different depositional layers from within or outside the combustion structure and then subdivide these into specific MFT representing different characteristic elements of the combustion structure. Due to the limited number of samples, the experimentally burned mosses have not been considered for the microfacies approach.

2.3 Lipid biomarker analysis

The archaeology of lipid biomarkers involves identifying the origin of organic residues recovered in archaeological contexts, by comparing archaeological compounds to modern-day plants and animals (Evershed, 1993).

A biological marker or biomarker is a molecular fossil that originated from formerly living organisms (Peters et al., 2005). Biomarkers are organic substances that provide information on past human activity, acting like a "chemical fingerprint" that can be matched to present organisms (Evershed, 2008). Some structures are direct indicators of their origin, and some structures can be more broadly classified (Evershed, 2008).

Lipids are a broad class of molecules that are produced by living organisms (Evershed, 1993). They are mainly composed of carbon, hydrogen, and oxygen and form a wide array of structures (Evershed, 1993). Lipids have hydrophobic properties, which reduces their solubility in water (Evershed, 1993); nevertheless, other degradational processes of chemical or microbial origin can affect the lipids' structure (Evershed, 1993). Lipids include fats, oils, waxes, terpenes, and sterols (Christie and Han, 2010; Gunstone, 1996) originating from different sources of organisms (Evershed, 1993). Due to their hydrophobic qualities, lipids are great candidates as biomarkers in archaeological settings since the compounds stay *in situ* and are not affected by leaching through water (Evershed, 1993, 2008). Compared with other biomolecules, lipids are less susceptible to decay due to their low polarity (Evershed, 2008).

In archaeological contexts, the organic residue recovered usually consists of a mixture of compounds that have undergone postdepositional alterations (Evershed, 1993, 2008). Here, the use of gas chromatography (GC) and gas chromatography-mass spectrometry (GCMS) comes into place, allowing the separation of molecules by weight and nature. It is possible for altered compounds to trace back their original source in reference to their biochemical mechanisms and pathways (Evershed, 2008).

2.3.1 Significance

There has always been an interest in amorphous organic materials found at archaeological sites (Evershed, 1993). Nowadays, an increasing number of scientists are employing lipid biomarker analysis on archaeological material (Evershed, 2008).

This has been made possible by analytical techniques, which can achieve molecular-level resolution (Evershed, 2008). The invention of gas chromatography paved the way for these analytical techniques (James and Martin, 1952), and they have been performed on archaeological organic residues for the last five decades (Condamin et al., 1976; Evershed, 1993; Evershed et al., 1999; Marchbanks, 1989; Patrick et al., 1985).

Most lipid biomarker studies in archaeology have been conducted on residues absorbed in ceramic vessel walls (Evershed, 2008 and references therein). Analyses of absorbed residues in pottery stand out due to the residues' great preservation potential and the ability to know what was contained in the vessel in the past.

The lipid biomarker approach on archaeological sediments is applied to a lesser extent. Generally, lipid biomarker analysis on sediment is challenging due to less favorable preservation of lipids than ceramic objects (Evershed, 2008). Lipids have a better preservation potential in pottery since entrapment of lipids in organic or mineral matrices reduces the loss of biomolecules by diffusion and a reduction of microbial activity (Eglinton and Logan, 1991; Evershed et al., 1992). Nevertheless, preservation in sediment is possible depending on environmental conditions such as temperature, light, and moisture (Eglinton and Logan, 1991). For instance, waterlogging or extreme aridity are both favorable for lipid preservation, while constant fluctuations in environmental conditions are detrimental (Evershed, 2008).

There are only a few studies of lipid biomarkers applied on archaeological sediments so far, most of them focusing on fecal biomarkers in middens and soils (Birk et al., 2012; Bull et al., 1999; Prost et al., 2017; Shillito et al., 2013; Sistiaga et al., 2014).

Recently, lipid residues preserved in archeological fires have begun to move into focus, and different researchers have successfully extracted and analyzed lipid compounds from sedimentary contexts related to archaeological fire. The studies span a broad geographical and chronological range (Choy et al., 2016; Kedrowski et al., 2009; Leierer et al., 2019; Leierer et al., 2020; Lejay et al., 2016). Generally, lipid biomarkers are well preserved in selected Middle Paleolithic combustion structures (Mallol et al., 2019; March et al., 2017), in which preservation is limited to particular facies within the structure (March et al., 2017) (see upcoming Chapter 3 and 4). Lipid biomarker fire research in archaeology is still a young subdiscipline, and part of the initial work is dedicated to building experimental reference material and exploring preservation conditions and the thermal alteration process (Buonasera et al., 2019; Jambrina-Enríquez et al., 2018; Lejay et al., 2016; March et al., 2014). In studies of archaeological sediment, relevant findings include the identification of polycyclic aromatic hydrocarbons as a marker of anthropogenic fire (Brittingham et al., 2019) and of different stenols and stanols, both fecal biomarkers, that have been found in Neanderthal combustion structure sediment and both of which indicate that these hominids had a mixed meat and plant diet (Sistiaga et al., 2014). In another study, *n*-alkyl nitriles were found to be useful as thermal markers and to differentiate animal and plant origin among the charred components of combustion structures (Jambrina-Enríquez et al., 2019). The advent of sedimentary lipid biomarker studies in archaeology has also motivated work towards methodological advances. Recent studies have improved lipid residue quantification and calibration methods (Herrera-Herrera et al., 2020; Herrera-Herrera and Mallol, 2018) and have shown the potential of extracting sedimentary lipids directly from drill dust of micromorphological blocks, which provide a spatially and temporally accurate (contextualized) sample that may, in turn, be analyzed with visual reference to sedimentary components identified microscopically (Rodríguez de Vera et al., 2020).

2.3.2 Sampling

For sampling lipid biomarkers from archaeological contexts, bulk sediment samples need to be extracted. Samples were selected from points of interest while avoiding spots of bioturbation and modern contamination. Sterilized metal tools were used to scrape off the sediment's exposed surface to avoid modern contamination. Then, sterilized metal tools were used to collect approximately 7 g of sediment, which was placed in pre-fired aluminum foil and packed. Samples were stored at -20 °C until analysis at AMBI Lab.

Experimental samples of Weissia moss for Case Study III were scraped off a limestone boulder in the vicinity of the archaeological site, using sterilized metal tools and placed into pre-fired aluminum foil. This sample was also stored at -20 °C until further preparation. In the lab, the moss was dried for 48 hours at 60 °C and then subsampled into chunks of approximately 1g and placed in ceramic crucibles. The crucibles were covered with aluminum foil to replicate a limited O_2 supply. Experimental burnings were conducted using a Nabertherm B180 muffle furnace with a heating rate of ±26 °C/min (Kuo et al., 2008). Five burnings were conducted at 150, 250, 350, 450, and 550 °C for one hour, respectively. Between each burning event, the furnace was cleaned at 550 °C for 1 h. Samples were weighed before and after burning, to document weight loss.

Additionally, two experimental moss fires were conducted in the field, taking the same source material (Weissia moss) from the same sampling location. Mosses were placed on aluminum foil and were burnt without kindling using pine needles and twigs as tinder. Subsequently, the samples were stored at -20 °C and transported to the AMBI Lab, where they were subsampled.

2.3.3 Lipid extraction, analysis, and quantification

To prepare archaeological samples for lipid extraction, they were oven-dried at 60 °C for 48 h using a Nabertherm P330 oven (Gamarra and Kahmen, 2015). Archaeological and experimental samples were then homogenized using an agate mortar and pestle. Samples were subsampled to either 5 g or 7 g for archaeological samples or between 0.9 g and 0.5 g for burnt experimental samples.

To obtain the total lipid extract (TLE), the sediment or burnt moss was mixed with dichloromethane/methanol (DCM/MeOH) 9:1 v/v using 8 mL of that solution per gram of sample. This was done for three cycles of 30 minutes in a sonicator bath (<30 °C) and subsequent centrifugation (10 min at 4700 rpm) followed by filtering through annealed glass wool (Jambrina-Enríquez et al., 2018; Leierer et al., 2019). The TLE was then evaporated using N_2 at 40 °C and reconstituted with DCM.

The TLE was then separated into six fractions according to their polarity using solid-phase extraction (SPE) on a silica gel column (1 g silica 70-230 mesh, 0.1 g sand 50-70 mesh, both previously fired at 450 °C during 10 h). They were eluted utilizing different solvents for each polarity and fraction (see Table 3). The different fractions were evaporated with N_2 at 30 °C and stored until measurement at -20 °C. Before measurement, the internal standard (IS, 8mg/L) was added, and the sample was reconstituted with solvent (Table 3). For samples from Case Study II, only *n*-alkanes were measured.

Fraction No.	Fraction	Elution	Internal standard	Reconstitution volume
1	*n*-alkane	3/8 dead volume (DV), n-hexane	5α-androstane	150 μL of DCM
2	Aromatics	2 DV, 8:2 v/v n-hexane/DCM	5α-androstane	50 μL of DCM
3	Ketones	2 DV, DCM	5α-androstan-3-ol	50 μL of DCM
4	Alcohols	2 DV of 1:1 v/v DCM:Ethyl acetate (EtOAc)	5α-androstan-3-ol	40 μL of DCM + 10 μL EtOAc
5	Acids and diols	2 DV EtOAc	Methyl C19:0	40 μL of DCM + 10 μL EtOAc
6	Other compounds	2 DV MeOH	Methyl C19:0	40 μL of DCM + 10 μL EtOAc

Table 3: Summary of lipid fractionation procedure and reconstitution for chromatographic analysis. DV≈ 1300 μL

The alcohol fraction was prepared by transforming alcohols into trimethylsilyl (TMS) esters. This was done by adding 100 μL of N,O-Bis(trimethylsilyl)trifluoroacetamide (BSTFA) + trimethylchlorosilane (TCMS) 99:1 v/v and 100 μL of pyridine to the extract, derivatizing at 80 °C for 1 hour, drying and reconstituting with 10 μL Ethyl Acetate (EtOAc) and 40 μL DCM.

Fatty acids were derivatized to methyl esters by adding 5 mL of MeOH, 400 μL of H_2SO_4 to the extract, and heating them at 70 °C for 240 min. They were then neutralized with a saturated sodium bicarbonate solution, extracted three times with 3 mL hexane, dried under nitrogen, and reconstituted with 40 μL DCM + 10 μL EtOAc.

Each sample and its fractions were analyzed using gas chromatography (GC) with a coupled mass-selective detector (GC-Agilent 7890B, MSD Agilent 5977A) and equipped with an HP-5ms capillary column ((5% phenyl)-methylpolysiloxane, length: 30 m, ID: 250 μm, film thickness 0.25 μm; Agilent Technologies). The GC was programmed to an initial temperature of 70 °C (held 2 min), then heated at a heating rate of 12 °C/min to 140 °C and to a final temperature of 320 °C at a heating rate of 3 °C/min (held 15 min) with helium as carrier gas (flow of 2 mL/min). The multimode injector (MMI) was held at a split ratio of 5:1 at an initial temperature of 70 °C for 0.85 min and heated to 300 °C at a programmed rate of 720 °C/min. The MS was used under the following conditions: transfer line, ion source, and quadrupole were set at 280 °C, 230 °C, and 150 °C respectively, electron ionization energy level was -70 eV, and the analyzer was operated in full scan mode (m/z 40-580).

Compounds were identified by comparing their retention times and mass spectra with those of reference compounds (mix *n*-alkanes n-C8 – n-C40, 500 mg/L in DCM; 37 component FAME mix C4–C24, concentration in DCM varied from 200 to 600 mg/L; and fatty acids C26:0, C28:0, and C30:0) and the NIST mass spectra library.

n-Alkanes were quantified using matrix-matched calibration curves (Herrera-Herrera and Mallol, 2018) by plotting the Area/AreaIS ratio against the concentration of the reference compounds that were dissolved in the matrix and extracted with the previously described procedure. For doing this, the four most intense fragment ions in the mass spectra were used (*n*-Alkanes: m/z 43, 57, 71, and 85; IS: m/z 67, 95, 81, and 245). Correlation coefficients for calibration curves were higher than 0.9904.

Concentrations of *n*-alkanes were plotted and interpreted in µg per gram of dry sediment (µg/gds) with their correspondent confidence intervals. In the instance of Case Study I, the Carbon Preference Index (CPI) was calculated. This is the ratio of the quantity of odd *n*-alkanes against the quantity of even *n*-alkanes and helps to evaluate the distribution of *n*-alkanes (Marzi et al., 1993). Originally the CPI was and is used to identify the biological origin of plants (Bush and McInerney, 2013; Cranwell et al., 1987; Eglinton and Hamilton, 1967), the degree of diagenesis (Diefendorf et al., 2011; Zech et al., 2011) or the paleoclimate (Ortiz et al., 2010; Xie et al., 2004) but recently it has also been used as a measure of heat alteration (Almendros and González-Vila, 2012; Jambrina-Enríquez et al., 2018; Kuhn et al., 2010). Larger CPI values hereby indicate a greater preference for odd chain lengths and a better preservation/lower burning alteration. For the calculation of the CPI, the revised formula by Marzi et al. (1993) was used:

$$CPI=\frac{([C23]+[C25]+[C27]+[C29]+[C31]+[C33]+[C35])+([C25]+[C27]+[C29]+[C31]+[C33]+[C35]+[C37])}{2\times([C24]+[C26]+[C28]+[C30]+[C32]+[C34]+[C36])}$$

Quantities measured for each *n*-alkane chain length have been inferred from the peak area of the unquantified sample to match previous publication standards (Herrera-Herrera et al., 2020).

2.3.4 Pyrolysis

Pyrolysis was carried out for selected samples of Case Study I, using a CDS Pyroprobe 500 (CDS Analytical, Oxford, PA) coupled to the Agilent GC-MS through and a split/splitless injector (AMBI Lab, La Laguna, Spain). Quartz tubes with a quartz filler rod were filled with samples ranging from a weight of 9 mg to 13.8 mg and sealed with a hand-made plug of quartz wool. The prepared tube was then introduced into the coil of the resistively heated Pt filament. The pyrolizer was initially set at 300 °C for 1 s, then the temperature was increased to 700 °C at a rate of 20 °C/ms and held for 15 s. The transfer line was maintained at 300 °C. The GC separation and MS conditions were set at the same state as the previously used one to analyze liquid fractions.

2.3.5 Compound-specific carbon isotope analysis (CSIA) of *n*-alkanes

n-Alkanes of Case Study I were subjected to compound-specific carbon isotope (CSIA) measurements. Measurements were conducted using a Thermo Scientific Isotope Ratio Mass Spectrometer Delta V Advantage coupled to a GC Trace 1310 through a Conflo IV interface with a temperature converter GC Isolink II (AMBI Lab, La Laguna, Spain). The injection of the samples was accomplished using a Programmed Temperature Vaporising (PTV) injector (splitless mode) with an evaporation step with the temperature increasing from 60 °C to 79 °C (held 30 s, rate 10 °C/min), a transfer stage increasing to 325 °C (held 3 min, rate 10 °C/s) and a cleaning temperature increased to 350 °C (held 3 min, rate 14 °C/s). A Trace Gold 5-MS (Thermo Scientific) fused silica capillary column was fitted to the GC (30 m x 0.25 mm, 0.25 µm film thickness). The carrier gas was helium at a flow rate set of 1.5 mL/min, and the oven was programmed as follows: from 70 °C (held 2 min) to 140 °C at 12 °C/min, from 140 °C to 320 °C (held 15 min) at 3 °C/min. The combustion reactor temperature was maintained at 1000 °C.

Measurements were repeated three times per sample, while data was acquired and processed using Isodat 3.0 (Thermo Scientific). An *n*-alkane Schimmelmann type A6 mixture (n-C16 to n-C30) was used to normalize the $\delta^{13}C$ values to the Vienna Pee Dee Belemnite (VPDB) scale. The standard deviation of the measurements was smaller than 0.50 ‰.

2.4 TC, TIC, and TOC

Total organic carbon measurements are a standard procedure coupled to lipid biomarker analysis to understand the amount of lipid biomarkers present in the sediment compared with other organic compounds.

Bulk samples were sent away to get them tested for their total carbon (TC), total inorganic carbon (TIC), and total organic carbon (TOC) content. The analysis was done using a LECO SC 144DR furnace at Instituto Prentice de Ecología (IPE-CSIC), Spain.

2.5 Experimental heating of El Salt stratigraphic unit XI sediment

This heating experiment is related to Case Study II, where the rubification process that led to a RL in a substrate such as that of El Salt, was investigated. A series of controlled lab burnings were conducted using presumably unburned sediment from stratigraphic unit XI. For each heating event, approximately 0.8 g of sediment was placed into a ceramic crucible and heated in a muffle furnace (Nabertherm B180). Heating intervals were between 100 °C and 800 °C in steps of 100 °C in oxic conditions. The furnace's heating rate was ±26 °C/min (Kuo et al., 2008), and the designated temperature was kept constant for 1 h. After 1 h, the crucibles were extracted and cooled down to room temperature.

Case Study I

Insights into the timing, intensity, and natural setting of Neanderthal occupation from the geoarchaeological study of combustion structures: A micromorphological and biomarker investigation of El Salt, unit Xb, Alcoy, Spain.

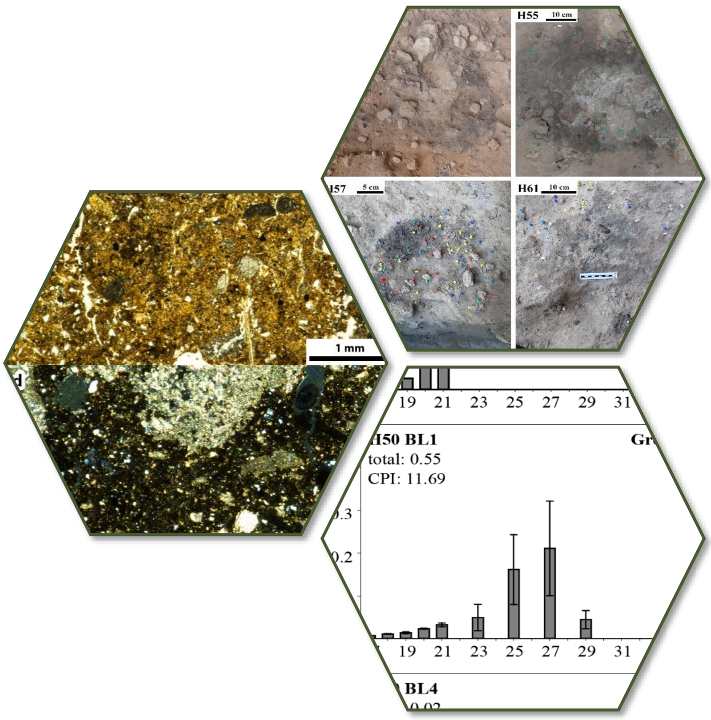

3. Case Study I: Study of a combustion structure assemblage

Insights into the timing, intensity, and natural setting of Neanderthal occupation from the geoarchaeological study of combustion structures: A micromorphological and biomarker investigation of El Salt, unit Xb, Alcoy, Spain

Lucia Leierer[1,2,*], Margarita Jambrina-Enríquez[1], Antonio V. Herrera-Herrera[1], Rory Connolly[1,2], Cristo M. Hernández[2], Bertila Galván[2], Carolina Mallol[1,2] https://doi.org/10.1371/journal.pone.0214955

[1] Instituto Universitario de Biorgánica Antonio González, Universidad de La Laguna, La Laguna, Santa Cruz de Tenerife, Spain
[2] Departamento de Geografía e Historia. Área de Prehistoria (Facultad de Humanidades), Universidad de La Laguna, Campus de Guajara, La Laguna, Santa Cruz de Tenerife, Spain
* Corresponding author: Lucia Leierer

ABSTRACT:

Middle Paleolithic lithic and faunal assemblages throughout Eurasia reflect short-term Neanderthal occupations, which suggest high group mobility. However, the timing of these short-term occupations, a key factor to assess group mobility and territorial range, remains unresolved. Anthropogenic combustion structures are prominent in the Middle Paleolithic record and conceal information on the timing and intensity, and natural setting of their associated human occupations. This paper examines a concentration of eleven combustion structures from unit Xb of El Salt, a Middle Paleolithic site in Spain, through a geoarchaeological approach, in search of temporal, human impact, and paleoenvironmental indicators to assess the timing, intensity, and natural setting of the associated human occupations. The study was conducted using micromorphology, lipid biomarker analysis, and compound-specific isotope analysis. Results show *in situ* hearths built on different diachronic topsoils rich in herbivore excrements and angiosperm plant residues with rare anthropogenic remains. These data are suggestive of low impact, short-term human occupations separated by relatively long periods of time, with possible indicators of seasonality. Results also show an absence of conifer biomarkers in the mentioned topsoils and the presence of conifer charcoal among the fuel residues (ash), indicating that firewood was brought to the site from elsewhere. A microscopic and molecular approach in the study of combustion structures allows us to narrow down the timescale of archaeological analysis and contributes valuable information towards an understanding of Neanderthal group mobility and settlement patterns.

3.1 Case Study I: Introduction

What is the approximate amount of time that Neanderthal groups occupied any given place in the landscape? How much time passed before they returned to that same place? These questions are key to understand Neanderthal group mobility and settlement patterns.

So far, these questions have not been properly answered using the current proxies applied in Middle Paleolithic archaeology.

Some proxies are especially helpful for distinguishing broadly between long-term and short-term occupations. Cleaning behaviors and maintenance activities can point to long-term occupations (Binford, 2002; Spagnolo et al., 2018; Stevenson, 1991; Vaquero, 2012; Vaquero et al., 2015) as evidenced by raked-out hearths (Goldberg, 2003; Kuhn et al., 2009; Meignen et al., 2007; Schiegl et al., 2003) or thick ash deposits indicative of recurrent refueling (Mallol et al., 2007; Meignen et al., 2008; Wattez, 1992). The origin of lithic raw material might help in differentiating long-term occupation (raw material acquisition nearby the site) from short-term occupations (raw material acquisition from farther away as reflective of high group mobility) (Richter, 2006; Vaquero, 2012). Additionally, occupation length estimates can be made on the basis of material assemblage accumulation density (Conard and Prindiville, 2000; Lourdeau, 2011). Also, carnivore activity on the faunal assemblages might indicate short term occupations since leftover bones would still be fresh and more appealing to carnivores (Vaquero, 2012; Yellen, 1991). Another method that has been used to frame the timing of human occupations in an archaeological context is dental wear analysis, which looks at seasonal markers in anthropogenic tooth remains to identify the season in which the animal has died. A stratigraphic unit with several teeth representing the same season commonly implies different, diachronic short-term seasonal occupations (Rivals et al., 2009a; Sánchez-Hernández et al., 2014).

So far, based on a combination of the above-mentioned proxies, the Middle Paleolithic archaeological record throughout Europe and the Near East reflects short-term human occupations (Cep and Waiblinger, 2001; Conard and Prindiville, 2000; Galván et al., 2014a; Hovers, 2001; Lourdeau, 2011; Machado et al., 2013; Machado et al., 2016; Machado and Pérez, 2015; Marks and Chabai, 2001; Moncel et al., 2011; Mora et al., 2004; Rivals et al., 2009a; Roebroeks and Tuffreau, 1999; Rosell et al., 2015; Straus, 1982; Vallverdú et al., 2005a; Villaverde et al., 1996; Wallace and Shea, 2006).

Still, the timing of Neanderthal short-term occupations remains unresolved. A key to address this issue is isolating single occupation episodes. Most proxies of occupation duration are based on the analysis of remains recovered from archaeological palimpsest deposits (Bailey, 2007; Carrancho et al., 2016; Henry, 2012; Lucas, 2005; Vaquero and Pastó, 2001) representing several occupation episodes. Dissecting Middle Paleolithic palimpsest deposits into single occupation episodes is not only essential to approach human behavior and change (Machado et al., 2013; Mallol and Hernández, 2016; Sullivan, 1992), but is also a prerequisite to assess the time between human occupations. In Paleolithic contexts, archaeological palimpsests can be dissected through lithic raw material units, faunal and lithic refits, archaeostratigraphy or tooth microwear analysis (Bargalló et al., 2016; Chacón et al., 2015; Machado et al., 2013; Machado et al., 2015; Machado and Pérez, 2015; Rivals et al., 2009a; Sañudo et al., 2016; Spagnolo et al., 2016; Vaquero et al., 2015). High-resolution geoarchaeological techniques have also shown to help approach single human occupation episodes (Cabanes et al., 2010; Carrancho et al., 2016; Mallol et al., 2013a; Miller et al., 2013; Polo-Díaz et al., 2016).

A very powerful source for palimpsest dissection and for studying isolated occupations are combustion structures. Hearths have been considered as a central element around which human activities take place (Binford, 1978; Binford, 1998; Fisher and Strickland, 1991; Jones, 1993; O'Connell, 1987; Yellen, 1977), and according to ethnoarchaeological research, most activities are carried out around hearths in household areas (Fisher and Strickland, 1991; Jones, 1993; O'Connell et al., 1991; O'Connell, 1987; Yellen, 1977). Thus combustion structures are considered as basic elements of a single occupation episode (Henry, 2012; Machado et al., 2013; Vallverdú et al., 2005b; Vaquero and Pastó, 2001), and consequently, they can aid in discerning a minimal number of occupation episodes (Vaquero and Pastó, 2001).

In the Middle Paleolithic, fire residues are present in the majority of sites (Roebroeks and Villa, 2011) and often comprise well-preserved combustion structures with distinct perimeters and internal stratigraphy. Crucially, such good preservation states could be indicative of short-term occupation or low occupation intensity, as continuous presence of humans at a site might result in obliterated raked-out hearths (Goldberg, 2003; Kuhn et al., 2009; Meignen et al., 2007; Schiegl et al., 2003). Very few Middle Paleolithic combustion structures with thick ash layers have been documented (Goldberg, 2003; Meignen et al., 2007). Most sites have yielded combustion structures with thin (less than 2 cm-thick) ash layers (Roebroeks and Villa, 2011), suggesting a prevalence of short-lived fires, in opposition to refueled fires used over weeks and months, which have been shown to result in thick ash deposits (Mallol et al., 2007; Meignen et al., 2008; Wattez, 1992).

According to published descriptions of Middle Paleolithic combustion structures (Martínez-Moreno et al., 2004; Vallverdú Poch et al., 2012; Vaquero and Pastó, 2001; Zieba et al., 2008), their macroscopic appearance generally conforms with the structure of simple, flat, circular, multi-layered structures exhibiting a succession of a reddish or brownish layer at the base (here onwards Red Layer or RL), overlain by a dark brown to black layer (BL) and capped by a gray to whiteish layer (WL) (Mallol and Henry, 2017). Previous studies have hypothesized that the WL contains combustion-related residues, while the BL and RL are the combustion substrate representing burned topsoil beneath the fire (Machado et al., 2015; Mallol et al., 2013a; Mallol et al., 2017). If we consider the ephemeral archaeological fingerprint of short-term human occupations, Middle Paleolithic BL and RL deposits are unlikely to yield behavioral evidence. Instead, they hold the potential to provide paleoenvironmental information because they contain residues of the natural vegetation cover prior to the occupation and the combustion event. On the other hand, any behavioral evidence associated with Neanderthal short-lived fires should be found in Middle Paleolithic WL deposits, which may conceal clues on Neanderthal behavior.

At present, although the Middle Paleolithic fire record has been widely investigated (Allué et al., 2012; Cabanes et al., 2010; Courty et al., 2012; Heyes et al., 2016; Koller et al., 2001; Pastó et al., 2000; Picornell-Gelabert et al., 2017; Sandgathe, 2017; Théry-Parisot, 2002b; Vidal-Matutano, 2016; Vidal-Matutano et al., 2017; Vidal-Matutano et al., 2018; Yravedra and Uzquiano, 2013), it has not been sufficiently studied from a geoarchaeological perspective as to characterize the formation and post-depositional modification of individual combustion structures. This shortcoming hampers our assessment of Neanderthal occupations based on the combustion structure record as introduced in the previous paragraphs. First, identification of short-lived hearths is not possible with the naked eye because relighting, rake-out and distinguishing between single and multiple burning events requires microscopic examination (Mallol et al., 2017). Second, there are a plethora of natural taphonomic factors that may modify the macroscopic appearance of combustion structures (Mallol et al., 2017). Third, the nature of WL and BL deposits lies in their components, which are often only sedimentary and identifiable at microscopic and molecular scales. Altogether, in-depth microstratigraphic investigations of Middle Paleolithic combustion structures have the potential to provide information on Neanderthal behavior and environmental contexts and at the same time indicate isolated occupation episodes, which might help to decipher the timing of short-term occupations.

To pursue such investigation, we selected stratigraphic unit X from the Middle Paleolithic site of El Salt in Spain. El Salt has yielded numerous flat combustion structures. In the field, these showed apparently good preservation states, with distinct outlines and internal stratigraphy. In certain areas, and especially in stratigraphic unit X, these combustion structures are partially overlapping or superimposed. In this context, a dense archaeological palimpsest involving multiple combustion structures reflect either many successive short-term occupations with isolated combustion structures (Lourdeau, 2011; Machado et al., 2013; Rivals et al., 2009a; Sánchez-Hernández et al., 2014; Vallverdú et al., 2005b; Vaquero, 2008) or fewer, longer occupations with multiple synchronous hearths (Rivals et al., 2009b; Thiébaut et al., 2009; Vaquero et al., 2012).

Galván (2014a) proposed that SU X (35 cm thick, dated to 52.3 ± 4.6 kA (Galván et al., 2014b)) possibly represents recurrent, brief, low impact Neanderthal occupations, based on an integrated archaeostratigraphic study of lithic refits, raw material procurement, knapping activity and the number of single discarded flint artifacts, the minimal number of individuals obtained from zooarchaeological analyses and the number of combustion structures (Machado et al., 2016; Machado and Pérez, 2015).

In this paper, we present the results of a geoarchaeological study coupling micromorphology and lipid biomarker analysis of a combustion structure assemblage from El Salt SU Xb to explore how these combustion structures formed. Archaeological soil micromorphology is the microscopic study of *in situ* preserved archaeological sediment, which can aid in the characterization of depositional and postdepositional processes. Lipid biomarker analysis is the study of lipid molecular compounds that can be traced to a particular biological origin. Both methods combined will be used here to assess if the human occupations associated with the combustion structures were low impact and short-termed, as previously formulated, and to provide an estimate of the time period between occupations. Given the common presence of distinct BLs deposits among the SU Xb combustion structures and the fact that organic matter preservation potential in charred contexts is quite high (Braadbaart and Poole, 2008; Mallol et al., 2013a; Weiner, 2010), we expect to obtain significant information through the systematic microstratigraphic analysis of these combustion structure assemblages.

3.2 Case Study I: Materials

This Case Study encompasses a selection of 11 combustion structures from the stratigraphic unit Xb (Fig. 2). Combustion structures were chosen according to their availability of micromorphological and biomarker samples, respectively. Combustion structure H61 only yielded bulk sediment samples for biomarker analysis. Samples were extracted, analyzed, and studied according to the standard procedure described above.

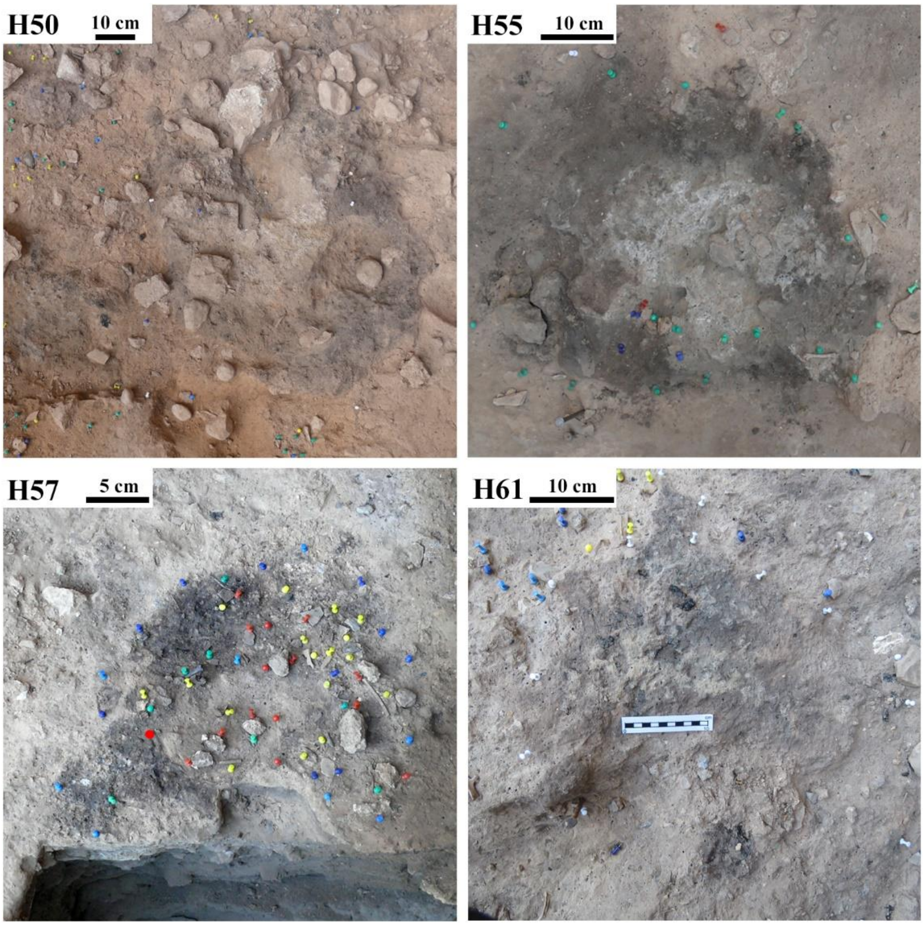

Fig. 2: Field photos of selected combustion structures from the combustion structure assemblage.

This assemblage of combustion structures was visually divided into two clusters. One cluster is closer to the site's travertine wall (H44b, H45, H57, and H61) entitled the "inner" cluster and one "outer" cluster positioned slightly farther away from the back wall (H46, H52, H53a, H53b, and H50) (see Fig. 3).

This categorization is based on a difference in sedimentary composition observed in the field. Generally, both areas consist of brownish yellow, massive, unsorted, gravelly-silty sand with abundant tufa and travertine fragments. However, the sediment of the "outer" area is more compact and contains fewer archaeological remains (flint flakes and bone fragments), while the sediment of the "inner" area is looser and more stratified. Four out of the 11 selected combustion structures display a clear white layer (WL) in the field. All other combustion structures only include a BL-RL succession (see Fig. 3). Nevertheless, all combustion structures comprise circular perimeters and contain burnt bone; thus, they are most likely to represent combustion structures. Other components present in the combustion features are flint flakes, charcoal as well as burnt limestone, and travertine clasts.

Micromorphological samples (n=12) contain the RL-BL(-WL) succession of the combustion structure as well as over- or underlying sediment from stratigraphic unit Xb (here onwards Xb), which appears unaffected by fire processes (see Appendix 1 and 2). Additionally, a micromorphology block (n=1) taken from a farther distance away from the combustion structures serves as a control sample. Biomarker samples (n=27) are taken from mostly the BL's (n=14) of the combustion structures, but also RL (n=3) and WL (n=5) samples are available, as well as control samples of the presumably unburned stratigraphic unit Xb (n=5).

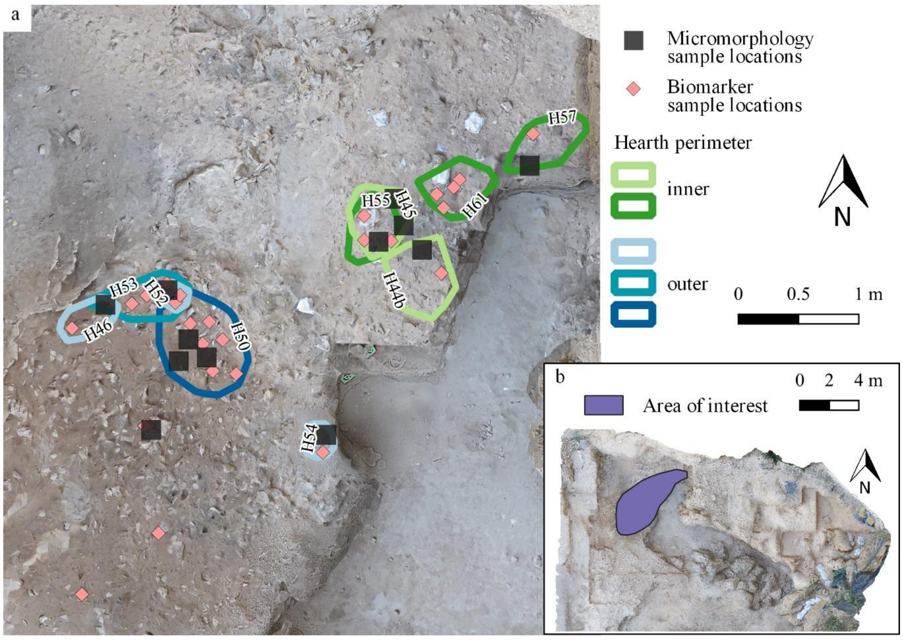

Fig. 3: Combustion structures of unit Xb—El Salt. a) Georeferenced orthophotograph extracted from 3D photogrammetric model of the site created in the 2017 field season showing the combustion structures selected for this study (georeferenced BL perimeters) and associated micromorphology and biomarker samples. b) Georeferenced orthophotograph (same as in a) of the whole site, with indicated location of the area of interest for this study.

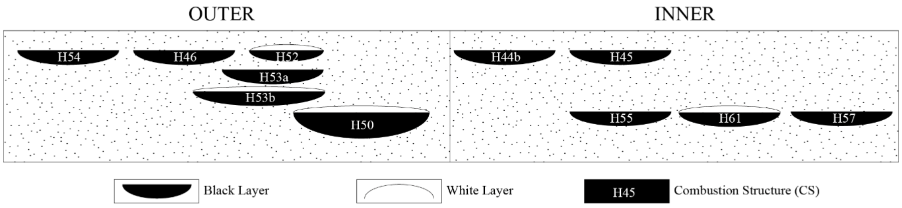

	CS	WL *	BL *	RL	Comments	Bioturbation	Truncation
INNER	H44b		2.5	x	Lower BL of two, separated by ashy sediment		
	H45		2.5				
	H55		4				
	H57		1.5		BL forms a ring structure around an unburned inner zone		
	H61	0.2	< 0.5		Outer limits eroded		
OUTER	H46		1			x (burrow)	
	H50	1	~ 4	x	Cobble-sized imprints with ashy sediment in BL, BL bowl shaped, dark and greasy		
	H52	0.4	0.5				x
	H53a		1				x
	H53b	0.2	2-5				
	H54		1		BL diameter 15 cm		x

Fig. 4: Schematic drawing showing the stratigraphic position of the selected combustion structures. Combustion structures as observed in the field with facies thickness in cm (*).

3.3 Case Study I: Results

3.3.1 Micromorphology

3.3.1.1 Lithology, main components, porosity, microstructure, and postdepositional features

All micromorphological samples share a common lithological composition – representing the sediment of stratigraphic unit Xb, which is dominated by sand-sized limestone fragments with quartz grain inclusions, sand-sized detritic travertine and tufa fragments, and fine sand-sized quartz crystals. These detritic mineral components are most abundant in the control and Xb samples and few or rare in the BLs, where organic components make up the bulk of the sedimentary mass. Travertine and tufa grains show signs of burning in BL and WL, brown or gray zones in plane-polarized light (PPL), and recrystallized zones in crossed polarized light (XPL) (Fig. 5m and n).

Anthropogenic and biogenic components are charcoal (Canti, 2017), few fat-derived char fragments (Fig. 5i) (Mallol et al., 2017), common bone (Villagran et al., 2017) and teeth (Villagran et al., 2017), massive coprolites (Fig. 5g and h) (Brönnimann et al., 2017b), fibrous coprolites (Fig. 5j and k) (Brönnimann et al., 2017a) and *Celtis australis* seed coats (Fig. 5o) (Mallol et al., 2013a) with variations in the degree of burning depending on the facies. Plant residues appear browned or blackened (Fig. 5f and l). A description of these components is presented in Table 4, further describing their abundance and representation in combustion structures and facies.

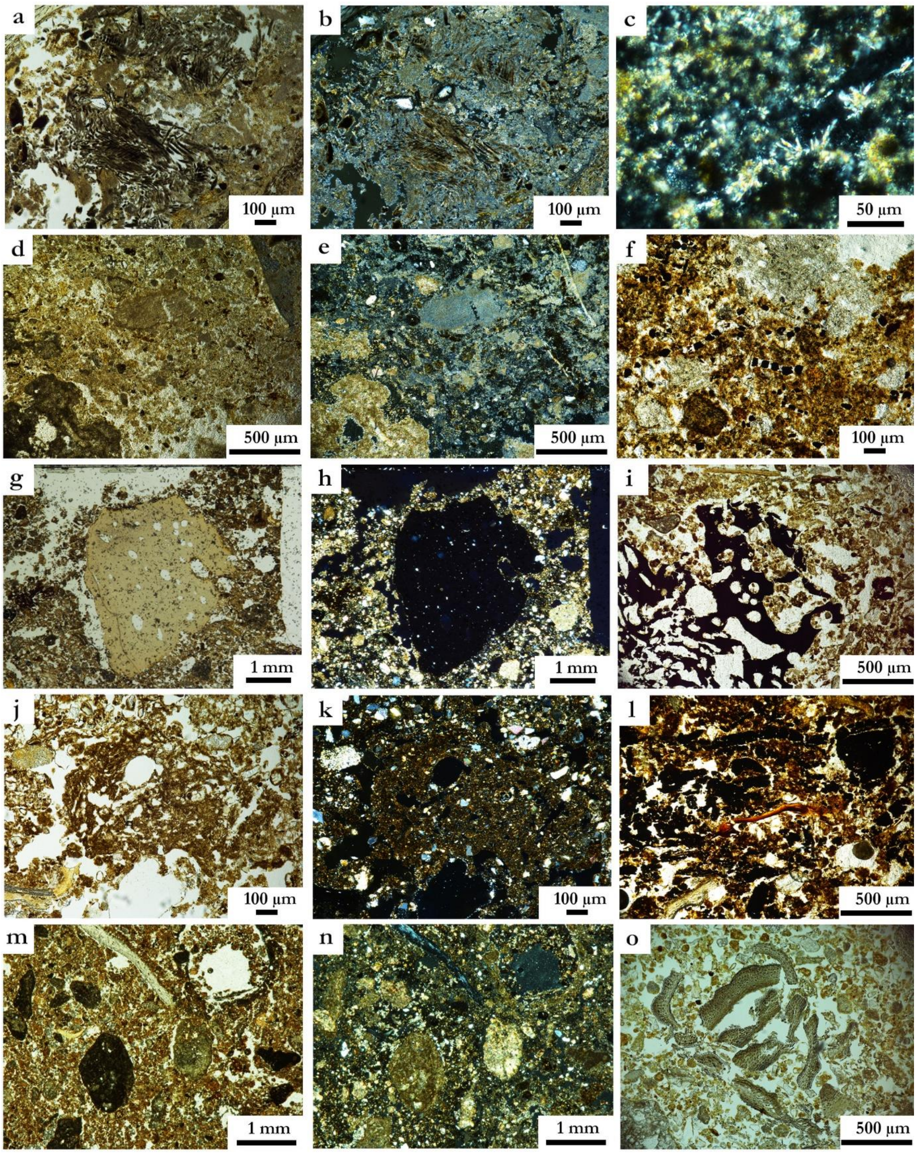

Fig. 5: Components identified in the micromorphological samples. a) wood ash (PPL), b) wood ash (XPL), c) needle fiber calcite (XPL), d) ashes (PPL), ashes (XPL), f) unidentified square black particles (PPL), g) burnt bone (PPL), h) burnt bone (XPL), i) animal fat-derived char (PPL), j) fibrous coprolite (PPL), k) fibrous coprolite (XPL), l) blackened plant particles (PPL), m) burned tufa (PPL), n) burned tufa (XPL), o) celtis australis seed coats (PPL).

Component	Description and comments	Representative combustion structures (and abundance*)
Bone fragments	Sand-sized fragments of predominantly small mammals, reptiles, or fish and lower proportion of indistinct fragments, possibly macrofauna In Control and RL, mostly unburned, in BL commonly burned and in WL calcined	All (3)
Teeth	From rodents	H46 BL (1), Xb (2)
Celtis australis seed coats		H44b BL (2), H53b BL (2), H53b WL (1), H53a WL (1), H55 BL (1), Xb (2)
Flint flakes	Sand-sized flakes and flake fragments, occasionally fissured	H44b BL (1), H50 WL (3), H55 BL (1), Xb (1)
Fibrous coprolites	Herbivore origin In some cases, fine mass is almost entirely made up of fibrous coprolites with diffuse boundaries	All (3)
Massive coprolites	From omnivores or carnivores	Xb (2)
Wood charcoal	Some fragments identified as pine Rounded in BL and UL, angular in WL	H44b BL (1), H50 BL (1), H53 RL (1), H53 BL (1), H55 BL (1), H57 WL (1), Xb (1)
Blackened plant residues	Fine-medium sand size Morphology suggestive of degraded plant tissue	All (3)
Unidentified square black particle	Subhorizontally aligned or isolated subangular cuboids 50 x 50 µm	H57 BL (3), H57 RL (3), Xb (1)
Animal fat-derived char fragments	Consisting of a massive black matrix with vesicular voids and fissures	Xb (1)
Calcitic eggshell fragments		H50 WL (1), Xb (1)

Table 4: Components identified in the sample set. Their description and their extent within the sediment and combustion structures with associated abundances (* abundance: 1=rare to few, 2=common to frequent, 3=abundant)

The fine mass of stratigraphic unit Xb is composed of undifferentiated, locally calcitic-crystallitic phosphatized clayey silt (Fig. 6a and b). In some cases, the input of fibrous coprolites is very dominant, creating a fibrous coprolitic matrix (Fig. 6a). Matrices of BLs resemble the fibrous coprolitic matrix, with a prevalence of blackened/charred organic material, and matrices of WLs are composed of diagenetic calcitic ash (Fig. 5a, b, d, and e).

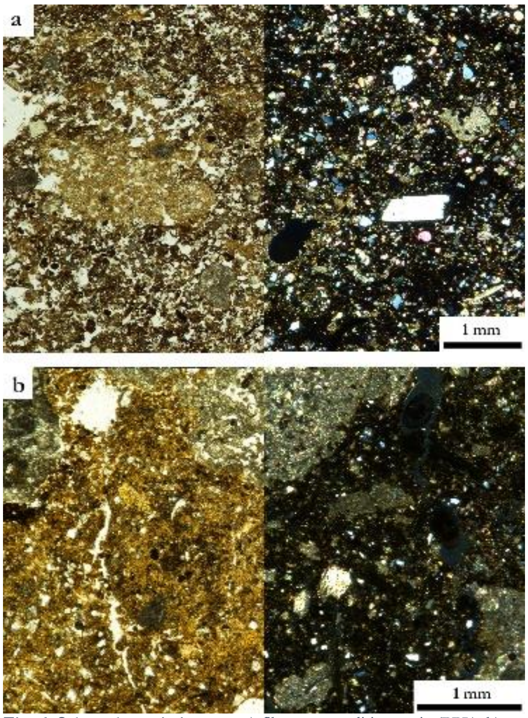

Fig. 6: Selected matrix images. a) fibrous coprolitic matrix (PPL), b) fibrous coprolitic matrix (XPL), c) phosphatic matrix (PPL), phosphatic matrix (XPL).

The prevailing porosity encompasses vughs and compound packing voids, with localized channels and a few randomly oriented planes. Microstructures resulting from that porosity are vughy microstructure, granular microstructure, and intergrain microaggregate microstructure.

Post depositional processes are bioturbation and diagenesis. Bioturbation is identified as being a mild physical postdepositional process, comprising local changes in the microstructure, which do not affect the overall ability to interpret or to differentiate individual microfacies units. Diagenesis can be observed in partial decalcification of the groundmass and the presence of phosphatized areas and locally abundant gypsum crystals and gypsum crystal pseudomorphs. The calcitic ash of the WL was also affected by diagenesis, exhibiting local isotropic or recrystallized domains (Fig. 5c) and collapse zones with intrusive overlying sediment.

3.3.1.2 Microfacies types (MFT's)

The sample set resulted in 45 MFU, which correspond to the observed WL, BL, RL, and Xb sediment (see Appendix 2). Accordingly, the MFUs were grouped into 12 MFT (Table 5). MFTs were established using matrix color, frequency of fibrous coprolites, organics particles, and degree of bioturbation in Xb, BL, and RL sediment. The WLs were grouped according to the presence or absence of wood ash and degree of diagenesis. A detailed description of the MFT and which facies is represented in them can be found in Table 5.

MFT	Layer	MFT description	Facies represented
1	BL	Dark brown fibrous coprolite-rich matrix with common black organic particles	H44b BL, H45 BL, H46 BL, H53b BL, H50 BL, H54 BL, H55 BL
2	RL	Reddish-brown fibrous coprolite-rich matrix with common black organic particles	H52 RL, H53b RL, H57 RL
3	Xb	Weakly bioturbated brownish-yellow fibrous coprolite-rich matrix	
4	WL	Pale brownish-yellow fibrous coprolite-rich matrix with diagenetic wood ash	H50 WL
5	BL	Dark brown matrix with abundant fibrous coprolites and black organic particles	H52 BL, H53a BL, H57 BL
6	Xb	Brownish-yellow matrix with few fibrous coprolites and few black organic particles	
7	Xb	Bioturbated brownish-yellow matrix with few fibrous coprolites and few black organics	
8	WL	Grey matrix with *in situ*, well-preserved wood ash	H55 WL
9	WL	Grey matrix of *in situ*, diagenetic wood ash with few calcined bone fragments	H57 WL, H52 WL
10	WL	Brownish-grey matrix with diagenetic wood ash	H53a WL, H53b WL

Table 5: MFT of combustion structure assemblage of SU Xb.

3.3.2 TC, TIC, and TOC

It was possible to get TC, TIC and TOC data on 9 samples. Average values of TC were 6.39 %, of TIC 5.09 % and of TOC 1.30 %. The BL on average yielded the highest quantity of TOC (2.08 %, n=4), before control (TOC = 0.76 %, n=2), WL (TOC = 0.69 %) and RL (TOC = 0.60 %, n=2) samples. The highest percentage of TIC is shown by the BL (5.18 %, n=4) and the lowest by the Controls (4.84 %, n=2) (see Table 6)

Sample	TC (%)	TIC (%)	TOC (%)
H44b WL	5.80	5.11	0.69
H45 BL	7.58	4.83	2.75
H46 BL	6.99	5.49	1.50
H50 RL	5.48	5.07	0.41
H52 BL	7.17	5.11	2.06
H52 UL	6.03	5.25	0.78
H57 BL	7.29	5.28	2.01
C2	5.89	5.25	0.65
C4	5.30	4.42	0.88
Avg. WL	5.80	5.11	0.69
Avg. BL	5.81	4.14	1.66
Avg. RL	5.48	5.07	0.41
Avg. control	5.60	4.84	0.76
Avg. all	6.39	5.09	1.30
Min. all	5.30	4.42	0.41
Max. all	7.58	5.49	2.75

Table 6: TC, TIC and TOC of selected combustion structures of SU Xb

3.3.3 Lipid biomarkers

3.3.3.1 *n*-Alkanes

Twenty-seven loose sediment samples were available for the analysis of *n*-alkanes. The data from those analyses exhibit a distribution of *n*-alkanes ranging between nC_{17} and nC_{35}. The total concentration in these samples varies from 0.02 µg/gds (H50 BL4) to 9.32 µg/gds (H50 BL2). Averages according to their origin result in the lowest values for the BLs (n=14; 0.96 µg/gds), and subsequently WLs (n=5; 1.57 µg/gds), Control and Xb (n=5; 1.85 µg/gds) and RLs (n=3; 2.50 µg/gds) (Fig. 7).

CPI values (n=27) vary from 0.17 (H55 BL2) to 28.84 (C2).

By using CPI values as a measure of alteration, *n*-alkane profiles were divided into three groups, representing three stages of alteration. The groups allocated to each sample and *n*-alkane profiles can be found in Fig. 7. The first group represents the presumably unaltered samples, which show pronounced odd long-chained peaks with a maximum peak at C31 and none or only small even peaks. Their CPI values are ranging above 15. Contained samples are the four control samples, H55 Xb, which represents Xb sediment below H55 and H50 BL1. The second group includes moderately altered samples containing an *n*-alkane profile with high distinct odd long-chained peaks and a presence of short and even chained peaks. Their highest peaks at C27, C31, and C33 can be compared to those of Group 1; nevertheless, samples have a CPI ranging from 1.09 to 4.49. Samples included in this group are H44b WL, H46 BL, H50 WL, H50 BL2, H50 BL3, H50 BL4, H50 RL, H53a WL, H54 BL, H55 BL1, H57 BL, H61 WL1. Group 3 represents samples that are highly altered, showing a predominance in short-chain and even *n*-alkanes. This group's CPI is lying between 0.16 and 0.44. Samples included in this category are H45 BL, H52 BL, H53a BL, H53b BL, H55 BL2, H61 WL2, H61 BL, and H61 RL.

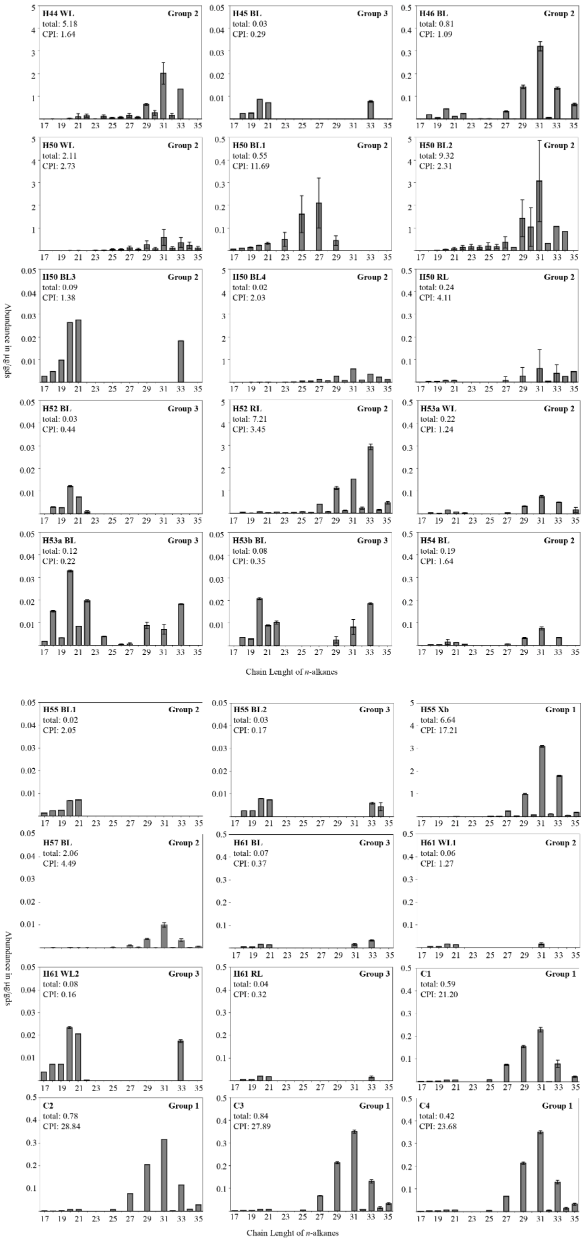

Fig. 7: N-alkane profiles of combustion feature facies. Abundances of alkanes with chain lengths from 17 to 35 in µg/gds with three different scales on the y-axis. Error ranges are shown according to their standard deviation. For H50 BL3, H50 BL4 and C2 the error ranges are lower than 0.004 µg/gds. Graphs show total alkane content (µg/gds), CPI and alteration group.

Samples without a pronounced alteration (Group 1 and Group 2) can be analyzed according to their dominant peaks. The majority of samples' highest peak is C31, though the most dominant peak for H52 RL is C33, and the most dominant peak of H50 BL1 is C27 (Fig. 7).

3.3.3.2 Other lipid fractions

No Polycyclic aromatic hydrocarbons could be detected in the aromatic fraction (fraction 2) or through pyrolysis. Also, Ketones could not be detected in any of the samples. Nonetheless, Betulin, Betulinaldehyde, Lupeol, β-Amyrin, Fucoxanthin, Stigmasta-3,5-diene, Stigmasterol, Cholesterol, 1-Hexacosanol, 1-Octacosanol, 1-Tetracosanol, Docosanol, and Squalene could be detected. The dominant fatty acids in the samples were 16:0 (palmitic acid) and 18:0 (stearic acid).

3.3.3.3 CSIA of *n*-Alkanes

Twenty-six samples yielded results for compound-specific carbon isotopes of *n*-alkanes comprising BLs, WLs, RLs, and Xb of 11 combustion structures and four control samples. Due to the dominance of odd-numbered *n*-alkanes with long chain lengths in the samples, the interpretation of compound-specific δ13C was focused on the $\delta^{13}C$ analysis of C_{29} and C_{31}. $\delta^{13}C$ values for C_{29} range from -34.4 to -29.4 ‰, with an average of -32.0 ‰ and values for C_{31} range between -35.3 and -31.1 with an average of -32.9 ‰ (Fig. 8).

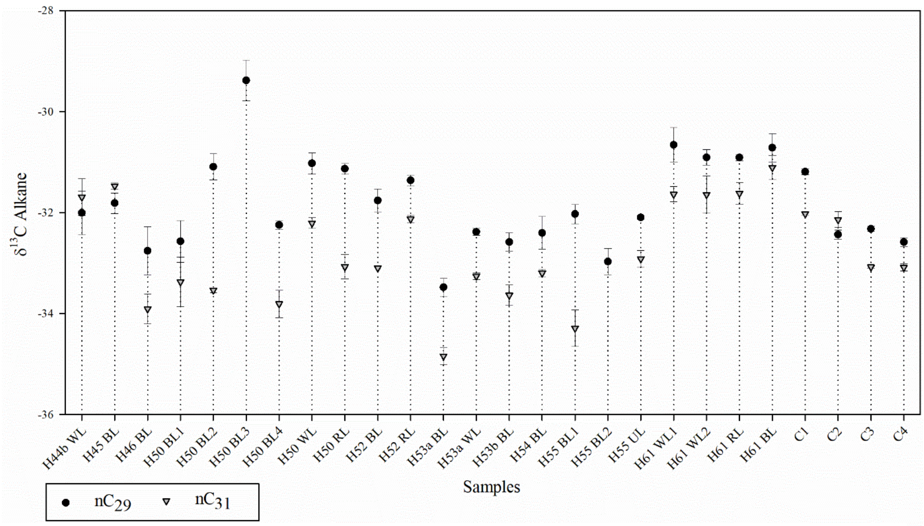

Fig. 8: δ13C compound specific alkane profiles. Combustion structures on the x-axis and δ13C values on the y-axis, displaying the isotopic value of the alkane nC29 and nC31 with error ranges according to the standard deviation.

3.4 Case Study I: Discussion

3.4.1 Formation of the SU Xb combustion structures

3.4.1.1 Micromorphological observations

Macroscopically, the eleven combustion structures studied here are similar in size, shape, internal stratigraphy, and associated archaeological material. Micromorphologically, clear ash layers could be identified in H52, H55, and H57, and diagenetically altered ash layers in H50, H53a, and H53b. Four of the combustion structures showed no ash at all (H44b, H45, H46, H54). All of these combustion structures are *in situ* while comprising an intact internal stratification (RL, BL, WL), observable on the micro-scale (Mallol et al., 2017). Occasional mild bioturbation is limited to a small scale, rarely exceeding the boundaries of the individual layers. For H61, only bulk samples were available.

All of the BLs represent sedimentary substrates rather than a layer of fuel residues. They mainly contain variable proportions of herbivore coprolite residues and black unidentified plant tissue.

In their composition and microstructure, the BLs of SU Xb are comparable to those from the overlying SU Xa (Mallol et al., 2013a). They consist of a loose, fibrous coprolite-rich sedimentary matrix with common geogenic detritus, microfaunal bone remains, degraded topsoil plant matter, a few charcoal fragments, and very few flint fragments. Fibrous coprolites and fibrous coprolite-rich sediment have been previously reported in herbivore dung deposits (Brönnimann et al., 2017a; Macphail and Goldberg, 2010). Thus, the BLs possibly represent undisturbed natural topsoils occupied by herbivores and later charred by anthropogenic fire. Crucially, the presence of common geogenic detrital mineral grains and scattered, finely comminuted degraded plant matter and microfaunal bone indicate they are natural topsoils and not purely dung nor fuel. The plant matter is present in the form of unidentified fibrous or massive black particles originating from topsoil vegetation (Deák et al., 2017). The original morphology of the perishable plant parts (parenchyma or collenchyma) was not observed; therefore, the plant matter must have undergone a certain degree of degradation prior to combustion, possibly corresponding to amorphous lignin-rich tissue (Babel, 1975; Ismail-Meyer, 2017) or remains of the epidermis, which are hard to decompose (Bal, 1973; Stoops, 2010). Crucially, the SU Xb control sediment samples yielded very few, scattered black particles. The longest sequence of hearths in the studied area consists out of four roughly overlapping combustion structures (H52, H53a, H53b, and H50). Considering the geogenic and pedogenic nature of their respective BLs, the site must have been unoccupied by humans in between each of the combustion events.

The human impact was not observed apart from the effect of burning that resulted in the BLs. Only rare flint fragments and macrofaunal bone remains were identified, and no signs of trampling were observed. Charcoal fragments are also scarce. Some of them have been identified as conifer, possibly *Pinus nigra or Pinus sylvestris*, in accordance with previous anthracological evidence from SU Xb (Vidal-Matutano et al., 2018). Given the detrital, mixed composition of the BLs and the roundness and smoothness of the charcoal fragments, which are few, these are possibly reworked, deriving from nearby, preceding combustion events.

Regarding the WLs, no anthropogenic components were identified in any of them, suggesting that the activities carried out around them did not involve tossing refuse into the fire, at least in significant amounts, nor cooking practices involving deposition of bone or char residues in the fire. Most of them showed signs of postdepositional reworking or diagenetic alteration. Strong bioturbation and mixing with the overlying sediment were observed in both H50 WL and H53 WL, in addition to strong decalcification in H53 WL.

3.4.1.2 Total organic carbon

The preservation of organic matter (TOC) in BLs is better than in WLs, RLs, and Xb. This is in agreement with previous studies by Mallol et al. (Mallol et al., 2013a), underlining the potential of charred organic matter to preserve biomarker fingerprints. This implies that temperatures in the BLs are sufficiently low as to preserve organic matter but at the same time high enough to produce non-biodegradable combustion residues.

3.4.1.3 Lipid biomarkers

The lipid compounds identified conform with the BL deposits representing former topsoils. The triterpenoids Betulin, Lupeol, and β-Amyrin are angiosperm biomarkers (Diefendorf et al., 2014; Otto et al., 2005; Stout, 1992). Terpenoids originate mainly from leaves, bark (Diefendorf et al., 2014), and resins (Diefendorf et al., 2014; Langenheim, 2003), while triterpenoids are indicative of angiosperms and diterpenoids of gymnosperms (Diefendorf et al., 2012). In SU Xb, the anthracological record indicates that conifers represent the predominant wood fuel type (Vidal-Matutano, 2016; Vidal-Matutano et al., 2017; Vidal-Matutano et al., 2018), and thus diterpenoids originating from tree resin were expected to be present in the combustion structure sediment (Beck et al., 1989; Diefendorf et al., 2014; Mills and White, 1977), especially since conifers, as members of the Pinaceae family, produce high quantities of resin (Langenheim, 2003). However, no gymnosperm biomarkers were identified in any of the BL samples. This is in agreement with the BLs representing a charred vegetated surface under the fires and not fuel residues. Considering that terpenoids would mainly derive from leaves of trees in the immediate surroundings of the site and only triterpenoids are present, we can assume that the site was surrounded by angiosperms prior to the combustion events. Although diterpenoids are naturally underrepresented because they are less abundant than triterpenoids (Diefendorf et al., 2012), an absolute absence of diterpenoids makes it less likely that gymnosperms grew in the vicinity of the site. Consequently, the conifer wood used to fuel the fires was possibly collected off-site.

Other indicators of angiosperm input are aliphatic compounds, including 1-Hexacosanol, 1-Octacosanol, 1-Tetracosanol, and Docosanol (Otto et al., 2005), all of which are present in our samples. A prevalence of nC_{29} and nC_{31} as dominant *n*-alkanes points to the presence of leaves from higher plants as well (Cranwell, 1978; Eglinton, 1970; Eglinton and Hamilton, 1967; Jambrina-Enríquez et al., 2018; Rieley et al., 1991). A possible source of leaves could be the Celtis tree (*Celtis australis*) since Celtis seed coats are present throughout the thin sections; likewise, Celtis phytoliths have been previously reported for SU Xa (Mallol et al., 2013a; Rodríguez-Cintas and Cabanes, 2015).

Given the interpretation of BLs as topsoil, it is important to determine whether the black microscopic plant residues identified microscopically are blackened by charring, biodegradation, or both. Our micromorphological observations suggest some degree of biodegradation (see above). However, our biomarker data show the presence of Stigmasta-3.4--diene and Stigmasterol, which are biomarkers of burnt plant biomass (Otto et al., 2005). In addition, no homophanes or hopenes, which are bacterially derived triterpenes (Stout, 1992), were identified. We only observed a few black plant parts in the SU Xb sediment control samples, and the *n*-alkane profiles of these samples do not show any alteration on the molecular scale of the *n*-alkanes. Thus, bacterial degradation is unlikely, and the varying degrees of alteration in the *n*-alkane profile observed in most of our BLs and WLs is possibly due to burning and is comparable to previously reported data from plant biomass burning (Eckmeier and Wiesenberg, 2009). This raises the question of the temperatures reached in the BLs as a result of subsurface heat penetration.

Given that our samples show a predominant angiosperm leafy content with a strong probability of the presence of Celtis trees, we can compare our data to a recent study involving controlled heating experiments on *Celtis australis* leaves, bark, branches, and twigs (Jambrina-Enríquez et al., 2018) to provide estimates of the temperatures at which our BLs were heated. Accordingly, our strongly altered samples (Group 3) were possibly burned to temperatures higher than 350 °C (Jambrina-Enríquez et al., 2018) but possibly lower than 500 °C (Wiesenberg et al., 2009), moderately altered samples (Group 2) were heated in the range between 150 °C and 350 °C (Jambrina-Enríquez et al., 2018) and unaltered samples (Group 1) were not heated to more than 150 °C (Jambrina-Enríquez et al., 2018). Overall, these temperatures are within the range documented for experimental combustion structure substrates with an organic-rich substrate (González-Pérez et al., 2004; Mallol et al., 2013a). Other experimental fires conducted on a plain substrate or organic poor substrates reach higher subsurface temperatures (Aldeias et al., 2016 and references therein).

One exception is BL1 of H50, which showed dominant peaks in nC_{25} and nC_{27}, suggesting the presence of twigs or branches (Jambrina-Enríquez et al., 2018). Jambrina-Enríquez et al. (2018) show that this *n*-alkane profile changes with combustion at temperatures higher than 150 °C, suggesting that the H50 BL did not reach temperatures higher than 150° C and thus the twigs or branches were not fuel but topsoil residues.

Regarding our biomarker data for the WLs, none of them shows highly altered *n*-alkane profiles, contrary to our expectations. This lack of alteration might be explained by the effect of bioturbation and diagenesis, which is prominent in these samples, as shown by our micromorphological data. Possibly, the *n*-alkane profile obtained contains a mixed signal of both the original ash layer and unburned sediment postdating the combustion structures. Despite this mixing, the CPI values of the WLs indicate the lowest *n*-alkane preservation, whereas the best *n*-alkane preservation according to the CPI was recorded in the control samples. This suggests that even when mixing WL and Xb, the CPI remains lower than that of the BL. Further work is required to better understand the effects of intrusive ashy sediments on CPI values.

3.4.1.4 Compound-specific stable carbon isotopes of *n*-alkanes

The $\delta^{13}C$ values of nC_{29} and nC_{31} *n*-alkanes range between -35.3 and-29.4. These values are indicative of plants with a C3 photosynthetic pathway (Bi et al., 2005; Collister et al., 1994; Jambrina-Enríquez et al., 2018; Wiesenberg et al., 2004). Important to note is that the isotopic values fluctuate up to 5‰ in the sample set. This variation is not related to the combustion structures or their facies (WL, BL, RL). In fact, the highest variability was observed in different samples within the BLs of H50. This variability could be explained by differences in plant functional types (e.g., grasses, deciduous angiosperms, evergreen gymnosperms) (Diefendorf et al., 2010). As previously discussed, the *n*-alkane profile of H50 BL1 stands out for showing the presence of twigs and branches, suggesting a more heterogeneous composition with regards to plant matter. Additionally, the micromorphological data from H50 BL, which shows a pronounced fibrous planar microstructure, demonstrates a distinctive pattern exclusive to H50 BL.

Since most of the samples belong to combustion contexts, the question arises as to the effect of heating on isotopic values. Above 330-360 °C, an increasing depletion in ^{12}C takes place, which can be attributed to the cleavage of 12C-12C bonds (Bjorøy et al., 1992). On the other hand, Diefendorf et al. (2015) report a shift of compound-specific *n*-alkane $\delta^{13}C$ values up to 2‰ in either direction depending on species and chain length, at a temperature higher than 200-250 °C. Thus, a shift in the compound-specific *n*-alkane $\delta^{13}C$ values would corroborate that BL and WL represent, in fact, burning if all other parameters are ruled out. As shown by our *n*-alkane data, a good number of our samples appear to have been heated to more than 250 °C. Even so, the heterogeneous composition of the organic matter (different plant tissues) should be considered. Jambrina-Enríquez et al. (2018) reported that the xylem from Celtis branches and twigs was enriched by ∼2‰ in ^{13}C relative to leaves, whereas bark was depleted by ∼3‰ in ^{13}C relative to leaves and that shifts of $\delta^{13}C$ values with increasing combustion temperature are different within plant tissues (leaves, bark, and xylem). Therefore, our isotope data must be taken with caution, and further basic research comparing compound-specific carbon isotope values of fresh and burned plants is needed.

3.4.2 Implications for the timing and intensity of Neanderthal occupations at El Salt SU Xb

The good preservation states of the SU Xb combustion structures as observed in the field are corroborated by our joint micromorphological and geochemical data. The degree of bioturbation, as well as diagenesis, is moderately low, and the BLs represent *in situ* combustion substrates. These combustion substrates were natural vegetated surfaces with decayed leaves and herbivore excrements, which possibly accumulated when humans were away. No signs of human activity were observed besides the lighting of simple, flat fires on these surfaces. Material remains observed microscopically are very few burnt bone residues in the ash layers (WLs) and trace amounts of scattered bone and flint flakes in BLs, RLs, and Xb. Only ephemeral signs of human activity were found in the WLs microscopically. On this basis and focusing on the relative stratigraphic position of the four superimposed, diachronic combustion features from the outer area (H50, H53b, H53a, H52), we propose that the SU Xb combustion structure assemblage represents at least four low-impact human occupation episodes (minimal number of occupations) separated by unknown periods of time during which the place was not occupied by humans. No stratigraphic discontinuities, signs of erosion, or long time pedogenesis was observed, suggesting that the amount of time of site abandonment was limited.

The charred plant matter contained in the BLs may provide additional clues to narrow down the timing of human occupations at El Salt SU Xb. Aside from blackening and possible shrinkage (Canti, 2017), charring is not expected to change the original morphology of plant tissue. Thus, we can assume that the morphology of the black particles we observed reflect the state of the plant matter present in the topsoil at the time of burning. As previously discussed, our microscopic, charred plant matter, morphologically amorphous lignin-rich tissue, possibly reflects the remains of moderately degraded angiosperm plants. Given this evidence, we can hypothesize that the fires were not made in the fall, in which case they would have charred a fresh leaf cover. Generally, the brittle parts of leaves (parenchyma and collenchyma) decay within a few months after deposition (Ismail-Meyer, 2017), so human occupations in El Salt SU Xb possibly did not take place during the fall season.

Furthermore, our results also suggest that the Neanderthal groups that occupied El Salt during the formation of SU Xb did not stay there for prolonged amounts of time, which would have resulted in obliterated, re-lit hearths and higher amounts of anthropogenic remains. Instead, they arrived, occupied the place, leaving the previously uninhabited natural surfaces intact, except for localized burning, and left before these had been obliterated by natural or anthropogenic processes.

3.4.3 Inter- and Intra-site comparison of the combustion structure assemblage

To corroborate our interpretation of brief human occupations separated by relatively long periods of time and further explore the consequences of short-term occupations at El Salt, we need to compare our data with other stratigraphic units or sites in the Iberian Peninsula comprising combustion structure, lithic and faunal assemblages.

El Salt stratigraphic unit Xa has been rigorously analyzed using different methods. Micromorphology conducted on selected combustion structures also yielded BLs representing charred plant litter (Mallol et al., 2013a). The black layers are up to 2 centimeters thick, and some are covered with a thin WL (Mallol et al., 2013a). *n*-Alkane data from those combustion structures appear to support our data in having the highest peaks at 29 and 31 and showing signs of heat alteration (Mallol et al., 2013a). This evidence also points to relatively long periods of site abandonment in stratigraphic unit Xa.

Lithic raw materials of SU Xa were gathered within a 20 km radius and mostly within a 5 km radius (Machado and Pérez, 2015; Molina Hernández et al., 2010), supporting short occupation episodes and high mobility (Richter, 2006; Vaquero, 2012). Flint cores are uncommon and are possibly part of the habitually transported gear, which, together with evidence of tool recycling, was interpreted as reflecting high group mobility (Machado and Pérez, 2015). The low sedimentation proposed in stratigraphic unit Xa that made tool recycling possible in SU Xa is supported in the nature of the palimpsest of SU Xb, whereas the approximately 2 cm thick organic soil covering the site at the arrival might have made a straightforward recovery of tools more challenging. Indirect evidence of carnivore activity like marks from teeth and digestion, isolated anatomical remains, and coprolites were detected (Machado and Pérez, 2015; Pérez et al., 2015; Pérez et al., 2017a), supporting long periods of site abandonment and short-term occupations (Sanz et al., 2017; Straus, 1982; Vaquero, 2012; Yellen, 1991). Finally, a layer of up to 7 cm-thick of archaeologically sterile sediment was recorded within SU Xa, interpreted as a period of site abandonment of decades to more than a century (Machado and Pérez, 2015). Lithic and faunal analyses of SU Xb are ongoing and preliminary observations point to similar animal processing, lithic raw material procurement, and technological patterns as observed for Xa.

Other Middle Paleolithic Iberian sites dating roughly to the same period as SU Xb have also yielded rich anthropogenic combustion records, but these cannot be directly compared to our dataset because, in the majority of cases, there is no associated micromorphological or lipid biomarker data. Available field descriptions of combustion structures show the presence of BLs mainly in open air or rockshelter settings (Courty et al., 2012; Eixea Vilanova et al., 2011-2012; Rosell et al., 2015), with similar shape and thickness to those in our dataset and could also represent short term combustion events (Eixea Vilanova et al., 2011-2012; Rosell et al., 2015). In caves, combustion structures are composed of a reddened substrate in connection with burned anthropogenic material, and occasionally ashes (Cabrera et al., 2004; Fernández Peris et al., 2012; Fernández Peris et al., 2014; Maillo-Fernandez et al., 2014), with a lack of BLs formed from charring organic-rich substrate, as expected for a sheltered space unaffected by soil-forming processes. Micromorphological analyses have been conducted at Bolomor cave where combustion structures were identified as having a short duration (Fernández Peris et al., 2012; Fernández Peris et al., 2014), and Esquilleu cave, which is at a considerable distance from El Salt where combustion structures exhibit trampling and diagenesis (Cabanes et al., 2010; Mallol et al., 2010). A comparison with the SU Xb structures might be confounding, as those fires were made in cave settings, whereas our dataset is from an open-air setting. Accordingly, micromorphological comparison with our dataset is not possible.

A third site rich in combustion remains, similar age, and associated micromorphological data is Abric Romaní. Abric Romaní is a rockshelter site around 370 km north of El Salt. Combustion structures exhibit BLs composed of plant and organo-mineral remains, with humified, charred, or calcined components in level J (Vallverdú Poch, 2002) and level O (Courty et al., 2012). Combustion structures in both levels are considered to be identical (Courty et al., 2012). Even though conifer wood was used to fuel the fires, the carbonaceous polymorphs present in the BLs are not derived from the fuel (Courty et al., 2012). Comparing our data to microphotographs of combustion structures of Abric Romaní, we observe similarities between their graphitic vitreous carbon and our amorphous plant material (Courty et al., 2012). Thus, fires in Abric Romaní, like the ones in El Salt, were possibly made on organic-rich substrates after relatively long abandonment periods.

3.5 Concluding remarks

Our study of El Salt SU Xb adds to the few Middle Paleolithic sites in Europe that have yielded well-preserved combustion structures as confirmed through microstratigraphic analyses: Such as Abric Romani (Courty et al., 2012; Pastó et al., 2000; Vallverdú et al., 2005b), Gorham's Cave (Macphail and Goldberg, 2000b), Grotte XIV (Karkanas et al., 2002; Rigaud et al., 1995), Klissoura Cave (Karkanas et al., 2004), Lakonis Cave (Karkanas, 2002), Pech de l'Azé IV (Dibble et al., 2009; Goldberg and Berna, 2010), Roc de Marsal (Goldberg et al., 2012), Vanguard Cave (Macphail and Goldberg, 2000b), and El Salt SU Xa (Mallol et al., 2013b).

The BLs of combustion features from El Salt SU Xb were formed through anthropogenic burning of an underlying organic-rich natural surface in an environment vegetated by angiosperms, including Celtis trees and intermittently occupied by herbivores and Neanderthals. These fires were fueled by wood gathered away from the site. The paucity of Neanderthal occupation during the formation of El Salt SU Xb, possibly representing at least four successive low impact human occupation events, with enough time in between to allow for the formation of an organic-rich soil and occupations most likely in winter, spring and summer.

The results from this study show the good preservation of lipid molecules in Paleolithic sedimentary contexts, supporting the implementation of organic chemistry in geoarchaeological research. In the case of combustion features, our data show not only that lipid molecules preserve well in burnt sediment but also how lipid biomarker analysis may contribute basic information to corroborate evidence of burning, provide temperature estimates, and aid in the taxonomic identification of charred organic matter, all of which are a necessary complement to micromorphological data. Our biomarker results were limited by a lack of reference material on lipid biomarkers and compound-specific carbon isotopes of plants, plant functional types, and seeds burned at different temperatures.

In sum, micromorphology combined with lipid biomarker analysis is a powerful approach to investigate anthropogenic combustion-related archaeological contexts from a microstratigraphic perspective, which can contribute valuable information on the timing and intensity of Neanderthal occupations as well as the natural setting of the site. These are key factors of group mobility and settlement patterns.

Case Study II

It's getting hot in here – Microcontextual study of a potential pit hearth at the Middle Paleolithic site of El Salt, Spain.

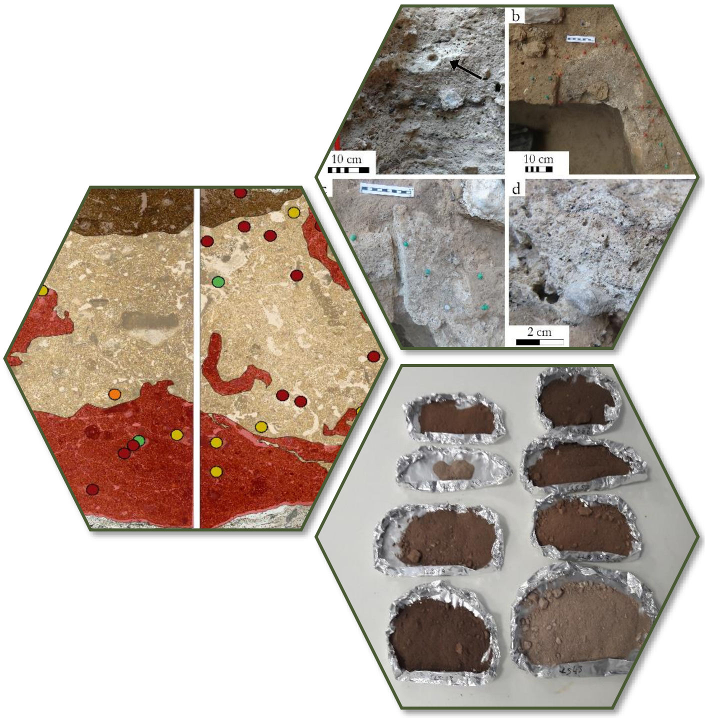

4. Case Study II: Investigation of a pit hearth

It's getting hot in here – Microcontextual study of a potential pit hearth at the Middle Paleolithic site of El Salt, Spain

Lucia Leierer [a,b,*], Ángel Carrancho Alonso [c], Leopoldo Pérez [d,e], Ángela Herrejón Lagunilla [f], Antonio V. Herrera-Herrera [a], Rory Connolly [a,b], Margarita Jambrina-Enríquez [a,g], Cristo M. Hernández Gómez [b,h], Bertila Galván [b], Carolina Mallol [a,b] https://doi.org/10.1016/j.jas.2020.105237

[a] Instituto Universitario de Biorgánica Antonio González, Universidad de La Laguna, La Laguna, Santa Cruz de Tenerife, Spain.
[b] Departamento de Geografía e Historia, Área de Prehistoria (Facultad de Humanidades), Universidad de La Laguna, Campus de Guajara, La Laguna, Santa Cruz de Tenerife, Spain.
[c] Área de Prehistoria, Departamento de Historia, Geografía y Comunicación. Universidad de Burgos. Edificio I+D+I, Plaza Misael Bañuelos s/n, 09001 Burgos, Spain.
[d] IPHES, Institut Català de Paleoecologia Humana i Evolució Social, Zona Educacional 4. Campus Sescelades URV (Edifici W3), 43007 Tarragona, Spain.
[e] Àrea de Prehistoria, Universitat Rovira i Virgili (URV), Avinguda de Catalunya, 35, 43002 Tarragona, Spain.
[f] Departamento de Física. Universidad de Burgos. Escuela Politécnica Superior (Campus Río Vena). Avda. Cantabria s/n, 090006. Burgos, Spain.
[g] Departamento de Biología Animal, Edafología y Geología, Facultad de Ciencias, Sección de Biología, Universidad de La Laguna, La Laguna, Tenerife, Spain
[h] Departamento de Didácticas específicas. Facultad de Educación. Universidad de La Laguna. Tenerife. Spain
* Corresponding author: Lucia Leierer

ABSTRACT:

By studying combustion structures, which conceal information about anthropogenic activity, we might learn about their makers. This is especially important for remote time periods like the Middle Paleolithic, whose archaeological record comprises numerous combustion structures. The majority of these are simple, flat, open hearths, although a small number of features situated in pit-like depressions have been recorded. Given that combustion structures built on a flat surface can result in pit-like color alteration of the underlying sediment, accurate identification of pit hearths is a crucial step prior to behavioral interpretation. Here we present a comprehensive study of a possible pit hearth from the Middle Paleolithic site of El Salt, Spain, using a microcontextual approach combining micromorphology, lipid biomarker analysis, archaeomagnetism, and zooarchaeology. This pit hearth involves a true depression containing a thick plant ash deposit. It reached very high temperatures, possibly multiple burning events, and long combustion times. Morphologically distinct combustion structures in a single archaeological context may indicate different functions and thus a diverse fire technology, pointing to Neanderthal behavioral variability.

4.1 Case Study II: Introduction

Fire has played an important role in human lives since the late Pleistocene, as evidenced by different Middle Paleolithic and Middle Stone Age deeply stratified sites with archaeological fire throughout their sequence (e.g., Courty et al., 2012; Galván et al., 2014a; Goldberg et al., 2009b; Mallol et al., 2013a; Vaquero and Pastó, 2001; Wadley, 2006). Thus, we can study archaeological combustion structures from these remote periods to learn about their makers. These structures may convey information on aspects of pyrotechnology (e.g., fuel use, fire temperature, fire intensity, hearth maintenance) (Mentzer, 2012), which as any other technology, reflects behavior and culture (e.g., Schiffer et al., 2001; Vitezović, 2013 and references therein). In order to obtain relevant information from an archaeological combustion structure, which is sedimentary in nature, it is necessary to apply geoarchaeological techniques (Miller, 2011). In recent years, different methodologies to study combustion structures as artifacts have been incorporated into archaeological method and theory (Mallol et al., 2017; Mallol and Henry, 2017; Mentzer, 2012; Mentzer, 2017; Miller, 2011; Stahlschmidt et al., 2020), and there is a growing number of case studies on this topic (e.g., Aldeias et al., 2012; Haaland et al., 2017; Miller et al., 2013).

The Middle Paleolithic fire record comprises numerous combustion features (Roebroeks and Villa, 2011 and references therein). The vast majority of these are generally described as simple open hearths, which are basic, flat structures without stone linings or surface preparation (James et al., 1989; Leierer et al., 2019; Mallol et al., 2013a; Mallol et al., 2017; Meignen et al., 1989; Mellars, 1996; Olive and Taborin, 1989; Roebroeks and Villa, 2011). Research into this fire evidence from different perspectives has provided information about aspects of Neanderthal fire technology. For instance, although there is widespread evidence of wood ash and charcoal as the main fuel source, other fuel sources have been documented, including bones (Costamagno et al., 2005; Costamagno et al., 2008; Théry-Parisot, 2002a; Yravedra et al., 2016; Yravedra and Uzquiano, 2013), lignite (Théry-Parisot and Meignen, 2000) and liquid hydrocarbons (Courty et al., 2012). There is evidence of fire use to facilitate woodwork (Aranguren et al., 2018), for smoking purposes (Vidal-Matutano et al., 2017), and the possibility to produce tar (Koller et al., 2001; Kozowyk et al., 2017; Niekus et al., 2019; Pawlik and Thissen, 2011; Schmidt et al., 2019; Wragg Sykes et al., 2015). Some of this evidence points towards pyrotechnological traditions involving fire use for purposes other than cooking and obtaining warmth and light. However, our knowledge on Neanderthal pyrotechnology is still very poor.

We might gain information from Middle Paleolithic combustion structures by focusing on their shape. A basic element of archaeological artifact analysis is morphology, a formal attribute that can be linked to culture and technology (Debénath and Dibble, 1994; Hunt and Bortolini, 2016). Although most Middle Paleolithic combustion structures are simple and flat, in a few cases, they are delimited by stones or are concave, forming a depression or pit into the substrate. Middle Paleolithic fires placed in a depression have been reported at several sites (Table 7). These combustion structures have been variably described and analyzed (see Table 7). The function and other technological aspects of these pit hearths remain unknown.

Site	Hearth description	References
Champlost	15 cm deep accumulation of ashes, heated bones, and lithics	(Farizy, 1994; Villeneuve and Farizy, 1989)
Abric Romaní	amongst numerous flat hearths, few built on natural depressions, few with a concave morphology	(Gabucio et al., 2017; Vallverdú Poch et al., 2012; Vaquero et al., 2001)
Oscurusciuto	2 m wide 15 cm deep hearth, containing heated bone, lithics, and rubified sediment	(Boscato and Ronchitelli, 2008; Villa et al., 2009)
Divje babe 1	one hearth with a 1 m diameter located in a depression	(Paunovic et al., 2002)
Roca dels Bous	large hearth made in a 20 cm deep depression, at least used twice	(Martínez-Moreno et al., 2004)
Kebara Cave	a few hearths with diameters over 80 cm and a thickness of around 25–45 cm, filled with ashes and charcoal, and hypothetically representing successive burning events	(Meignen et al., 2007)
Hayonim Cave	large, well-delimited thick wood ash deposits with over 110 cm in diameter and a thickness of 10 –12 cm	(Goldberg and Bar-Yosef, 1998)

Table 7: Sites with combustion structures placed in a depression, hearth description, and accompanying references.

Interpreting archaeological combustion structures in depressions as anthropogenic pit hearths solely based on field observation can be misleading since experimental studies have shown that downward heat transfer in a fire made on a flat surface may result in a shallow, pit-like color alteration of the underlying sediment (Aldeias et al., 2016; Bellomo, 1993; Brodard et al., 2015; Mallol et al., 2013b; March et al., 2014; Pérez et al., 2017b). Such structures cannot be interpreted as anthropogenic pit hearths, as they did not involve intentional preparation of a pit or depression (Aldeias et al., 2016), raising the question of how many correctly identified Neanderthal pit hearths there are. Likewise, hearth cleaning activities might result in pit-like structures showing ripped-up soil aggregates of the underlying substrate (Mallol et al., 2007).

Anthropogenic pit fires or pit hearths have been defined as combustion structures with a bowl- or U-shape, a depth of not more than 1 m and a diameter of 0.6 to 1 m (Groenendijk, 1987; Huisman et al., 2019; Peeters and Niekus, 2017). In archaeological contexts, the most commonly occurring pit hearths can be found in the Mesolithic record of the Netherlands, Belgium, and northern Germany (Groenendijk, 1987), but also in other periods like the Bronze Age (Løvschal and Fontijn, 2019) and the Ninevite 5 period (Smogorzewska, 2012). There are a few ethnographic or ethnoarchaeological descriptions of pit hearths from native Americans (Skibo and Schiffer, 2008), seminomadic pastoralists (Zerboni et al., 2013), and contemporary hunter-gatherers (Mallol et al., 2007). A pit hearth is constructed through the excavation of the substrate, which limits the amount of oxygen in the fire (Mallol et al., 2017; Skibo and Schiffer, 2008). The temperatures reached in pit hearths seem to be lower than in flat hearths but more stable and spatially homogeneous (March, 1992; March et al., 2014; Peeters and Niekus, 2017). Thus, their morphology and thermal properties allow for different and more specialized functions than simple flat combustion structures. In the ethnographic record, there are pit hearths for hide smoking (Skibo and Schiffer, 2008), charcoal burning (Zerboni et al., 2013), and cooking (Mallol et al., 2007; Wandsnider, 1997). A study summarizing ethnographic data from cooking pits associates them with roasting big amounts of either plants or fatty meat "for extended periods of time and subjected to moderate to high heat" (Wandsnider, 1997, p. 28).

Given that the presence of pit hearths in the Middle Paleolithic would suggest technological or functional variation in fire use, microcontextual investigations of possible pit hearths can be of considerable value to behavioral research on Neanderthals (Aldeias et al., 2016; Haaland et al., 2017; Meignen et al., 2007). So far, successful identifications of Middle Paleolithic pit hearths using a microcontextual approach have been conducted in Kebara and Hayonim Cave (Goldberg and Bar-Yosef, 1998; Meignen et al., 2007).

At the Middle Paleolithic site of El Salt, a plausible pit hearth was found at the boundary of two depositional layers (stratigraphic units Xb and XI). This is, so far, the only combustion feature that is not flat in the entire archaeological fire record of the site (in over a total of 90 combustion features). Normally at El Salt, combustion structures are simple, flat, with black sedimentary layers (here onwards BL) interpreted as charred topsoils (Leierer et al., 2019; Mallol et al., 2013a). In contrast, the possible pit hearth does not exhibit a BL. Instead, it comprises a thick, whitish-grey sedimentary layer (WL) filling a small, irregular depression and reddish sediment (red layer or RL) at the base (Fig. 1, Fig 2). In order to investigate the nature of this peculiar combustion feature and to contribute to the understanding of Neanderthal fire technology, in this paper, we applied a microcontextual and multidisciplinary approach combining micromorphology, lipid biomarker analysis, archaeomagnetism, and zooarchaeology.

4.2 Case Study II: Material – Combustion structure H77

Combustion structure H77, which was cut and partially lost during the excavations of 1960-61, was exposed during the 2018 field season. A clear pit shape was visible on the profile left by the 1960 excavations (Fig. 9a). It is located at the boundary between stratigraphic unit Xb and XI. The feature was covered by a lens of grey sandy silt (Field name: Lsg11), which was reported to be texturally different from the prevailing sedimentary facies in this unit. Directly beneath facies Lsg11 was the WL of feature H77. As can be seen on the 1960 profile (Fig. 9a), The WL was thicker towards the center of the feature, with a maximum thickness of 5 cm. Upon excavation of the WL, which was loose and massive and contained a few fresh rootlets, a

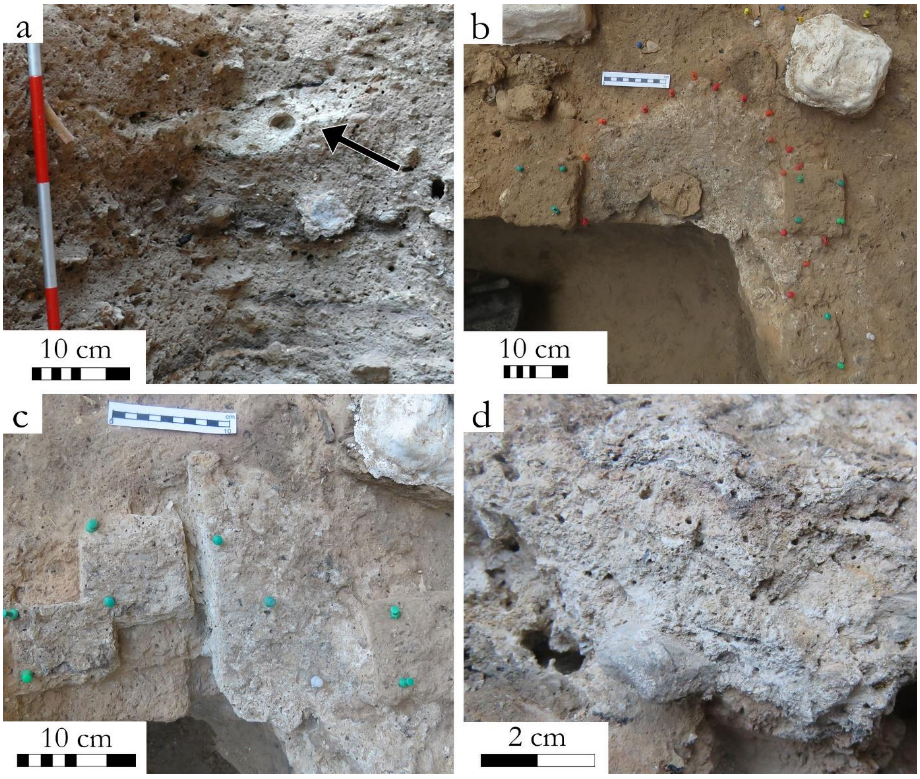

Fig. 9: Selected field photos of H77. a) Profile view of H77 from the year 2012. Note thick ash layer (arrow) that exhibits a slight bowl shape. b) Photograph of perimeter of the WL of H77 (red pins) and surroundings of combustion structure exposing the stratigraphic unit Lsg11 c) H77 during excavation while separated in two parts, in the left part, the WL has already been excavated and the RL and two archaeomagnetism samples are exposed. On the right part the upper surface of WL is exposed and has not been excavated there yet d) detailed view of the profile of the WL that was created by cutting the feature in two parts. The profile is viewed from the left part of the feature looking towards the right part.

sloping, reddish-brown (RL) sedimentary surface was exposed (see Fig. 9c, Fig. 10). The RL showed a massive appearance and was approximately 2 cm thick at the center of the feature, thinning out towards the periphery.

The archaeological assemblage stratigraphically associated with feature H77 comprises a concentration of calcined bone (n=7), including a shaft fragment of around 8 cm. There were also a few cm long charcoal fragments and a few flint objects (n=4). All the remains were found towards the bottom of the WL. The underlying RL deposit contained a larger archaeological assemblage, with 18 flint objects and seven bone fragments.

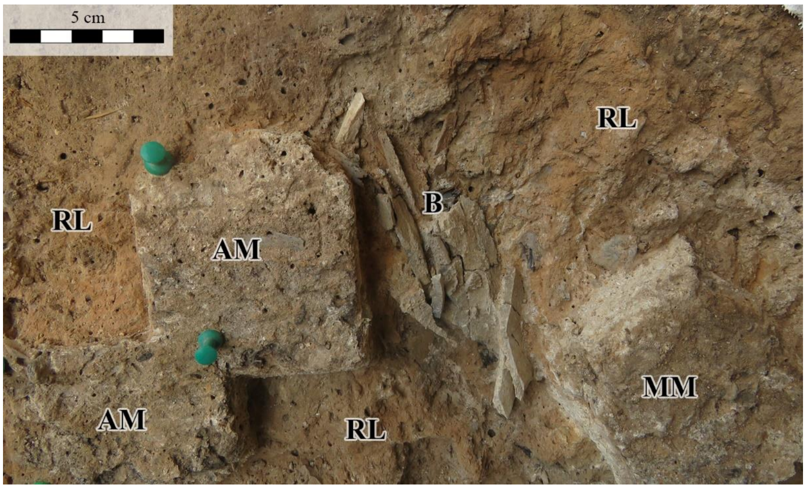

Fig. 10: Field photo of an area of H77 including the two archaeomagnetism samples of the WL (AM), the micromorphology block Salt-18-8 (MM), the underlying red layer (RL) and a deer tibia in 14 fire-cracked pieces (B).

4.3 Case Study II: Methods specific for this study

4.3.1 Archaeomagnetic and rock-magnetic analyses

To obtain the highest accuracy and prevent the breakage of the hand block samples during sampling, we used plaster of Paris. A horizontal surface was created by dripping the plaster on the surface of every hand-block. A piece of methacrylate was carefully pressed onto the plaster while wet, and a pair of bubble levels was used for leveling. Before removing every hand-block, a line pointing to the magnetic North was drawn with a Brunton compass on the dry plaster.

Before cutting the hand-blocks, they were consolidated using a mixture of sodium silicate (*water glass*) and distilled water (75:25). 13 cubic specimens (~ 10 cm^3) were obtained from the uppermost part of these blocks (0-2 cm of depth) to study their natural remanent magnetization (NRM) directional stability.

The progressive demagnetization of NRM was performed both by stepwise thermal (TH) and alternating field (AF) demagnetization. However, TH demagnetization was mostly applied to assess the heating temperature of these samples. NRM was measured with a 755 Superconducting Rock Magnetometer (2G). Stepwise TH demagnetization was performed in 20 heating steps from room temperature up to 600 ºC using a TD48 – SC (ASC) shielded thermal demagnetizer. The AF demagnetization was carried out in

20 steps up to a peak field of 100 mT with the demagnetization unit of the 2G cryogenic magnetometer. The direction of the characteristic remanent magnetization (ChRM) of all specimens was determined by principal component analysis (Kirschvink, 1980) using the *Remasoft* software (Chadima and Hrouda, 2006). The mean archaeomagnetic direction was calculated using Fisher (1953) statistics.

With the aid of a Variable Field Translation Balance (Magnetic Measurements), different experiments were performed to further constrain the magnetic properties of the samples. The analyses comprised progressive isothermal remanent magnetization (IRM) acquisition curves, hysteresis loops (± 1 T), backfield coercivity curves, and thermomagnetic curves up to 700 ºC in air. These measurements were carried out on bulk sediment (~ 450 mg) from every sample and facies studied and at different depths. The results were interpreted using the *RockMagAnalyzer* 1.0 software (Leonhardt, 2006). All the palaeomagnetic and rock-magnetic analyses were carried out at the laboratory of paleomagnetism of Burgos University, Spain.

4.3.2 Faunal analysis

For quantification, all bone fragments were taxonomically and anatomically identified whenever possible, while non-identified specimens were classified into three categories (long, flat, or articular) and associated with a weight-size category based on bone density, circumference, and the thickness of the cortical surface: large-sized > 300 kg, medium-sized 100-300 kg, small-sized 5-100 kg, and very small-sized < 5 kg (Bunn, 1986; Palomo et al., 2007; Uerpmann, 1973). In this work, we employed only three measures of abundance: number of remains (NR), minimal number of element (MNE), and minimal number of individuals (MNI). The whole bone surface was analyzed using macroscopic and microscopic techniques to identify biostratinomic and diagenetic modifications. Possible anthropogenic features (percussion, fracture, butchering marks, thermal alteration) or features associated with predators (tooth marks, digestion) were quantified, as well as possible diagenetic processes such as erosion, sedimentary concretions, roots action, weathering, pigmentation, and trampling (Binford, 1981; Blasco Sancho, 1992; Denys and Patou-Mathis, 2014; Domínguez-Rodrigo and Yravedra, 2009; Fernandez-Jalvo and Andrews, 2016; Shipman, 1981; Shipman and Rose, 1983; Villa and Mahieu, 1991; Yravedra, 2006).

4.4 Case Study II: Results

4.4.1 Micromorphology

Together, all the thin sections analyzed (six from inside the feature, two from outside but closely related) provided a microscopic overview of the entire combustion structure. We identified four microfacies types (here onwards: MFTs) which can be correlated with the macroscopic field facies. These MFTs are, from base to top: MFT XI, MFT RL, MFT WL, and MFT Lsg11 (Fig. 11). Since lithology, components, and post-depositional processes share comparable characteristics throughout the sample set, they will be presented separately in the following paragraphs. Changes in frequency or composition within an MFT will be noted in the description of the MFTs. A detailed description of every microfacies unit can be found in the appendix (Appendix 3).

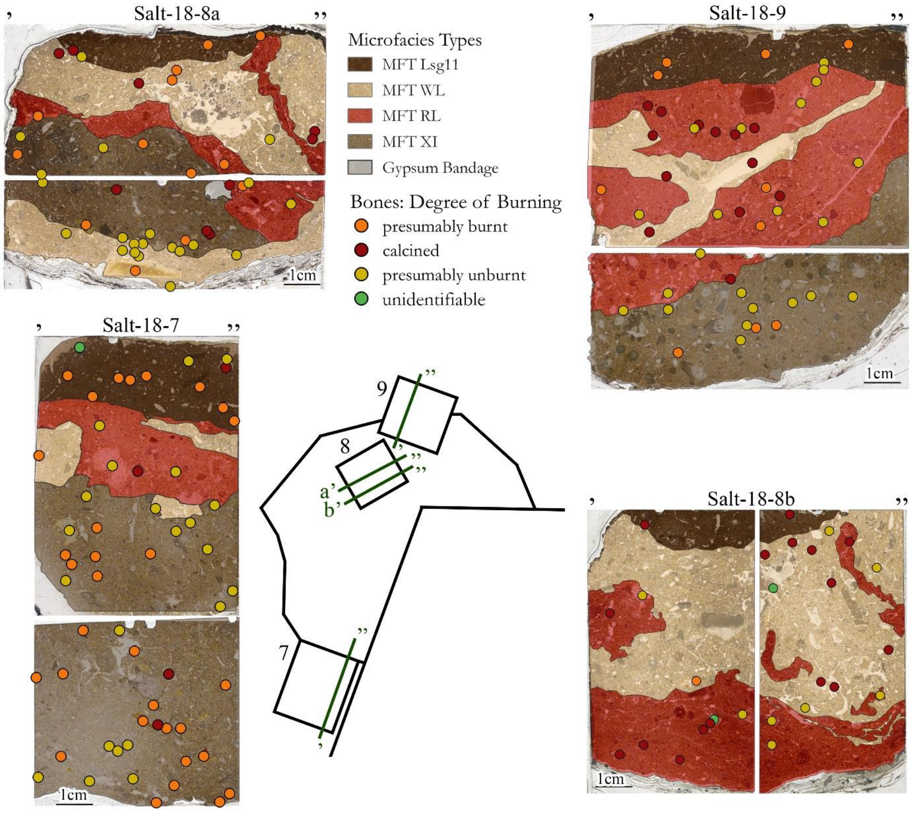

Fig. 11: Location of micromorphology blocks and their corresponding thin sections. Different colors indicate the microfacies types (MFT) and dots indicate the location and degree of burning of bones bigger than 1.5 mm.

4.4.1.1 Lithology

The lithological composition of the sample set is homogenous and characteristic of El Salt SU Xb, as has been previously documented (Leierer et al., 2019). The sediment is sandy and detritic, with subrounded, quartz-rich limestone fragments, subrounded travertine and tufa fragments, and few subrounded quartz grains. These components show variations in abundance, degrees of weathering, and burning throughout the different MFTs (see Appendix 3). Some of the tufa fragments are brownish grey in PPL due to burning (Mallol et al., 2013a).

4.4.1.2 Other Components

Anthropogenic and biogenic components are frequent in the sample set and are listed and described in Table 8 and presented in Fig. 12.

Component	Description	MFT XI	MFTR L	MFTW L	MFT Lsg11
Ash	Woody and nonwoody plant-ash in different states of preservation			x	
Wood charcoal	Some fragments identified as pine	x		(x)	x
Black organic residues	Fine to medium sand size, possibly charred	x			x
Fibrous coprolite	Herbivore origin	x	x		x
Massive coprolite	Omnivore/carnivore origin	x	x		x
Celtis australis seed coats	Abundant throughout the sample set, some burned	x	x	x	x
Possible animal fat-derived char fragments	Very few particles of massive black matrix with vesicular voids and fissures commonly identified as charred liquid drops of fat (Clark and Ligouis, 2010; Goldberg et al., 2009b; Miller et al., 2009)	x			
Bones	Abundant throughout sample set, Predominantly microfauna and lower proportion of nondistinctive fragments, possibly macrofauna	x	x	x	x
Teeth	From rodents	x	x	x	
Flint flakes	Sand-sized flakes and flake fragments, some burned, visible as crazing (fine pattern of cracks)(Angelucci, 2017)		x		x

Table 8: Anthropogenic and biogenic components found in the sample set, their description, and their presence (marked with an "x") or absence (empty cell) in the specific MFT. Cells marked with an "(x)" represent a single occurrence of that component within the MFT.

Microscopic faunal remains exhibit different degrees of burning. All bone fragments (excluding teeth) larger than 1.5 mm were mapped, and their approximate degree of burning was subjectively classified, resulting in 173 bones with four possible degrees of burning: Calcined (n=42), presumably burnt (n=55), presumably unburnt (n=73) and unidentified (n=3) (see Fig. 11). The subjective classification was done according to optical differences in color (in PPL) and birefringence (in XPL), following reference material of experimentally heated bone and micromorphological guidelines for their characterization (Villagran et al., 2017). The distribution of the altered bones is random in all MFTs, while MFT XI and MFT Lsg11 have a predominance of heated bone and MFT RL and MFT WL a predominance of calcined bone. The abundance of bone is lower in the MFT WL compared to all other MFTs.

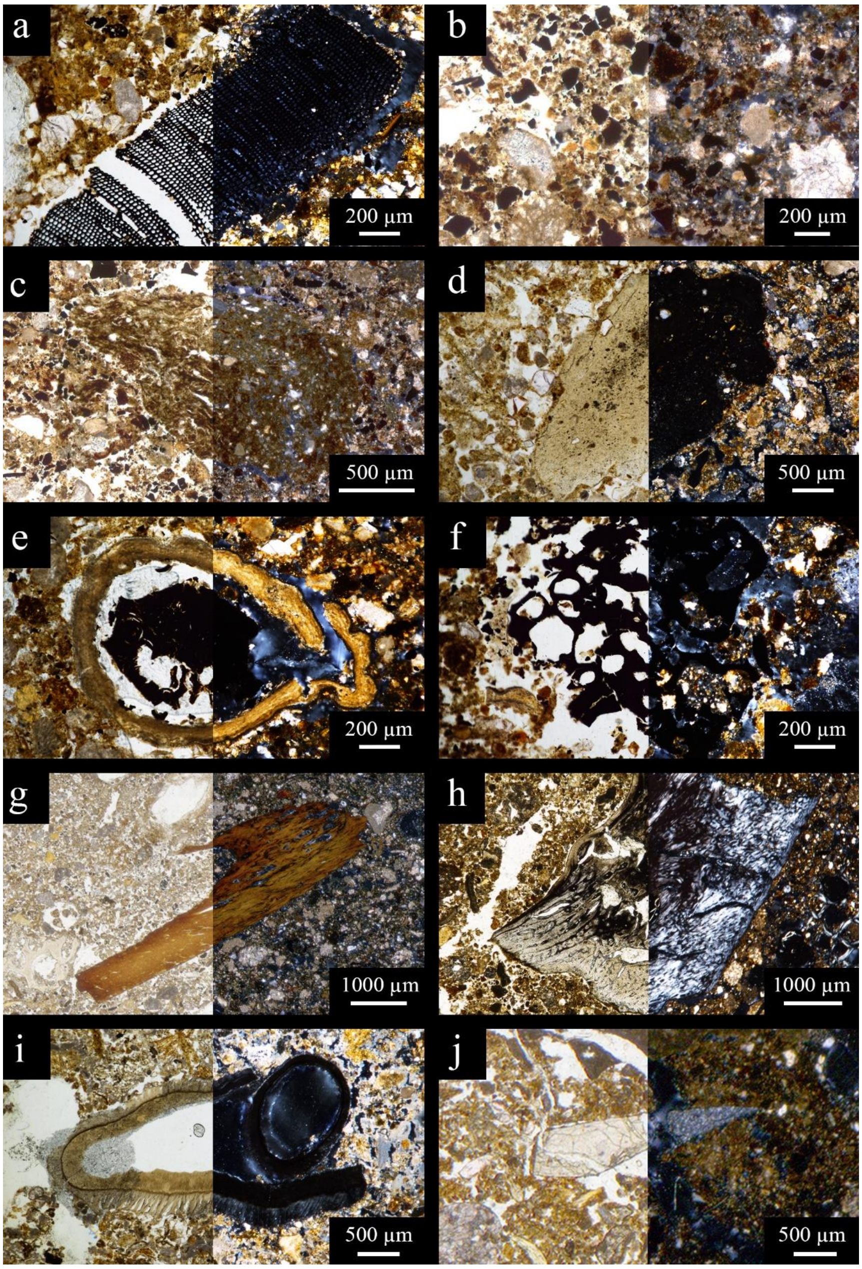

Fig. 12: Components mentioned in Table 8 as microphotograph. Each microphotograph represents PPL on the left side of the picture and XPL on the right side of the picture. a) charcoal, b) black organic particles, c) fibrous coprolite, d) massive coprolite, e) intact Celtis australis seed coat containing its charred seed, f) possibly fat derived char, g) heated bone, h) calcined bone, i) tooth, j) heated flint flake.

4.4.1.3 Post-depositional processes

The entire sample set is slightly disturbed by bioturbation. However, the degree of bioturbation is small enough to enable a good comparison amongst the different MFTs. A majority of the void structure is dominated by channels and chambers. A small number of passage features could be observed as well. Nevertheless, physical transformation due to bioturbation is at a small scale, without disturbance of the general sedimentary structure. In a few instances, bioturbation took place at the boundary of two distinct MFTs, where sediment from one layer was mixed into the other layer in the form of a passage feature.

Part of the sample set shows post-depositional decalcification (Karkanas and Goldberg, 2010a). MFT XI and MFT RL are more strongly decalcified than MFT Lsg11, whereas the ashes of MFT WL are the least decalcified. MFT XI and MFT Lsg11 contain massive coprolites, and some voids are internally hypocoated with a phosphatic stain.

4.4.1.4 Microfacies types (MFTs)

4.4.1.4.1 MFT XI

MFT XI has a dark brown color in PPL. At high magnification, the groundmass is brownish yellow, and it is evident that the dark brown color observed in the naked eye and at low magnification is due to the common presence of charcoal and black organic residues. In XPL, the b-fabric is only weakly crystallitic, indicating decalcification. The mineral grains are also affected by decalcification. Intergrain microaggregate microstructures are predominant and are complemented by subangular blocky microstructures. Voids are complex packing voids, channels, and chambers. Anthropogenic components like possible fat-derived char, charcoal, and bone are very abundant.

4.4.1.4.2 MFT RL

MFT RL exhibits massive reddish-brown sediment in PPL, devoid of organic material. The b-fabric resembles that of MFT XI. Depending on the position of the thin section within the feature, the RL is thicker, more reddish, without organic material (towards the center) or thinner, less red with very little organic matter (towards the periphery). In some areas, especially towards the center of the combustion structure, the upper part of the RL exhibits horizontal planes. Microstructure and voids are, apart from the planes, similar to that of MFT XI.

4.4.1.4.3 MFT WL

The thickness of the WL in thin section is up to 5 cm, and the boundaries to over- and underlying units are sharp. MFT WL appears pale-yellowish brown in PPL and locally blueish grey or light grey in XPL. It is locally fibrous and composed exclusively of wood ash and unidentified plant ash. The light grey zones show a crystallitic b-fabric in XPL and contain calcium carbonate pseudomorphs of calcium oxalate, specifically calcitic wood ash rhombs (Fig. 13a–c), while the blueish grey zones lack rhombs and show scattered micritic crystals (Fig. 13d–i). The ashes in these areas are submicroscopic, which influences their interference color (Canti, 2003). Additionally, ash particles resembling plant structures are encountered within the blueish grey zones (Fig. 13i, j). They have a dark red color and are fibrous. Bigger particles have a cell structure preserved.

The microstructure is predominantly intergrain microaggregate and vughy with occasional channels. MFT WL contains very few components – besides ash – the most abundant being bone fragments, followed by lower amounts of tooth fragments and *Celtis australis* seed coats.

4.4.1.4.4 MFT Lsg11

In regard to color, microstructure, voids, and the presence of anthropogenic components, MFT Lsg11 and MFT XI appear to be similar; however, MFT Lsg11 shows less decalcification of the matrix. The dark brown color of MFT Lsg11 is due to the presence of charcoal and black organic residues.

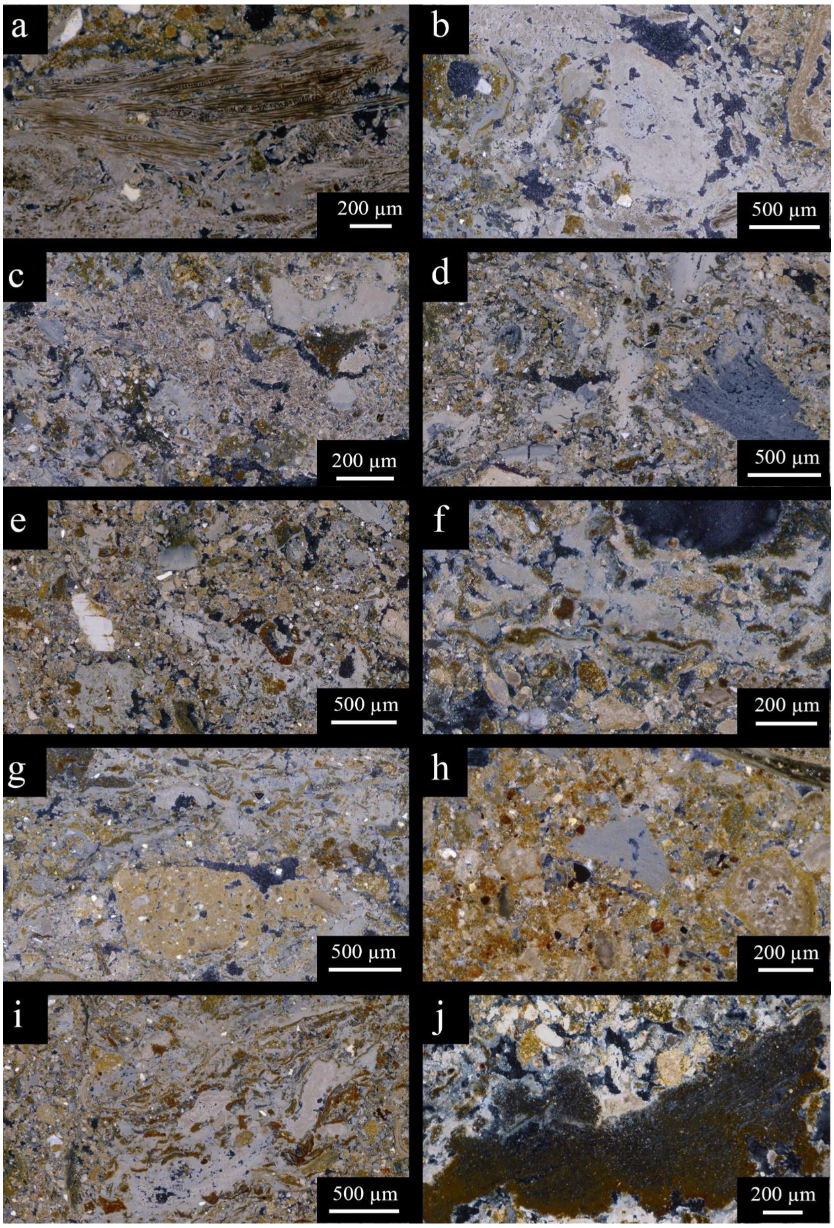

Fig. 13: Microphotographs of ashes taken in XPL: a) fresh wood ash in the form of calcium carbonate pseudomorphs of calcium oxalate(ash rhombs and rods), b) micritic mass of fine crystalline calcitic ash and carbonate pseudomorphs, c) fresh wood ash as carbonate pseudomorphs together with micritic mass of ashes, d) micritic mass of ashes of different crystal sizes according to the difference in color, e) micritic mass of ashes intermixed with sediment, f) micritic mass of ash crystals recrystallized around remains of reddish plant fiber, g) aggregate of RL sediment (passage feature) within micritic mass of ashes, h) aggregate of micritic ashes within the RL, i) accumulation of reddish plant fibers surrounded by recrystallized micritic ashes, j) close-up of large fibrous tissue fragment with preserved cell structure embedded in micritic ashes.

4.4.2 Lipid biomarkers – *n*-alkanes

We obtained *n*-alkane data from 8 loose sediment samples from inside the combustion feature (WL: n=4, RL: n=1) and from surrounding sediment on top (Lsg11: n=1) and on the bottom (SU XI: n=2) (Fig. 14). The concentration of total *n*-alkanes is rather low with an average of 0.113 micrograms per gram of dry sediment (µg/gds) with the highest concentration of 0.59 µg/gds (BM18 – Lsg11) and the lowest concentration of 0.005 in WL samples (BM37, BM43). We can broadly distinguish between samples from within the feature and samples around it. The RL and WL samples from within the feature are low in total alkane concentration (0.018 µg/gds n=5) with dominant peaks in shorter chains between C18 and C21. The surrounding samples have a higher total alkane concentration of 0.656 µg/gds (n=4) with dominant peaks in C31 and C35 and an odd-over-even predominance.

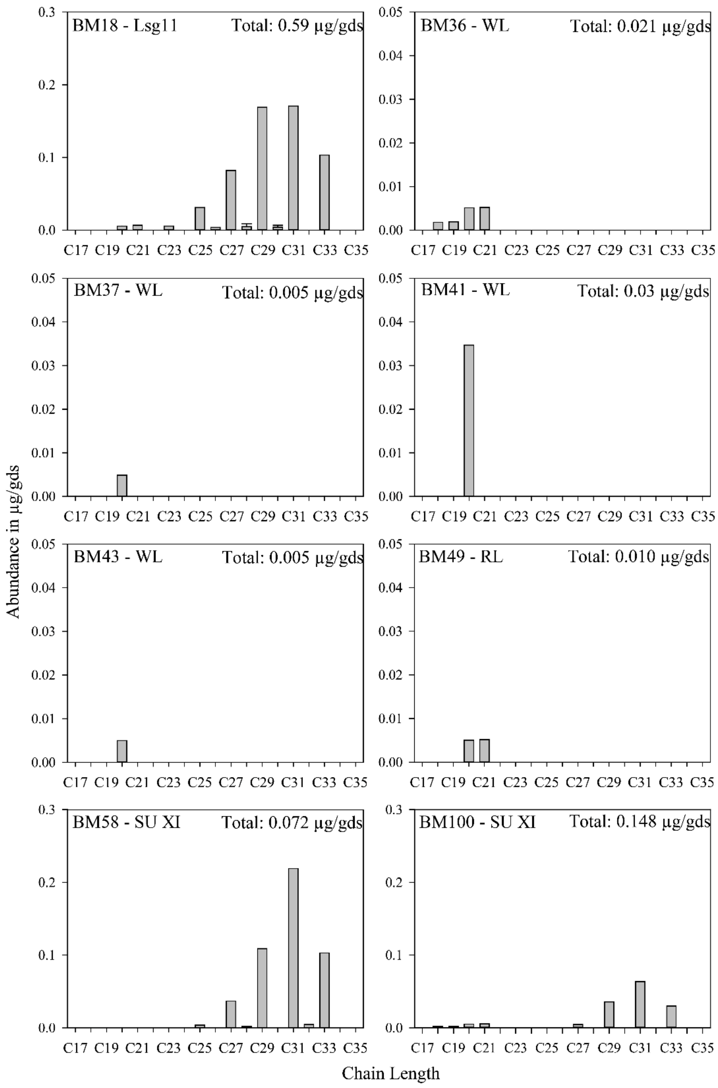

Fig. 14: *n*-Alkane profiles of samples related to H77. Graphs show name of the sample, total *n*-alkane concentration and abundances of *n*-alkanes from chain length of C17 to C35 with two different scales on the y-axis. Error ranges are shown according to their standard deviation. Error ranges not visible are lower than 0.0009.

4.4.3 TC, TIC, and TOC

We obtained TC, TIC, and TOC data on eight samples. Averaging the different facies, RL has the lowest amount of TOC (0.24 %, n=1), followed by WL (0.56 %, n=4), Lsg11 (1.77 %, n=1) and SU XI (2.57 %, n=2). For detailed values, see Table 9.

	TC (%)	TIC (%)	TOC (%)
BM 18 (Lsg11)	6.32	4.55	1.77
BM 36 (WL)	7.07	6.34	0.73
BM 37 (WL)	6.81	6.50	0.31
BM 40 (WL)	5.45	4.71	0.74
BM 43 (WL)	6.48	6.02	0.46
BM 49 (RL)	6.03	5.80	0.24
BM 58 (SU XI)	6.95	4.57	2.38
BM 100 (SU XI)	8.20	5.44	2.76
Average	6.66	5.49	1.17
Average Lsg11	6.32	4.55	1.77
Average WL	6.45	5.89	0.56
Average RL	6.03	5.80	0.24
Average SUXI	7.57	5.00	2.57

Table 9: TC, TIC, and TOC values of selected samples in percent.

4.4.4 Controlled heating experiments

Colors ranged from dark reddish-brown (on the Munsell soil color chart 5YR 3/4) (100 °C) to reddish-yellow (5YR 6/6) (800 °C) (see Fig. 15) (Munsell Color (Firm), 2010). We did not observe color change between 100 to 300 °C. At 400 °C, the sediment turned lighter in color but remained reddish-brown (5YR 4/4). From 500 to 600 °C, a change in color towards a very light reddish-brown was noted (5YR 5/4), and towards light reddish-yellow at 700 and 800 °C (5YR 6/6).

Fig. 15: Color change after controlled burning of sediment from SU XI at different temperatures for 1 h.

4.4.5 Archaeomagnetic results

Initial natural remanent magnetization (NRM) intensities of the WL are between 2.8 x 10^{-4} and 1.75 x 10^{-4} Am^2kg^{-1} while susceptibility varies between 5.5 x 10^{-6} and 4.0 x 10^{-6} m^3kg^{-1}. In the RL, NRM values vary between 4.5 x 10^{-4} and 4.3 x 10^{-5} Am^2kg^{-1} and susceptibilities oscillate between 5.45 x 10^{-6} and 9.6 x 10^{-7} m^3kg^{-1}. For both parameters, WL samples show higher values compared to the RL, suggesting that the concentration of ferromagnetic (*s.l.*) particles are higher in the WL.

Fig. 16 shows the values of the Königsberger (Q_n) ratio for both facies. The Q_n ratio (Koenigsberger, 1938; Stacey, 1967) is a magnetic parameter which relates to the remanent and induced magnetization ([Q_n = NRM / (χH)], where χ is the magnetic susceptibility and H the intensity of the local magnetic field). This parameter is commonly used to characterize burnt archaeological materials or igneous rocks and is considered a measurement of stability to indicate a sample's capability of maintaining a stable remanence, such as thermal remanent magnetization (TRM). All values but one are over unity, indicating that the magnetization is most probably of thermal origin and are in the range of other burnt archaeological and experimental materials such as hearths, pottery, or fireplaces (e.g., Francés-Negro et al., 2019; Herrejón Lagunilla et al., 2019; Kapper et al., 2014).

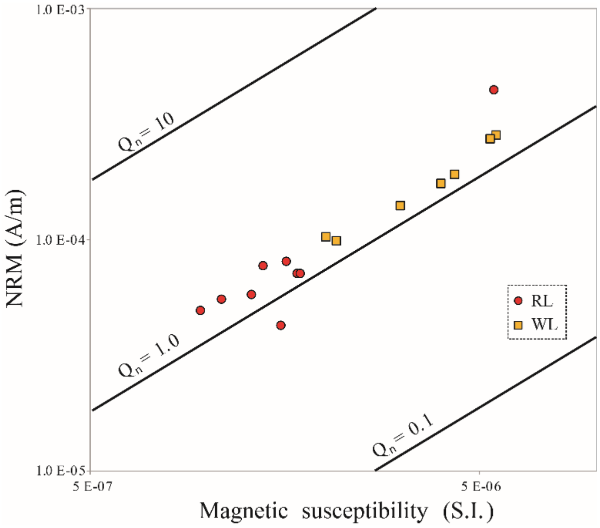

Fig. 16: The natural remanent magnetization (NRM) versus the bulk magnetic susceptibility (S.I.), showing lines of constant Koenigsberger ratio (Qn) between 0.1 and 10. RL = Red layer. WL = white layer.

The orthogonal NRM demagnetization diagrams obtained in both facies are characterized by high intensities of magnetization and stable and reproducible directions (Fig. 17). All specimens exhibit a low temperature secondary viscous component unblocking up to 200 – 250 ºC. The characteristic remanent magnetization (ChRM) direction is isolated from 250 ºC to 580 – 600 ºC, systematically showing normal polarity. Exceptionally, in a single case, the ChRM direction is defined between 200 and 500 ºC in a RL sample (Fig. 17b). This behavior reflects a partial thermoremanent magnetization (pTRM) caused by the lower temperature reflected in this sample. A high-temperature (HT) component can be observed between 500 and 600 ºC (Fig. 17b). The maximum unblocking temperature (max TUB) of the pTRM would indicate the maximum heating temperature experienced by this RL during its last heating. It seems logical to expect some variability in the temperatures reached by the burnt facies of prehistoric combustion features (e.g., Carrancho et al., 2009), especially considering that the RL is underlying the WL, thus further away from the heat source. In any case, the dominant behavior in the NRM directional stability of both burnt facies is defined by highly magnetic, univectorial, stable normal polarity diagrams, most probably carrying a TRM. This observation is also supported by the Q_n ratio values, and the thermomagnetic results explained below.

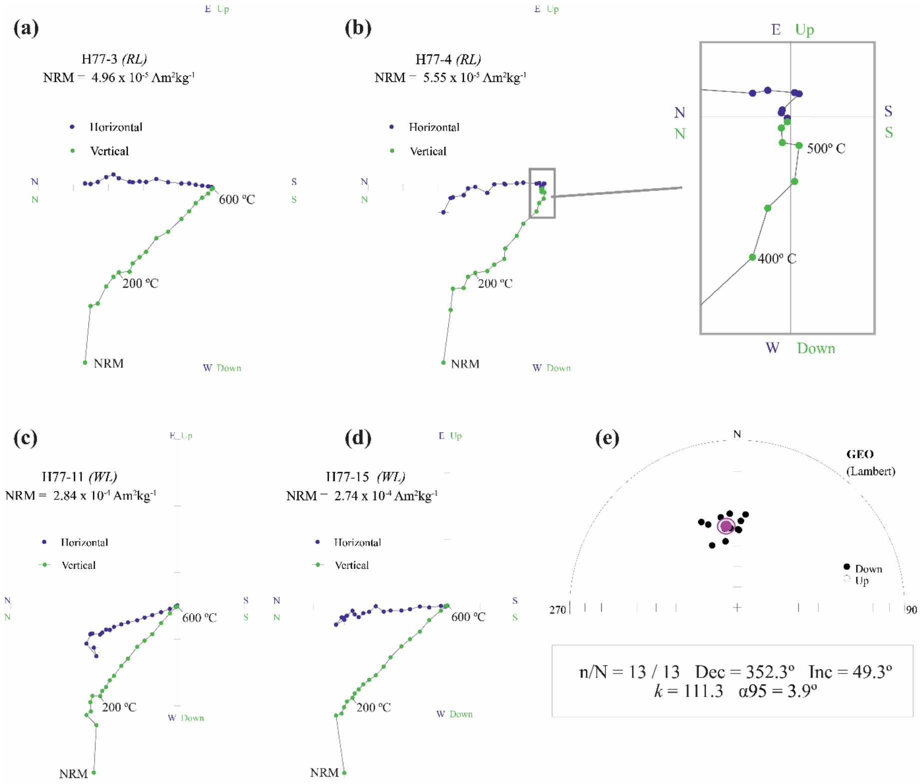

Fig. 17: (a-d) Representative orthogonal NRM thermal demagnetization plots from combustion structure H77. Green (blue) symbols represent the vertical (horizontal) projections of vector endpoints. The sample code, intensity (NRM) and type of facies studied are shown for each sample. RL = red layer; WL = while layer. For clarity, the last steps of panel b are blown up showing a high-temperature component. **(e) An equal-area projection of all ChRM directions**, with the mean direction calculated at sample level and the α95 confidence circle (in pink). n/N = number of specimens considered / analyzed; Dec. = declination; Inc. = inclination; k = precision parameter; α95, semi-angle of confidence.

Regarding the magnetic properties, the WL maximum values of magnetization in the isothermal remanent magnetization (IRM) curves are higher than those from the RL. A similar trend is detected in thermomagnetic curves, in which a decreasing pattern in depth is also observed (Fig. 18a–j). The main magnetic carrier is, in all cases, a slightly substituted magnetite with Curie temperatures (TC) around 580 ºC. In general, there is a progressive decrease in the intensity of magnetization as a function of depth. Although the RL subsamples show some variability, their values are within the same order of magnitude (Fig. 18a–e). The decrease in the magnetization intensity as a function of depth is especially clear in the ash subsamples (Fig. 18f–j). In both facies, a total or very high degree of reversibility is observed, perhaps with the only exception of the deepest WL sample (Fig. 18i). In any case, the WL is magnetically more intense than the RL since it underwent higher temperatures generating a higher concentration of ferrimagnetic (s.s.) minerals (magnetite).

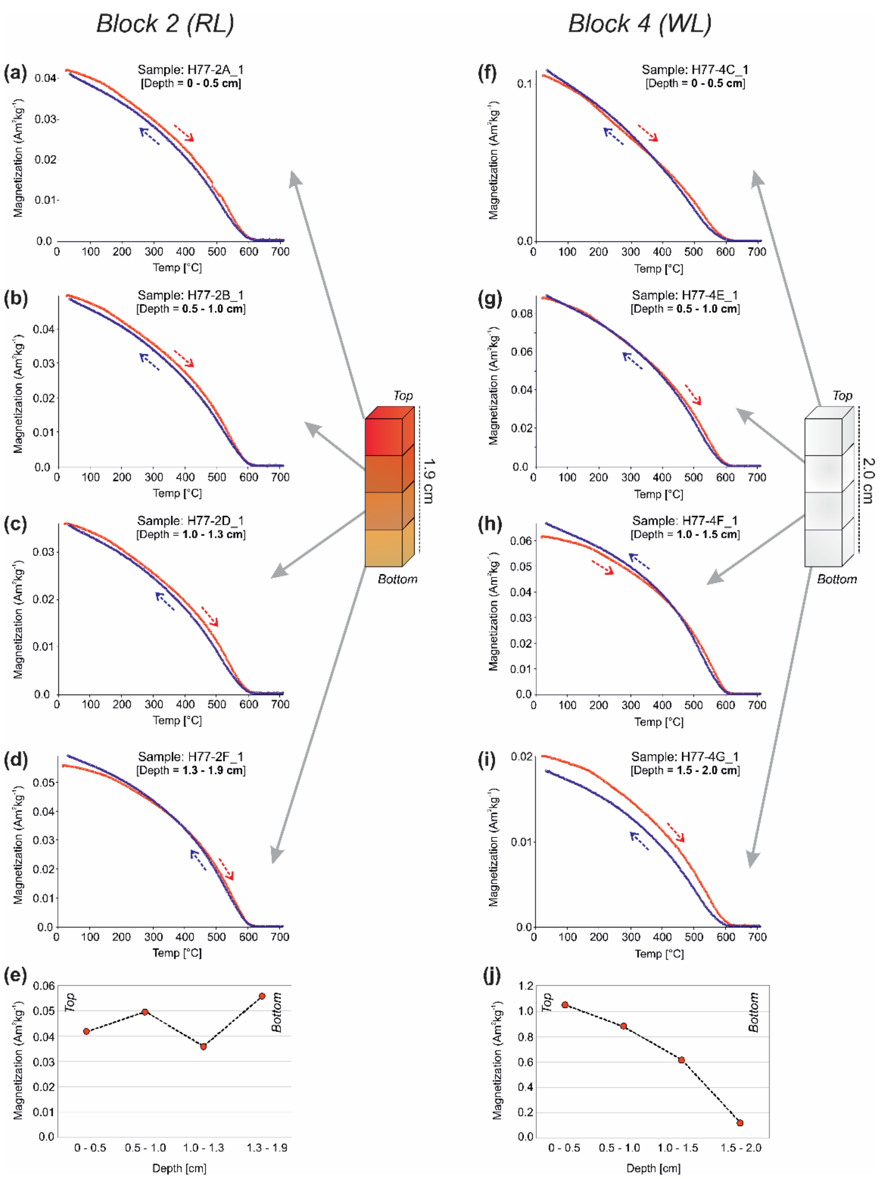

Fig. 18: Thermomagnetic curves analyzed as a function of depth for (a-e) block 2 (red-layer or RL) and (f-j) block 4 (white layer or WL). Sample code, depth and magnetization intensity are indicated for every sample. Heating (cooling) cycles are shown in red (blue) with their respective arrows. Panels e and j represent the variation of the magnetization intensity at room temperature for the heating cycle of every sample at different depths for both blocks.

4.4.6 Faunal analysis

The bone remains associated with and recovered from H77 are very scarce, with only 13 NR (number of remains) that are split into 11 NME (minimal number of element) and 2 MNI (minimum number of individuals) (Table 10): one prime deer (*Cervus elaphus*) and one rabbit (*Oryctolagus cuniculus*). The remains are, for the most part, composed of long bone fragments, with a few instances of cranial or axial parts.

At a taphonomic level, all bone fragments exhibit thermal alteration, with a higher degree of surface modification in the layers closest to the heat source, as shown by the degree of burning and presence of cracks. For example, a single deer tibia was collected in 14 fire-cracked fragments (Fig. 10). However, signs of anthropogenic modification (e.g., slicing marks, scraping marks, dental imprints) are generally absent, and only five fresh fractures were recorded (Table 11).

	Abundance			Taphonomic alterations					
Taxa	NR	MNE	MNI	Thermal Alt.	Fracture fresh	Fracture dry	Mixed Fracture	Manganese	Root-marks
Cervus elaphus	3	3	1 (Prime)	3	1		2	2	
Oryctolagus cuniculus	1	1	1	1	1	4		1	
Medium size	3	1	-	3	2		1	1	1
Small size	1	-	-	1				1	
Undetermined	5	1	-	3	1			2	1
	13	6	2	11	5	4	3	7	2

Table 10: Measures of abundance and quantification of taphonomic alterations of faunal remains in H77.

Taxa	Anat. Element	Facies	Fragment	Type	Origin	Agent	Distribution	Color	Modification
Cervus elaphus	Ribs	WL	550	Thermal alt.	Fire	Anthropic	Total	Grey	Cracks
Cervus elaphus	Radius	WL	500	Thermal alt.	Fire	Anthropic	Total	Black	Cracks
Cervus elaphus	Tibia	WL	050	Thermal alt.	Fire	Anthropic	Total	Bl/G/Wh	Cracks
Oryctolagus cuniculus	Long bone	RL	050	Thermal alt.	Fire	Anthropic	Total	Black/Grey	-
Medium size	Cranial	RL	050	Thermal alt.	Fire	Anthropic	Total	Grey/White	Scaling
Medium size	Long bone	RL	050	Thermal alt.	Fire	Anthropic	Partial	Brown/Grey	-
Medium size	Long bone	RL	050	Thermal alt.	Fire	Anthropic	Total	Black	-
Small size	Long bone	WL	050	Thermal alt.	Fire	Anthropic	Total	Brown/Black	-
Undetermined	Cranial	WL	051	Thermal alt.	Fire	Anthropic	Total	White	Cracks
Undetermined	Undetermined	RL	050	Thermal alt.	Fire	Anthropic	Total	Grey/White	Cracks
Undetermined	Long bone	RL	050	Thermal alt.	Fire	Anthropic	Total	Brown/Grey	-

Table 11: Main features observed in the H77 heated bone.

4.5 Case Study II: Discussion

Our multiproxy study indicates that the H77 combustion feature represents an *in situ* pit hearth. Below, we discuss different lines of evidence from the geoarchaeological and zooarchaeological techniques applied, which provided clues about the nature of the feature, its degree of preservation, temperature estimates, and its possible use history.

4.5.1 H77: a well preserved *in situ* pit hearth

Thick ash layers (of up to 20 cm) documented in Paleolithic contexts are typically interpreted as ash dumps based on their micromorphological features (Berna and Goldberg, 2008; Meignen et al., 2007). In the case of H77, an ash dump in the pit is improbable. First, the WL filling the small depression is composed of primary plant ash. Second, in agreement with experimental data from (Aldeias et al., 2016), the RL at the surface of the depression is thicker towards the center of the combustion structure (see Salt-18-9 in Fig. 11), indicating *in situ* burning. The absence of a black layer underlying the H77 ash deposit is a notable difference from the other El Salt combustion structures, in which such black sedimentary layers are composed of charred decayed plant remains and excrements (Case Study I) (Mallol et al., 2013a). Instead, H77 contains a thick RL completely devoid of organics. This RL resembles SU XI in all aspects (e.g., lithology, components, microstructure) except for the absence of organic matter and the red color, suggesting the same depositional source.

Further evidence of *in situ* burning was obtained through archaeomagnetism. Our results clearly show that all the samples are highly magnetic and stable and that they have efficiently recorded the direction of the Earth's magnetic field at the time of the last burning and subsequent cooling. The magnetization intensity values are similar to those reported for burnt facies in prehistoric combustion structures (e.g., Carrancho et al., 2009; Kapper et al., 2014). The Qn ratio values point out that the mechanism of magnetization is most likely a thermoremanence (TRM). Furthermore, the stable orthogonal NRM demagnetization diagrams with reproducible directions and a good statistical grouping also indicate an efficient record of the magnetization through a TRM as well as good preservation of the original combustion structure. If the samples had undergone severe mechanical reworking (e.g., by trampling, bioturbation, etc.), the dispersion of the ChRM directions in the stereogram would be significantly higher with lower k values. Considering the reasonably low dispersion obtained (k = 111.3) and the age of this combustion structure (*ca.* 55 ky B.P.), the preservation level of H77 is very good.

This agrees with macro and microstratigraphic-scale observations. The contact between the RL and the WL is sharp, which is common in combustion structures (Mallol et al., 2017), and does not show any signs of post-depositional disturbance. No microscopic ripped-up clasts or mixing between the two layers was observed, except for two instances of ash embedded in the RL, which will be discussed in the fire use history section below. The absence of ripped-up aggregates from the underlying substrate speaks against hearth cleaning activities and thus incidental production of a pit (Mallol et al., 2007). Regarding the formation of the pit, it could have been intentionally excavated, or it could have been present prior to the fire as a natural depression.

4.5.2 Estimating burning temperatures

Reddening and absence of organics together point towards high-temperature combustion. Organic matter is oxidized between 500 and 550 °C, where it gets converted to carbon dioxide and ash (Heiri et al., 2001; Wang et al., 2011). At these temperatures, both fresh and charred organics disappear from the sedimentary matrix. Thus, the RL must have been exposed to such temperatures for some time. Rubification is the reddening of iron-containing soils or sediment from heat (Röpke and Dietl, 2017). Experiments have shown that organic substrates rubify less than inorganic sediments (Aldeias et al., 2016; Berna et al., 2007; Canti and Linford, 2000; Mallol et al., 2013a; March et al., 2014). Nevertheless, the temperature at which reddening occurs is unclear. Different experimental burning studies report rubification at different temperatures which taken together yield a broad range (250 °C to 800 °C) (Berna et al., 2007; Gualtieri and Venturelli, 1999; Mathieu and Stoops, 1972; Röpke and Dietl, 2017), suggesting that sediment type may be an influential variable. Some sediments show no reddening even at high temperatures (Berna et al., 2007; Canti and Linford, 2000). In an experimental study in which fires were made on the natural substrate surrounding the El Salt site, only 2 out of 25 of the resulting combustion structures yielded reddish layers at their base (Mallol et al., 2013b). One structure, with a 9 mm thick patchy RL directly underneath the ash layer, was from a fire made on artificially wet sediment, fueled with a total of 24.4 kg of pine wood for 6–7 hours (Mallol et al., 2013b). The resulting RL was interpreted to originate from mineral dehydroxylation upon fast water evaporation rather than high temperatures (Mallol et al., 2013a). The other structure yielded a 0.5 cm thick RL directly underneath the ash layer. It resulted from a fire made on very compact, inorganic sediment fueled for 3 hours (Mallol et al., 2013a). Our results from experimental lab burning of SU XI sediment, which comprises abundant black organic residues and charcoal fragments (see MFT XI), showed that rubification started at 500 °C and was strongest at 700 to 800 °C (see Fig. 15).

From the experiments described above, we can reasonably speculate that the H77 combustion structure represents three possible scenarios: a pit hearth 1) made on organics-containing sediment whose temperatures (at the substrate) may have reached at least 500 °C, or 2) made on inorganic sediment whose temperatures might have not necessarily exceeded 500 °C, or 3) made on wet sediment. The presence of microscopic horizontal fissures observed at the upper part of the H77 RL in the samples closest to the center of the structure suggest that the substrate reached high temperatures, as reported in previous experiments (Mallol et al., 2013a; Mallol et al., 2013b). As discussed below, our lipid biomarker and archaeomagnetism data also agree with this hypothesis and are both against the wet substrate scenario and the inorganic sediment scenario.

Our *n*-alkane data indicate that the RL and WL were exposed to high heat. These sedimentary layers yielded low *n*-alkane concentrations with dominant peaks at C20 and C21 indicative of degradation. A record of degradation implies that the original sediment contained some organic matter. Possible causes for degradation are either thermal (Eckmeier and Wiesenberg, 2009) or microbial (Brittingham et al., 2017).

Microbial degradation would generally affect the whole sample set, and the surrounding sedimentary facies (Lsg11 and SU XI) showed better preservation and no signs of alteration; hence microbial degradation is unlikely. Thermal degradation was shown in experimental work on *n*-alkanes of *Celtis australis* leaves, bark, branches, and twigs, which represent similar *n*-alkane patterns as the H77 assemblage with dominant peaks at C20 at temperatures higher than 350 °C (Jambrina-Enríquez et al., 2018). Another study on a combustion structure assemblage from El Salt SU X showed comparable patterns in several BL and WL (see Case Study I). By comparing our data with these results, an estimated burning temperature of much higher than 350 °C can be proposed for the H77 fire. Comparing our data to Wiesenberg et al. (2009), who conducted charring experiments with rye and maize, temperatures might have even exceeded 500 °C.

Regarding our archaeomagnetism data, the high degree of thermomagnetic reversibility recorded in the thermomagnetic curves (coincidence between the heating and cooling cycles) indicates that both WL and RL underwent high heating temperatures, most likely > 600–700 °C. Otherwise, they would not show such high reversibility upon laboratory re-heating to those temperatures as probably, their ferromagnetic mineralogy would not be stabilized. The stable and reproducible directional behavior of the NRM orthogonal demagnetization plots is also compatible with high-temperature heating.

In a single case, a p-TRM seems to have been recorded in a RL sample that would have reached a maximum temperature of 460–500 °C (Fig. 17). This might be explained by the internal temperature variability expected for simple anthropogenic combustion structures (Canti and Linford, 2000). The considerable thickness of the ashes of the H77 combustion structure (up to 5 cm) is also indicative that a significant amount of fuel was burnt, which would favor reaching high temperatures. In any case, the high NRM intensities observed, Q_n ratio values > 1, stable orthogonal NRM demagnetization plots with quite reproducible directions, and high reversibility in the thermomagnetic curves all indicate high-temperature heating and the record of a TRM. These criteria have already been observed in other archaeomagnetic studies on prehistoric fires as proof of stable remanences and well-heated materials (e.g., Carrancho et al., 2012).

In the literature, the burning temperatures of pit hearths are still being discussed. There is a consensus that pit hearths do not reach the same high temperatures as flat combustion structures (March et al., 2014; Peeters and Niekus, 2017) due to the insulating effects of the pit depression and reduced oxygen input (Mallol et al., 2017), which also renders combustion slower, incomplete and more charcoal-rich (March, 1992; March et al., 2014). Another factor that limits burning temperatures is the rapid infilling of the pit with ash and charcoal, which are both thermally insulating (Aldeias et al., 2016; Canti and Linford, 2000; March et al., 2014). March et al. (2014) report average temperatures above ground in experimental combustion structures with simple flat hearth temperatures at 335 °C and pit hearth temperatures at 273 °C. Other experimental flat combustion structures reach maximum mean temperatures of 600 °C (Bellomo, 1993) or their maximum temperatures range from 600–1000 (Bentsen, 2012, 2013; Braadbaart et al., 2012; Canti and Linford, 2000; Sievers and Wadley, 2008; Stiner et al., 1995). Evidently, higher temperatures than reported in March et al. (2014) can be reached.

Factors that seem to influence temperatures reached on the surface are the number of heatings, the quantity of fuel, conductivity of the substrate as well as the position within the combustion structure (Carrancho and Villalaín, 2011) and in the subsurface are amongst others intensity of heat, duration, sedimentary moisture and compaction (Aldeias et al., 2016).

Despite these conditions and considering our different proxies, our temperature estimates for H77 would be between 500 °C and 600 °C for the RL. These temperatures are relatively high compared to other experimental values of pit hearths but might not be impossible to reach. Even if temperatures reached are slightly lower than in the experimental flat fires, if kept burning for long enough, temperatures between 500–600 °C might be reached in the uppermost few centimeters (Aldeias et al., 2016).

4.5.3 Approaching the use history of the H77 pit hearth: Fuel and repeated use

Microscopically, the H77 plant ash observed throughout the WL samples consists of well-preserved calcium carbonate pseudomorphs of calcium oxalate in a mass of fine crystalline, birefringent, calcareous material (Canti, 2003), as has been previously described for partially dissolved and recrystallized wood ash (Canti, 2003; Shahack-Gross et al., 2008). Recrystallization of wood ash is a common diagenetic process in archaeological contexts (Goldberg et al., 2009b; Karkanas et al., 2007; Madella et al., 2002; Shahack-Gross et al., 2008; Zerboni, 2011). In H77, there is also residual reddish fibrous matter mixed with the recrystallized ash (see Fig. 13 i and j), resembling experimentally burned moss (Mallol et al., 2017). However, the color of this fibrous matter does not suggest charring or calcination. Given that the alkane signature of the WL does not indicate input of fresh plant matter (see Fig. 14), a possible explanation might be plant pseudomorphs, which are common in ashes (Mallol et al., 2017 and references therein) associated with clay that may have been coating the plant at the time of combustion (Goldberg et al., 2009a). For now, the nature of the plant fuel that was mixed with wood in H77 remains unknown.

How intense was the use of the H77 pit hearth? Considering possible volume reduction of the original ash deposit due to slight dissolution and compaction (Schiegl et al., 1994; Schiegl et al., 1996), the preserved ash volume in H77 is considerable. This could have resulted from a single, long-duration combustion event or a complex use history involving different relighting episodes. Both scenarios may involve massive, thick ash deposits (Mallol et al., 2007). Weiner et al. (2002) state that the absence of charcoal in a combustion structure and therefore the white color of its ashes might be indicative of repeated burning at the same location. H77 RL and WL contained only one charcoal fragment in sample Salt-18-8a, with a diameter of about 1 cm, fractured *in situ*, and concentrated in the upper third of the WL.

Slight reworking, relighting, or repeated use of the structure is evidenced in sample Salt-18-8b, which exhibits two ash lenses embedded in the RL, and sample Salt-18-7, which shows thin ash concentrations underlying the RL. Such evidence points to the structure's complex formation history. These ash lenses and concentrations have not been disturbed by bioturbation, so it is highly likely that they are *in situ*. According to previous experiments, relighting a combustion structure after a short time might not always show characteristic stratigraphic features and thus go unnoticed (Mallol et al., 2013b), while relighting of hearths after a long hiatus can be recognized as stacked combustion structures that either have successions of BL and WL or laminated WLs (Berna and Goldberg, 2008; Goldberg, 2003; Goldberg et al., 2009b; Meignen et al., 2007). Here, it is unlikely that there was a long hiatus between the burning events since sedimentation would have affected the entire surface of the hearth and not only a small patch within the combustion feature. It is more likely that part of the sediment from the wall of the pit fell on top of the initial ash layer and was possibly rubified upon subsequent burning.

Finally, additional information on the use history of the H77 pit hearth comes from the faunal assemblage contained in the ash deposit. Although it is too small to draw any conclusions about anthropogenic activity besides intentional burning, it seems clear that the bone remains represent animal refuse (mainly red deer) that was tossed in the flames. Unintentional burning of bone fragments that might have been lying on the surface is unlikely, as all the bone specimens are strongly heated to levels close to calcination, which has been experimentally shown to correspond to the bone in direct contact with fire (Mallol et al., 2013a; Pérez et al., 2017b). The bone could have been tossed in the fire as fuel or for other purposes or reasons.

4.5.4 Final remarks

The H77 combustion structure is located at the interface of stratigraphic units X and XI. It is embedded in stratigraphic unit XI and covered by stratigraphic unit X, suggesting a possible correlation with human occupations taking place sometime between the end of the formation of the SU XI deposit and the deposition of unit X. Archaeological excavation of El Salt SU XI has only just begun, and there is no fire record to compare or results with. If we compare H77 with the SU X fire record, which has been extensively studied (Leierer et al., 2019; Mallol et al., 2013a; Vidal-Matutano, 2016; Vidal-Matutano et al., 2017; Vidal-Matutano et al., 2018), it is one of a kind. Neither the morphology nor the temperature reached in H77 has been encountered in El Salt before. The microscopic appearance of the ashes and the fibrous material is also undocumented. Future experiments to generate ash from different plants are needed to determine possible fuel sources.

The differences in morphology between flat hearths and pit hearths are considerable. In artifacts, differences in morphology represent variability in function and hence culture and technology (Debénath and Dibble, 1994; Hunt and Bortolini, 2016). Given that combustion structures are artifacts, morphologically distinct combustion structures may indicate different functions and thus a diverse fire technology. Even though we do not know the function of H77, we can assume it is different by comparing it with ethnographic cases. Pit hearths are normally used for hide smoking (Skibo and Schiffer, 2008), charcoal burning (Zerboni et al., 2013), and cooking (Mallol et al., 2007; Wandsnider, 1997). While flat combustion structures might also be used for cooking, it is likely that the food gets affected differently by a variation in heat transfer (Mallol et al., 2017). Thus, the deliberate use of a pit hearth reflects variation in fire technology. Regarding the comparably high temperatures reached in this fire, there might have been an intent to keep this fire burning with such high temperatures. This is evidence of Neanderthal behavioral variability (e.g., Burke, 2006; Kuhn, 1995; Scott, 2011; Speth, 2010).

4.6 Case Study II: Conclusion

H77 is an *in situ* combustion structure that we interpret as an anthropogenic fire made in a pit by Neanderthal groups living at El Salt prior to the SU X occupations. Whether the pit was dug out or was a natural depression remains unknown. Our multiproxy data indicate that the fire reached high temperatures (500–600 °C in the RL) and possibly had a complex use history. The fuel consisted of a mix of wood and another undetermined plant, and during its use, animal refuse (especially ribs, radius, and tibia of red deer) was tossed in it.

So far, H77 is the only pit hearth documented at the site, which has yielded over 90 combustion features, and one of the few pit hearths documented in the Eurasian Neanderthal record. The addition of well-documented pit hearths to the Neanderthal record implies variability in fire technology and supports overall Neanderthal behavioral variability, an aspect that had not previously been explored through the fire record.

For this study, we have applied a novel multiproxy, microcontextual approach. Although soil micromorphology has been previously used to reconstruct anthropogenic fire formation processes, there are very few studies combining this technique with lipid biomarker analysis to pin down fuel sources and burning temperatures. Coupling these two techniques with archaeomagnetism is also unprecedented. In order to advance our knowledge on the function and technological variability of Neanderthal fire, more Middle Paleolithic combustion structures need to be studied using similar multiproxy, microcontextual approaches. For the specific case of H77, further experiments, including ones with single and multiple-use pit hearths made on organic, inorganic, and wet sediment, need to be performed to test our present hypotheses.

Case Study III

Hot Moss: Micromorphology and lipid content of burnt Weissia moss and their interest to Geoarchaeology

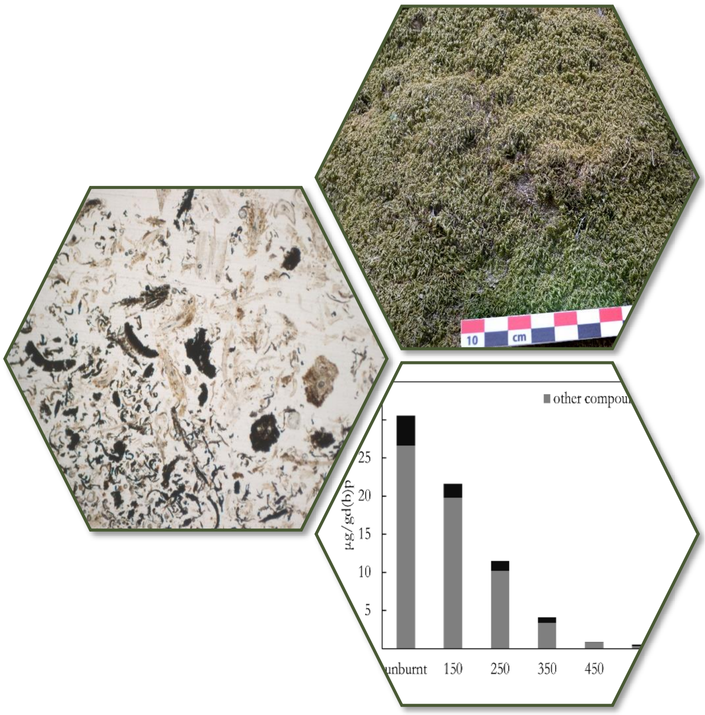

5. Case Study III: Moss

Hot Moss: Micromorphology and lipid content of burnt Weissia moss and their interest to Geoarchaeology

Lucia Leierer [a,b,*], Antonio V. Herrera-Herrera [a], Carolina Mallol [a,b]

[a] Instituto Universitario de Biorgánica Antonio González, Universidad de La Laguna, La Laguna, Santa Cruz de Tenerife, Spain.
[b] Departamento de Geografía e Historia, Área de Prehistoria (Facultad de Humanidades), Universidad de La Laguna, Campus de Guajara, La Laguna, Santa Cruz de Tenerife, Spain.
* Corresponding author: Lucia Leierer

ABSTRACT:

Despite their widespread natural distribution, mosses are rarely uncovered in archaeological contexts. They are often be overlooked due to their small size and poor preservation potential. In the realm of anthropogenic fire and pyrotechnology, peat moss has been documented as fuel, but ordinary moss has not. Peat has been shown to be a common, handy fuel used for at least 2000 years (Andriesse, 1988). Micromorphological investigations of combustion structures from the El Salt Middle Paleolithic site in Spain have revealed the use of an unknown fuel source exhibiting a moss-like appearance. Here, we carried out a comprehensive experimental study in which mosses from the Weissia species were burnt and analyzed using micromorphology and lipid biomarker analysis with the aim to create reference material for future comparison with archaeological material. The lipid compounds identified provide insight into the thermal alteration of mosses and highlight a series of potential Weissia moss biomarkers. Regarding micromorphology, similarities could be drawn between the experimental charred moss and the undetermined archaeological particles observed in the combustion structure samples from El Salt. However, these were insufficient for determination. Our data contribute reference material to an ever-growing body of experimental samples for studies on archaeological combustion features and for archaeological research at large.

5.1 Case Study III: Introduction

What we broadly call mosses are approximately 14,000 species belonging to the taxonomic division of Bryophyta (Asakawa et al., 2013). Bryophyta are placed into the group of bryophytes together with marchantiophyta (liverworts, 6,000 species) and anthocerotophyta (hornworts 300 species) (Asakawa et al., 2013). Bryophytes are present everywhere globally, except in the sea (Asakawa et al., 2013). Mosses are non-vascular flowerless plants; thus, they belong to the simplest land plants (Klavina et al., 2015) but are essential elements for ecosystems (Klavina et al., 2015). Most mosses are small-sized, with their plant bodies reaching only a few centimeters in length (Sharma, 2014). Mosses do not possess roots, stems, or leaves but instead have rhizoids as roots, axis as stemlike structure, and phylloid as leaflike structures (Koch, 1956; Sharma, 2014).

From a biochemical viewpoint, mosses are not the focus of many studies. Some species have been studied for secondary metabolites (Dembitsky, 1993), and alkane content was studied for biochemistry and paleoclimatology (Baas et al., 2000). Chemically investigated moss species are calculated to be less than 2 % (Klavina et al., 2015; Markham, 1988). Additionally, lipids in mosses have not reached much attention (Klavina et al., 2015).

In archaeological contexts, mosses are rarely uncovered. Mosses are best preserved in anoxic, waterlogged conditions and are thus only sporadically recovered from archaeological deposits (Reitz and Shackley, 2012). Mainly, mosses have a poor preservation potential since they do not contain lignin, and their spores are not protected by sporopollenin (Reitz and Shackley, 2012). Furthermore, mosses might go unnoticed by excavators as a result of their delicate structure or because sampling strategies are unsuitable for their recovery (Reitz and Shackley, 2012). So far, the record of mosses in archaeological contexts is small, which is probably due to their preservation potential and recovery methods. Mosses have been recovered as cushion wrapped around handles of flint, daggers, and scrapers (Dickson, 1973; Henshall, 1964), as stuffing material for plugging cracks in timbers (Clark, 1971), as packing or bedding material (Dickson, 1973; Seaward and Williams, 1976) and as caulking material for boats (Allison and Godwin, 1947; Dickson, 1973; Dickson et al., 2013; Dickson and Ransom, 1968; Sheppard, 1922). Even Ötzi, the iceman, was found with 75 different species of bryophytes, including a few found in his bowels, which were informative about his last route that is believed to have been from the south by climbing up through the Schnalstal valley.

So far, mosses have never been uncovered as fuel, which could be due to limitations in the recovery methods. Research into the fuel of archaeological fire usually involves specialists in charcoal and phytolith analysis, and moss does not contain woody tissue, rarely phytoliths or any easily recoverable structures (Reitz and Shackley, 2012; Thummel et al., 2019). However, considering that peat, which is an accumulation of partially decayed organic matter containing peat mosses (Sphagnum), has and still is used as fuel in its dry state (Andriesse, 1988; Spedding, 1988), other kinds of mosses could also have been used as fuel in the past.

Unidentified plant matter exhibiting a moss-like appearance was observed in micromorphological thin sections from the ash layer of H77, a combustion structure from SU XI at El Salt Middle Paleolithic site in Spain. The microscopic plant matter showed a mix of crescent-shaped fibrous structures resembling clayey pseudomorphs after plant matter and recrystallized calcitic ash. These features showed recognizable similarities to thin sections from the ash layer of an experimental combustion structure resulting from a fireplace made on top of mossy and grassy topsoil (Mallol et al., 2017). The experimental combustion substrate contained charred plant matter that included delicate, undulating, intertwined plant structures (see Mallol et al., 2017 Fig 31.6 f). A microphotograph of a single moss axis with phylloids from the experimental combustion structure, burnt at temperatures below 200 °C, showed similarities with the unidentified plant tissue observed in the archaeological H77-ash layer (see Mallol et al., 2017 Fig 31.1 c). The addition of moss to Neanderthal fires, whether as fuel, accidentally attached to firewood, or merely as a part of the underlying natural substrate, is a likely possibility given the widespread natural presence of mosses in the Northern hemisphere. Identifying their residue in archaeological contexts would provide valuable clues to site formation, settlement patterns and pyrotechnological behavior, and the landscapes and vegetation associated with Neanderthal occupations.

An experimental approach is needed to interpret our archaeological samples. To the best of our knowledge, there is no published data (botanical or other) on the micromorphology or lipid content of burnt mosses. This study aims to create a reference collection of burnt moss for micromorphological and lipid biomarker analysis.

In this study, a moss sample of the genus Weissia was collected from the vicinity of the El Salt site and burned in field and controlled experiments at different temperatures. It was then analyzed using micromorphology and lipid biomarker analysis and compared with the archaeological ash samples of combustion structure H77.

5.2 Case Study III: Materials

Our experiments were carried out using moss growing in the vicinity of the El Salt site, ascribed to the genus Weissia. The genus Weissia belongs to the family Pottiaceae and is a xerophytic moss adapted to dry habitats while readily absorbing water (Malcolm and Malcolm, 2000; Stoneburner, 1985). The moss genus Weissia includes several species, each of which have been defined and described taxonomically and morphologically. Weissia mosses have not been examined under biochemical aspects, so this study is essential to create a reference database for this moss genus. Likewise, in the family of Pottiaceae, only three moss genera were studied under chemical aspects (Aboutabl et al., 1999; Üçüncü et al., 2010; Yamasaki et al., 2007).

A 15 cm x 15 cm bushy patch of green moss of the genus Weissia (family Pottiaceae in group Bryophyta) was peeled off a limestone boulder (see Fig. 19) and stored at -20°C until further analysis. Subsamples obtained from this piece of moss were separated into pieces for micromorphological analysis and lipid biomarker analysis. For micromorphological analysis, two pieces of moss were burnt at 350 °C and 550 °C, respectively. For lipid biomarker analysis, five samples of approximately 1 g were fired in steps of 100 °C from 150 °C to 550 °C, and one 0.2 g piece was left unburned.

Three experimental moss fires were conducted in the field, and two of these were chosen for lipid biomarker analysis. They were burned on top of aluminum foil and serve as comparative material for lipid biomarker analysis. The reason for using these field experiments for biomarker analysis besides our controlled burnings was to mimic archaeological, and thus uncontrolled, conditions and assess the likelihood of recovering useful moss biomarkers. These field experiments also helped us to observe the combustibility of common mosses. The moss was extracted as fresh samples from the limestone boulder and was subsequently burned. Due to the arid summer conditions on-site, the moss was pre-dried but still had an overall green color with patches of dry brown fibers. Pieces of incipient soil and small fragments of the limestone boulder were attached to the rhizoids of the moss. One experimental fire (Moss Fire 3, m3) was ignited with several matchsticks until most of it was charred. Apart from that, it exhibited a few patches that were brownish-green and seemingly unburnt, and the tips of some moss fibers were calcined. Moss Fire 4 (m4) was burnt differently to ensure complete burning of the moss. A batch of moss was placed on aluminum foil and stacked up with a layer of dried pine needles first and then a layer of dried twigs. The fire was ignited with a lighter and burned to completion, resulting in the moss, pine needles, and twigs being charred and calcined. The moss was mostly charred with areas of calcination, while the pine needles and twigs were mainly calcined. For analysis, Moss Fire 4 was preferentially subsampled to include only moss particles and excluded any twigs or pine needles.

The samples were then prepared and analyzed following the steps described in the materials and methods chapter.

Fig. 19: Moss sampling location and appearance.

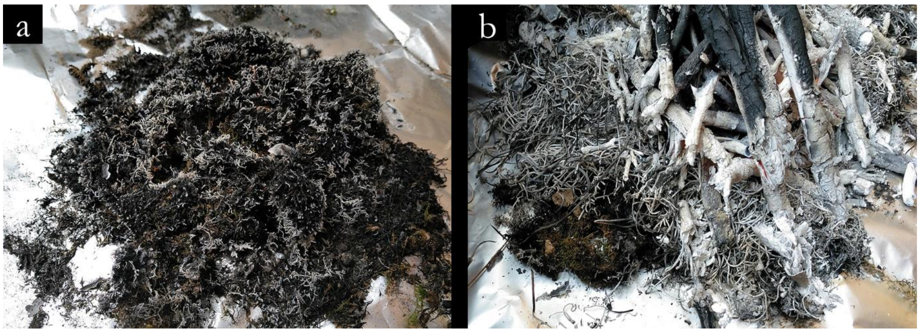

Fig. 20: Experimental moss fires burnt in the field. a) Moss Fire 3 (m3) ignited and burnt with several matchsticks; b) Moss Fire 4 (m4) burnt with pine needles and twigs. Here, the moss is seen as the lowest layer with predominantly charred fibers, whereas pine needles and twigs on top of the moss are predominantly calcined.

5.3 Case Study III: Results

5.3.1 Physical changes after burning

The sampled moss was dry due to the arid summer conditions of 2019 at the site of El Salt, which is in Alcoy, Spain (see Fig. 19). The moss had been growing on the limestone rock for several years, and an incipient, thin soil that was present at the interface had adhered to the moss rhizoids.

The moss burnt for micromorphological analysis exhibited a homogenous black color at 350 °C and a whitish-beige color at 550 °C (see Fig. 21). The moss fibers stayed intact since the samples were left undisturbed after burning. At 350 °C, traces of the soil adhering to the rhizoids of the moss were brown, and at 550 °C, the remains of the soil were slightly reddish-brown.

The moss burned for the lipid biomarker analysis showed changes in weight and appearance. Weight-loss was contingent on burning temperature, from 7.3% to 55.4% between 150 °C and 450 °C, and in total 48.1% weight loss at 550 °C.

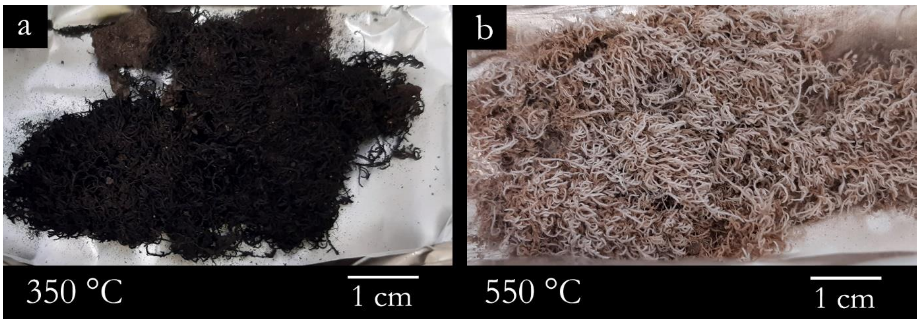

Fig. 21: Moss burnt for micromorphological analysis in the muffle furnace at a) 350 and b) 550 °C.

After drying the sample for biomarker analysis, the moss was still green and exhibited no shrinkage. Following the first stage of burning at 150 °C, the moss morphology mainly resembled fresh moss but was dried entirely and looked reddish-brown. Remains of the adhered soil were light brown. After 250 °C, the overall color of the moss had shifted to dark brown. The plant fibers had marginally shrunk, and the incipient charring process had darkened the plant fibers as well as the adhering soil to a darker brown color. At 350 °C, the moss was black, while the soil remained dark brown. The fibers had shrunk more. At 450 °C, no apparent difference from 350 °C was noted except for incipient calcination at the tips of a few fibers. A drastic change was evident at 550 °C, where most of the moss fibers were calcined, were whitish-beige in color, and had shrunk. The remaining soil was black.

Moss	wt before burning [g]	wt after burning[g]	wt loss [g]	wt loss [%]
150	1.0277	0.9526	0.0751	7.3
250	1.0524	0.8665	0.1859	17.7
350	1.0304	0.6509	0.3795	36.8
450	0.9896	0.4417	0.5479	55.4
550	1.0087	0.5235	0.4852	48.1

Table 12: Weight loss of moss while burning at different temperatures.

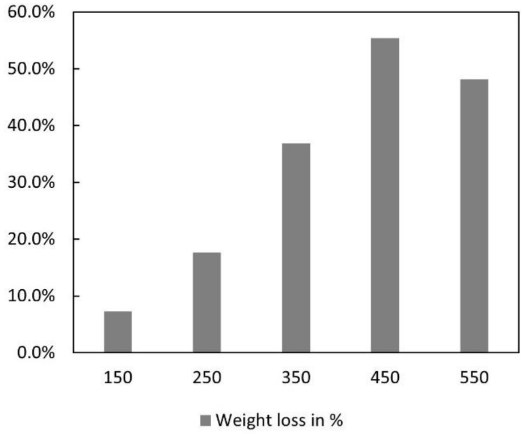

Fig. 22: Weight loss of moss after burning at different temperatures in wt%.

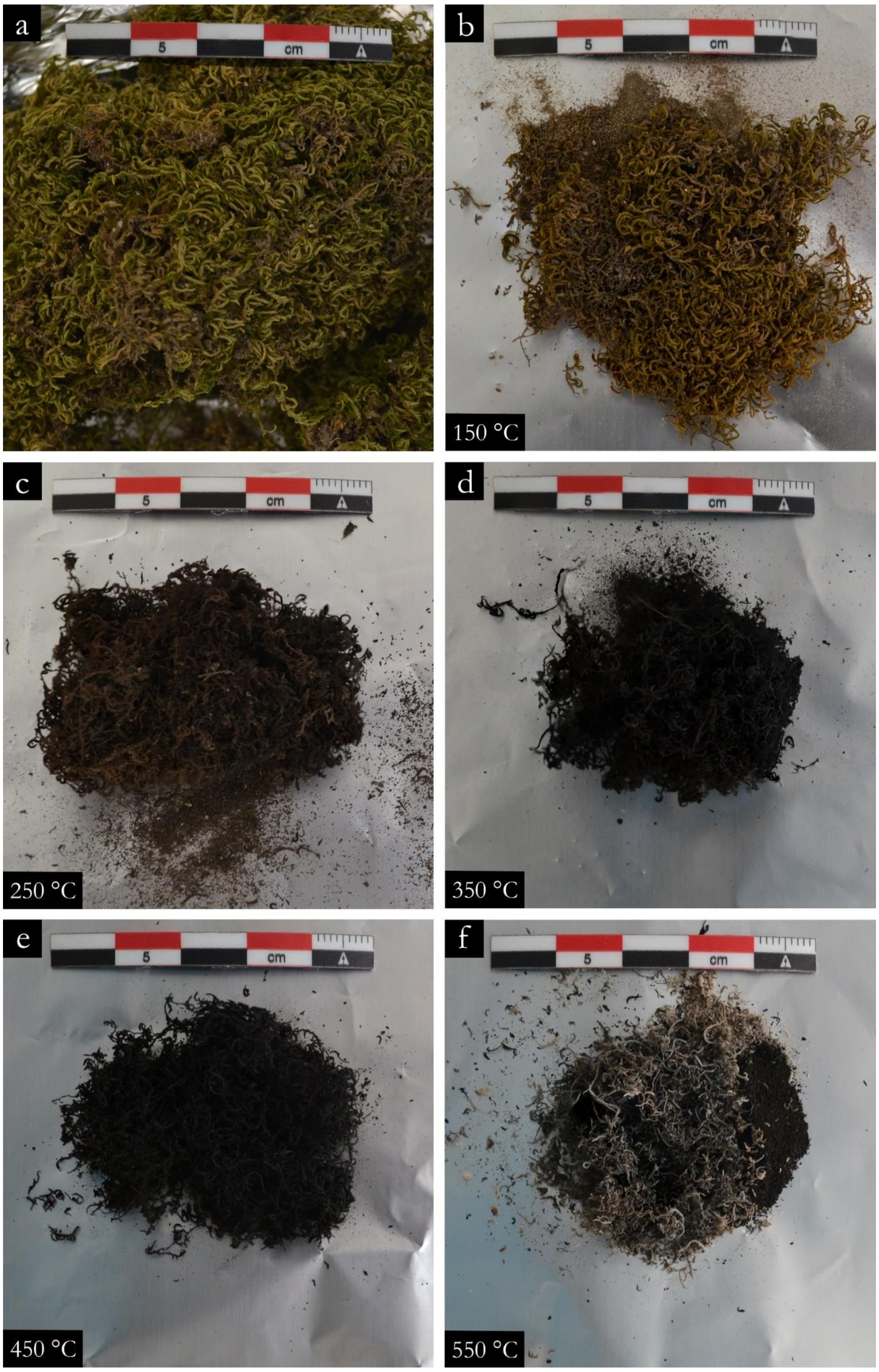

Fig. 23: Moss of the genus Weissia, a) after drying, b-f) burnt at different temperatures in the muffle furnace ranging from 150 to 550 °C as preparation for lipid biomarker extraction.

5.3.2 Micromorphological analysis of burnt and calcined mosses

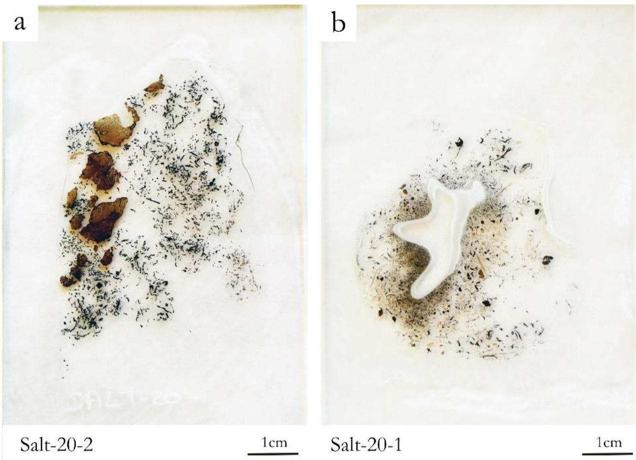

Fig. 24: Thin section scans of experimentally produced moss burnt at a) 350 °C and b) 550 °C.

Preparation of the samples for micromorphology resulted in two large thin sections (9x6 cm), one representing the burnt moss at 550 °C (Salt-20-1) and the other representing the burnt moss at 350 °C (Salt-20-2).

While looking clearly charred at 350 °C and ashy after burning at 550 °C (see Fig. 21), the difference between charred and ashy is not as clear under the microscope (see Fig. 24 and Fig. 25). At 350 °C, the moss is evenly charred (Fig. 25 a-d), whereas at 550 °C, both charred and calcined particles are present (Fig. 25 e-j). Fig. 25e shows grading from charred to ashy moss.

The integrity of the moss fibers is well preserved in both samples; however, the degree of fragmentation of plant particles is higher in the moss burnt to 550 °C. In the sample burned at 350 °C (see Fig. 25a-d), the axis and part of the leaves (phylloids) are clearly visible (Fig. 25 a-c), although some of the phylloids are broken and not in their natural anatomical position. Other charred amorphous material and charred particles with a cell structure or pores are present in the thin section as well (Fig. 25c). Undetermined charred fragments are also very abundant. In Fig. 25d, burnt tufa/limestone aggregates from the bedrock are interspersed with charred amorphous particles.

In the moss burnt to 550 °C (Fig. 25 e-j), particle fragmentation is more dominant than in the other sample. The axis is still clearly visible, while the phylloids are detached from it and can be seen as fragments (Fig. 25e, f). Even though the sample was burned to 550 °C, there are charred particles amidst the calcined ones (Fig. 25e, f). Fragments of tufa and adherent soil show signs of burning (Fig. 25e).

According to the data obtained from the sample burnt to 550 °C, moss ash can be characterized by axis and phylloid fragments and few amorphous plant particles. Aggregates, oxalates, or druses were absent in the entire sample set.

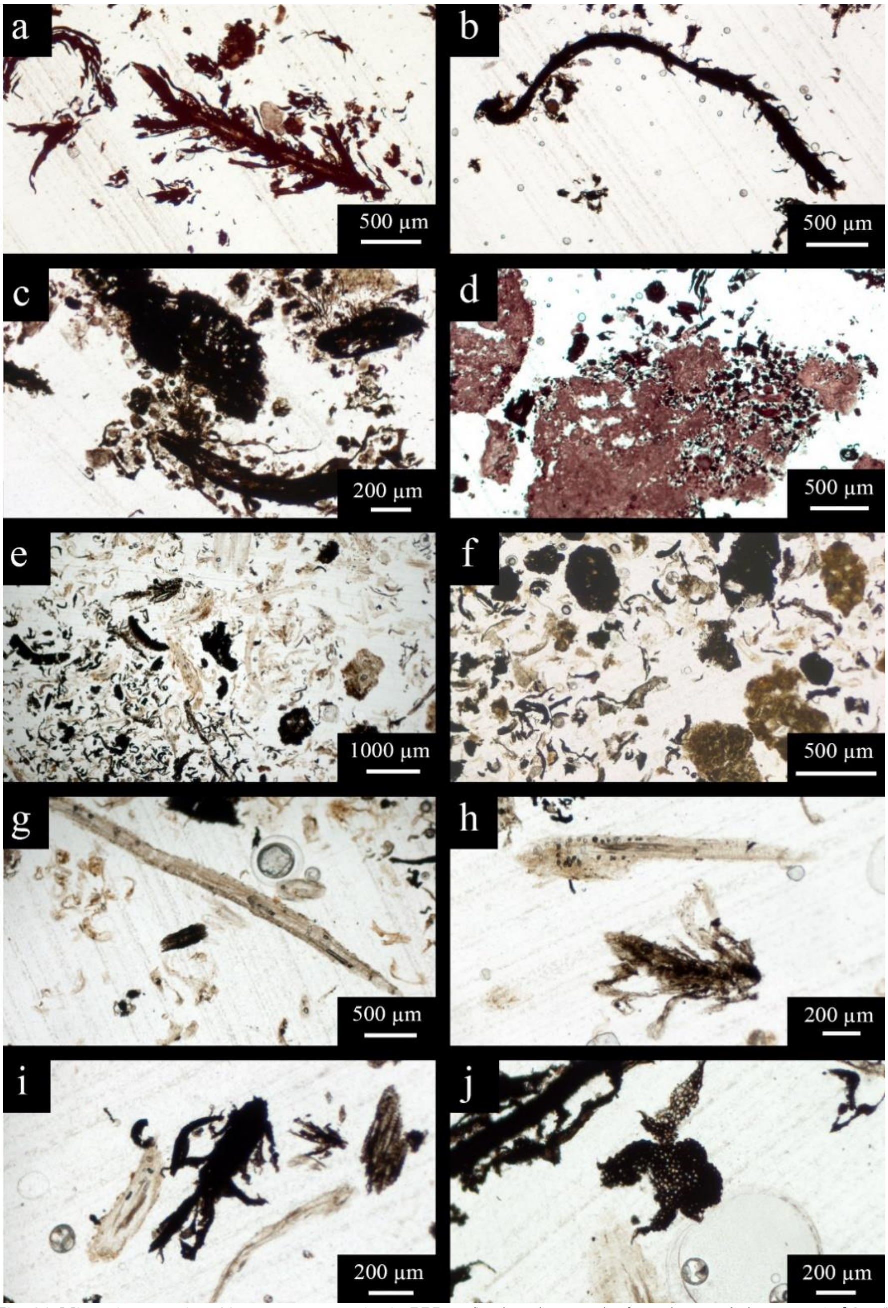

Fig. 25: Microphotographs of burnt moss samples in PPL. a-d) microphotographs from the sample burnt at 350 °C; e-j) microphotographs from the sample burnt at 550 °C. a) charred axis and phylloid of moss; b) charred axis and phylloids of moss, where tips of phylloids might be broken off; c) charred axis with few, long phylloids and other amorphous charred objects; d) heated tufa interspersed with small fragments of amorphous charred material; e) grading from charred to calcined moss fragments, axis and phylloids are present in the calcined area but are detached from another f) fragments of tufa, charred and calcined phylloids; g) the calcined axis and calcined phylloids detached from it; h) a calcined axis and a half charred/half calcined axis with phylloids still attached; i) charred and calcined axes, the charred one with phylloids still attached; j) peculiar charred structure.

5.3.3 Lipid biomarker analysis of burnt mosses

Lipids were extracted from 1) an unburnt fresh moss sample, 2) a series of samples burned in the muffle furnace from 150 to 550 °C in 100 °C intervals (150, 250, 350, 450, and 550) and 3) two experimentally produced moss fires in the field (m3: Moss Fire 3, m4: Moss Fire 4).

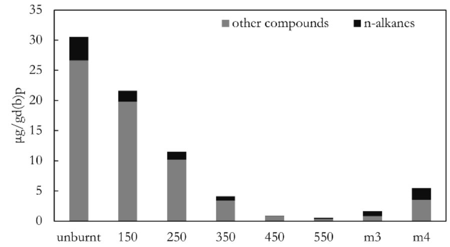

Fig. 26: Weight of all compounds extracted at different stages of burning (unb: unburnt, 150: 150 °C, …,550: 550 °C) and of two experimental fires (m3: Moss Fire 3; m4: Moss Fire 4). The weight in µg per gram of dry sediment is depicted for *n*-alkanes in black and for other components in grey.

After lipid extraction, the weight of all the extracted compounds was summed up in µg per gram of dry plant (µg/gdp) as well as µg per gram of dry burnt plant (µg/gdbp), resulting in the total lipid content. In the graphs, the concentrations are given in µg/gd(b)p, since both unburnt dry and burnt dry plant is included. In Fig. 26 and Fig. 27, the total lipid content was divided into *n*-alkanes and the remaining compounds. The total weight of all compounds in the unburnt moss sample was 30.5 µg/gdp. The burnt samples had a lower total lipid content that decreased with increasing temperature. The sample burned at 150 °C had a lipid content of 21.6 µg/gdbp, decreasing to 11.5 µg/gdbp at 250 °C, 4.1 µg/gdbp at 350 °C, 0.9 µg/gdbp at 450 °C and 0.5 µg/gdbp at 550 °C. The two field experimental samples had moderately low total lipid content with m3 at 1.6 µg/gdbp and m4 at 5.5 µg/gdbp. The concentration of *n*-alkanes also decreased with rising temperatures, being proportionally lower than the rest of the compounds except at 350 and 550 °C where the n-alkanes showed higher proportions (19 and 5% n-alkanes compared to 13 and 1% other compounds) In Moss Fires 3 and 4 the proportion of *n*-alkanes is significantly higher than other lipid compounds (21 and 50 % *n*-alkanes compared to 3 and 13 % other compounds). The total amount of lipid compounds in Moss Fires 3 and 4 (1.6 and 5.5 µg/gdbp) correspond roughly to the lipid amounts reported for experimental moss burning at 350 and 450 °C.

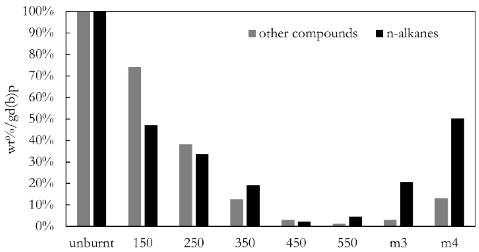

Fig. 27: Percentage of weight of extracted compounds with the unburnt sample representing 100%. Other compounds are depicted in grey, while *n*-alkanes are depicted in black.

The Weissia moss *n*-alkane profile shows a characteristic pattern (Fig. 28). In the unburnt sample, the dominant peaks are C33 and C31, with minor peaks at C20, C23, C24, and C25. At 150 °C, the profile is similar to the unburnt moss, with a decrease in C33 and C31 and a new peak at C29. C33 and C31 were still dominant, while mid-chain length n-alkanes decreased, ranging from C20 to C25.

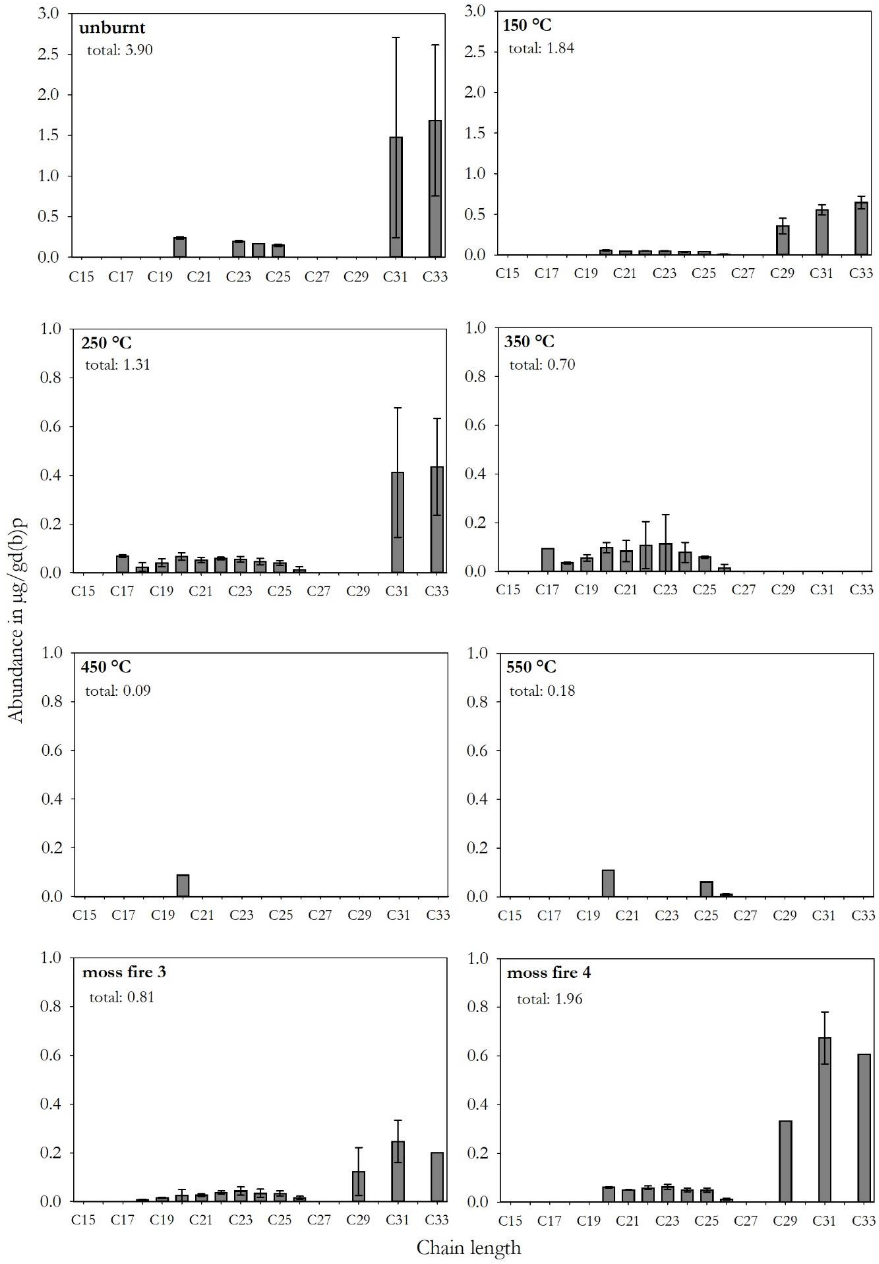

Fig. 28: *n*-Alkane profiles of samples at different stages of controlled burning and from field experiments. Graphs show name of the sample and abundances of *n*-alkanes from chain length of C15 to C33 with two different scales on the y-axis depicting concentrations in µg/gd(b)p. Error ranges are shown according to their standard deviation.

At 250 °C, despite the further decrease, C33 and C31 are still the most dominant *n*-alkanes. Mid- and lower-chain *n*-alkanes ranged from C17 through C26. At 350 °C, the long-chain peaks disappeared, and the *n*-alkane profile was dominated by low to mid-chain *n*-alkanes distributed in a smoothed curve between C17 and C26. A smoothed curve distribution was already recognizable at 250 °C and predictable at 150 °C. Another drastic change in the *n*-alkane profile occurred at 450 °C, where all peaks disappear except for C20. Similarly, at 550 °C, only the C20, C25, and C26 peaks are present, the most dominant being C20.

The two moss fires made in the field show similar *n*-alkane profiles to the unburnt moss and the burnt moss at 150 °C. Both experimental fires exhibit the long-chained *n*-alkanes C29, C31, and C33, with the highest peak at C31, followed by C33 and C29. Additionally, the mid-chain *n*-alkanes are distributed in a smoothed curve from C18 to C26 in Moss Fire 3 and C20 to C26 in Moss Fire 4.

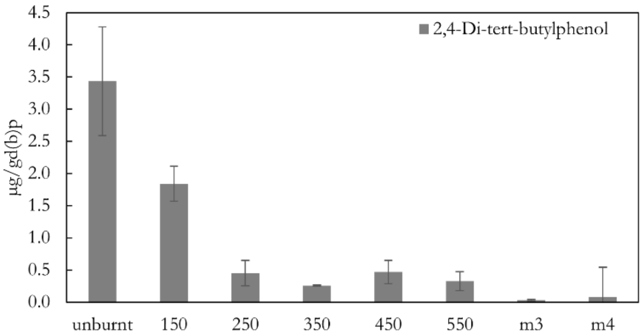

Fig. 29: The concentration of 2,4-Di-tert-butylphenol throughout the sample set. Y-axis in µg/gdp, error ranges are shown according to their standard deviation.

Regarding the total amount of lipids, the highest concentration was detected in the unburnt sample (see Fig. 26), while the highest number of different compounds was observed in the sample burned at 150 °C (see Appendix 4). Only a few compounds are present in all samples throughout the different stages of heating and the experimental field samples. One of those compounds present in all samples is 2,4-Di-tert-butylphenol, a toxic lipophilic phenol present in some organisms. The amount of 2,4-Di-tert-butylphenol is highest in the unburnt sample and decreased with increasing temperature up to 350 °C, slightly increasing at 450 °C only to decrease at 550 °C. In Moss Fires 3 and 4, concentrations were relatively low (see Fig. 29).

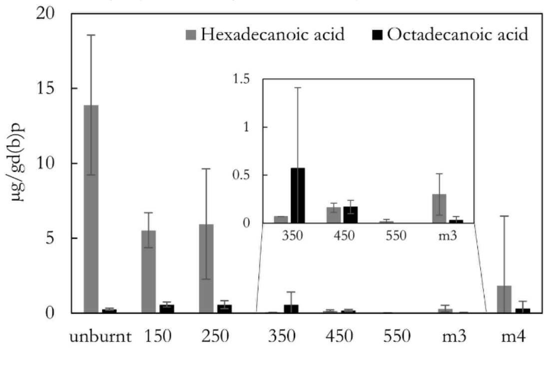

Fig. 30: Concentrations of the fatty acids Hexadecanoic acid and Octadecanoic acid within the sample set. Concentrations are measured in µg/gdp. Error ranges are shown according to their standard deviation. Please regard the zoomed in chart with lower y-axis values for a better visibility of the samples low in concentration.

Other compounds present in almost all samples are Hexadecanoic acid and Octadecanoic acid. Both belong to the group of fatty acids and are long-chain saturated fatty acids. Hexadecanoic acid (C 16:0) is significantly more dominant than Octadecanoic acid (C 18:0) in the unburnt sample. The peaks of Hexadecanoic acid decreased at 150 and 250 °C, while Octadecanoic acid peaks increased moderately. At 350 °C, the peak of Octadecanoic acid is dominant, and at 450 °C, both peaks show similar values. At 550 °C, only a low concentration of Hexadecanoic acid remained. In m3 and m4, Hexadecanoic acid was the dominant peak, and Octadecanoic acid was present in low concentrations. Other saturated fatty acids are present in lower concentrations, such as Docosanoic acid, Dodecanoic acid, Eicosanoic acid, Hexacosanoic acid, Hexanedioic acid, Nonanedioic acid, Nonanoic acid, Pentadecanoic acid, Tetracosanoic acid, and Tetradecanoic acid. Their concentrations can be retrieved from Appendix 4.

Sterols are compounds known to occur in plants, animals, fungi, and bacteria. The sterols present in the Weissia moss are Campesterol, γ-Sitosterol, and Stigmasterol, all known as plant sterols (phytosterols). Additionally, β-Sitosterol, another phytosterol, is present in Moss Fire 4. The concentration of the sterols is highest at 150 °C (see Fig. 31). The unburnt sample contains more sterols than the sample burnt at 250 °C, while the sample at 250 °C does not contain any γ-Sitosterol and from 350 °C and higher, no sterols were preserved. In Moss Fires 3 and 4, Campesterol and Stigmasterol are present, and in Moss Fire 4, β-Sitosterol was observed.

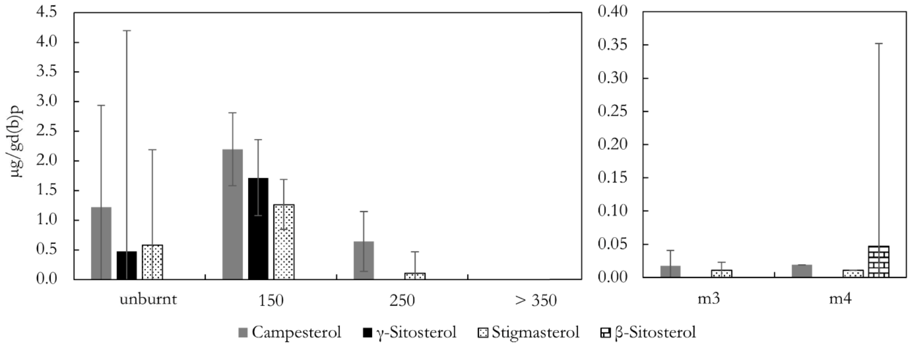

Fig. 31: Concentrations of sterols within the sample set. Concentrations are measured in µg/gdp. Error ranges are shown according to their standard deviation.

Fig. 32 depicts two compounds. Phytol is an acyclic diterpene alcohol, and Neophytadiene is a sesquiterpenoid. Both compounds have their highest concentration at 150 °C. In the unburnt sample, the peak of Neophytadiene is dominant; at 150 °C, slightly less dominant, and at 250 °C, both peaks show similar values. From 350 °C onwards, the peaks are not preserved, and in the field fires, Neophytadiene is only present in Moss Fire 4.

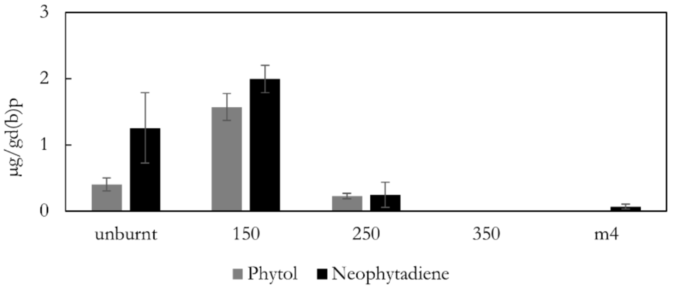

Fig. 32: Concentrations of Phytol and Neophytadiene within the sample set. Concentrations are measured in µg/gdp. Error ranges are shown according to their standard deviation.

Another noteworthy compound is Hexadecanitrile, which was encountered in both field experiments (m3, m4) and in the controlled sample at 350 °C. It is present in higher concentrations in the experimental field fires than in the controlled burning.

Other compounds characteristic for the unburnt sample of Weissia moss are: 4,8,12,16-Tetramethylheptadecan-4-olide; (3β,24R)- acetate Ergost-5-en-3-ol; Linoleic acid, Lupeol, Stigmast-5-en-3-ol, oleate, (3β, 24S)-Stigmast-5-en-3-ol Stigmast-5-ene; Stigmasta-3,5-diene; (3β,22Z)-acetate-Stigmasta-5,22-dien-3-ol; Stigmastan-3,5-diene; and 3,4-dehdihydro-Stigmastan-6.33-dien. The concentration of these compounds, as well as additional compounds at different heating stages and the field experiments, can be looked up in Appendix 4.

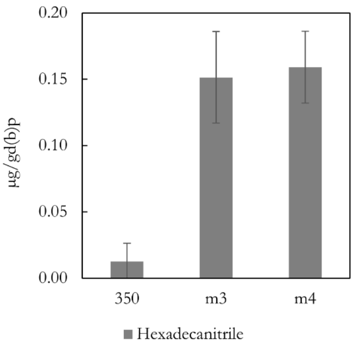

Fig. 33: Concentrations of Hexadecanitrile within the sample set. Concentrations are measured in µg/gdp. Error ranges are shown according to their standard deviation.

5.4 Case Study III: Discussion

5.4.1 Burning process

The samples' weight loss during controlled heating was between 7.3 % at 150 °C and 55.4 % at 450 °C (see Fig. 22). The weight loss at 550 °C was 48.1 %. The weight loss between 150 °C and 350 °C was gradual and deviated at 450 °C, at which there was more weight loss than at 550 °C. A study on thermogravimetric burning of peat moss concluded that there were six stages of pyrolysis reactions between 100 and 900 °C and four stages between 100 and 600 °C (Wen et al., 2020). The first mass loss at 150 °C corresponded with the loss of moisture (Wen et al., 2020), the second and third at 280 with the decomposition of hemicellulose, and at 350 °C with the decomposition of cellulose (Sophonrat et al., 2018; Wen et al., 2020). Lignin decomposes between 250 and 550 °C, with the most significant mass loss from 400 to 480 °C (Wen et al., 2020). According to this study, weight loss should be linear. The outlier at 450 °C could be attributed to remains of sediment still adhering to the sample during burning. Previous thermogravimetric sediment analyses report similar stages of pyrolysis (Wu and Luo, 2018). The first stage describes the loss of water between 40 and 160 °C and accounts for 12.15 % of the weight loss, and the second stage occurs between 160 to 250 °C and accounts for 23.36 % of weight loss. This is where light organic compounds and macromolecules of organic matter decompose (Wu and Luo, 2018). The third stage corresponds with a 10.41 % weight loss taking place between 520 to 780 °C and is attributed to the decomposition of macromolecules in organic matter, tar, and coke, previously formed during stage two (Wu and Luo, 2018). Until around 400 °C, the weight loss of moss and sediment were similar, but beyond 400 °C, the weight loss of sediment was over 12 % less than that of the moss. Thus, the higher weight loss at 450 °C could be attributed to having less adhering sediment than the samples burnt at 350 and 550 °C. The amount of sediment within the moss samples can additionally be estimated according to Fig. 23, where the least amount of sediment is visible in the sample burnt at 450 °C.

5.4.2 Micromorphology

The thin sections of moss burnt at 350 °C and 550 °C showed certain similarities and differences. The charred moss particles look similar in both thin sections, but only the thin section at 550 °C contains calcined particles. Also, the degree of fragmentation of the plant particles is higher in the moss burnt to 550 °C.

At 350 °C, all organic compounds were charred, and no fresh plant material remained. Differences between fresh and charred moss were visible in the degree of preservation of the axis and phylloids. In most cases in the charred sample, the phylloids were attached to the axis, whereas the degree of fragmentation of the phylloids varied, ranging from barely fragmented (see Fig. 25a, c) to highly fragmented (see Fig. 25b). The observed variability in fragmentation may be due to different reasons. One reason could be the differential burning of axis and phylloids due to differential freshness and moisture content. The samples used for micromorphological analysis were collected during an arid summer and showed dry domains. Thus, prior to burning, they showed zones with fresh, green axes and phylloids and zones with dried out yellow-brown axes and phylloids. Later, in the lab, they were dried at room temperature, possibly involving locally concentrated additional moisture and leading to localized delayed charring and lower degrees of fragmentation. In other studies involving charred moss, moisture content disappears between 40 and 160 °C (Wen et al., 2020). This might explain moisture retention of experimentally burned moss up to between 40 and 160 °C reported by Wen et al. (2020). Another reason for differential fragmentation could be mechanical breakage due to sample handling during the thin section manufacture process. A third reason could be natural anatomical variation (thinner, weaker vs. thicker, stronger phylloids). For now, there is insufficient evidence to explain the causes for the observed variability in fragmentation. Nevertheless, our observations and the moisture-retention capacity of moss suggest that variable moisture content at the onset leads to delayed dehydration during the burning process. This hypothesis could be tested with additional drying of the mosses at 160 °C, followed by burning at 350 °C and 550 °C, respectively. In the meantime, the influence of moss anatomical variability and possible mechanical breakage during laboratory handling cannot be ruled out.

Special attention has to be given to the unique occurrence of burnt tufa/limestone aggregates from the bedrock interspersed with charred amorphous particles as seen in Fig. 25d. Mosses are amongst the first plants to colonize rock surfaces (Jackson, 2015). Mosses attach themselves to the substrate using their rhizoids (Malcolm and Malcolm, 2000) and release weak organic and carbonic acids that enhance chemical weathering (Jackson, 2015; Lenton et al., 2012). This weathering is the basis for establishing an incipient soil (Jackson, 2015; Schaetzl and Anderson, 2005). A snapshot of this process can be seen in Fig. 25d, where weathered limestone particles were accidentally collected and charred together with the moss sample. Weathering is visible in the aggregate's porous and rough, serrate appearance, and the fine organic particles represent rhizoids and degraded older parts of the moss.

At 550 °C, a part of the moss was calcined while another part remained charred. Calcination and calcitic ash formation occur between 400 and 500 °C in oxic conditions when calcium oxalate forms and subsequently transforms into calcium carbonate upon rehydration (Canti and Brochier, 2017). Consequently, the temperature of 550 °C should be sufficient to calcinate the entire sample. As with differential fragmentation, the presence of charred particles in the 550 °C sample might be explained by differential moisture content at the onset.

The experimentally charred moss depicted in Mallol et al. (2017, p. 304, Fig. 31.1c) is very similar to the experimentally charred moss from this Case Study. Both represent axis and phylloids. The unidentified plant structures in the archaeological H77 ash layer have no similarity to neither Mallol et al.'s moss nor this moss. No charred moss axes or charred amorphous moss plant structures were identified in any of the H77 samples. Furthermore, no weathered tufa remains, such as those reported for the experimental moss sample, were identified.

On the other hand, the broken, detached, loosely distributed charred phylloids (Fig. 25e, f) resemble the reddish, crescent-shaped, thin particles documented in the H77 ash layer. They are arched in a similar way and exhibit similar lengths. However, the archaeological H77 particles are thinner (see Fig. 34 for visual comparison). As discussed in Case Study II, the archaeological particles' reddish color might originate from clay coating of the surface of plant material and thus might represent clay pseudomorphs after plant matter (Goldberg et al., 2009a; Mallol et al., 2017). A surface coating would explain the thinness of the archaeological plant matter since it does not represent the plant material itself but a coating on the plant's surface. If only the phylloids and not the axes were coated, this would also explain the missing axes in the archaeological sample. The presence of such clayey pseudomorphs in the ash layer is consistent with the associated high temperatures, at which the actual plant would have been calcined and subsequently altered through diagenetic processes (Canti and Brochier, 2017).

Accurate micromorphological identification of the plant material discovered in the H77 archaeological sample is challenging. Hypothetical clay coatings from an archaeological combustion structure are not comparable with actual calcined plant material produced under controlled conditions. The shape of the broken-off phylloids seems to coincide with the shape of the plant material pseudomorphs of the archaeological sample. However, in the absence of moss axes, there is not enough evidence to correlate the archaeological and experimental samples. Further comparisons with different reference plant matter are necessary.

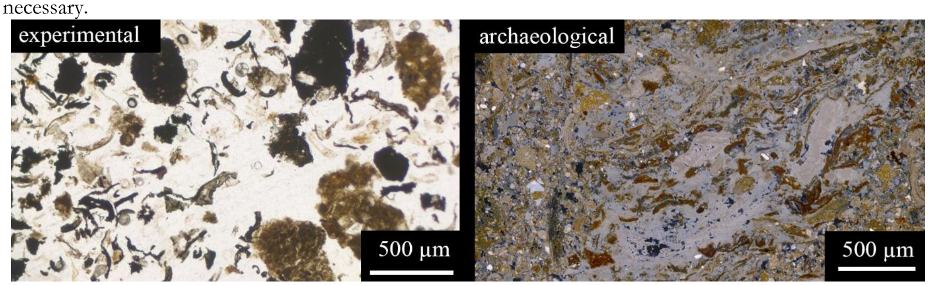

Fig. 34: A comparison between the experimentally created moss sample and the archaeological undetermined plant in the ash layer of H77. The same scale was used for both microphotographs. Experimental: Remains of broken off phylloids and burnt tufa aggregates created by burning moss for 550 °C. Archaeological: Undetermined plant particles embedded in the ash layer of the H77 pit hearth from Case Study II. More examples can be found in Fig. 13 for the archaeological material and Fig. 25 for the experimental material.

5.4.3 The chemical signature

5.4.3.1 The lipid content of Weissia moss

Before discussing the thermal alteration process of moss, it is necessary to summarize the lipid profile of the unburned moss.

The *n*-alkane graph of the unburnt moss sample shows dominant peaks at C31 and C33 and lower peaks at C20, C23, C24, and C24. This profile is different from the usual *n*-alkane profile of higher plants, which have their dominant peaks at C27, C29, and C31 (Eglinton and Hamilton, 1967). To our knowledge, this is the first-reported Weissia moss *n*-alkane profile, so it can be used as a reference for unburnt Weissia moss. The only commonly documented moss *n*-alkane content and distribution is from Sphagnum moss, which has its dominant peaks at 23 and 25 (Bush and McInerney, 2013; Nott et al., 2000; Pancost et al., 2002). Here, the peaks at 23 and 25, together with the peaks at 19 and 24, are very low and would not contribute significantly to the sediment after deposition, especially since the chemical signature in sediments is always a mixture of compounds (Evershed, 2008). Thus, Weissia moss displays a significantly different *n*-alkane profile than Sphagnum moss, and we can use this difference in lipid biomarker analysis.

Besides the *n*-alkanes, the main components present are the saturated fatty acids. Fatty acids are made up of a carboxylic acid and an aliphatic chain (Moss et al., 1995), are some of the most common lipids naturally present, and are regularly encountered in archaeological contexts (Evershed, 1993; Gunstone, 1996). Hexadecanoic acid, Octadecanoic acid, and Tetracosanoic acid, the phytosterols Campesterol, γ-Sitosterol, and Stigmasterol. These compounds are commonly found in most plants (Meyers and Ishiwatari, 1993; Mumtaz et al., 2020; Tamura et al., 1991; Volkman, 1986). The compounds 2,4-Di-tert-butylphenol, Phytol, and Neophytadiene are present in the unburnt Weissia moss, and although they are not exclusive to this genus or family, they are less common in the plant kingdom than the ones mentioned above.

5.4.3.2 Controlled experimental burning

Heating and burning of organic matter result in the thermal alteration of lipid molecular compounds. The process has been previously experimentally described and discussed, especially for *n*-alkanes and other compounds (Diefendorf et al., 2015; Jambrina-Enríquez et al., 2018; Jambrina-Enríquez et al., 2019; Knicker et al., 2013; Malainey et al., 1999). The moss data collected in this study is consistent with the data presented in the cited works. The main thermal alteration process taking place is a gradual decrease in lipid compound concentrations at each successive burning phase.

The *n*-alkane profiles of the moss samples burnt at different temperatures show typical signs of thermal degradation which are, an overall decrease in the total amount of alkanes, lower concentrations of long-chain *n*-alkanes, the dominance of even homologs, and a higher content of mid-chain *n*-alkanes (centered around C20 – C22) (Diefendorf et al., 2015; Jambrina-Enríquez et al., 2018; Knicker et al., 2013) resulting from the thermal breakdown of long-chain *n*-alkanes (Knicker et al., 2013). The hotter the burning temperature, the more the long chains break down, and the more the larger compounds disappear.

At 150 °C, two interesting changes can be pointed out. Some compounds show higher values at 150 °C than at the unburnt state. These higher values can be attributed to enrichment in particular compounds and the pyrogenic formation of new ones to the detriment of those breaking down sooner due to their higher susceptibility to heat. This process will be discussed later in more detail for each individual compound. The other change is a change in the number of compounds present at 150 °C (n=33) compared to the number of compounds in the unburnt sample (n=19) (see Appendix 4). This change can also be explained by early onset beginning degradation and transformation of compounds into new compounds that were not present in the unburnt sample.

Phenols are compounds that have one or more hydroxy groups attached to a benzene or other arene ring (Moss et al., 1995). 2,4-Di-tert-butylphenol, a lipophilic phenol, is a common natural product found in at least 169 species, including bacteria, fungi, diatoms, liverworts, pteridiphyta, gymnosperms, dicots, monocots, and animals (Zhao et al., 2020). In liverworts, the closest relatives, the compound was identified in Marchantia linearis (Kumara, 2014). In this study, we identified this compound in normal concentrations throughout the burning process up to 550 °C and in the unburnt sample (see Fig. 29). This means the compound seems not to be as susceptible to thermal degradation as other compounds. Still, degradation is present, which is almost up to 50 % between the unburnt and the 150 °C samples. Additional pyrogenic formation through thermal degradation of certain compounds, might play a significant role in the thermal alteration process, as evidenced through a higher concentration at 450 °C compared to 250 and 350 °C and the higher concentration at 550 °C compared to 350 °C.

Interpreting fatty acid compounds in archaeological combustion contexts is challenging because they are susceptible to heat (Kedrowski et al., 2009) and to biodegradation (Evershed et al., 2002; Malainey et al., 1999), so different fatty acid types and concentrations in archaeological contexts might result from a variety of processes. In the burnt moss samples, both saturated and unsaturated fatty acids were recovered. Here, only saturated fatty acids will be discussed, especially Hexadecanoic acid (C 16:0) and Octadecanoic acid (C 18:0) since unsaturated fatty acids are prone to degrade quickly in archaeological settings, and C 16:0 and C 18:0 are the fatty acids with the highest concentrations (Evershed et al., 2002; Malainey et al., 1999). During the burning process, Hexadecanoic acid decreased significantly while Octadecanoic acid first increased and then decreased (see Fig. 30). Thermal breakdown reduces the concentration and number of fatty acids in a sample (Malainey et al., 1999). Polyunsaturated and long-chain fatty acids with a chain length of 20 or more are prone to a fast deterioration (Malainey et al., 1999), whereas saturated fatty acids are least affected (Malainey et al., 1999). In an experimental degradation study, the concentration of saturated fatty acids increased with the loss of unsaturated fatty acids (Malainey et al., 1999). This could also be the case between the controlled moss sample at 150 and 250 °C and the increase of Octadecanoic acid until 350 °C.

Sterols are essential lipids in all eukaryotic organisms (Brocks and Summons, 2003), and phytosterols are sterols from plants. All the sterols identified in the controlled experiments are common phytosterols (Campesterol, γ-Sitosterol, and Stigmasterol). When heated or burned, these compounds degrade and form (pyrogenic) compounds, including oxidized phytosterols, fragmented phytosterol molecules, volatile compounds, and oligomers. (Barriuso et al., 2012; Rudzińska et al., 2009). Degradation intensity in sterols is affected by temperature and time (Rudzińska et al., 2009). Barriuso et al. (2012) state that Campesterol is most susceptible to degradation, similar to β-Sitosterol and then Stigmasterol. In the Weissia moss, no degradation was visible at 150 °C, and it shows an increase in the concentration of compounds at this temperature, possibly reflecting the degradation of certain compounds and their transformation into sterols. At 250 °C, sterols were degraded and decreased in their concentration: γ-Sitosterol could not be detected. Campesterol had degraded by approximately 48 %, and Stigmasterol had degraded by 81 %. At 350 °C, no sterols were detected. This data does not agree with the data from Barriuso et al. (2012), which showed higher degradation of Campesterol and β-sitosterol than stigmasterol and cholesterol. A possible explanation for this disagreement is that in Barriuso et al.'s study, sterols were the only components heated, so their degradation was most likely straightforward to track and control. Here, the increase in Campesterol, γ-Sitosterol, and Stigmasterol may have been partly due to contributions from degrading compounds other than sterols. Rudzińska et al. (2009) note that at a heating time of 1 hour at a point between 120 and 180 °C, a step in degradation susceptibility appears, at which compounds are degraded between half or two thirds their weight, while between 0 and 120 °C, the compounds only degrade up to 14 % on average. Additionally, a number of studies indicate that sterol degradation occurs over a temperature of 150 °C (Barriuso et al., 2012 and references therein). Thus, two likely factors prevail to explain the increase in compounds observed at 150 °C: The breakdown and transformation of other molecules into sterols and the minimal degradation of sterols themselves at 150 °C.

Other compounds found include the alcohols Neophytadiene and Phytol. The presence of Neophytadiene, a diterpene/sesquiterpenoid, and plant metabolite, has been discovered in some mosses (Aulacomnium palustre, Climacium dendroides, Dicranum polysetum, Hylocomium splendens, Pleurozium schreberi, Polytrichum commune, Polytrichum juniperum, Ptilium crista-castrensis, Rhytidiadelphus triquetrus, Sphagnum fallax, Sphagnum magellanicum, Sphagnum rubellum, Sphagnum tenellum) in different concentrations (Klavina et al., 2015). Similarly, Phytol, a diterpene/acyclic diterpene alcohol, was identified in the above-mentioned moss types (Klavina et al., 2015) and ten other types of mosses (Suire et al., 2000). Nevertheless, Neophytadiene and Phytol are not moss biomarkers. They have been identified in other plants as well. The observed thermal degradation pattern (see Fig. 32) resembles the degradation pattern observed in sterols, with a loss of compounds at 350 °C, low concentrations, and degradation at 250 °C, and higher concentrations than the unburnt sample at 150 °C. As in the case of sterols, the increase in concentrations at 150 °C can be explained by either a degradation of these compounds at higher temperatures or a breakdown and transformation of other lipids into these compounds. It is also likely that both factors affect the increase in concentrations.

5.4.3.3 Field experimental burning

Field experiments resulting in Moss Fires 3 and 4 were conducted to gain insight into the recovery potential and the potential to find biomarkers or pyromarkers of moss-related lipid compounds in a fire that is not purely made of moss.

When conducting the experiments, it became apparent that it was impossible to ignite and burn a fire solely using moss fuel. Even though the summer conditions had dried out the moss, it still retained enough moisture to hamper combustion. This obstacle was resolved by constantly reigniting the moss with matchsticks in Moss Fire 3 and using dry pine leaves and twigs as tinder to ignite and fuel the fire in Moss Fire 4. In both cases, the moss was smoldering rather than burning throughout the combustion process. These uncontrolled field conditions mark the difference between the field experimental moss fires and the controlled moss burnings. In the field, the fires were burning for a short duration with the help of a tinder, and the temperature was unknown. Nevertheless, certain similarities were found between the controlled and field experiments.

Comparing the weight of *n*-alkanes and other compounds in the field experimental burnt moss with the controlled experimental samples would broadly estimate the burning temperature of Moss Fire 3 to between 350 and 450 °C and Moss Fire 4 to between 250 and 350 °C (see Fig. 26). Considering there was another fuel (besides moss) included in the field combustions, these estimations might not be accurate. As an example, Fig. 27 shows a significantly higher percentage of n-alkanes compared to all other compounds in the charred moss (burned in the field) compared to our unburnt moss reference. This can be attributed to the presence of charred pine needles. Pine needles, which are gymnosperms, have a lower concentration of *n*-alkanes than angiosperms (Bush and McInerney, 2013), higher than Weissia moss. In Bush and McInerney (2013), angiosperms are reported to have on average 506 μg/g dry leaf, gymnosperms 46 μg/g dry leaf, and sphagnum moss 149 μg/g dry plant. Here, the unburnt moss sample contains 3.9 μg/g dry plant. No published data about the *n*-alkane content of any Weissia moss species was available, and we take our reference as a standard.

The *n*-alkane profile of the Moss Fires 3 and 4 resemble the controlled unburnt and burnt moss at 150 °C and 250 °C. However, both moss fires have their dominant peak at C31 instead of at C33 like the controlled moss samples. This profile might reflect the contribution of the pine needles since the C33 *n*-alkane peak in pine is relatively low (Bojović et al., 2012; Bush and McInerney, 2013; Cranwell, 1973; Mitić et al., 2018). Additionally to the contribution of pine in the *n*-alkanes, Dehydroabietic acid, a diterpenoid, and a characteristic biomarker for conifers was recovered (Otto et al., 2006; Otto and Simpson, 2005; Simpson and Simpson, 2012). Even though the sample was subsampled to analyze mainly moss, the contribution of pine needles was still detectable.

Regarding other compounds, the Moss Fires 3 and 4 samples show similarities with the controlled moss fire samples. This is not unusual since many lipid compounds, including different fatty acids and sterols, are found in different plant types (Meyers and Ishiwatari, 1993; Mumtaz et al., 2020; Tamura et al., 1991; Volkman, 1986). Notwithstanding, recurrent compounds in the controlled burnt Weissia moss samples, including 2,4-Di-tert-butylphenol and Neophytadiene, were also identified in the field burnt moss. Despite not being exclusive Weissia moss biomarkers, these compounds may help narrow down the kinds of plant residues present in archaeological sediment samples.

The thermal degradation of the lipid compounds present in Moss Fire 3 and 4 places both samples into a burning temperature of more than 150 °C, most likely between 250 °C and 350 °C. Both fires contain Campesterol and Stigmasterol, which in the controlled burnings disappears at 350 °C. Furthermore, Hexadecanitrile, a biomarker for biomass burning (Jambrina-Enríquez et al., 2019; Simoneit et al., 2003), was only found in the control burning sample at 350 °C and in Moss Fire 3 and 4.

5.4.4 Final remarks

Once having characterized micromorphological features and lipid molecular compounds possibly indicative of the presence of burnt moss, how do we interpret the possible presence of burnt moss residues in Neanderthal combustion structure H77? Our field burning experiments show that moss is not an efficient fuel when pursuing combustion. Even air-dried mosses retain a significant amount of moisture and are hard to combust. Therefore, the presence of burnt moss residues in archaeological contexts might be explained by other pyrotechnological behaviors or accidental burning of naturally present moss, such as in the experimental case reported by Mallol et al. (2013). Further experiments and ethnoarchaeological investigations of smoking hearths could shed light on different techniques that might require the use of moss as fuel, cover, or other pyrotechnological components.

For now, the data on Middle Paleolithic fire suggests that auxiliary combustibles, besides wood, were rarely used (Hovers and Belfer-Cohen, 2013). If this is correct, the possible contribution of mosses in the H77 pit hearth could derive from either from mosses having been present on the substrate and accidentally burnt as described in Mallol et al. (2013) or accidentally adhered to woody fuel, which would be expected if the fuel was deadwood, as previously shown for El Salt (Vidal-Matutano et al., 2017). Previous studies were showing that plant residues in archaeological combustion black layers are typically charred and that ash layers do not typically preserve charred particles or lipid molecular compounds (Buonasera et al., 2019; Jambrina-Enríquez et al., 2019; Leierer et al., 2019; Mallol et al., 2017). This suggests that the presence of charred particles or lipid compounds is unlikely for H77, which consists of thick ash layers that reached high temperatures. Lipids of other fractions, besides *n*-alkanes, were not analyzed in the H77 ash layer because the low concentration of n-alkanes, due to thermal degradation, present in this layer implied the likely absence of more polar lipid compounds (see Fig. 14) (Cranwell, 1981). Accidentally adhered moss would more likely result in clay pseudomorphs after total combustion of the organic matter. Alternatively, the Middle Paleolithic fire record conceals unexplored complexity that has gone overlooked due to the lack of microscopic and biomolecular approaches. Future microcontextual investigations of different Middle Paleolithic combustion structures could resolve this issue.

5.5 Case Study III: Conclusion

This study has provided the first reference of unburnt and burnt Weissia moss and its characteristic thermal alteration profile. It has also shown that it is possible to identify burnt moss using micromorphology and lipid biomarker analysis. Under the microscope, moss structures are recognizable as long as anatomical connections are preserved to some extent, such as the presence of phylloids attached to their axes. Chemically, the presence of specific lipid compounds such as Neophytadiene, Phytol, and 2,4-Di-tert-butylphenol might point to the presence of Weissia moss, although these are not taxonomically exclusive, and identification requires other proxies. Statistical analyses of the obtained biomarkers as well as isotopic analysis of the fatty acids C16:0 and C18:0 might aid in distinguishing the presence of mosses in archaeological sediments. This highlights the need to conduct additional experiments involving mosses in the context of combustion structures as well as to explore additional ethnoarchaeological data on the uses of moss in combustion contexts. Further experimental studies might be necessary to burn other plant material surrounding the site and analyze their microscopic and molecular characteristics.

General discussion

6. General discussion

The results of our microcontextual investigation of Neanderthal combustion structures from El Salt have provided information regarding Neanderthal pyrotechnology and settlement patterns, as well as paleoenvironmental information relevant to Neanderthal adaptations. This discussion is divided thematically into different subsections. I first summarize the main results from three case studies with emphasis on how they may relate to relevant aspects of Neanderthal behavior and paleoenvironments. Then, I present a general discussion centered on the way in which these results, in combination with other behavioral proxies, may help advance current debates on Neanderthals and the relevance of the methodology applied in this thesis. I end the discussion with future perspectives for further research on the Neanderthal combustion features from El Salt and elsewhere.

6.1 Summary of Results

In Case Study I, a systematic microstratigraphic analysis was conducted to study a combustion structure assemblage from stratigraphic unit Xb. The objectives were to explore the formation of the combustion structures, identify isolated occupation episodes, assess whether the occupations associated with the combustion structures were low impact and short-term, and estimate a time period between successive occupations. The results from applying high-resolution geoarchaeological methods to the sediment of combustion structures were significant. The combustion structures were formed through anthropogenic burning on top of an organic-rich natural surface. This surface, consisting of angiosperm leaves, including Celtis trees, and herbivore coprolites, was charred and blackened in the process of combustion. Fuel for the fires was gathered away from the site. At least four successive occupation events were identified, all of which generally being low impact. Due to the formation of organic-rich soils prior to each combustion episode, it is estimated that enough time had elapsed in between occupation episodes. According to the state of the charred organic soil, occupations took place most likely in winter, spring, or summer.

In Case Study II, a microcontextual and multidisciplinary approach was carried out to obtain high-resolution data of a possible pit hearth. The main objectives of that Case Study were to examine the integrity of the combustion structure and the formation of the pit hearth, whether it was intentionally dug out or placed in a natural depression. The application of the multidisciplinary methods provided significant results, the combination of which allowed most of the research questions to be answered. The combustion structure was confirmed to have been placed *in situ* in a depression within the stratigraphic unit XI sediment. Each method that was applied confirmed that the fire reached high temperatures of over 500 °C in the underlying sediment. The pit hearth might have had a complex use history involving animal refuse tossed in the flame, mixed fuel sources including wood and another unidentified source, high temperatures, and possibly long burning times. This evidence reflects pyrotechnological variability and, thus, Neanderthal behavioral variability. Important to note here is the thickness of the ash layer compared to the ash layers of the first Case Study. Whereas the thinness of the white layer in Case Study I point towards a low impact, short-term human occupations, in Case Study II, the thick ash layer might suggest a longer-term occupation (Mallol et al., 2007; Meignen et al., 2008; Wattez, 1992). This might point to a change in settlement dynamics between stratigraphic units X (Case Study I) and XI (Case Study II) (see Chapter 6.2.1).

Case Study III was motivated by the undetermined nature of the pit hearth's ash deposit. A set of experiments was performed to compare archaeological data with experimentally heated mosses, which were possible fuel sources based on the presence of conspicuous fibrous, delicate microscopic structures observed within the ash deposit samples from Case Study II. Micromorphology and lipid biomarker analysis were carried out on experimentally burnt mosses, and the resulting data were compared with the archaeological counterpart. The results show that moss input in sedimentary residues from an anthropogenic fire can be identified micromorphologically under certain conditions. In the case of the H77 pit hearth, the presence of moss is possible but could not be ascertained. From a biomolecular perspective, identification of specific lipid compounds may point to the presence of Weissia moss, but these cannot be considered as distinct biomarkers. If future research corroborates the presence of moss in the H77 pit hearth, the question remains as to the pyrotechnological role of this plant. Our experimental observations suggest that it is not an efficient fuel, and explanations such as accidental input (moss adhered to woody fuel, moss present on the soil substrate), a smoke-related fire function, and others need to be contemplated. This study provided a reference dataset of the mentioned moss-related lipid compounds, their thermal degradation profile, and their pyrogenic byproducts. This data is valuable for future biomolecular investigations of sedimentary fire residues.

6.2 Contribution to current debates on Neanderthal behavior

6.2.1 Group mobility and settlement patterns

Taken together, the results of the three case studies touched on several relevant aspects of Neanderthal behavior. One relates to group mobility and settlement patterns. The results from Case Study I show a series of at least four consecutive, short-termed and low-impact occupations with enough time between them for wildlife to occupy the site, reflecting high group mobility. On the other hand, the results from Case Study II document a Neanderthal combustion structure that was fueled for a longer time than what we had observed among the structures related to SU X's short occupations. As discussed below, whether this difference reflects a difference in occupation duration (brief bivouac-type camps vs. occupation lasting several months) or not remains unknown.

Our definition of short-and long-term occupations primarily originates from ethnographic data by comparing modern hunter-gatherers with Paleolithic groups (Binford, 1980; Kelly, 1983). According to ethnographic observations, long-term occupations are characterized by an intra-site spatial organization of activities, site maintenance through secondary dumping areas (Bartram et al., 1991; O'Connell et al., 1991), and long-time refueling of combustion structures (Mallol et al., 2007). Archaeologically, long-term occupations are characterized by combustion structures with thick ash layers (Meignen et al., 2008; Wattez, 1992), high density of bone remains (Picin and Cascalheira, 2020), high artifact density, on-site production of lithic materials (Kuhn, 2013; Surovell and Brantingham, 2007), and spatial organization of the living space (Picin and Cascalheira, 2020). Cleaning and maintenance activities can also be attributed to long-term occupations (Binford, 2002; Spagnolo et al., 2018; Stevenson, 1991; Vaquero, 2012; Vaquero et al., 2015), resulting in raked-out hearths (Goldberg, 2003; Kuhn et al., 2009; Meignen et al., 2007; Schiegl et al., 2003). Short-term occupations are characterized by low-density deposits, high frequencies of transported and modified tools (Kuhn, 2013; Surovell and Brantingham, 2007), limited *in situ* knapping and butchering, low impact, no spatial organization of the site (Picin and Cascalheira, 2020), and carnivore damage on the bones (Vaquero, 2012; Yellen, 1991). Hearths from short occupation contexts are flat, simple, and exhibit thin ash layers (Mallol et al., 2007; Martínez-Moreno et al., 2004; Vallverdú Poch et al., 2012; Vaquero and Pastó, 2001; Zieba et al., 2008).

The majority of Middle Paleolithic sites have been interpreted as short-term occupations (Cep and Waiblinger, 2001; Conard and Prindiville, 2000; Galván et al., 2014a; Hovers, 2001; Lourdeau, 2011; Machado et al., 2013; Machado et al., 2015; Machado et al., 2016; Machado and Pérez, 2015; Marks and Chabai, 2001; Moncel et al., 2011; Mora et al., 2004; Rivals et al., 2009a; Roebroeks and Tuffreau, 1999; Rosell et al., 2015; Straus, 1982; Vallverdú et al., 2005a; Villaverde et al., 1996; Wallace and Shea, 2006). However, a few examples of possible long-term occupations have been documented, such as units XI-VIII in Kebara (Meignen et al., 1998; Meignen, 2019; Speth et al., 2012), Abric Romaní Level J (Vaquero, 2012), Aragó Cave Level G (Rivals et al., 2009b), and Saint-Césaire Level Egpf (Thiébaut et al., 2009).

So far, research at El Salt conforms to the characteristic short-term occupation settlement patterns documented for Neanderthals. Specifically previously examined SU Xa, which targeted palimpsest dissection through a multiproxy approach to elucidate settlement patterns (Machado and Pérez, 2015; Molina Hernández et al., 2010) and corroborate previous evidence of high group mobility (Machado and Pérez, 2015; Pérez et al., 2020).

As previously discussed (see Chapter 3.4.3), stratigraphic unit Xb generally resembles SU Xa regarding its microstratigraphic geogenic, biogenic, and anthropogenic features and its biomolecular lipid signatures. These similarities suggest similar depositional and postdepositional conditions. However, there is insufficient archaeological data to interpret the formation of this stratigraphic unit in terms of time and the nature of the human occupations associated with it. For now, our geoarchaeological data (Case Study I) has provided rough time estimates that suggest successive, brief, low impact human occupations with relatively long periods of time between them. This suggests that stratigraphic units Xa and Xb could represent Neanderthal groups with similar behavior regarding their settlement and mobility patterns.

A recent archaeomagnetic study of undisturbed sedimentary samples from SU Xb (Herrejón Lagunilla, 2020) provided data and interpretations of the possible minimum time intervals between the combustion structures. A few of these combustion structures are the same ones studied here (Case Study I). The archaeomagnetic results indicate with a 95% confidence that the combustion structures - which were found on a single apparent surface, are diachronic, with several decades between them. Specifically, a minimum of 36 years elapsed between H50 and H57, 136 years between H50 and H55, and 30 years between H55 and H57 (Herrejón Lagunilla, 2020). These interpretations agree with the ones presented in Case Study

I: that there were long-term intervals between individual occupations and their corresponding combustion structures; sufficient time for incipient soil formation. Taken together, both lines of evidence underpin the possible high group mobility of the El Salt SU Xb Neanderthals.

The thick ash layer and possible complex use history of combustion structure H77 from SU XI presented in this thesis (Case Study II) reflect a longer burning duration compared to the overlying stratigraphic unit Xb. Estimates on burning duration based on ash thickness point to a burning time of at least several days (Schiegl et al., 1994; Schiegl et al., 1996), a timeframe that covers both short and long-termed occupations. Rough estimates on the ash volume of H77 according to its sizes (ø 30 cm, 5 cm depth), result in a volume of about 2300 cm^3 (Formula of the volume of semi-ellipsoid: $V = 2/3 * \pi *$ radius * radius * depth). According to the average volume of ash after burning 5 kg of wood (321 cm^3) (Schiegl et al., 1994; Schiegl et al., 1996), it would take approximately 36 kg of wood to fill the basin shape of H77. However, the actual amount of wood was probably even higher due to the compaction and diagenesis of ashes (Schiegl et al., 1994; Schiegl et al., 1996). To completely burn this amount of wood, H77 must have burnt for several consecutive hours, or for several days, if the fire did not burn continuously.

An ethnoarchaeological study reported a combustion structure with similar characteristics of the ash layer, which had been burnt a few times a day for a duration of two months (Mallol et al., 2007). The combustion structure exhibited a 7 cm thick ash layer; however, during its time of use, it was periodically maintained by scooping out ashes (Mallol et al., 2007). Hearth maintenance, such as scooping out ashes, was not observed in H77. The possible reworking goes in line with the evidence for relighting and must have happened at the beginning of the firing process.

Also, in possible relation to the issue of time is the thick RL of up to 2 cm of H77. Archaeomagnetic analyses confirmed temperatures of at least 600 °C for the RL, and according to Aldeias et al. (2016), it takes up to 2.5 hours of continuous heating at 950 °C to reach 600 °C at 2 cm below the surface. In a field experimental fire fueled by charcoal on top of limestone-sand and quartz, 600 °C at 2 cm below the surface is reached after 5 hours (Aldeias et al., 2016). In clayey silt, reaching a temperature of 600 °C at 2 cm would take even longer (Aldeias et al., 2016). Due to the presence of H77 in a pit structure and its resulting limits to reach high temperatures such as the insulating effects of the pit and the rapid infilling of ashes, the fire must have burned for at least several hours if not days to reach such a high temperature in the RL.

Several other lines of evidence support the H77 combustion structure's complex use history: the uncommonly high temperatures that left behind a combustion structure containing no charred plant remains and the possible reworking and relighting during its use, visible in microstratifications of the RL and WL. For now, this evidence agrees with the existence of a longer-term Neanderthal combustion structure, possibly indicating longer-term Neanderthal occupation in SU XI relative to those documented in SU Xa and Xb. To corroborate that the H77 combustion structure possibly represents human occupation lasting months rather than days, archaeological evidence of maintenance behaviors, such as hearth rake out and ash dumping, which can be identified using micromorphology (Goldberg, 2003; Kuhn et al., 2009; Mallol et al., 2007; Meignen et al., 2007; Schiegl et al., 2003), could be sought in future investigations of SU XI, as such behaviors have been described in long-term hunter-gatherer occupation contexts (Binford, 2002; Spagnolo et al., 2018; Stevenson, 1991; Vaquero, 2012; Vaquero et al., 2015).

Diachronic change in settlement dynamics has been previously documented in Kebara (Meignen, 2019), another Neanderthal site. Considering this evidence, which is suggestive of Neanderthal behavioral variability, a possible change in settlement dynamics from longer-termed occupation episodes in SU XI relative to SU X at El Salt deserves further investigation from multiple lines of research. Besides the previously mentioned micromorphological indicators of long-term human occupation, the presence of an archaeological record reflective of diverse domestic activities, as has been documented in long-term basecamps (Binford, 1980, 1982), could be sought.

The geoarchaeological, microcontextual proxies of Neanderthal behavior presented in this thesis provide clues for advancing current debates surrounding Neanderthal settlement dynamics and group mobility. However, further multidisciplinary studies yielding multiproxy data are necessary to resolve inconclusive aspects and contribute robusticity to our interpretations. For now, SU Xa's, convincing evidence points towards low-impact, short-term occupations and defines the Neanderthals as having high group mobility. Complementary geoarchaeological, microcontextual data on this stratigraphic unit could provide further support. For SU Xb, multidisciplinary archaeological data needs to be obtained to test the geoarchaeological interpretations presented here and to be able to compare Stratigraphic units Xa and Xb. For SU XI, multidisciplinary investigations, including geoarchaeology, have not been carried out yet, as excavations have not unearthed the deposit yet. Future work will shed light on the preliminary ideas presented here.

In this dissertation, I present data obtained through a bottom-up approach, based on hypothesis building from direct empirical evidence. This approach leaves many of the "big questions" unanswered but at the same time, reveals which questions can be more readily addressed through investigations of the archaeological record. In the topic of hunter-gatherer settlement patterns, hypotheses are often built from ethnographic observation, and the degree to which the ethnographic reality and observations derived from it are comparable with the archaeological and geoarchaeological counterpart, is questionable. Future increase in archaeological and geoarchaeological data with comparable degrees of resolution will validate or reject the ethnographic models and advance the current debates on Neanderthal settlement patterns.

6.2.2 Neanderthal pyrotechnology

Anthropogenic actions and natural processes related to fires could be differentiated and determined for all studied combustion structures of case studies I and II, bringing us closer to identifying Neanderthal pyrotechnological behavior. Following these considerations, at El Salt, our studies have revealed the existence of two main types of combustion structures: Simple, flat structures built on a vegetated surface and a hearth placed in a pit that reached very hot temperatures and burned for a long duration and presumably multiple times.

Most Middle Paleolithic sites contain combustion structures (Roebroeks and Villa, 2011 and references therein), and a great majority of them are simple, flat, circular, sometimes multi-layered structures with distinct perimeters and visible internal stratigraphy (RL-BL-WL) (Martínez-Moreno et al., 2004; Vallverdú Poch et al., 2012; Vaquero and Pastó, 2001; Zieba et al., 2008). As discussed before, at El Salt, these combustion structures reflect short-term occupations, in agreement with the currently accepted hypothetical Neanderthal settlement patterns (see Chapter 6.2). At El Salt, combustion structures show variation in size, proportions of components such as flint and bones tossed in the fire (see Chapter 3), and fuel type input (Vidal-Matutano, 2016; Vidal-Matutano et al., 2017; Vidal-Matutano et al., 2018). These variations could reflect variation in Neanderthal behavior or explain random variation or variation in material availability. For now, the sample is too small for statistical analysis.

Besides variable size, components, and fuel types, El Salt combustion structures also show variable wood ash deposits. However, some degree of variation could be explained by erosion rather than pyrotechnological variability. In the investigated combustion structure assemblage of SU Xb, four out of eleven combustion structures comprise an ash layer, ranging in thicknesses between 2 and 10 mm. It can be assumed that each combustion structure initially comprised an ash layer, most likely with varying thickness, but some ash layers were preserved, while other ash layers disappeared. The disappearance of the ash layer can be either explained by mechanical erosion such as aeolian processes or by the chemical dissolution of calcite (Mallol et al., 2017). In fact, the preservation of ashes of these four combustion structures and the pit hearth is peculiar, since El Salt is regarded as an open-air (Galván et al., 2014a; Galván et al., 2014b) or semi-open-air site (Vidal-Matutano, 2016; Vidal-Matutano et al., 2017; Vidal-Matutano et al., 2018), and open-air sites rarely preserve ashes (Friesem et al., 2014a and references therein). This preferential preservation could be explained through partial protection of the site by the inclination of the limestone wall and by possible rapid covering by leaves in the fall as experimentally demonstrated by Mallol et al. (2013a; 2013b). Nevertheless, the difference between the ash layer of H77 and the ashes of the combustion structure assemblage of Xb is significant and is unlikely to arise from different weathering or erosion conditions.

The pit hearth-type at El Salt is so far represented by a single occurrence in SU XI. It is different from all the studied SU X combustion structures in different ways. It was built in an anthropogenically or naturally formed pit, does not possess a black layer, and has been heated to temperatures that exceed those usually reached in documented archaeological and experimental flat and pit hearths (Aldeias et al., 2016; Bellomo, 1993; Bentsen, 2012, 2013; Braadbaart et al., 2012; Canti and Linford, 2000; March et al., 2014; Peeters and Niekus, 2017; Sievers and Wadley, 2008; Stiner et al., 1995). Whether the pit was dug out or naturally present, the fire was most likely intentionally placed in the pit. The fact that the entire fill of the pit consists of ash components indicates that the pit was empty at the time of burning. This evidence suggests that the El Salt Neanderthals had pyrotechnological knowledge involving a distinction between flat and pit hearths.

Archaeological and experimental studies have shown that pit hearths can be used for hide smoking, charcoal burning, and cooking (Mallol et al., 2007; Skibo and Schiffer, 2008; Wandsnider, 1997; Zerboni et al., 2013). These activities require lower temperatures than those usually associated with flat surface fires (March et al., 2014; Peeters and Niekus, 2017). Lower temperatures can be achieved by reduced oxygen input from the contained depression and the rapid infilling of thermally insulating charcoal and ash (Aldeias et al., 2016; Canti and Linford, 2000; Mallol et al., 2017; March et al., 2014), resulting in a slower, incomplete combustion rich in charcoal (March, 1992; March et al., 2014). However, these observations are not in accordance with the H77 pit hearth results, since we estimated temperatures in the H77 substrate (RL) of between 500 °C and 600 °C, and complete combustion. At this point, the function of a pit hearth reaching high temperatures and the pyrotechnological operational sequences underlying its making remains unexplained.

Previous evidence of different elements of Neanderthal pyrotechnology that were *not* identified in our studies include the use of bone fuel (Costamagno et al., 2005; Costamagno et al., 2008; Théry-Parisot, 2002a; Yravedra et al., 2016; Yravedra and Uzquiano, 2013), and the use of lignite and liquid hydrocarbons as fuel (Courty et al., 2012; Théry-Parisot and Meignen, 2000). Even though the input of bones into the fire has been documented at H77, the number of bones compared to the amount of wood ashes suggest that bones were not a significant fuel source. Instead, the bones were most likely tossed in the fire as refuse. El Salt conforms to the bulk of Neanderthal cases, in which wood is the primary fuel source and supplementary fuels are not documented (Albert et al., 1999; Albert et al., 2012; Madella et al., 2002; Shahack-Gross et al., 2008). Notably, the cited evidence comes from investigations carried out using methods that might overlook certain fuel residues such as lignite and liquid hydrocarbons. The techniques used in our studies are appropriate to identify such fuel types. At El Salt, the use of rotten wood fuel was identified and interpreted as evidence of smoking fire practice (Vidal-Matutano et al., 2017). Through Case Study III, we found Weissia moss being a possible additive to fires, even though use as auxiliary fuel is unlikely.

Besides fuel source variability, several Middle Paleolithic sites have yielded evidence of variability in hearth morphology: Grotte du Bison (a 20x30 cm stone-lined hearth) (Baffier and Girard, 1997; Farizy, 1990; Leroi-Gourhan, 1961), Vilas Ruivas (two crescent-shaped stone structures, one with a hearth inside of it, the other with two) (Bicho, 2004; Raposo, 1995), Les Canalettes (a stone-lined hearth) (Meignen, 1993; Théry-Parisot and Meignen, 2000), Bolomor (two stone-lined hearths) (Fernández Peris, 2007), Port Pignot (a rectangular hearth surrounded by stones) (Cliquet and Lautridou, 2009), Abri du Rozel (a stone-lined hearth) (van Vliet-Lanoë et al., 2006) and Pech de l'Azé II (some stone-lined hearths) (Bordes, 1971; Straus, 1989). So far, we did not identify stone-lined hearths at El Salt SUs X and XI. One of the SU Xb combustion structures, H50, showed peculiar macroscopic features in the field: its BL, which was greasy to the touch and very dark in color, preserved cobble-sized imprints on its surface (see Fig. 3). The data presented here (Case Study I) show that the greasy BL is made up of a heterogeneous mixture of plant matter, including wood and most likely twigs or branches, as well as a significant amount of fibrous material. Although the function of combustion structure H50 remains unknown, its peculiar macroscopic and microstratigraphic features suggest further variation in El Salt SU Xb's combustion structures. At a higher level, these data suggest variable and possibly complex Neanderthal pyrotechnological behavior.

As Speth (2004) described in his (news) article on Neanderthal mental competence, inadequate cognitive abilities were ascribed to Neanderthals, solely on negative or missing evidence. Today, archaeological science has provided some of the formerly missing evidence and shown variable use of space

(Henry, 2003; Henry et al., 2004; Spagnolo et al., 2018; Vallverdú et al., 2010), evidence for sophisticated stone tool technology (e.g., Delpiano et al., 2019), tar production (Koller et al., 2001; Kozowyk et al., 2017; Niekus et al., 2019; Pawlik and Thissen, 2011; Schmidt et al., 2019; Wragg Sykes et al., 2015), wooden tool manufacture (Aranguren et al., 2018) and fiber technology (Hardy et al., 2013; Hardy et al., 2020). Regarding pyrotechnology, As shown in this investigation and discussed in the paragraphs above, there is a growing body of evidence suggesting that Neanderthals were competent fire makers and had a rich and diverse pyrotechnology.

6.3 Methodological Considerations

In this work, micromorphology and lipid biomarker analysis helped answer the initial research questions. Recalling the chapters on the significance of both methods and the benefits of their combination (Chapter 2.2.1and 2.3.1), they are indeed well-suited techniques to analyze and interpret archaeological combustion features (Allué et al., in prep; Mallol et al., 2017). The results obtained through micromorphology corroborate the great potential of this independent geoarchaeological technique to obtain empirical data on behavioral, paleoenvironmental, and genetic aspects of archaeological sedimentary contexts related to combustion. Specifically, micromorphology allowed us to study Neanderthal combustion features from El Salt SUs X and XI at small (microscopic) scales of observation, which helped identify and contextualize components of biogenic, anthropogenic, and lithological origin. Microscopically thin rubified sedimentary layers and ash layers could be identified and examined and helped create a comprehensive picture of Neanderthal combustion structures. Furthermore, micromorphology contributed to SU Xb's palimpsest dissection by identifying occupation and abandonment periods and a low Neanderthal impact on the sediment and combustion structures. Micromorphology also provided insights into possible anthropogenic reworking and relighting activities in combustion structure H77 and, together with data from other techniques, allowed us to examine the degree of heating of the underlying red layer.

Lipid biomarker analysis is a relatively new approach in archaeological combustion feature research. Nevertheless, it yielded relevant data, and it was possible to integrate it with the micromorphological data towards meaningful interpretations. The lipid biomarker studies presented here contribute to the small set of literature on this topic (Brittingham et al., 2019; Lejay et al., 2016; Sistiaga et al., 2014; Sistiaga Gutiérrez et al., 2011). Our case studies show that the *n*-alkane analysis can contribute valuable information besides what this kind of analysis is best known for: providing paleoenvironmental data based on the identification of particular plant-type biomarkers present in this lipid fraction. In this thesis, the *n*-alkanes provided pyrotechnological information relevant to advance our knowledge of Neanderthal pyrotechnology. Along the lines of previous work (Diefendorf et al., 2015; Eckmeier and Wiesenberg, 2009; Jambrina-Enríquez et al., 2018; Jambrina-Enríquez et al., 2019; Knicker et al., 2013; Wiesenberg et al., 2009), here we showed that thermal alteration of plants leads to specific *n*-alkane thermal degradation profiles and these can be used as proxies to identify in situ burning in archaeological contexts or approach the history of individual archaeological combustion features. Other components found in our case studies, particularly the terpenoids, were shown to be good indicators for vegetation present in the site's natural surroundings. Lipid preservation in the BL and combustion substrate sediments from El Salt SUs X and XI is good and allows for identifying a diversity of compounds, many of them biomarkers. This observation motivates future lipid biomarker research at different Neanderthal sites. Although good lipid preservation at El Salt may be partly due to geographic and diagenetic factors, previous studies set forth the potential of combustion-related black sedimentary layers as sources of lipid biomolecular residues (Buonasera et al., 2019; Mallol et al., 2013a) and suggest that targeting geographically distant and diagenetically different archaeological contexts, might also yield well-preserved lipids.

In combination, the micromorphological and biomolecular lipid data helped build a comprehensive picture of the archaeological combustion features from El Salt SUs X and XI. Both kinds of data complemented each other at different stages of the analysis and later, at the interpretative stage. Micromorphology served as a map to contextualize the lipid biomarker samples within the combustion structure. By identifying diagenetic and physical processes (such as bioturbation, anthropogenic reworking), we had the necessary information on the depositional source and state of preservation of the sedimentary context to assess the meaning of the lipid data. In turn, biomolecular lipid analysis aided micromorphological interpretation in narrowing down possible sources of unidentified black particles and amorphous black matter observed in the thin sections. For interpretation of the ash layers, we turned to micromorphology again, as high temperatures break down lipid molecular compounds and they disappear. Instead, the micromorphology of the ash components (microstructures, pseudomorphs, and fire-resistant residues helped to identify fuel sources. In sum, a combined use of micromorphology and lipid biomarker analysis from a geoarchaeological perspective, with the resulting data from each technique complementing the other at different stages of the investigation, can lead to archaeologically significant contributions.

6.4 Future perspectives

Based on these conclusions, archaeologists should consider applying this sampling and analysis strategy to other Middle Paleolithic sites and their combustion structures to aid in piecing together a general knowledge of Neanderthals and their behavior. This would facilitate the comparison of Neanderthal behavior across regions and timeframes. It would enable us to see patterns in hearth construction, anthropogenic input, pyrotechnology, and settlement patterns. An extensive study of pit hearths or pit structures from other Middle Paleolithic sites would be especially interesting to enable a comparison to the pit hearth from El Salt.

Geoarchaeologists should continue collecting and analyzing reference samples for both micromorphology and lipid biomarker analysis to build a database with possible contributions to the interpretation of the archaeological fire record and to facilitate the identification of compounds at the site level. In case of negative results and mismatches between the reference sample and undetermined archaeological material, researchers should not be discouraged. Negative results are also useful and should be included in the reference database for future research advances.

Future research is needed to determine the possible change in settlement dynamics identified in El Salt SU XI. This entails excavation and multidisciplinary investigations of the archaeological record (lithics, faunal remains, combustion features, and the microscopic and molecular record). Regarding the geoarchaeological strategy for the investigation of combustion features at El Salt, I recommend following a similar methodology as in SU X, based on systematic, georeferenced sampling for archaeomagnetism, micromorphology, phytolith analysis, geochemistry (organic and inorganic), and flotation for anthracology. Such multidisciplinary strategy will allow for empirically founded interpretations of Neanderthal behavior and coherent comparisons between SUs X and XI.

General conclusions

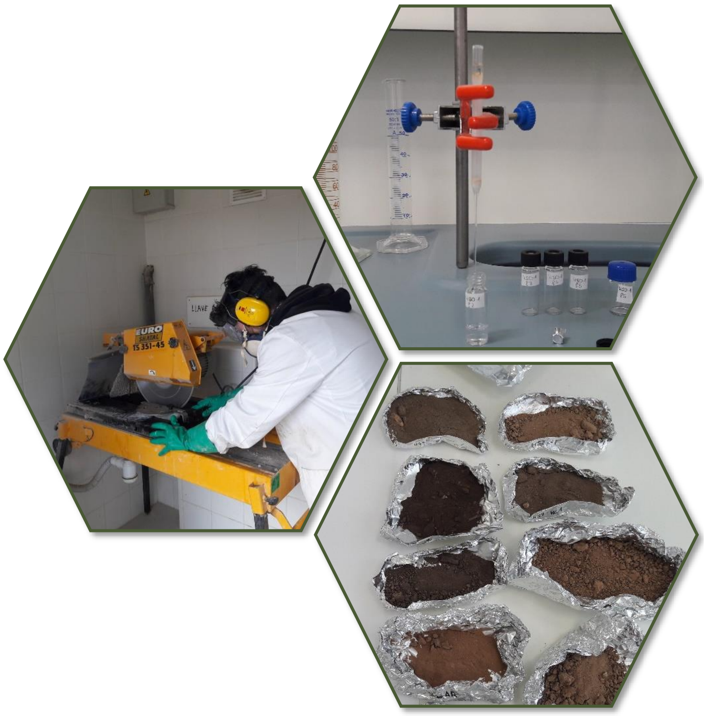

7. General Conclusions

This thesis was aimed at advancing our knowledge on Neanderthal behavior by gaining insight into Neanderthal pyrotechnology, group mobility, and settlement patterns. High-resolution, microcontextual, geoarchaeological investigations of a series of Neanderthal combustion structures and their surrounding sediment were carried out using combined micromorphology and lipid biomarker analysis. The objectives of this dissertation were: 1) to identify isolated occupation episodes, 2) to obtain high temporal and spatial resolution data related to fire use within possible single occupation events, 3) to determine anthropogenic (and other) residues preserved in Neanderthal combustion structures and 4) to explore the resulting data through experimentation.

These objectives were solved to an acceptable degree. Single occupation episodes were identified in Case Study I, which enabled the acquisition of temporal and spatial data in the form of microscopic and molecular data. For Case Study I and II, possible sources of anthropogenic and natural input into the combustion structures were determined, providing pyrotechnological information and information about the natural paleovegetation at the site. Finally, an experimental approach was undertaken to explore the undetermined fuel source observed in combustion structure H77, showing moss as a solid reference to which we compared our archaeological material, after which the presence of moss in this fire still cannot be ruled out.

The results contributed information on different aspects of the behavior of the Neanderthal groups living at El Salt during the times in which stratigraphic units X and XI formed. This information is summarized below.

Regarding Neanderthal settlement dynamics:

- The SU Xb Neanderthal occupations had a low impact on their sedimentary substrate, which is predominantly geogenic and biogenic in its composition and structure and shows a weak anthropogenic signature.
- The time elapsed between successive Neanderthal occupation episodes during the formation of SU Xb was sufficiently long to enable incipient soil formation and significant buildup of biogenic refuse (excrements and plant litter).
- Evidence of low impact human occupation and prolonged site abandonment suggests high group mobility.
- SU XI preserves a pit hearth with a thick ash layer and signs of reworking and relighting, which could reflect longer-termed occupations compared to those from SU X.
- The possibility of long-term Neanderthal occupation in SU XI based on the pit hearth evidence raises the possibility of a change in settlement dynamics from stratigraphic unit XI to X, which would imply Neanderthal behavioral variability.

Regarding Neanderthal pyrotechnology:

- El Salt SU Xb combustion structures conform to our previous knowledge on the characteristic types of Neanderthal fires: simple, flat, short-lived fires fueled by pine wood.
- In selecting their woody fuel, Neanderthals excluded tree species present in the immediate surroundings.
- El Salt SU XI pit hearth is evidence of Neanderthal pyrotechnological variability and suggests complex (unknown) pyrotechnological operational sequences.
- Neanderthals made high-temperature fires, as evidenced by the SU XI pit hearth.
- Moss is an inefficient fuel that hampers combustion. Its possible presence in Neanderthal combustion structure residues remains unexplained.
- Future excavations, geoarchaeological studies of combustion structures, and the study of fauna and lithics are needed to accept or deny the hypothesis of a shift in settlement patterns in XI. Until then, we need to refrain from generalizing the observations made on H77 to the remaining combustion structure assemblage of SU XI. Nevertheless, H77 is an exceptional combustion structure due to its different characteristics such as burning duration, high temperatures reached, and the placement in the pit, and describes variability in pyrotechnology and variability in general Neanderthal behavior. This is an important puzzle piece towards a better understanding of Neanderthals.

In the future, this research can be followed up by further multidisciplinary investigations, including:

- High-resolution geoarchaeological investigation of SU Xa for future comparison to the data from SU Xb presented here.
- Analysis of the lithic and faunal record from SU Xb for its combination with existing anthracological and geoarchaeological data (archaeomagnetic data and data from this thesis).
- Multidisciplinary archaeological excavation and analysis (combined lithic, zooarchaeological, anthracological, and high-resolution geoarchaeological studies) of SU XI for future comparison with data from SU X and to test the settlement dynamics hypothesis that emerged from our investigation of the SU XI pit hearth.
- Multidisciplinary archaeological excavation and analysis (combined lithic, zooarchaeological, anthracological, and high-resolution geoarchaeological studies) of Neanderthal contexts to compare resulting data from the data presented here and gain insight on Neanderthal behavior and on the scope of our combined geoarchaeological methodology when considering variables such as geography and diagenesis.
- Experiments and ethnoarchaeological investigations to elucidate the possible reasons for the presence of moss in archaeological combustion features, including possible functions of moss in fire-related human activities or accidental input.

- Experimental burning of additional plants related with anthropogenic combustion activities based on ethnographic evidence to engross the existing micromorphological and lipid biomarker reference database.

The combination of micromorphology and lipid biomarker analysis in combustion structure research has proven particularly useful. The lipid biomarker data suggests that the lipid sedimentary record may be well preserved and yield beneficial data despite the age of the sedimentary deposit.

I hope this dissertation will motivate other researchers and archaeologists to apply similar methods to investigate combustion structures at other Middle Paleolithic sites. In the future, a comprehensive corpus of high-resolution data on Neanderthal combustion features will lead to a better understanding of Neanderthal pyrotechnology and behavior across a wide geological and temporal range.

So far, we still "have only indirect means of knowing the courage and activity of the Neanderthals in the chase" (Osborn, 1914 p. 211), but by utilizing geoarchaeological and multidisciplinary analyses, we can, in fact, decipher their behavior through these indirect means.

References

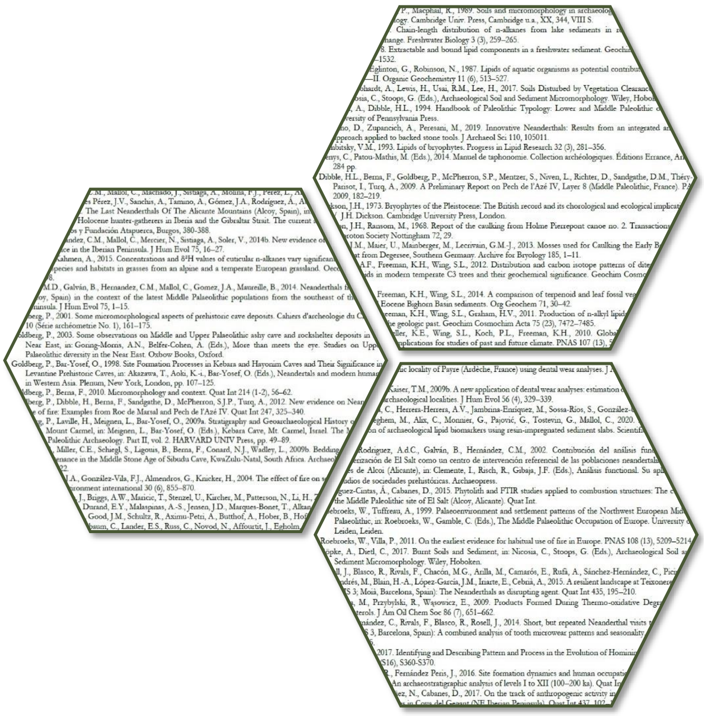

8. References

Aboutabl, E., Afifi, M., Ghaem, N., Yokoyama, R., Fukuyama, Y., Asakawa, Y., 1999. Aromatic Compounds from the Egyptian Moss *Eucladium Verticillatum* (Brid) B. S. G. J Hattori Bot Lab 86, 175–178.

Albert, R.M., Berna, F., Goldberg, P., 2012. Insights on Neanderthal fire use at Kebara Cave (Israel) through high resolution study of prehistoric combustion features: Evidence from phytoliths and thin sections. Quat Int 247, 278–293.

Albert, R.M., Lavi, O., Estroff, L., Weiner, S., Tsatskin, A., Ronen, A., Lev-Yadun, S., 1999. Mode of Occupation of Tabun Cave, Mt Carmel, Israel During the Mousterian Period: A Study of the Sediments and Phytoliths. J Archaeol Sci 26 (10), 1249–1260.

Albert, R.M., Weiner, S., Bar-Yosef, O., Meignen, L., 2000. Phytoliths in the Middle Palaeolithic Deposits of Kebara Cave, Mt Carmel, Israel: Study of the Plant Materials used for Fuel and Other Purposes. J Archaeol Sci 27 (10), 931–947.

Aldeias, V., 2017. Experimental Approaches to Archaeological Fire Features and Their Behavioral Relevance. Curr Anthropol 58 (16), 191-205.

Aldeias, V., Dibble, H.L., Sandgathe, D., Goldberg, P., McPherron, S.J.P., 2016. How heat alters underlying deposits and implications for archaeological fire features: A controlled experiment. J Archaeol Sci 67, 64–79.

Aldeias, V., Goldberg, P., Sandgathe, D., Berna, F., Dibble, H.L., McPherron, S.P., Turq, A., Rezek, Z., 2012. Evidence for Neandertal use of fire at Roc de Marsal (France). J Archaeol Sci 39 (7), 2414–2423.

Allison, J., Godwin, H., 1947. Report on plant material associated with the Ferriby prehistoric boats. Proc. Prehist. Soc. 13, 138.

Allué, E., Cabanes, D., Sol, A., Sala, R., 2012. Hearth Functioning and Forest Resource Exploitation Based on the Archeobotanical Assemblage from Level J, in: Carbonell i Roura, E. (Ed.), High Resolution Archaeology and Neanderthal Behavior. Vertebrate Paleobiology and Paleoanthropology. Springer Netherlands, Dordrecht, pp. 373–385.

Allué, E., Mallol, C., Aldeias, V., Burguet-Coca, A., Cabanes, D., Carrancho, Á., Connolly, R., Leierer, L., Mentzer, S.M., Miller, C.E., Sandgathe, D.M., Stahlschmidt, M.C., Théry-Parisot, I., Vaquero, M., in prep. Fire and fuel in the European Middle Palaeolithic, in: Romagnoli, F., Rivals, F., Benazzi, S. (Eds.), Updating the Neanderthals: Understanding Behavioural Complexity in the Late Middle Palaeolithic.

Almendros, G., González-Vila, F.J., 2012. Wildfires, soil carbon balance and resilient organic matter in Mediterranean ecosystems. A review. SJSS 2, 8–33.

Andriesse, J.P., 1988. Nature and management of tropical peat soils. FAO soils bulletin 59. Food and Agriculture Organization of the United Nations, Rome.

Anesin, D., 2016. Dinamiche formative di due siti di riferimento del Paleolitico nella Penisola Iberica sud-orientale.: Analisi micromorfologica dei depositi di Cueva Antón e Cueva Negra (Spagna, Murcia). Doctorate Thesis, Trento, Italy.

Angelucci, D.E., 2003. Geoarchaeology and micromorphology of Abric de la Cativera (Catalonia, Spain). Catena 54 (3), 573–601.

Angelucci, D.E., 2017. Lithic Artefacts, in: Nicosia, C., Stoops, G. (Eds.), Archaeological Soil and Sediment Micromorphology. Wiley, Hoboken, pp. 223–230.

Angelucci, D.E., Anesin, D., Susini, D., Villaverde, V., Zapata, J., Zilhão, J., 2018. A tale of two gorges: Late Quaternary site formation and surface dynamics in the Mula basin (Murcia, Spain). Quat Int 485, 4–22.

Aranguren, B., Revedin, A., Amico, N., Cavulli, F., Giachi, G., Grimaldi, S., Macchioni, N., Santaniello, F., 2018. Wooden tools and fire technology in the early Neanderthal site of Poggetti Vecchi (Italy). PNAS 115 (9), 2054–2059.

Arpin, T.L., Mallol, C., Goldberg, P., 2002. Short contribution: A new method of analyzing and documenting micromorphological thin sections using flatbed scanners: Applications in geoarchaeological studies. Geoarchaeology 17 (3), 305–313.

Arriolabengoa, M., Iriarte, E., Aranburu, A., Yusta, I., Arnold, L.J., Demuro, M., Arrizabalaga, A., 2018. Reconstructing the sedimentary history of Lezetxiki II cave (Basque Country, northern Iberian Peninsula) using micromorphological analysis. Sediment Geol 372, 96–111.

Arteaga, I., Angelucci, D., Carbonell, E., Courty, M.-A., Vallverdú Poch, J., 2000. Microfacies and sedimentary environment of the upper-middle palaeolithic boundary at Abric Romaní (Capellades, Barcelona). Cuaternario y geomorfología: Revista de la Sociedad Española de Geomorfología y Asociación Española para el Estudio del Cuaternario 15 (1-2), 15–30.

Asakawa, Y., Ludwiczuk, A., Nagashima, F., 2013. Chemical constituents of bryophytes: Bio- and chemical diversity, biological activity, and chemosystematics. Progress in the chemistry of organic natural products 95. Springer, Wien, London.

Baas, M., Pancost, R., van Geel, B., Sinninghe Damsté, J.S., 2000. A comparative study of lipids in Sphagnum species. Org Geochem 31 (6), 535–541.

Babel, U., 1975. Micromorphology of Soil Organic Matter, in: Gieseking, J.E. (Ed.), Soil Components. Springer Berlin Heidelberg, Berlin, Heidelberg, pp. 369–473.

Baffier, D., Girard, M., 1997. Le karst d'Arcy-sur-Cure (Yonne) et ses occupations humaines paléolithiques. Quaternaire 8 (2), 245–255.

Bailey, G., 2007. Time perspectives, palimpsests and the archaeology of time. J Anthropol Archaeol 26 (2), 198–223.

Bal, L., 1973. Micromorphological analysis of soils: Lower levels in the organization of organic soil materials. Soil Survey Paper 6, Wageningen.

Bargalló, A., Gabucio, M.J., Rivals, F., 2016. Puzzling out a palimpsest: Testing an interdisciplinary study in level O of Abric Romaní. Quat Int 417, 51–65.

Barriuso, B., Otaegui-Arrazola, A., Menéndez-Carreño, M., Astiasarán, I., Ansorena, D., 2012. Sterols heating: Degradation and formation of their ring-structure polar oxidation products. Food Chem, 706–712.

Bartram, L.E., Kroll, E.M., Bunn, H.T., 1991. Variability in Camp Structure and Bone Food Refuse Patterning at Kua San Hunter-Gatherer Camps, in: Jochim, M., Kroll, E.M., Price, T.D. (Eds.), The Interpretation of Archaeological Spatial Patterning. Interdisciplinary Contributions to Archaeology. Springer US, Boston, MA, pp. 77–148.

Bar-Yosef, O., Vandermeersch, B., Arensburg, B., Belfer-Cohen, A., Goldberg, P., Laville, H., Meignen, L., Rak, Y., Speth, J.D., Tchernov, E., Tillier, A.-M., Weiner, S., Clark, G.A., Garrard, A., Henry, D.O., Hole, F., Roe, D., Rosenberg, K.R., Schepartz, L.A., Shea, J.J., Smith, F.H., Trinkaus, E., Whalen, N.M., Wilson, L., 1992. The Excavations in Kebara Cave, Mt. Carmel [and Comments and Replies]. Curr Anthropol 33 (5), 497–550.

Beck, C.W., Smart, C.J., Ossenkop, D.J., 1989. Residues and Linings in Ancient Mediterranean Transport Amphoras, in: Allen, R.O. (Ed.), Archaeological Chemistry IV, vol. 220. Advances in Chemistry. American Chemical Society, Washington, DC, pp. 369–380.

Bellomo, R.V., 1993. A Methodological Approach for Identifying Archaeological Evidence of Fire Resulting from Human Activities. J Archaeol Sci 20 (5), 525–553.

Bentsen, S.E., 2012. Size matters: Preliminary results from an experimental approach to interpret Middle Stone Age hearths. Quat Int 270, 95–102.

Bentsen, S.E., 2013. Controlling the Heat: An Experimental Approach to Middle Stone Age Pyrotechnology. S Afr Archaeol 68 (198), 137–145.

Berna, F., Behar, A., Shahack-Gross, R., Berg, J., Boaretto, E., Gilboa, A., Sharon, I., Shalev, S., Shilstein, S., Yahalom-Mack, N., Zorn, J.R., Weiner, S., 2007. Sediments exposed to high temperatures: Reconstructing pyrotechnological processes in Late Bronze and Iron Age Strata at Tel Dor (Israel). J Archaeol Sci 34 (3), 358–373.

Berna, F., Goldberg, P., 2008. Assessing Paleolithic pyrotechnology and associated hominin behavior in Israel. Isr J Earth Sci 56 (2), 107–121.

Bi, X., Sheng, G., Liu, X., Li, C., Fu, J., 2005. Molecular and carbon and hydrogen isotopic composition of n-alkanes in plant leaf waxes. Org Geochem 36 (10), 1405–1417.

Bicho, N., 2004. The Middle Paleolithic occupation of southern Portugal, in: Conard, N.J. (Ed.), Settlement dynamics of the Middle Paleolithic and Middle Stone Age. Tübingen publications in prehistory. Kerns, Tübingen, pp. 597–608.

Binford, L.R., 1978. Nunamiut ethnoarchaeology. (Studies in archeology). Academic Press, New York.

Binford, L.R., 1980. Willow Smoke and Dogs' Tails: Hunter-Gatherer Settlement Systems and Archaeological Site Formation. Am Antiq 45 (1), 4–20.

Binford, L.R., 1981. Bones: Ancient men in modern myths. Studies in archaeology. Acad. Press, New York NY, XXVII, 320 S.

Binford, L.R., 1982. The archaeology of place. J Anthropol Archaeol 1 (1), 5–31.

Binford, L.R., 1998. Hearth and home: The spatial analysis of ethnographically documented rock shelter occupations as a template for distinguishing between human and hominid use of sheltered space, in: Middle Palaeolithic and Middle Stone Age settlement systems. Proceedings of the XIII UISPP Congress (pp. 229-239), Forli: Abaco.

Binford, L.R., 2002. In pursuit of the past: Decoding the archaeological record; with a new afterword. Univ. of California Press, Berkeley, Calif.

Birk, J.J., Dippold, M., Wiesenberg, G.L.B., Glaser, B., 2012. Combined quantification of faecal sterols, stanols, stanones and bile acids in soils and terrestrial sediments by gas chromatography-mass spectrometry. J Chromatogr A 1242, 1–10.

Bjorøy, M., Hall, P.B., Hustad, E., Williams, J.A., 1992. Variation in stable carbon isotope ratios of individual hydrocarbons as a function of artificial maturity. Org Geochem 19 (1-3), 89–105.

Blasco Sancho, M.F., 1992. Tafonomía y prehistoria: Métodos y procedimientos de investigación. Monografías arqueológicas 36. Departamento de Ciencias de la Antigüedad (Prehistoria) Universidad de Zaragoza, Zaragoza, 254 pp.

Boggs, S., 2006. Principles of sedimentology and stratigraphy, 4th ed. Pearson Prentice Hall, Upper Saddle River, N.J.

Bojović, S., Sarac, Z., Nikolić, B., Tešević, V., Todosijević, M., Veljić, M., Marin, P.D., 2012. Composition of n-alkanes in natural populations of Pinus nigra from Serbia - chemotaxonomic implications. Chem Biodivers 9 (12), 2761–2774.

Bordes, F., 1971. Observations sur l'Acheuléen des grottes en Dordogne. Munibe (Antropologia-Arkeologìa) (23), 5–23.

Boscato, P., Ronchitelli, A., 2008. Strutture di combustione in depositi del Paleolitico medio del Sud Italia. AJPA, 218–225.

Braadbaart, F., Poole, I., 2008. Morphological, chemical and physical changes during charcoalification of wood and its relevance to archaeological contexts. J Archaeol Sci 35 (9), 2434–2445.

Braadbaart, F., Poole, I., Huisman, H.D.J., van Os, B., 2012. Fuel, Fire and Heat: An experimental approach to highlight the potential of studying ash and char remains from archaeological contexts. J Archaeol Sci 39 (4), 836–847.

Brittingham, A., Hren, M.T., Hartman, G., 2017. Microbial alteration of the hydrogen and carbon isotopic composition of n -alkanes in sediments. Org Geochem 107, 1–8.

Brittingham, A., Hren, M.T., Hartman, G., Wilkinson, K.N., Mallol, C., Gasparyan, B., Adler, D.S., 2019. Geochemical Evidence for the Control of Fire by Middle Palaeolithic Hominins. Sci Rep 9 (1), 15368.

Briz Godino, I., Álvarez, M., Balbo, A., Zurro, D., Madella, M., Villagrán, X., French, C., 2011. Towards high-resolution shell midden archaeology: Experimental and ethnoarchaeology in Tierra del Fuego (Argentina). Quat Int 239 (1-2), 125–134.

Brocks, J.J., Summons, R.E., 2003. Sedimentary Hydrocarbons, Biomarkers for Early Life, in: Holland, H.D., Turekian K.K (Eds.), Treatise on Geochemistry. Elsevier, pp. 63–115.

Brodard, A., Lacanette-Puyo, D., Guibert, P., Lévêque, F., Burens, A., Carozza, L., 2015. A new process of reconstructing archaeological fires from their impact on sediment: A coupled experimental and numerical approach based on the case study of hearths from the cave of Les Fraux (Dordogne, France). Archaeol Anthropol Sci 8 (4), 673–687.

Brönnimann, D., Ismail-Meyer, K., Rentzel, P., Pümpin, C., Lisá, L., 2017a. Excrements of Herbivores, in: Nicosia, C., Stoops, G. (Eds.), Archaeological Soil and Sediment Micromorphology. Wiley, Hoboken.

Brönnimann, D., Pümpin, C., Ismail-Meyer, K., Rentzel, P., Égüez, N., 2017b. Excrements of Omnivores and Carnivores, in: Nicosia, C., Stoops, G. (Eds.), Archaeological Soil and Sediment Micromorphology. Wiley, Hoboken, pp. 67–81.

Bull, I.D., Simpson, I.A., van Bergen, P.F., Evershed, R.P., 1999. Muck 'n' molecules: Organic geochemical methods for detecting ancient manuring. Antiquity 73 (279), 86–96.

Bunn, H.T., 1986. Patterns of skeletal representation and hominid subsistence activities at Olduvai Gorge, Tanzania, and Koobi Fora, Kenya. J Hum Evol 15 (8), 673–690.

Buonasera, T., Herrera-Herrera, A.V., Mallol, C., 2019. Experimentally Derived Sedimentary, Molecular, and Isotopic Characteristics of Bone-Fueled Hearths. J Archaeol Method Theory 67 (6), 1327–1375.

Burke, A., 2006. Neanderthal settlement patterns in Crimea: A landscape approach. J Anthropol Archaeol 25 (4), 510–523.

Bush, R.T., McInerney, F.A., 2013. Leaf wax n-alkane distributions in and across modern plants: Implications for paleoecology and chemotaxonomy. Geochim Cosmochim Acta 117, 161–179.

Cabanes, D., Mallol, C., Expósito, I., Baena, J., 2010. Phytolith evidence for hearths and beds in the late Mousterian occupations of Esquilleu cave (Cantabria, Spain). J Archaeol Sci 37 (11), 2947–2957.

Cabrera, V., Pike-Tay, A., Quirós, F., 2004. Trends in Middle Paleolithic settlement in Cantabrian Spain: The Late Mousterian at Castillo Cave, in: Conard, N.J. (Ed.), Settlement dynamics of the Middle Paleolithic and Middle Stone Age, vol. 2. Tübingen publications in prehistory. Kerns, Tübingen.

Canti, M., Brochier, J.E., 2017. Plant Ash, in: Nicosia, C., Stoops, G. (Eds.), Archaeological Soil and Sediment Micromorphology. Wiley, Hoboken, pp. 147–154.

Canti, M.G., 2003. Aspects of the chemical and microscopic characteristics of plant ashes found in archaeological soils. Catena 54 (3), 339–361.

Canti, M.G., 2017. Charred Plant Remains, in: Nicosia, C., Stoops, G. (Eds.), Archaeological Soil and Sediment Micromorphology. Wiley, Hoboken, pp. 141–142.

Canti, M.G., Linford, N., 2000. The Effects of Fire on Archaeological Soils and Sediments: Temperature and Colour Relationships. Proc. Prehist. Soc. 66, 385–395.

Carrancho, Á., Villalaín, J.J., 2011. Different mechanisms of magnetisation recorded in experimental fires: Archaeomagnetic implications. Earth Planet Sci Lett 312 (1-2), 176–187.

Carrancho, Á., Villalaín, J.J., Angelucci, D.E., Dekkers, M.J., Vallverdú, J., Vergès, J.M., 2009. Rock-magnetic analyses as a tool to investigate archaeological fired sediments: A case study of Mirador cave (Sierra de Atapuerca, Spain). Geophys J Int 179 (1), 79–96.

Carrancho, Á., Villalaín, J.J., Vallverdú, J., Carbonell, E., 2016. Is it possible to identify temporal differences among combustion features in Middle Palaeolithic palimpsests?: The archaeomagnetic evidence: A case study from level O at the Abric Romaní rock-shelter (Capellades, Spain). Quat Int 417, 39–50.

Carrancho, Á., Villalaín, J.J., Vergès, J.M., Vallverdú, J., 2012. Assessing post-depositional processes in archaeological cave fires through the analysis of archaeomagnetic vectors. Quat Int 275, 14–22.

Cep, B., Waiblinger, J., 2001. The use of cave and open-air sites in southern Germany, in: Conard, N.J. (Ed.), Settlement dynamics of the Middle Paleolithic and Middle Stone Age. Tübingen publications in prehistory. Kerns, Tübingen, pp. 251–263.

Chacón, M.G., Bargalló, A., Gabucio, M.J., Rivals, F., Vaquero, M., 2015. Neanderthal Behaviors from a Spatio-Temporal Perspective: An Interdisciplinary Approach to Interpret Archaeological Assemblages, in: Conard, N.J., Delagnes, A. (Eds.), Settlement dynamics of the Middle Paleolithic and Middle Stone Age, IV. Tübingen publications in prehistory. Kerns, Tübingen, pp. 253–294.
Chadima, M., Hrouda, F., 2006. Remasoft 3.0 a user-friendly paleomagnetic data browser and analyzer. TraGe 27, 20–21.
Choy, K., Potter, B.A., McKinney, H.J., Reuther, J.D., Wang, S.W., Wooller, M.J., 2016. Chemical profiling of ancient hearths reveals recurrent salmon use in Ice Age Beringia. PNAS 113 (35), 9757–9762.
Christie, W.W., Han, X., 2010. Lipid analysis: Isolation, separation, identification and lipidomic analysis, 4th ed. ed. Oily Press lipid library 24. Oily Press, Bridgwater.
Churchill, S.E., 2014. Thin on the ground: Neandertal biology, archeology and ecology. Foundation of Human Biology v.10. Wiley, Hoboken, 453 pp.
Clark, G., 1971. Excavations at Star Carr: An early mesolithic site at Seamer Near Scarborough Yorkshire. Cambridge University Press, s.l.
Clark, J.L., Ligouis, B., 2010. Burned bone in the Howieson's Poort and post-Howieson's Poort Middle Stone Age deposits at Sibudu (South Africa): Behavioral and taphonomic implications. J Archaeol Sci 37 (10), 2650–2661.
Cliquet, D., Lautridou, J.-P., 2009. Les occupations humaines du Pléistocène moyen de Normandie dans leur cadre environnemental. Quaternaire (vol. 20/3), 305–320.
Collister, J.W., Rieley, G., Stern, B., Eglinton, G., Fry, B., 1994. Compound-specific δ 13C analyses of leaf lipids from plants with differing carbon dioxide metabolisms. Org Geochem 21 (6-7), 619–627.
Conard, N.J., Prindiville, T.J., 2000. Middle palaeolithic hunting economies in the Rhineland. Int J Osteoarchaeol 10 (5), 286–309.
Condamin, J., Formenti, F., Metais, M.O., Michel, M., Blond, P., 1976. The Application of Gas Chromatography to the Tracing of Oil in Ancient Amphorae. Archaeometry 18 (2), 195–201.
Costamagno, S., Théry-Parisot, I., Brugal, J.P., Guibert, R., 2005. Taphonomic consequences of the use of bones as fuel. Experimental data and archaeological applications, in: , Biosphere to lithosphere: new studies in vertebrate taphonomy. Oxbow Books, Oxford, pp. 51–62.
Costamagno, S., Théry-Parisot, I., Castel, J.-C., Brugal, J.-P., 2008. Combustible ou non? Analyse multifactorielle et modèles explicatifs sur des ossements brûlés paléolithiques. BAR Int. S 1914.
Courty, M.A., 2001. Microfacies Analysis Assisting Archaeological Stratigraphy, in: Goldberg, P., Holliday, V.T., Ferring, C.R. (Eds.), Earth Sciences and Archaeology. Springer US, Boston, MA, pp. 205–239.
Courty, M.A., Carbonell, E., Vallverdú Poch, J., Banerjee, R., 2012. Microstratigraphic and multi-analytical evidence for advanced Neanderthal pyrotechnology at Abric Romani (Capellades, Spain). Quat Int 247, 294–312.
Courty, M.A., Goldberg, P., Macphail, R., 1989. Soils and micromorphology in archaeology, 1. publ ed. Cambridge manuals in archaeology. Cambridge Univ. Press, Cambridge u.a.
Cranwell, P.A., 1973. Chain-length distribution of n-alkanes from lake sediments in relation to post-glacial environmental change. Freshw Biol 3 (3), 259–265.
Cranwell, P.A., 1978. Extractable and bound lipid components in a freshwater sediment. Geochim Cosmochim Acta 42 (10), 1523–1532.
Cranwell, P.A., 1981. Diagenesis of free and bound lipids in terrestrial detritus deposited in a lacustrine sediment. Org Geochem 3 (3), 79–89.
Cranwell, P.A., Eglinton, G., Robinson, N., 1987. Lipids of aquatic organisms as potential contributors to lacustrine sediments—II. Org Geochem 11 (6), 513–527.
Deák, J., Gebhardt, A., Lewis, H., Usai, R.M., Lee, H., 2017. Soils Disturbed by Vegetation Clearance and Tillage, in: Nicosia, C., Stoops, G. (Eds.), Archaeological Soil and Sediment Micromorphology. Wiley, Hoboken, pp. 233–264.
Debénath, A., Dibble, H.L., 1994. Handbook of Paleolithic Typology: Lower and Middle Paleolithic of Europe. University of Pennsylvania Press.
Delpiano, D., Zupancich, A., Peresani, M., 2019. Innovative Neanderthals: Results from an integrated analytical approach applied to backed stone tools. J Archaeol Sci 110, 105011.
Dembitsky, V.M., 1993. Lipids of bryophytes. Prog Lipid Res 32 (3), 281–356.
Denys, C., Patou-Mathis, M., 2014. Manuel de taphonomie. Collection archéologiques. Éditions Errance, Arles.
Dibble, H.L., Berna, F., Goldberg, P., McPherron, S.P., Mentzer, S., Niven, L., Richter, D., Sandgathe, D.M., Théry-Parisot, I., Turq, A., 2009. A Preliminary Report on Pech de l'Azé IV, Layer 8 (Middle Paleolithic, France). PA 2009, 182–219.
Dickson, J.H., 1973. Bryophytes of the Pleistocene: The British record and its chorological and ecological implications. Cambridge University Press, London.
Dickson, J.H., Ransom, M., 1968. Report of the caulking from Holme Pierrepont canoe no. 2. Transactions of the Thoroton Society Nottingham 72, 1–29.
Dickson, J.M., Maier, U., Mainberger, M., Lecrivain, G.M.-J., 2013. Mosses used for Caulking the Early Bronze Age Logboat from Degersee, Southern Germany. Archive for Bryology 185, 1–11.

Diefendorf, A.F., Freeman, K.H., Wing, S.L., 2012. Distribution and carbon isotope patterns of diterpenoids and triterpenoids in modern temperate C3 trees and their geochemical significance. Geochim Cosmochim Acta 85, 342–356.

Diefendorf, A.F., Freeman, K.H., Wing, S.L., 2014. A comparison of terpenoid and leaf fossil vegetation proxies in Paleocene and Eocene Bighorn Basin sediments. Org Geochem 71, 30–42.

Diefendorf, A.F., Freeman, K.H., Wing, S.L., Graham, H.V., 2011. Production of n-alkyl lipids in living plants and implications for the geologic past. Geochim Cosmochim Acta 75 (23), 7472–7485.

Diefendorf, A.F., Mueller, K.E., Wing, S.L., Koch, P.L., Freeman, K.H., 2010. Global patterns in leaf 13C discrimination and implications for studies of past and future climate. PNAS 107 (13), 5738–5743.

Diefendorf, A.F., Sberna, D.T., Taylor, D.W., 2015. Effect of thermal maturation on plant-derived terpenoids and leaf wax n -alkyl components. Org Geochem 89-90, 61–70.

Domínguez-Rodrigo, M., Yravedra, J., 2009. Why are cut mark frequencies in archaeofaunal assemblages so variable?: A multivariate analysis. J Archaeol Sci 36 (3), 884–894.

Eckmeier, E., Wiesenberg, G.L.B., 2009. Short-chain n-alkanes (C16–20) in ancient soil are useful molecular markers for prehistoric biomass burning. J Archaeol Sci 36 (7), 1590–1596.

Eglinton, G., 1970. Chemical Fossils. Scientific American [Offprint]. Freeman.

Eglinton, G., Hamilton, R.J., 1967. Leaf Epicuticular Waxes. Science 156 (3780), 1322–1335.

Eglinton, G., Logan, G.A., 1991. Molecular preservation. Philos Trans R Soc Lond B Biol Sci 333 (1268), 315-27; discussion 327-8.

Égüez, N., Mallol, C., Martín-Socas, D., Camalich, M.D., 2016. Radiometric dates and micromorphological evidence for synchronous domestic activity and sheep penning in a Neolithic cave: Cueva de El Toro (Málaga, Antequera, Spain). Archaeol Anthropol Sci 8 (1), 107–123.

Eixea Vilanova, A., Villaverde Bonilla, V., Zilhão, J., Sanchis Serra, A., Morales Pérez, J.V., Real Margalef, C., Bergadà Zapata, M.M., 2011-2012. El nivel IV del abrigo de la Quebrada (Chelva, Valencia): análisis microespacial y valoración del uso del espacio en los yacimientos del Paleolítico Meido valenicano. Neanderthales en Iberia: últimos avances en la investigación del Paleolítico Medio ibérico 33, 127–158.

Elefanti P., Panagopoulou, E., Karkanas, P., 2008. The transition from the Middle to the Upper Palaeolithic in the southern Balkans: The evidence from the Lakonis I Cave, Greece. Eurasian Prehistory 5, 85–95.

Evershed, R., Heron, C., Charters, S., Goad, L., 1992. The survival of food residues: New methods of analysis, interpretation and application.

Evershed, R.P., 1993. Biomolecular archaeology and lipids. World Archaeol 25 (1), 74–93.

Evershed, R.P., 2008. Organic Residue Analysis in Archaeology: The Archaeological Biomarker Revolution. Archaeometry 50 (6), 895–924.

Evershed, R.P., Dudd, S.N., Charters, S., Mottram, H., Stott, A.W., Raven, A., van Bergen, P.F., Bland, H.A., 1999. Lipids as carriers of anthropogenic signals from prehistory. Philos Trans R Soc Lond B Biol Sci 354 (1379), 19–31.

Evershed, R.P., Dudd, S.N., Copley, M.S., Berstan, R., Stott, A.W., Mottram, H., Buckley, S.A., Crossman, Z., 2002. Chemistry of Archaeological Animal Fats. Acc Chem Res 35 (8), 660–668.

Fagoaga, A., Laplana, C., Marquina-Blasco, R., Machado, J., Marin-Monfort, M.D., Crespo, V.D., Hernández, C.M., Mallol, C., Galván, B., Ruiz-Sánchez, F.J., 2019. Palaeoecological context for the extinction of the Neanderthals: A small mammal study of Stratigraphic Unit V of the El Salt site, Alcoi, eastern Spain. Palaeogeogr Palaeoclimatol Palaeoecol 530, 163–175.

Fagoaga, A., Ruiz-Sánchez, F.J., Laplana, C., Blain, H.-A., Marquina, R., Marin-Monfort, M.D., Galván, B., 2017. Palaeoecological implications of Neanderthal occupation at Unit Xb of El Salt (Alcoi, eastern Spain) during MIS 3 using small mammals proxy. Quat Int 481, 101–112.

Farizy, C., 1990. Du Moustérien au Châtelperronien à Arcy-sur-Cure: un état de la question, in: Farizy, C. (Ed.), Paléolithique moyen récent et paléolithique supérieur ancien en Europe. Ruptures et transitions; examen critique des documents archéologiques; actes du colloque international de Nemours, 9 - 10 - 11 mai 1988. Mémoires du Musée de préhistoire d'Ile-de-France 3. Ed. APRAIF, Nemours, pp. 281–290.

Farizy, C., 1994. Spatial Patterning of Middle Paleolithic Sites. J Anthropol Archaeol 13 (2), 153–160.

Faus Terol, E., 2000. Recursos Líticos y Gestion de Talla de la Industria Lítica Musteriense de les Coves d'Estroig (Cocentaina, Alacant). Alberri 13.

Fernández Peris, J., 2007. La Cova del Bolomor (Tavernes de la Valldigna, Valencia). Las industrias líticas del Pleistoceno medio en el ámbito del Mediterráneo peninsular. Serie de Trabajos varios 108.

Fernández Peris, J., Barciela, V., Blasco, R., Cuartero, F., Hortelano, L., Sañudo, P., 2014. Bolomor Cave, Valencia, Spain, in: Sala Ramos, R. (Ed.), Pleistocene and Holocene hunter-gatherers in Iberia and the Gibraltar Strait. The current archaeological record. Univ. de Burgos y Fundación Atapuerca, Burgos, pp. 323–331.

Fernández Peris, J., González, V.B., Blasco, R., Cuartero, F., Fluck, H., Sañudo, P., Verdasco, C., 2012. The earliest evidence of hearths in Southern Europe: The case of Bolomor Cave (Valencia, Spain). Quat Int 247, 267–277.

Fernandez-Jalvo, Y., Andrews, P., 2016. Atlas of Taphonomic Identifications: 1001+ Images of Fossil and Recent Mammal Bone Modification. Vertebrate Paleobiology and Paleoanthropology. Springer Netherlands, Dordrecht, s.l.

Fisher, J.W., Strickland, H.C., 1991. Dwellings and Fireplaces: Keys to Efe Pygmy Campsite Structure., in: Gamble, C., Boismier, W.A. (Eds.), Ethnoarchaeological approaches to mobile campsites. Hunter-gatherer and pastoralist case studies. International Monographs in Prehistory, Ann Arbor, Mich.

Fisher, R., 1953. Dispersion on a Sphere. Proc R Soc A 217 (1130), 295–305.

Flügel, E., 1982. Microfacies Analysis of Limestones. Springer Berlin Heidelberg, Berlin, Heidelberg.

Francés-Negro, M., Carrancho, Á., Pérez-Romero, A., Arsuaga, J.L., Carretero, J.M., Iriarte, E., 2019. Storage or cooking pots?: Inferring pottery use through archaeomagnetic assessment of palaeotemperatures. J Archaeol Sci 110, 104992.

Friesem, D.E., Zaidner, Y., Shahack-Gross, R., 2014a. Formation processes and combustion features at the lower layers of the Middle Palaeolithic open-air site of Nesher Ramla, Israel. Quat Int 331, 128–138.

Friesem, D.E., Karkanas, P., Tsartsidou, G., Shahack-Gross, R., 2014b. Sedimentary processes involved in mud brick degradation in temperate environments: A micromorphological approach in an ethnoarchaeological context in northern Greece. J Archaeol Sci 41, 556–567.

Fumanal García, M.P., 1994. El yacimiento musteriense de El Salt (Alcoi, País Valenciano): rasgos geomorfológicos y climatoestratigrafía de sus registros. SAGVNTVM 27, 39–55.

Gabucio, M.J., Fernández-Laso, M.C., Rosell, J., 2017. Turning a rock shelter into a home. Neanderthal use of space in Abric Romaní levels M and O. Hist Biol 30 (6), 743–766.

Galván, B., Hernández, C.M., Mallol, C., Machado, J., Sistiaga, A., Molina, F.J., Pérez, L., Afonso, R., Garralda, M.D., Mercier, N., Morales Pérez, J.V., Sanchis, A., Tamino, A., Gómez, J.A., Rodríguez, Á., Abreu, I., Vidal-Matutano, P., 2014a. El Salt. The Last Neanderthals Of The Alicante Mountains (Alcoy, Spain), in: Sala Ramos, R. (Ed.), Pleistocene and Holocene hunter-gatherers in Iberia and the Gibraltar Strait. The current archaeological record. Univ. de Burgos y Fundación Atapuerca, Burgos, pp. 380–388.

Galván, B., Hernández, C.M., Mallol, C., Mercier, N., Sistiaga, A., Soler, V., 2014b. New evidence of early Neanderthal disappearance in the Iberian Peninsula. J Hum Evol 75, 16–27.

Gamarra, B., Kahmen, A., 2015. Concentrations and δ^2H values of cuticular n-alkanes vary significantly among plant organs, species and habitats in grasses from an alpine and a temperate European grassland. Oecologia 178 (4), 981–998.

Garralda, M.D., Galván, B., Hernandez, C.M., Mallol, C., Gomez, J.A., Maureille, B., 2014. Neanderthals from El Salt (Alcoy, Spain) in the context of the latest Middle Palaeolithic populations from the southeast of the Iberian Peninsula. J Hum Evol 75, 1–15.

Goldberg, P., 2001. Some micromorphological aspects of prehistoric cave deposits. Cahiers d'archeologie du CELAT 10 (Série archéometrie No. 1), 161–175.

Goldberg, P., 2003. Some observations on Middle and Upper Palaeolithic ashy cave and rockshelter deposits in the Near East, in: Goring-Morris, A.N., Belfer-Cohen, A. (Eds.), More than meets the eye. Studies on Upper Palaeolithic diversity in the Near East. Oxbow Books, Oxford pp.19-23.

Goldberg, P., Bar-Yosef, O., 1998. Site Formation Processes in Kebara and Hayonim Caves and Their Significance in Levantine Prehistoric Caves, in: Akazawa, T., Aoki, K.-i., Bar-Yosef, O. (Eds.), Neandertals and modern humans in Western Asia. Plenum, New York, London, pp. 107–125.

Goldberg, P., Berna, F., 2010. Micromorphology and context. Quat Int 214 (1-2), 56–62.

Goldberg, P., Dibble, H., Berna, F., Sandgathe, D., McPherron, S.J.P., Turq, A., 2012. New evidence on Neandertal use of fire: Examples from Roc de Marsal and Pech de l'Azé IV. Quat Int 247, 325–340.

Goldberg, P., Laville, H., Meignen, L., Bar-Yosef, O., 2009a. Stratigraphy and Geoarchaeological History of Kebara Cave, Mount Carmel, in: Meignen, L., Bar-Yosef, O. (Eds.), Kebara Cave, Mt. Carmel, Israel. The Middle and Upper Paleolithic Archaeology. Part II, vol. 2. HARVARD UNIV Press, pp. 49–89.

Goldberg, P., Miller, C.E., Schiegl, S., Ligouis, B., Berna, F., Conard, N.J., Wadley, L., 2009b. Bedding, hearths, and site maintenance in the Middle Stone Age of Sibudu Cave, KwaZulu-Natal, South Africa. Archaeol Anthropol Sci 1 (2), 95–122.

González-Pérez, J.A., González-Vila, F.J., Almendros, G., Knicker, H., 2004. The effect of fire on soil organic matter--a review. Environ Int 30 (6), 855–870.

Green, R.E., Krause, J., Briggs, A.W., Maricic, T., Stenzel, U., Kircher, M., Patterson, N., Li, H., Zhai, W., Fritz, M.H.-Y., Hansen, N.F., Durand, E.Y., Malaspinas, A.-S., Jensen, J.D., Marques-Bonet, T., Alkan, C., Prufer, K., Meyer, M., Burbano, H.A., Good, J.M., Schultz, R., Aximu-Petri, A., Butthof, A., Hober, B., Hoffner, B., Siegemund, M., Weihmann, A., Nusbaum, C., Lander, E.S., Russ, C., Novod, N., Affourtit, J., Egholm, M., Verna, C., Rudan, P., Brajkovic, D., Kucan, Z., Gusic, I., Doronichev, V.B., Golovanova, L.V., Lalueza-Fox, C., La Rasilla, M. de, Fortea, J., Rosas, A., Schmitz, R.W., Johnson, P.L.F., Eichler, E.E., Falush, D., Birney, E., Mullikin, J.C., Slatkin, M., Nielsen, R., Kelso, J., Lachmann, M., Reich, D., Paabo, S., 2010. A draft sequence of the Neandertal genome. Science 328 (5979), 710–722.

Groenendijk, H.A., 1987. Mesolithic hearth-pits in the Veenkoloniën (prov. Groningen, the Netherlands), defining a specific use of fire in the Mesolithic. Palaeohistoria (29).

Gualtieri, A.F., Venturelli, P., 1999. In situ study of the goethite-hematite phase transformation by real time synchrotron powder diffraction. Am Min 84 (5-6), 895–904.

Gunstone, F.D., 1996. Fatty Acid and Lipid Chemistry. Springer US, Boston, MA.

Haaland, M.M., Friesem, D.E., Miller, C.E., Henshilwood, C.S., 2017. Heat-induced alteration of glauconitic minerals in the Middle Stone Age levels of Blombos Cave, South Africa: Implications for evaluating site structure and burning events. J Archaeol Sci 86, 81–100.
Hardy, B.L., Moncel, M.-H., Daujeard, C., Fernandes, P., Béarez, P., Desclaux, E., Chacon Navarro, M.G., Puaud, S., Gallotti, R., 2013. Impossible Neanderthals?: Making string, throwing projectiles and catching small game during Marine Isotope Stage 4 (Abri du Maras, France). Quat Sci Rev 82, 23–40.
Hardy, B.L., Moncel, M.-H., Kerfant, C., Lebon, M., Bellot-Gurlet, L., Mélard, N., 2020. Direct evidence of Neanderthal fibre technology and its cognitive and behavioral implications. Sci Rep 10 (1), 4889.
Heiri, O., Lotter, A.F., Lemcke, G., 2001. Loss on ignition as a method for estimating organic and carbonate content in sediments: reproducibility and comparability of results. Journal of Paleolimnology 25 (1), 101–110.
Henry, D., 2012. The palimpsest problem, hearth pattern analysis, and Middle Paleolithic site structure. Quat Int 247, 246–266.
Henry, D.O., 2003. Behavioral Organization at Tor Faraj, in: Henry, D.O. (Ed.), Neanderthals in the Levant. Behavioral organization and the beginnings of human modernity. New approaches to anthropological archaeology. Continuum, London, New York, pp. 237–269.
Henry, D.O., Hietala, H.J., Rosen, A.M., Demidenko, Y.E., Usik, V.I., Armagan, T.L., 2004. Human Behavioral Organization in the Middle Paleolithic: Were Neanderthals Different? Am Anthropol 106 (1), 17–31.
Henshall, A., 1964. A dagger-grave and other cist burials at Ashgrove Methilhill Fife. Proceedings of the Society of Antiquaries of Scotland 97, 166–179.
Herrejón Lagunilla, Á., 2020. Estudios Arqueomagnéticos en Materiales Quemados Prehistóricos de la Penisula Ibérica. Aplicaciones Geochronológicas y Geoarqueológicas. Tesis doctoral.
Herrejón Lagunilla, Á., Carrancho, Á., Villalaín, J.J., Mallol, C., Hernández, C.M., 2019. An experimental approach to the preservation potential of magnetic signatures in anthropogenic fires. PloS one 14 (8), e0221592.
Herrera-Herrera, A.V., Leierer, L., Jambrina-Enríquez, M., Connolly, R., Mallol, C., 2020. Evaluating different methods for calculating the Carbon Preference Index (CPI): Implications for palaeoecological and archaeological research. Org Geochem 146, 104056.
Herrera-Herrera, A.V., Mallol, C., 2018. Quantification of lipid biomarkers in sedimentary contexts: Comparing different calibration methods. Org Geochem 125, 152–160.
Heyes, P.J., Anastasakis, K., Jong, W. de, van Hoesel, A., Roebroeks, W., Soressi, M., 2016. Selection and Use of Manganese Dioxide by Neanderthals. Sci Rep 6, 22159.
Hovers, E., 2001. Territorial behavior in the Middle Paleolithic of the Southern Levant.
Hovers, E., Belfer-Cohen, A., 2013. On Variability and Complexity. Curr Anthropol 54 (8), 337-357.
Huisman, D.J., Niekus, M.J.L.T., Peeters, J.H.M., Geerts, R.C.A., Müller, A., 2019. Deciphering the complexity of a ‘simple’ mesolithic phenomenon: Indicators for construction, use and taphonomy of pit hearths in Kampen (the Netherlands). J Archaeol Sci 109, 104987.
Hunt, A., Bortolini, E. (Eds.), 2016. The Oxford Handbook of Archaeological Ceramic Analysis. Oxford University Press.
Ismail-Meyer, K., 2017. Plant Remains, in: Nicosia, C., Stoops, G. (Eds.), Archaeological Soil and Sediment Micromorphology. Wiley, Hoboken, pp. 121–135.
Iturbe, G., Carrión, J., Pérez, E., Martínez Valle, R., Calatayud, P.M., Garralda, M., Vandermeersch, B., 1997. Cova Beneito (Muro, Alicante): Una perspectiva interdisciplinar. Recerques del Museu d'Alcoi 2, 23–88.
Jackson, T.A., 2015. Weathering, secondary mineral genesis, and soil formation caused by lichens and mosses growing on granitic gneiss in a boreal forest environment. Geoderma 251-252, 78–91.
Jambrina-Enríquez, M., Herrera-Herrera, A.V., Mallol, C., 2018. Wax lipids in fresh and charred anatomical parts of the Celtis australis tree: Insights on paleofire interpretation. Org Geochem, 147–160.
Jambrina-Enríquez, M., Herrera-Herrera, A.V., Rodríguez de Vera, C., Leierer, L., Connolly, R., Mallol, C., 2019. n-Alkyl nitriles and compound-specific carbon isotope analysis of lipid combustion residues from Neanderthal and experimental hearths: Identifying sources of organic compounds and combustion temperatures. Quat Sci Rev 222, 105899.
James, A.T., Martin, A.J.P., 1952. Gas-liquid partition chromatography; the separation and micro-estimation of volatile fatty acids from formic acid to dodecanoic acid. Biochem J 50 (5), 679–690.
James, S.R., Dennell, R.W., Gilbert, A.S., Lewis, H.T., Gowlett, J.A.J., Lynch, T.F., McGrew, W.C., Peters, C.R., Pope, G.G., Stahl, A.B., 1989. Hominid Use of Fire in the Lower and Middle Pleistocene: A Review of the Evidence [and Comments and Replies]. Curr Anthropol 30 (1), 1–26.
Jones, K.T., 1993. The Archaeological Structure of a Short-Term Camp., in: Hudson, J. (Ed.), From Bones to Behavior: Ethnoarchaeological and Experimental Contributions to the Interpretation of Faunal Remains. Southern Illinois University, Carbondale, Illinois, pp. 101–114.
Kapper, K.L., Anesin, D., Donadini, F., Angelucci, D.E., Cavulli, F., Pedrotti, A., Hirt, A.M., 2014. Linking site formation processes to magnetic properties. Rock- and archeomagnetic analysis of the combustion levels at Riparo Gaban (Italy). J Archaeol Sci 41, 836–855.
Karkanas, P., 2002. Micromorphological studies of Greek prehistoric sites: New insights in the interpretation of the archaeological record. Geoarchaeology 17 (3), 237–259.

Karkanas, P., 2010. Geology, stratigraphy and site formation processes of the Upper Palaeolithic and later sequence in Klisoura Cave 1. Eurasian Prehistory 7 (2), 15–36.
Karkanas, P., Brown, K.S., Fisher, E.C., Jacobs, Z., Marean, C.W., 2015. Interpreting human behavior from depositional rates and combustion features through the study of sedimentary microfacies at site Pinnacle Point 5-6, South Africa. J Hum Evol 85, 1–21.
Karkanas, P., Goldberg, P., 2010a. Phosphatic Features, in: Stoops, G. (Ed.), Interpretation of micromorphological features of soils and regoliths, 1. ed. ed. Elsevier, Amsterdam.
Karkanas, P., Goldberg, P., 2010b. Site formation processes at Pinnacle Point Cave 13B (Mossel Bay, Western Cape Province, South Africa): resolving stratigraphic and depositional complexities with micromorphology. J Hum Evol 59 (3-4), 256–273.
Karkanas, P., Koumouzelis, M., Kozlowski, J.K., Sitlivy, V., Sobczyk, K., Berna, F., Weiner, S., 2004. The earliest evidence for clay hearths: Aurignacian features in Klisoura Cave 1, southern Greece. Antiquity 78 (301), 513–525.
Karkanas, P., Pavlopoulos, K., Kouli, K., Ntinou, M., Tsartsidou, G., Facorellis, Y., Tsourou, T., 2011. Palaeoenvironments and site formation processes at the Neolithic lakeside settlement of Dispilio, Kastoria, Northern Greece. Geoarchaeology 26 (1), 83–117.
Karkanas, P., Rigaud, J.-P., Simek, J.F., Albert, R.M., Weiner, S., 2002. Ash Bones and Guano: A Study of the Minerals and Phytoliths in the Sediments of Grotte XVI, Dordogne, France. J Archaeol Sci 29 (7), 721–732.
Karkanas, P., Shahack-Gross, R., Ayalon, A., Bar-Matthews, M., Barkai, R., Frumkin, A., Gopher, A., Stiner, M.C., 2007. Evidence for habitual use of fire at the end of the Lower Paleolithic: site-formation processes at Qesem Cave, Israel. J Hum Evol 53 (2), 197–212.
Karkanas, P., van de Moortel, A., 2014. Micromorphological analysis of sediments at the Bronze Age site of Mitrou, central Greece: Patterns of floor construction and maintenance. J Archaeol Sci 43, 198–213.
Kedrowski, B.L., Crass, B.A., Behm, J.A., Luetke, J.C., Nichols, A.L., Moreck, A.M., Holmes, C.E., 2009. GC/MS Analysis of Fatty Acids from Ancient Hearth Residues at the Swan Point Archaeological Site. Archaeometry 51 (1), 110–122.
Kelly, R.L., 1983. Hunter-Gatherer Mobility Strategies. J Anthropol Res 39 (3), 277–306.
Kirschvink, J.L., 1980. The least-squares line and plane and the analysis of palaeomagnetic data. Geophys J Int 62 (3), 699–718.
Klavina, L., Springe, G., Nikolajeva, V., Martsinkevich, I., Nakurte, I., Dzabijeva, D., Steinberga, I., 2015. Chemical Composition Analysis, Antimicrobial Activity and Cytotoxicity Screening of Moss Extracts (Moss Phytochemistry). Molecules 20 (9), 17221–17243.
Klein, R.G., 2009. The human career: Human biological and cultural origins, 3rd ed. ed. University of Chicago Press, Chicago.
Knicker, H., Hilscher, A., La Rosa, J.M. de, González-Pérez, J.A., González-Vila, F.J., 2013. Modification of biomarkers in pyrogenic organic matter during the initial phase of charcoal biodegradation in soils. Geoderma 197-198, 43–50.
Koch, L.F., 1956. Notes on Bryological Terminology. Bryologist 59 (1), 23.
Koenigsberger, J.G., 1938. Natural residual magnetism of eruptive rocks. J. Geophys. Res. 43 (3), 299.
Koller, J., Baumer, U., Mania, D., 2001. High-Tech in the Middle Palaeolithic: Neandertal-Manufactured Pitch Identified. Eur J Archaeol 4 (3), 385–397.
Kozowyk, P.R.B., Soressi, M., Pomstra, D., Langejans, G.H.J., 2017. Experimental methods for the Palaeolithic dry distillation of birch bark: implications for the origin and development of Neandertal adhesive technology. Sci Rep 7 (1), 8033.
Kubiena, W.L., 1938. Micropedology. Collegiate Press, Inc., Ames, Iowa.
Kuhn, S.L., 1995. Mousterian Lithic Technology: An Ecological Perspective. Princeton University Press.
Kuhn, S.L., 2013. Roots of the Middle Paleolithic in Eurasia. Curr Anthropol 54 (8), 255-268.
Kuhn, S.L., Stiner, M.C., Güleç, E., Ozer, I., Yilmaz, H., Baykara, I., Açikkol, A., Goldberg, P., Molina, K.M., Unay, E., Suata-Alpaslan, F., 2009. The early Upper Paleolithic occupations at Uçağizli Cave (Hatay, Turkey). J Hum Evol 56 (2), 87–113.
Kuhn, T.K., Krull, E.S., Bowater, A., Grice, K., Gleixner, G., 2010. The occurrence of short chain n-alkanes with an even over odd predominance in higher plants and soils. Org Geochem 41 (2), 88–95.
Kumara, M., 2014. Comparison of GC-MS analysis of phytochemicals in the ethanolic extracts of Marchantia linearis Lehm & Lindenb. and Marchantia polymorpha L. (Bryophyta). Int J Pharm Sci 5 (5), 1981–1987.
Kuo, L.-J., Herbert, B.E., Louchouarn, P., 2008. Can levoglucosan be used to characterize and quantify char/charcoal black carbon in environmental media? Org Geochem 39 (10), 1466–1478.
Langenheim, J.H., 2003. Plant resins: Chemistry, evolution, ecology, and ethnobotany. Timber Press, Portland, Or, 586 pp.
Leierer, L., Carrancho Alonso, Á., Pérez, L., Herrejón Lagunilla, Á., Herrera-Herrera, A.V., Connolly, R., Jambrina-Enríquez, M., Hernández Gómez, C.M., Galván, B., Mallol, C., 2020. It's getting hot in here – Microcontextual study of a potential pit hearth at the Middle Paleolithic site of El Salt, Spain. J Archaeol Sci 123 (7), 105237.
Leierer, L., Jambrina-Enríquez, M., Herrera-Herrera, A.V., Connolly, R., Hernández, C.M., Galván, B., Mallol, C., 2019. Insights into the timing, intensity and natural setting of Neanderthal occupation from the geoarchaeological

study of combustion structures: A micromorphological and biomarker investigation of El Salt, unit Xb, Alcoy, Spain. PloS one 14 (4), e0214955.

Lejay, M., Alexis, M., Quénéa, K., Sellami, F., Bon, F., 2016. Organic signatures of fireplaces: Experimental references for archaeological interpretations. Org Geochem 99, 67–77.

Lenton, T.M., Crouch, M., Johnson, M., Pires, N., Dolan, L., 2012. First plants cooled the Ordovician. Nature Geosci 5 (2), 86–89.

Leonhardt, R., 2006. Analyzing rock magnetic measurements: The RockMagAnalyzer 1.0 software. Comput and Geosci 32 (9), 1420–1431.

Leroi-Gourhan, A., 1961. Les fouilles d'Arcy-sur-Cure (Yonne). Galip 4 (1), 3–16.

Lisá, L., Bajer, A., Válek, D., Květina, P., Šumberová, R., 2013. Micromorphological Evidence of Neolithic Rondel-like Ditch Infillings; Case Studies from Těšetice-Kyjovice and Kolín, Czech Republic. IANSA IV, 135–146.

Lourdeau, A., 2011. Stability in the Intermittence, in: Conard, N.J., Richter, J. (Eds.), Neanderthal Lifeways, Subsistence and Technology, vol. 19. Vertebrate Paleobiology and Paleoanthropology. Springer Netherlands, Dordrecht, pp. 167–186.

Løvschal, M., Fontijn, D., 2019. Directionality and axiality in the Bronze Age: Cross-regional landscape perspectives on 'fire pit lines' and other pitted connections. World Archaeol 51 (1), 140–156.

Lucas, G., 2005. The archaeology of time. Themes in archaeology. Routledge, London, New York.

Machado, J., Hernández, C.M., Mallol, C., Galván, B., 2013. Lithic production, site formation and Middle Palaeolithic palimpsest analysis: In search of human occupation episodes at Abric del Pastor Stratigraphic Unit IV (Alicante, Spain). J Archaeol Sci 40 (5), 2254–2273.

Machado, J., Mallol, C., Hernández, C.M., 2015. Insights into Eurasian Middle Palaeolithic Settlement Dynamics: The Palimpsest Problem, in: Conard, N.J., Delagnes, A. (Eds.), Settlement dynamics of the Middle Paleolithic and Middle Stone Age. Tübingen publications in prehistory. Kerns, Tübingen.

Machado, J., Molina, F.J., Hernández, C.M., Tarriño, A., Galván, B., 2016. Using lithic assemblage formation to approach Middle Palaeolithic settlement dynamics: El Salt Stratigraphic Unit X (Alicante, Spain). Archaeol Anthropol Sci 1 (2), 25.

Machado, J., Pérez, L., 2015. Temporal frameworks to approach human behavior concealed in Middle Palaeolithic palimpsests: A high-resolution example from El Salt Stratigraphic Unit X (Alicante, Spain). Quat Int 417, 66–81.

Machado Gutiérrez, J., Cristo Manuel Hernández Gómez, Bertila Galván Santos, 2011. Contribución teórico-metodológica al análisis histórico de palimpsestos arqueológicos a partir de la producción lítica. Un ejemplo de aplicación para el Paleolítico medio en el yacimiento de El Salt (Alcoy, Alicante). Recerques del Museu d'Alcoi (20), 33–46.

Macphail, R., Goldberg, P., 2000a. Macphail, R.I. and P. Goldberg, 2000. Geoarchaeological investigation of sediments from Gorham's and Vanguard Caves, Gibraltar, in: Stringer, C.B., Barton, R.N.E., Finlayson, J.C. (Eds.), Neanderthals on the Edge. Oxford Books, Oxford, pp. 183–200.

Macphail, R.I., 2014. Archaeological Soil Micromorphology, in: Smith, C. (Ed.), Encyclopedia of Global Archaeology. Springer New York, New York, NY, pp. 356–364.

Macphail, R.I., Crowther, J., Cruise, J., 2007. Micromorphology and post-Roman town research: the examples of London and Magdeburg, in: Henning, J. (Ed.), Post-Roman towns, trade and settlement in Europe and Byzantium. Vol. 1: The heirs of the Roman west. Millennium-Studien Bd. 5. W. de Gruyter, Berlin, New York, pp. 303–317.

Macphail, R.I., Cruise, G.M., Allen, M.J., Linderholm, J., Reynolds, P., 2004. Archaeological soil and pollen analysis of experimental floor deposits; with special reference to Butser Ancient Farm, Hampshire, UK. J Archaeol Sci 31 (2), 175–191.

Macphail, R.I., Goldberg, P., 2000b. Geoarchaeological investigations of sediments from Gorham's and Vanguard Caves, Gibralter: Microstratigraphical (soil micromorphological and chemical) signatures., in: Stringer, C.B. (Ed.), Neanderthals on the edge. Papers from a conference marking the 150th anniversary of the Forbes' Quarry discovery, Gibraltar. Oxbow Books, Oxford, pp. 183–200.

Macphail, R.I., Goldberg, P., 2010. Archaeological Materials, in: Stoops, G. (Ed.), Interpretation of micromorphological features of soils and regoliths, 1. ed. ed. Elsevier, Amsterdam, pp. 589–622.

Macphail, R.I., McAvoy, J.M., 2008. A micromorphological analysis of stratigraphic integrity and site formation at Cactus Hill, an Early Paleoindian and hypothesized pre-Clovis occupation in south-central Virginia, USA. Geoarchaeology 23 (5), 675–694.

Madella, M., Jones, M.K., Goldberg, P., Goren, Y., Hovers, E., 2002. The Exploitation of Plant Resources by Neanderthals in Amud Cave (Israel): The Evidence from Phytolith Studies. J Archaeol Sci 29 (7), 703–719.

Maillo-Fernandez, J., Arteaga, C., Iriarte-Chiapusso, M.-J., Fernández, A., Wood, R., Quirós, F., 2014. Cueva Morín, in: Sala Ramos, R. (Ed.), Pleistocene and Holocene hunter-gatherers in Iberia and the Gibraltar Strait. The current archaeological record. Univ. de Burgos y Fundación Atapuerca, Burgos, pp. 72–78.

Malainey, M.E., Przybylski, R., Sherriff, B.L., 1999. The Effects of Thermal and Oxidative Degradation on the Fatty Acid Composition of Food Plants and Animals of Western Canada: Implications for the Identification of Archaeological Vessel Residues. J Archaeol Sci 26 (1), 95–103.

Malcolm, B., Malcolm, N., 2000. Mosses and other bryophytes: An illustrated glossary. Micro-Optics Press, Nelson, N.Z.

Mallol, C., 2006. What's in a beach? Soil micromorphology of sediments from the Lower Paleolithic site of 'Ubeidiya, Israel. J Hum Evol 51 (2), 185–206.
Mallol, C., Cabanes, D., Baena, J., 2010. Microstratigraphy and diagenesis at the upper Pleistocene site of Esquilleu Cave (Cantabria, Spain). Quat Int 214 (1-2), 70–81.
Mallol, C., Henry, A., 2017. Ethnoarchaeology of Paleolithic Fire: Methodological Considerations. Curr Anthropol 58 (16), 217-229.
Mallol, C., Hernandez, C.M., Cabanes, D., Sistiaga, A., Machado, J., Rodríguez, Á., Pérez, L., Galván, B., 2013a. The black layer of Middle Palaeolithic combustion structures. Interpretation and archaeostratigraphic implications. J Archaeol Sci 40 (5), 2515–2537.
Mallol, C., Hernández, C., 2016. Advances in palimpsest dissection. Quat Int 417, 1–2.
Mallol, C., Hernández, C., Mercier, N., Falguères, C., Carrancho, Á., Cabanes, D., Vidal-Matutano, P., Connolly, R., Pérez, L., Mayor, A., Ben Arous, E., Galván, B., 2019. Fire and brief human occupations in Iberia during MIS 4: Evidence from Abric del Pastor (Alcoy, Spain). Sci Rep 9 (1), 18281.
Mallol, C., Hernández, C.M., Cabanes, D., Machado, J., Sistiaga, A., Pérez, L., Galván, B., 2013b. Human actions performed on simple combustion structures: An experimental approach to the study of Middle Palaeolithic fire. Quat Int 315, 3–15.
Mallol, C., Marlowe, F.W., Wood, B.M., Porter, C.C., 2007. Earth, wind, and fire: Ethnoarchaeological signals of Hadza fires. J Archaeol Sci 34 (12), 2035–2052.
Mallol, C., Mentzer, S.M., Miller, C.E., 2017. Combustion Features, in: Nicosia, C., Stoops, G. (Eds.), Archaeological Soil and Sediment Micromorphology. Wiley, Hoboken, pp. 299–330.
March, R.J., 1992. L'utilisation du bois dans les foyers préhistoriques: Une approche expérimentale. Bulletin de la Société Botanique de France. Actualités Botaniques 139 (2-4), 245–253.
March, R.J., Lucquin, A., Joly, D., Ferreri, J.C., Muhieddine, M., 2014. Processes of Formation and Alteration of Archaeological Fire Structures: Complexity Viewed in the Light of Experimental Approaches. J Archaeol Method Theory 21 (1), 1–45.
March, R.J., Whallon, R., Morley, M.W., 2017. Studying Neanderthal fire structures from Crvena Stijena, in: Whallon, R. (Ed.), Crvena Stijena in Cultural and Ecological Context. Multidisciplinary Archaeological Research in Montenegro, pp. 340–449.
Marchbanks, M.L., 1989. Lipid Analysis in Archaeology: An Initial Study of Ceramics and Subsistence at the George C. Davis Site. University of Texas at Austin.
Markham, K.R., 1988. Distribution of flavonoids in the lower plants and its evolutionary significance., in: Harborne, J.B. (Ed.), The Flavonoids. Advances in Research Since 1980. Springer, New York, NY, pp. 427–468.
Marks, A., Chabai, V., 2001. Constructing Middle Paleolithic settlement systems in Crimea: potentials and limitations, in: Conard, N.J. (Ed.), Settlement dynamics of the Middle Paleolithic and Middle Stone Age. Tübingen publications in prehistory. Kerns, Tübingen, pp. 179–204.
Martínez-Moreno, J., Mora, R., La Torre, I. de, 2004. Methodological Approach for Understanding Middle Palaeolithic Settlement Dynamics at La Roca dels Bous (Noguera, Catalunya, Northeast Spain, in: Conard, N.J. (Ed.), Settlement dynamics of the Middle Paleolithic and Middle Stone Age. Tübingen publications in prehistory. Kerns, Tübingen, pp. 393–413.
Marzi, R., Torkelson, B.E., Olson, R.K., 1993. A revised carbon preference index. Org Geochem 20 (8), 1303–1306.
Matarazzo, T., Berna, F., Goldberg, P., 2010. Occupation surfaces sealed by the Avellino eruption of Vesuvius at the Early Bronze Age village of Afragola in southern Italy: A micromorphological analysis. Geoarchaeology 37, 437-466.
Mathieu, C., Stoops, G., 1972. Observations pétrographiques sur la paroi d'un four à chaux carolingien. Arcme 2 (1), 347–354.
Mayor, A., Hernández, C., Machado, J., Mallol, C., Galvan, B., 2019. El estudio tecnológico de conjuntos líticos paleolíticos desde la perspectiva del episodio de ocupación humana: los casos de El Salt y El Pastor (Alcoi, Alacant). Recerques del Museu d'Alcoi 28, 7–26.
Mayor, A., Hernández, C.M., Machado, J., Mallol, C., Galván, B., 2020. On identifying Palaeolithic single occupation episodes: Archaeostratigraphic and technological approaches to the Neanderthal lithic record of stratigraphic unit xa of El Salt (Alcoi, eastern Iberia). Archaeol Anthropol Sci 12 (4), 25.
Meignen, L., 1993. L' abri des Canalettes: Un habitat moustérien sur les grands Causses (Nant, Aveyron); fouilles 1980 - 1986. Monographie du CRA 10. CNRS éd, Paris.
Meignen, L., 2019. Changes in the use of Kebara cave during the Middle Paleolithic and Upper Paleolithic times, in: Meignen, L., Bar-Yosef, O. (Eds.), The Middle and Upper Paleolithic Archaeology. Part II. Peabody Museum Press, Harvard University, Cambridge (US), pp. 413–455.
Meignen, L., Bar-Yosef, O., Goldberg, P., 1989. Les structures de combustion moustériennes de la grotte de Kébara (Mont Carmel, Israel), in: Olive, M., Taborin, Y. (Eds.), Nature et Fonction des Foyers Préhistoriques. Actes du Colloque International de Nemours 1987, pp. 141–146.
Meignen, L., Bar-Yosef, O., Goldberg, P., Weiner, S., 2000. Le feu au paléolithique moyen: Recherches sur les structures de combustion et le statut des foyers. l'exemple du Proche-Orient. PaleO 26 (2), 9–22.

Meignen, L., Beyries, S., J., S., O., B.A.R., 1998. Acquisition, traitement des matières animales et fonction du site au Paléolithique moyen dans la grotte de Kébara (Israël): Approche interdisciplinaire, in: Économie Préhistorique: Les Comportements de Subsistance au Paléolitique. XVIII Rencontres Internationales d'Archéologie et d'Histoire d'Antibes, Sophia-Antipolis, pp. 227–241.
Meignen, L., Goldberg, P., Albert, R., Bar-Yosef, O., 2008. Structures de combustion, choix des combustibles et degré de mobilité des groupes dans le Paléolithique moyen du Proche-Orient (grottes de Kebara et d'Hayonim, Israël), in: Théry-Parisot, I., Costamagno, S., Henry, A. (Eds.), Gestion des combustibles au paléolithique et au mésolithique: nouveaux outils, nouvelles interprétations, vol.13, Session WS21. BAR International Series: 1914. Oxford: Archaeopress, pp. 101–118.
Meignen, L., Goldberg, P., Bar-Yosef, O., 2007. The hearths at Kebara Cave and their role in site formation processes, in: Bar-Yosef, O., Albert, R.M. (Eds.), Kebara Cave, Mt. Carmel, Israel. The Middle and Upper Paleolithic archaeology. Bulletin / American School of Prehistoric Research 49. Peabody Museum of Archaeology and Ethnology Harvard Univ, Cambridge, Mass., pp. 91–122.
Mellars, P., 1996. The Neanderthal legacy: An archaeological perspective from western Europe. Princeton University Press, Princeton, N.J.
Mentzer, S.M., 2011. Macro- and micro-scale geoarchaeology of Üçağızlı caves I and II, Hatay, Turkey. Doctoral Thesis.
Mentzer, S.M., 2012. Microarchaeological Approaches to the Identification and Interpretation of Combustion Features in Prehistoric Archaeological Sites. J Archaeol Method Theory 21 (3), 616–668.
Mentzer, S.M., 2017. Hearths and Combustion Features, in: Gilbert, A.S., Goldberg, P., Holliday, V.T., Mandel, R.D., Sternberg, R.S. (Eds.), Encyclopedia of geoarchaeology. Encyclopedia of earth sciences series. Springer Reference, Dordrecht, Heidelberg, New York, London, pp. 411–424.
Meyers, P.A., Ishiwatari, R., 1993. Lacustrine organic geochemistry—an overview of indicators of organic matter sources and diagenesis in lake sediments. Org Geochem 20 (7), 867–900.
Miller, C., 2011. Deposits as Artifacts. TÜVA Mitteilungen (12), 91–107.
Miller, C.E., Conard, N.J., Goldberg, P., Berna, F., 2009. Dumping, sweeping and trampling: experimental micromorphological analysis of anthropogenically modified combustion features. Palethnologie 2, 25–37.
Miller, C.E., Goldberg, P., Berna, F., 2013. Geoarchaeological investigations at Diepkloof Rock Shelter, Western Cape, South Africa. J Archaeol Sci 40 (9), 3432–3452.
Miller, C.E., Sievers, C., 2012. An experimental micromorphological investigation of bedding construction in the Middle Stone Age of Sibudu, South Africa. J Archaeol Sci 39 (10), 3039–3051.
Mills, J.S., White, R., 1977. Natural Resins of Art and Archaeology Their Sources, Chemistry, and Identification. Stud Conserv 22 (1), 12–31.
Mitić, Z.S., Zlatković, B.K., Jovanović, S.Č., Nikolić, J.S., Nikolić, B.M., Stojanović, G.S., Marin, P.D., 2018. Diversity of needle n-alkanes, primary alcohols and diterpenes in Balkan and Carpathian native populations of Pinus nigra J.F. Arnold. Biochem Syst Ecol 80, 46–54.
Molina Hernández, F.J., 2016. El sílex del Prebético y Cuencas Neógenas en Alicante y sur de Valencia: Su caracterización y estudio aplicado al Paleolítico Medio. Doctoral Thesis.
Molina Hernández, F.J., Andoni Tarriño Vinagre, Bertila Galván Santos, Cristo Manuel Hernández Gómez., 2010. Áreas de aprovisionamiento de sílex en el Paleolítico Medio en torno al Abric del Pastor (Alcoi, Alicante). Estudio macroscópico de la producción lítica de la colección Brotons. Recerques del Museu d'Alcoi (19), 65–80.
Moncel, M.-H., Moigne, A.-M., Sam, Y., Combier, J., 2011. The Emergence of Neanderthal Technical Behavior: New Evidence from Orgnac 3 (Level 1, MIS 8), Southeastern France. Curr Anthropol 52 (1), 37–75.
Mora, R., Torre, la, I. de, Martínez-Moreno, J., 2004. Middle Palaeolithic mobility and land use in the Southwestern Pyrenees: the example of level 10 in La Roca dels Bous (Noguera, Catalunya, Northeast Spain), in: Conard, N.J. (Ed.), Settlement dynamics of the Middle Paleolithic and Middle Stone Age. Tübingen publications in prehistory. Kerns, Tübingen, pp. 415–435.
Moss, G.P., Smith, P.A.S., Tavernier, D., 1995. Glossary of class names of organic compounds and reactivity intermediates based on structure (IUPAC Recommendations 1995). Pure and Applied Chemistry 67 (8-9), 1307–1375.
Mumtaz, F., Zubair, M., Khan, F., Niaz, K., 2020. Analysis of plants lipids, in: Nabavi, S., Saeedi, M., Nabavi, Seyed, Sanches Silva, Ana (Eds.), Recent Advances in Natural Products Analysis. Elsevier, pp. 677–705.
Munsell Color (Firm), 2010. Munsell soil color charts: With genuine Munsell color chips. Grand Rapids, MI.
Nicosia, C., Stoops, G. (Eds.), 2017. Archaeological Soil and Sediment Micromorphology. Wiley, Hoboken.
Niekus, M.J.L.T., Kozowyk, P.R.B., Langejans, G.H.J., Ngan-Tillard, D., van Keulen, H., van der Plicht, J., Cohen, K.M., van Wingerden, W., van Os, B., Smit, B.I., Amkreutz, L.W.S.W., Johansen, L., Verbaas, A., Dusseldorp, G.L., 2019. Middle Paleolithic complex technology and a Neandertal tar-backed tool from the Dutch North Sea. PNAS 116 (44), 22081–22087.
Nott, C.J., Xie, S., Avsejs, L.A., Maddy, D., Chambers, F.M., Evershed, R.P., 2000. n-Alkane distributions in ombrotrophic mires as indicators of vegetation change related to climatic variation. Org Geochem 31 (2-3), 231–235.

O'Connell, J.F., Hawkes, K., Jones, N.B., 1991. Distribution of Refuse-Producing Activities at Hadza Residential Base Camps, in: Jochim, M., Kroll, E.M., Price, T.D. (Eds.), The Interpretation of Archaeological Spatial Patterning. Interdisciplinary Contributions to Archaeology. Springer US, Boston, MA, pp. 61–76.
O'Connell, J.F., 1987. Alyawara Site Structure and Its Archaeological Implications. Am Antiq 52 (1), 74–108.
Olive, M., Taborin, Y. (Eds.), 1989. Nature et Fonction des Foyers Préhistoriques: Actes du Colloque International de Nemours 1987.
Ortiz, J.E., Gallego, J.L.R., Torres, T., Díaz-Bautista, A., Sierra, C., 2010. Palaeoenvironmental reconstruction of Northern Spain during the last 8000calyr BP based on the biomarker content of the Roñanzas peat bog (Asturias). Org Geochem 41 (5), 454–466.
Osborn, H.F., 1914. Men of the Old Stone Age: Their Environent, Life and Art. Charles Scribner's Sons, New York.
Otto, A., Gondokusumo, R., Simpson, M.J., 2006. Characterization and quantification of biomarkers from biomass burning at a recent wildfire site in Northern Alberta, Canada. J Appl Geochem 21 (1), 166–183.
Otto, A., Simoneit, B.R.T., Rember, W.C., 2005. Conifer and angiosperm biomarkers in clay sediments and fossil plants from the Miocene Clarkia Formation, Idaho, USA. Org Geochem 36 (6), 907–922.
Otto, A., Simpson, M.J., 2005. Degradation and Preservation of Vascular Plant-derived Biomarkers in Grassland and Forest Soils from Western Canada. Biogeochemistry 74 (3), 377–409.
Palomo, L.J., Gisbert, J., Blanco, J.C., 2007. Atlas y libro rojo de los mamíferos terrestres de España. Dirección General para la Biodiversidad-SECEM, Madrid.
Pancost, R.D., Baas, M., van Geel, B., Sinninghe Damsté, J.S., 2002. Biomarkers as proxies for plant inputs to peats: An example from a sub-boreal ombrotrophic bog. Org Geochem 33 (7), 675–690.
Pastó, I., Allué, E., Vallverdú Poch, J., 2000. Mousterian hearths at Abric Romaní, Catalonia (Spain), in: Stringer, C.B. (Ed.), Neanderthals on the edge. Papers from a conference marking the 150th anniversary of the Forbes' Quarry discovery, Gibraltar. Oxbow Books, Oxford, pp. 59–67.
Patania, I., Goldberg, P., Cohen, D.J., Yuan, J., Wu, X., Bar-Yosef, O., 2019. Micromorphological and FTIR analysis of the Upper Paleolithic early pottery site of Yuchanyan cave, Hunan, South China. Geoarchaeology 35 (2), 143–163.
Patrick, M., Koning, A.J., Smith, A.B., 1985. Gas Liquid Chromatographic Analysis of Fatty acids in Food Residues from Ceramics Found in the Southwestern Cape, South Africa. Archaeometry 27 (2), 231–236.
Paunovic, M., Culiberg, M., Turk, I., 2002. Analysis of the content of hearths from the Mousterian site of Divje babe 1 (Slovenia). Razprave IV Razreda Sazu (43), 203–218.
Pawlik, A.F., Thissen, J.P., 2011. Hafted armatures and multi-component tool design at the Micoquian site of Inden-Altdorf, Germany. J Archaeol Sci 38 (7), 1699–1708.
Peeters, H., Niekus, M.J.L.T., 2017. Mesolithic Pit Hearths in the Northern Netherlands Function, Time-Depth and Behavioural Context, in: Digging in the Mesolithic. Ac tes de la séance de la Société préhistorique française, Châlons-en-Champagne. 29-30 mars 2016, pp. 225–239.
Pérez, L., 2019. Estrategias de subsistencia y dinámicas de asentamiento en los Valles de Alcoy durante el Paleolítico medio. Análisis zooarqueológico, tafonómico y paleoecológico de la secuencia arqueológica de El Salt. Doctoral Thesis.
Pérez, L., Machado, J., Hernández, C., Morales Pérez, J., Brugal, J.-P., Galvan, B., 2015. Arqueozoologia y arqueoestratigrafía del yacimiento de El Salt (Alcoi, Alicante): contribución metodológica para el análisis del registro faunístico contenido en palimpsestos arqueológicos del Paleolítico medio, in: Sanchis Serra, A. (Ed.), Preses petites i grups humans en el passat. II Jornades d'Arqueozoologia del Museu de Prehistòria de València. Museu de Prehistoria de València, València, pp. 223–244.
Pérez, L., Machado, J., Sanchis, A., Hernández, C., Mallol, C., Galvan, B., 2020. A High Temporal Resolution Zooarchaeological Approach to Neanderthal Subsistence Strategies on the Southeastern Iberian Peninsula: El Salt Stratigraphic Unit Xa (Alicante, Spain), in: Cascalheira, J., Picin, A. (Eds.), Short-Term Occupations in Paleolithic Archaeology. Definition and Interpretation, 1st ed. 2020 ed. Interdisciplinary Contributions to Archaeology. Springer International Publishing; Springer, Cham, pp. 237–289.
Pérez, L., Sanchis, A., Hernández, C., Galván, B., 2017a. Paleoecología de Macromamíferos Aplicada a los Conjuntos zooarqueológicos de el Salt. Interaccions entre felins i humans. III Jornades d'arquezoologia., 327–353.
Pérez, L., Sanchis, A., Hernández, C.M., Galván, B., Sala, R., Mallol, C., 2017b. Hearths and bones: An experimental study to explore temporality in archaeological contexts based on taphonomical changes in burnt bones. J Archaeol Sci Rep 11, 287–309.
Peters, K.E., Walters, C.C., Moldowan, J.M., 2005. The biomarker guide. - 1. Biomarkers and isotopes in the environment and human history, 2. ed. ed. Cambridge Univ. Press, Cambridge.
Picin, A., Cascalheira, J., 2020. Introduction to Short-Term Occupations in Palaeolithic Archaeology, in: Cascalheira, J., Picin, A. (Eds.), Short-Term Occupations in Paleolithic Archaeology. Definition and Interpretation, 1st ed. 2020 ed. Interdisciplinary Contributions to Archaeology. Springer International Publishing; Springer, Cham.
Picornell-Gelabert, L., Allué, E., Courty, M.A., 2017. An archaeology of fuels: Social and environmental factors in behavioural strategies of multi-resource management. Quat Int 431, 2–5.

Polo-Díaz, A., Benito-Calvo, A., Martínez-Moreno, J., Mora Torcal, R., 2016. Formation processes and stratigraphic integrity of the Middle-to-Upper Palaeolithic sequence at Cova Gran de Santa Linya (Southeastern Prepyrenees of Lleida, Iberian Peninsula). Quat Int 417, 16–38.

Prost, K., Birk, J.J., Lehndorff, E., Gerlach, R., Amelung, W., 2017. Steroid Biomarkers Revisited - Improved Source Identification of Faecal Remains in Archaeological Soil Material. PloS one 12 (1), e0164882.

Rampelli, S., Turroni, S., Mallol, C., Hernandez, C., Galván, B., Sistiaga, A., Biagi, E., Astolfi, A., Brigidi, P., Benazzi, S., Lewis, C.M., Warinner, C., Hofman, C.A., Schnorr, S.L., Candela, M., 2021. Components of a Neanderthal gut microbiome recovered from fecal sediments from El Salt. Communications biology 4 (1), 169.

Raposo, L., 1995. Ambientes, territorios y subsistencia en el Paleolítico Medio de Portugal. CMPL 6, 57–77.

Reitz, E.J., Shackley, M.L., 2012. Environmental archaeology. Manuals in archaeological method, theory and technique. Springer, New York.

Rellini, I., Firpo, M., Isetti, E., Rossi, G., Robb, J., Pian, D., Traverso, A., 2020. Micromorphological investigations at Scaloria Cave (Puglia, South-east Italy): New evidences of multifunctional use of the space during the Neolithic. Archaeol Anthropol Sci 12 (1), 1–21.

Richter, J., 2006. Neanderthals in their landscape, in: Demarsin, B., Otte, M. (Eds.), Neanderthals in Europe. Proceedings of the international conference, held in the Gallo-Roman Museum in Tongeren, vol. 117. Atvatvca 2, pp. 51–66.

Rieley, G., Collier, R.J., Jones, D.M., Eglinton, G., Eakin, P.A., Fallick, A.E., 1991. Sources of sedimentary lipids deduced from stable carbon-isotope analyses of individual compounds. Nature 352 (6334), 425–427.

Rigaud, J.-P., Simek, J.F., Ge, T., 1995. Mousterian fires from Grotte XVI (Dordogne, France). Antiquity 69 (266), 902–912.

Rivals, F., Moncel, M.-H., Patou-Mathis, M., 2009a. Seasonality and intra-site variation of Neanderthal occupations in the Middle Palaeolithic locality of Payre (Ardèche, France) using dental wear analyses. J Archaeol Sci 36 (4), 1070–1078.

Rivals, F., Schulz, E., Kaiser, T.M., 2009b. A new application of dental wear analyses: estimation of duration of hominid occupations in archaeological localities. J Hum Evol 56 (4), 329–339.

Rodríguez de Vera, C., Herrera-Herrera, A.V., Jambrina-Enríquez, M., Sossa-Ríos, S., González-Urquijo, J., Lazuen, T., Vanlandeghem, M., Alix, C., Monnier, G., Pajović, G., Tostevin, G., Mallol, C., 2020. Micro-contextual identification of archaeological lipid biomarkers using resin-impregnated sediment slabs. Sci Rep 10 (1), 20574.

Rodriguez Rodriguez, A.d.C., Galván, B., Hernández, C.M., 2002. Contribución del análisis funcional en la caracterización de El Salt como un centro de intervención referencial de las poblaciones neandertalianas en los Valles de Alcoi (Alicante), in: Clemente, I., Risch, R., Gibaja, J.F. (Eds.), Análisis functional. Su aplicación al estudios de sociedades prehistóricas. Archaeopress, pp. 121–132.

Rodríguez-Cintas, Á., Cabanes, D., 2015. Phytolith and FTIR studies applied to combustion structures: The case of the Middle Paleolithic site of El Salt (Alcoy, Alicante). Quat Int 431, 16–26.

Roebroeks, W., Tuffreau, A., 1999. Palaeoenvironment and settlement patterns of the Northwest European Middle Palaeolithic, in: Roebroeks, W., Gamble, C. (Eds.), The Middle Palaeolithic Occupation of Europe. University of Leiden, Leiden, pp. 121–138.

Roebroeks, W., Villa, P., 2011. On the earliest evidence for habitual use of fire in Europe. PNAS 108 (13), 5209–5214.

Röpke, A., Dietl, C., 2017. Burnt Soils and Sediment, in: Nicosia, C., Stoops, G. (Eds.), Archaeological Soil and Sediment Micromorphology. Wiley, Hoboken, pp. 173–180.

Rosell, J., Blasco, R., Rivals, F., Chacón, M.G., Arilla, M., Camarós, E., Rufà, A., Sánchez-Hernández, C., Picin, A., Andrés, M., Blain, H.-A., López-García, J.M., Iriarte, E., Cebrià, A., 2015. A resilient landscape at Teixoneres Cave (MIS 3; Moià, Barcelona, Spain): The Neanderthals as disrupting agent. Quat Int 435, 195–210.

Rudzińska, M., Przybylski, R., Wąsowicz, E., 2009. Products Formed During Thermo-oxidative Degradation of Phytosterols. J Am Oil Chem Soc 86 (7), 651–662.

Sánchez-Hernández, C., Rivals, F., Blasco, R., Rosell, J., 2014. Short, but repeated Neanderthal visits to Teixoneres Cave (MIS 3, Barcelona, Spain): A combined analysis of tooth microwear patterns and seasonality. J Archaeol Sci 49, 317–325.

Sandgathe, D.M., 2017. Identifying and Describing Pattern and Process in the Evolution of Hominin Use of Fire. Curr Anthropol 58 (16), 360-370.

Sañudo, P., Blasco, R., Fernández Peris, J., 2016. Site formation dynamics and human occupations at Bolomor Cave (Valencia, Spain): An archaeostratigraphic analysis of levels I to XII (100–200 ka). Quat Int 417, 94–104.

Sanz, M., Daura, J., Égüez, N., Cabanes, D., 2017. On the track of anthropogenic activity in carnivore dens: Altered combustion structures in Cova del Gegant (NE Iberian Peninsula). Quat Int 437, 102–114.

Schaetzl, R.J., Anderson, S., 2005. Soils: Genesis and geomorphology / Randall Schaetzl and Sharon Anderson. Cambridge University Press, Cambridge.

Schiegl, S., Conard, N., 2006. The Middle Stone Age sediments at Sibudu: results from FTIR spectroscopy and microscopic analyses. South African Humanit 18, 149–172.

Schiegl, S., Goldberg, P., Bar-Yosef, O., Weiner, S., 1996. Ash Deposits in Hayonim and Kebara Caves, Israel: Macroscopic, Microscopic and Mineralogical Observations, and their Archaeological Implications. J Archaeol Sci 23 (5), 763–781.

Schiegl, S., Goldberg, P., Pfretzschner, H.-U., Conard, N.J., 2003. Paleolithic burnt bone horizons from the Swabian Jura: Distinguishing between in situ fireplaces and dumping areas. Geoarchaeology 18 (5), 541–565.

Schiegl, S., Lev-Yadun, S., Bar-Yosef, S., El Goresy, A., Weiner, S., 1994. Siliceous aggregates from prehistoric wood ash: a major component of sediments in Kebara and Hayonim caves (Israel). Isr J Earth Sci (43), 267–278.

Schiffer, M.B., Skibo, J.M., Griffitts, J.L., Hollenback, K.L., Longacre, W.A., 2001. Behavioral Archaeology and the Study of Technology. Am Antiq 66 (4), 729–737.

Schmidt, P., Blessing, M., Rageot, M., Iovita, R., Pfleging, J., Nickel, K.G., Righetti, L., Tennie, C., 2019. Birch tar production does not prove Neanderthal behavioral complexity. PNAS 116 (36), 17707–17711.

Scott, B., 2011. Becoming Neanderthals: The earlier British Middle Palaeolithic. Oxbow Books, Oxford, Oakville, Conn.

Seaward, M.R.D., Williams, D., 1976. An interpretation of mosses found in recent archaeological excavations. J Archaeol Sci 3 (2), 173–177.

Shahack-Gross, R., Ayalon, A., Goldberg, P., Goren, Y., Ofek, B., Rabinovich, R., Hovers, E., 2008. Formation processes of cemented features in karstic cave sites revealed using stable oxygen and carbon isotopic analyses: A case study at middle paleolithic Amud Cave, Israel. Geoarchaeology 23 (1), 43–62.

Shahack-Gross, R., Marshall, F., Ryan, K., Weiner, S., 2004. Reconstruction of spatial organization in abandoned Maasai settlements: Implications for site structure in the Pastoral Neolithic of East Africa. J Archaeol Sci 31 (10), 1395–1411.

Sharma, O.P., 2014. Bryophyta. Series on diversity of microbes and cryptogams. McGraw Hill Education, New Delhi.

Sheppard, T., 1922. The Pre-historic Boat from Brigg. Mar Mirror 8 (8), 226–232.

Shillito, L.-M., Matthews, W., Bull, I., Williams, J., 2013. Biomolecular investigations of faecal biomarkers at Sheik-e Abad and Jani, in: Matthews, R., Matthews, W., Muḥammadīfar, Y.D. (Eds.), The earliest Neolithic of Iran. 2008 excavations at Sheikh-e Abad and Jani. CZAP reports 1. Oxbow Books, Oxford, UK, Oakville, CT pp. 105-115.

Shipman, P., 1981. Life history of a fossil: An introduction to taphonomy and paleoecology. Harvard Univ.Pr, Cambridge, Mass., London.

Shipman, P., Rose, J., 1983. Early hominid hunting, butchering, and carcass-processing behaviors: Approaches to the fossil record. J Anthropol Archaeol 2 (1), 57–98.

Sievers, C., Wadley, L., 2008. Going underground: Experimental carbonization of fruiting structures under hearths. J Archaeol Sci 35 (11), 2909–2917.

Simoneit, B.R.T., Rushdi, A.I., bin Abas, M.R., Didyk, B.M., 2003. Alkyl amides and nitriles as novel tracers for biomass burning. Environ Sci Technol 37 (1), 16–21.

Simpson, M.J., Simpson, A.J., 2012. The chemical ecology of soil organic matter molecular constituents. J Chem Ecol 38 (6), 768–784.

Sistiaga, A., Mallol, C., Galván, B., Summons, R.E., 2014. The Neanderthal meal: a new perspective using faecal biomarkers. PloS one 9 (6), e101045.

Sistiaga Gutiérrez, A., March, R., Gómez, C.M.H., Santos, B.G., 2011. Aproximación desde la química orgánica al estudio de los hogares del yacimiento del Paleolítico medio de El Salt (Alicante, España). Recerques del Museu d'Alcoi (20), 47–70.

Skibo, J.M., Schiffer, M.B., 2008. People and Things: A Behavioral Approach to Material Culture. Springer Science+Business Media LLC, New York, NY.

Smogorzewska, A., 2012. Fire Installations in Household Activities. Archaeological and ethnoarchaeological study from Tell Arbid (North-East Syria). PaleO 38 (1), 227–247.

Sophonrat, N., Sandström, L., Zaini, I.N., Yang, W., 2018. Stepwise pyrolysis of mixed plastics and paper for separation of oxygenated and hydrocarbon condensates. Appl Energy 229, 314–325.

Spagnolo, V., Marciani, G., Aureli, D., Berna, F., Boscato, P., Ranaldo, F., Ronchitelli, A., 2016. Between hearths and volcanic ash: The SU 13 palimpsest of the Oscurusciuto rock shelter (Ginosa – Southern Italy): Analytical and interpretative questions. Quat Int 417, 105–121.

Spagnolo, V., Marciani, G., Aureli, D., Berna, F., Toniello, G., Astudillo, F., Boschin, F., Boscato, P., Ronchitelli, A., 2018. Neanderthal activity and resting areas from stratigraphic unit 13 at the Middle Palaeolithic site of Oscurusciuto (Ginosa - Taranto, Southern Italy). Quat Sci Rev, 169–193.

Spedding, P.J., 1988. Peat. Fuel 67 (7), 883–900.

Speth, J., 2004. News flash: Negative evidence convicts Neanderthals of gross mental incompetence. World Archaeol 36 (4), 519–526.

Speth, J.D., 2010. The paleoanthropology and archaeology of big-game hunting: Protein, fat, or politics? Interdisciplinary Contributions to Archaeology. Springer, New York.

Speth, J.D., Meignen, L., Bar-Yosef, O., Goldberg, P., 2012. Spatial organization of Middle Paleolithic occupation X in Kebara Cave (Israel): Concentrations of animal bones. Quat Int 247 (5), 85–102.

Stacey, F.D., 1967. The Koenigsberger ratio and the nature of thermoremanence in igneous rocks. Earth Planet Sci Lett 2 (1), 67–68.

Stahlschmidt, M.C., Mallol, C., Miller, C.E., 2020. Fire as an Artifact—Advances in Paleolithic Combustion Structure Studies: Introduction to the Special Issue. J Paleo Arch 3 (4), 503–508.

Stevenson, M.G., 1991. Beyond the Formation of Hearth-Associated Artifact Assemblages, in: Jochim, M., Kroll, E.M., Price, T.D. (Eds.), The Interpretation of Archaeological Spatial Patterning. Interdisciplinary Contributions to Archaeology. Springer US, Boston, MA, pp. 269–299.
Stiner, M.C., Kuhn, S.L., Weiner, S., Bar-Yosef, O., 1995. Differential Burning, Recrystallization, and Fragmentation of Archaeological Bone. J Archaeol Sci 22 (2), 223–237.
Stoneburner, A., 1985. Variation and Taxonomy of Weissia in the Southwestern United States. II. Taxonomic Treatment. Bryologist 88 (4), 293–314.
Stoops, G., 2003. Guidelines for analysis and description of soil and regolith thin sections. Soil Science Soc. of America, Madison.
Stoops, G. (Ed.), 2010. Interpretation of micromorphological features of soils and regoliths, 1. ed. ed. Elsevier, Amsterdam.
Stoops, G., 2014. The "Fabric" of soil micromorphological research in the 20th century — A bibliometric analysis. Geoderma 213, 193–202.
Stoops, G., Nicosia, C., 2017. Introduction, in: Nicosia, C., Stoops, G. (Eds.), Archaeological Soil and Sediment Micromorphology. Wiley, Hoboken, pp. 1–7.
Stout, S.A., 1992. Aliphatic and aromatic triterpenoid hydrocarbons in a Tertiary angiospermous lignite. Org Geochem 18 (1), 51–66.
Straus, L.G., 1982. Carnivores and Cave Sites in Cantabrian Spain. J Anthropol Res 38 (1), 75–96.
Straus, L.G., 1989. On Early Hominid Use of Fire. Curr Anthropol 30 (4), 488–491.
Suarez Villagran, X., Gianotti, C., 2013. Earthen mound formation in the Uruguayan lowlands (South America): Micromorphological analyses of the Pago Lindo archaeological complex. J Archaeol Sci 40 (2), 1093–1107.
Suire, C., Bourgeois, G., Koponen, T., 2000. Some chemical constituents of thirteen mosses from the traditional Mniaceae family. J Hattori Bot Lab, 233–246.
Sullivan, A.P., 1992. Investigating the Archaeological Consequences of Short-Duration Occupations. Am Antiq 57 (1), 99–115.
Surovell, T.A., Brantingham, P.J., 2007. A note on the use of temporal frequency distributions in studies of prehistoric demography. J Archaeol Sci 34 (11), 1868–1877.
Tamura, T., Akihisa, T., Kokke, W., 1991. Naturally Occurring Sterols and Related Compounds from Plants, in: Patterson, G.W., Nes, W.D. (Eds.), Physiology and biochemistry of sterols. American Oil Chemists' Society, Champaign, Ill., pp. 172–228.
Théry-Parisot, I., 2002a. Fuel Management (Bone and Wood) During the Lower Aurignacian in the Pataud Rock Shelter (Lower Palaeolithic, Les Eyzies de Tayac, Dordogne, France). Contribution of Experimentation. J Archaeol Sci 29 (12), 1415–1421.
Théry-Parisot, I., 2002b. The gathering of firewood during Palaeolithic time, in: Charcoal Analysis. Methodological approaches, Paleoecological Results and Wood Uses. Proceedings of the Second International Meeting of Anthracology. Second International Meeting of Anthracology, Paris. BAR International series, pp. 243–250.
Théry-Parisot, I., Meignen, L., 2000. Économie des combustibles (bois et lignite) dans l'abri moustérien des Canalettes [L'expérimentation à la simulation des besoins énergétiques]. Gallia préhistoire 42 (1), 45–55.
Thiébaut, C., Meignen, L., Lévêque, F., 2009. Les dernières occupations moustériennes de Saint-Césaire (Charente-Maritime, France): Diversité des techniques utilisées et comportements économiques pratiqués. BSPF 106 (4), 691–714.
Thummel, R.V., Brightly, W.H., Strömberg, C.A.E., 2019. Evolution of phytolith deposition in modern bryophytes, and implications for the fossil record and influence on silica cycle in early land plant evolution. New Phytol 221 (4), 2273–2285.
Turq, A., Dibble, H.L., Goldberg, P., Mc Pherron, S.P., Sandgathe, D.M., Jones, H.L., Maddison, K., Maureille, B., Mentzer, S., Rink, J.W., Steenhuyse, A., 2011. Les fouilles récentes du Pech de l'Azé IV (Dordogne). Galip 53 (1), 1–58.
Üçüncü, O., Cansu, T.B., Ozdemir, T., Alpay Karaoğlu, Ş., Yayli, N., 2010. Chemical composition and antimicrobial activity of the essential oils of mosses (Tortula muralis Hedw., Homalothecium lutescens (Hedw.) H. Rob., Hypnum cupressiforme Hedw., and Pohlia nutans (Hedw.) Lindb.) from Turkey. Turk J Chem 34, 825–834.
Uerpmann, H.-P., 1973. Animal Bone Finds and Economic Archaeology: A Critical Study of 'Osteo-Archaeological' Method. World Archaeol 4 (3), 307–322.
Vallverdú, J., Allué, E., Bischoff, J.L., Cáceres, I., Carbonell, E., Cebrià, A., García-Antón, D., Huguet, R., Ibáñez, N., Martínez, K., Pastó, I., Rosell, J., Saladié, P., Vaquero, M., 2005a. Short human occupations in the Middle Palaeolithic level I of the Abric Romani rock-shelter (Capellades, Barcelona, Spain). J Hum Evol 48 (2), 157–174.
Vallverdú, J., Allué, E., Bischoff, J.L., Cáceres, I., Carbonell, E., Cebrià, A., García-Antón, D., Huguet, R., Ibáñez, N., Martínez, K., Pastó, I., Rosell, J., Saladié, P., Vaquero, M., 2005b. Short human occupations in the Middle Palaeolithic level i of the Abric Romaní rock-shelter (Capellades, Barcelona, Spain). J Hum Evol 48 (2), 157–174.
Vallverdú, J., Vaquero, M., Cáceres, I., Allué, E., Rosell, J., Saladié, P., Chacón, G., Ollé, A., Canals, A., Sala, R., Courty, M.A., Carbonell, E., 2010. Sleeping Activity Area within the Site Structure of Archaic Human Groups. Curr Anthropol 51 (1), 137–145.

Vallverdú Poch, J., 2002. Micromorphología de las facies sedimentarias de la Sierra de Atapuerca y del nivel J del Abric Romaní. Implicaciones geoarchaeológicas y paleoetnográficas.: Tesis doctoral presentada para obtener el grado de doctor del programa Ocupació del territorio: interpretacions històriques. Tesis doctoral, Tarragona.

Vallverdú Poch, J., Alonso, S., Bargalló, A., Bartrolí, R., Campeny, G., Carrancho, Á., Expósito, I., Fontanals, M., Gabucio, J., Gómez, B., Prats, J.M., Sañudo, P., Solé, À., Vilalta, J., Carbonell, E., 2012. Combustion structures of archaeological level O and mousterian activity areas with use of fire at the Abric Romaní rockshelter (NE Iberian Peninsula). Quat Int 247, 313–324.

van Vliet-Lanoë, B., Cliquet, D., Auguste, P., Folz, E., Keen, D., Schwenninger, J.-L., Mercier, N., Alix, P., Roupin, Y., Meurisse, M., Seignac, H., 2006. L'abri sous-roche du Rozel (France, Manche): Un habitat de la phase récente du Paléolithique moyen dans son contexte géomorphologique. Quaternaire 17 (3), 207–258.

Vannieuwenhuyse, D., 2017. Mind the gap: geoarchaeology and micromorphology of cave and rockshelter sequences from the Kimberley, north-west Australia. Doctoral Thesis.

Vannieuwenhuyse, D., O'Connor, S., Balme, J., 2017. Settling in Sahul: Investigating environmental and human history interactions through micromorphological analyses in tropical semi-arid north-west Australia. J Archaeol Sci 77, 172–193.

Vaquero, M., 2008. The history of stones: Behavioural inferences and temporal resolution of an archaeological assemblage from the Middle Palaeolithic. J Archaeol Sci 35 (12), 3178–3185.

Vaquero, M., 2012. Introduction: Neanderthal Behavior and Temporal Resolution of Archeological Assemblages, in: Carbonell i Roura, E. (Ed.), High Resolution Archaeology and Neanderthal Behavior. Vertebrate Paleobiology and Paleoanthropology. Springer Netherlands, Dordrecht, pp. 1–16.

Vaquero, M., Bargalló, A., Chacón, M.G., Romagnoli, F., Sañudo, P., 2015. Lithic recycling in a Middle Paleolithic expedient context: Evidence from the Abric Romaní (Capellades, Spain). Quat Int 361, 212–228.

Vaquero, M., Chacón, M.G., García-Antón, M.D., Gómez de Soler, B., Martínez, K., Cuartero, F., 2012. Time and space in the formation of lithic assemblages: The example of Abric Romaní Level J. Quat Int 247, 162–181.

Vaquero, M., Pastó, I., 2001. The Definition of Spatial Units in Middle Palaeolithic Sites: The Hearth-Related Assemblages. J Archaeol Sci 28 (11), 1209–1220.

Vaquero, M., Vallverdu, J., Rosell, J., Pasto, I., Allue, E., 2001. Neandertal Behavior at the Middle Palaeolithic Site of Abric Romani, Capellades, Spain. J Field Archaeol 28 (1/2), 93–114.

Vidal-Matutano, P., 2016. Firewood and hearths: Middle Palaeolithic woody taxa distribution from El Salt, stratigraphic unit Xb (Eastern Iberia). Quat Int 457, 74–84.

Vidal-Matutano, P., Henry, A., Théry-Parisot, I., 2017. Dead wood gathering among Neanderthal groups: Charcoal evidence from Abric del Pastor and El Salt (Eastern Iberia). J Archaeol Sci 80, 109–121.

Vidal-Matutano, P., Pérez-Jordà, G., Hernández, C.M., Galván, B., 2018. Macrobotanical evidence (wood charcoal and seeds) from the Middle Palaeolithic site of El Salt, Eastern Iberia: Palaeoenvironmental data and plant resources catchment areas. J Archaeol Sci Rep 19, 454–464.

Villa, P., Boscato, P., Ranaldo, F., Ronchitelli, A., 2009. Stone tools for the hunt: Points with impact scars from a Middle Paleolithic site in southern Italy. J Archaeol Sci 36 (3), 850–859.

Villa, P., Mahieu, E., 1991. Breakage patterns of human long bones. J Hum Evol 21 (1), 27–48.

Villagran, X.S., 2019. The Shell Midden Conundrum: Comparative Micromorphology of Shell-Matrix Sites from South America. J Archaeol Method Theory 26 (1), 344–395.

Villagran, X.S., Balbo, A.L., Madella, M., Vila, A., Estevez, J., 2011a. Experimental micromorphology in Tierra del Fuego (Argentina): Building a reference collection for the study of shell middens in cold climates. J Archaeol Sci 38 (3), 588–604.

Villagran, X.S., Balbo, A.L., Madella, M., Vila, A., Estevez, J., 2011b. Stratigraphic and spatial variability in shell middens: Microfacies identification at the ethnohistoric site Tunel VII (Tierra del Fuego, Argentina). Archaeol Anthropol Sci 3 (4), 357–378.

Villagran, X.S., Giannini, P.C.F., DeBlasis, P., 2009. Archaeofacies analysis: Using depositional attributes to identify anthropic processes of deposition in a monumental shell mound of Santa Catarina State, southern Brazil. Geoarchaeology 24 (3), 311–335.

Villagran, X.S., Huisman, D.J., Mentzer, S.M., Miller, C.E., Jans, M.M., 2017. Bone and Other Skeletal Tissues, in: Nicosia, C., Stoops, G. (Eds.), Archaeological Soil and Sediment Micromorphology. Wiley, Hoboken, pp. 9–38.

Villagran, X.S., Strauss, A., Alves, M., Oliveira, R.E., 2019. Virtual micromorphology: The application of micro-CT scanning for the identification of termite mounds in archaeological sediments. J Archaeol Sci Rep 24, 785–795.

Villaverde, V., Martínez Valle, R., Calatayud, P.M., Pilar Fumanal, M., 1996. Mobility and the role of small game in the Middle Paleolithic of the Central Region of the Spanish Mediterranean: A Comparison of Cova Negra with other Paleolithic deposits, in: Carbonell, E. (Ed.), The last neandertals, the first anatomically modern humans. A tale about the human diversity; cultural change and human evolution: the crisis at 40 KA BP. Porticos Librerias, Zaragoza.

Villeneuve, L., Farizy, C., 1989. Les témoins de combustion du gisement moustérien de Champlost (Yonne), in: Olive, M., Taborin, Y. (Eds.), Nature et Fonction des Foyers Préhistoriques. Actes du Colloque International de Nemours 1987, pp. 135–139.

Vitezović, S., 2013. From Artefacts to Behaviour: Technological Analyses in Prehistory. Anthropologie L1 (2), 175–194.
Volkman, J.K., 1986. A review of sterol markers for marine and terrigenous organic matter. Org Geochem 9 (2), 83–99.
Wadley, L., 2006. Partners in grime: results of multi-disciplinary archaeology at Sibudu Cave. South African Humanit 18, 315–341.
Wallace, I.J., Shea, J.J., 2006. Mobility patterns and core technologies in the Middle Paleolithic of the Levant. J Archaeol Sci 33 (9), 1293–1309.
Wandsnider, L., 1997. The Roasted and the Boiled: Food Composition and Heat Treatment with Special Emphasis on Pit-Hearth Cooking. J Anthropol Archaeol 16 (1), 1–48.
Wang, Q., Li, Y., Wang, Y., 2011. Optimizing the weight loss-on-ignition methodology to quantify organic and carbonate carbon of sediments from diverse sources. Environ Monit Assess 174 (1-4), 241–257.
Ward, I., Veth, P., Prossor, L., Denham, T., Ditchfield, K., Manne, T., Kendrick, P., Byrne, C., Hook, F., Troitzsch, U., 2017. 50,000 years of archaeological site stratigraphy and micromorphology in Boodie Cave, Barrow Island, Western Australia. J Archaeol Sci Rep 15, 344–369.
Wattez, J., 1988. Contribution à la connaissance des foyers préhistoriques par l'étude des cendres. BSPF 85 (10), 352–366.
Wattez, J., 1992. Dynamique de formation des structures de combustion de la fin du paléolithique au néolithique moyen: approche méthodologique et implications culturelles. Univ. de Paris 1.
Weiner, S., 2010. Microarchaeology: Beyond the visible archaeological record. Cambridge University Press, Cambridge, New York.
Weiner, S., Goldberg, P., Bar-Yosef, O., 2002. Three-dimensional Distribution of Minerals in the Sediments of Hayonim Cave, Israel: Diagenetic Processes and Archaeological Implications. J Archaeol Sci 29 (11), 1289–1308.
Weinstein-Evron, M., Tsatskin, A., Weiner, S., Shahack-Gross, R., Frumkin, A., Yeshurun, R., Zaidner, Y., 2012. A window into Early Middle Paleolithic Human Occupational Layers: Misliya Cave, Mounta Carmel, Israel. PA 2012, 202–228.
Wen, Y., Wang, S., Mu, W., Yang, W., Jönsson, P.G., 2020. Pyrolysis performance of peat moss: A simultaneous in-situ thermal analysis and bench-scale experimental study. Fuel 277, 118173.
Wiesenberg, G.L.B., Lehndorff, E., Schwark, L., 2009. Thermal degradation of rye and maize straw: Lipid pattern changes as a function of temperature. Org Geochem 40 (2), 167–174.
Wiesenberg, G.L.B., Schwarzbauer, J., Schmidt, M.W.I., Schwark, L., 2004. Source and turnover of organic matter in agricultural soils derived from n-alkane/n-carboxylic acid compositions and C-isotope signatures. Org Geochem 35 (11-12), 1371–1393.
Wragg Sykes, R.M., Coward, F., Hosfield, R., Pope, M., Wenban-Smith, F., 2015. To see a world in a hafted tool: birch pitch composite technology, cognition and memory in Neanderthals, in: Coward, F., Hosfield, R., Pope, M., Wenban-Smith, F. (Eds.), Settlement, Society and Cognition in Human Evolution. Cambridge University Press, New York, pp. 117–137.
Wu, Z., Luo, H., 2018. Pyrolysis Characteristics and Kinetic Analysis of Sediment from the Dianchi Lake in China. Int J Chem Eng (1), 1–7.
Xie, S., Guo, J., Huang, J., Chen, F., Wang, H., Farrimond, P., 2004. Restricted utility of δ 13 C of bulk organic matter as a record of paleovegetation in some loess–Paleosol sequences in the Chinese Loess Plateau. Quat Res 62 (1), 86–93.
Yamasaki, Y., Nakashima, S., Konno, H., 2007. A novel alpha-glucosidase from the moss Scopelophila cataractae. Acta Biochim Pol 54 (2), 401–406.
Yellen, J.E., 1977. Archaeological approaches to the present. Academic Press, New York.
Yellen, J.E., 1991. Small mammals: Post-discard patterning of !Kung San faunal remains. J Anthropol Archaeol 10 (2), 152–192.
Yravedra, J., 2006. Tafonomía aplicada a zooarqueología. UNED - Universidad Nacional de Educación a Distancia, Madrid.
Yravedra, J., Álvarez-Alonso, D., Estaca-Gómez, V., López-Cisneros, P., Arrizabalaga, Á., Elorza, M., Iriarte, M.J., Pardo, J.F.J., Ses, C., Uzquiano, P., 2016. New evidence of bones used as fuel in the Gravettian level at Coímbre cave, northern Iberian Peninsula. Archaeol Anthropol Sci 9, 1153–1168.
Yravedra, J., Uzquiano, P., 2013. Burnt bone assemblages from El Esquilleu cave (Cantabria, Northern Spain): Deliberate use for fuel or systematic disposal of organic waste? Quat Sci Rev 68, 175–190.
Zech, M., Pedentchouk, N., Buggle, B., Leiber, K., Kalbitz, K., Markovic, S., Glaser, B., 2011. Effect of leaf litter degradation and seasonality on D/H isotope ratios of n-alkane biomarkers. Geochim Cosmochim Acta 75, 4917–4928.
Zerboni, A., 2011. Micromorphology reveals in situ Mesolithic living floors and archaeological features in multiphase sites in central Sudan. Geoarchaeology 26 (3), 365–391.
Zerboni, A., Massamba N'Siala, I., Biagetti, S., Di Lernia, S., 2013. Burning without slashing. Cultural and environmental implications of a traditional charcoal making technology in the central Sahara. J Arid Environ 98, 126–131.

Zhao, F., Wang, P., Lucardi, R.D., Su, Z., Li, S., 2020. Natural Sources and Bioactivities of 2,4-Di-Tert-Butylphenol and Its Analogs. Toxins 12 (1).

Zieba, A., Sitlivy, V., Sobczyk, K., Kolesnik, A.V., 2008. Raw Material Exploitation and Intra-Site Spatial Distribution at Two Late Middle and Early Upper Paleolithic Sites in the Krakow Region: Piekary IIA and Ksiecia Jozefa. Archaeol Enthol Anthropol Eurasia 33 (1), 46–57.

9. Appendices

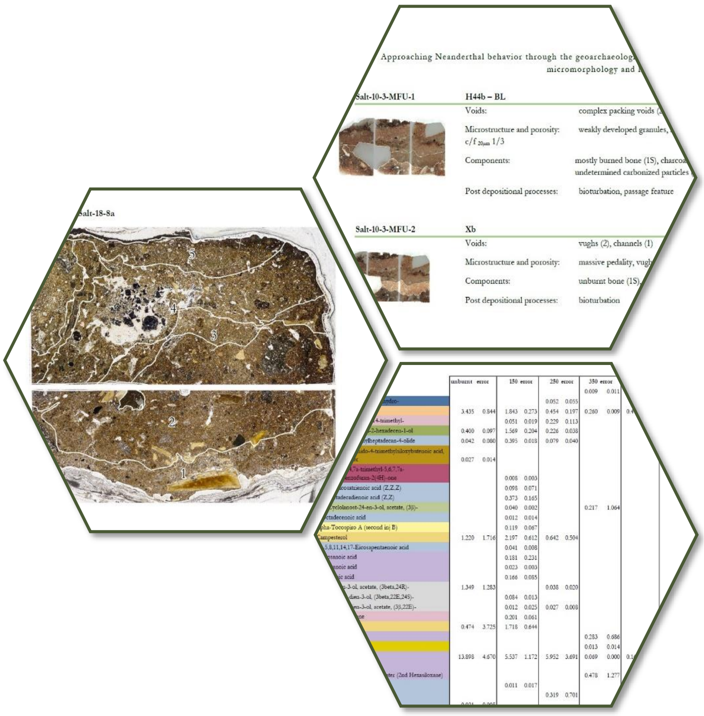

Appendix 1 – Case Study I – Thin sections of sample set, location, and hearth number

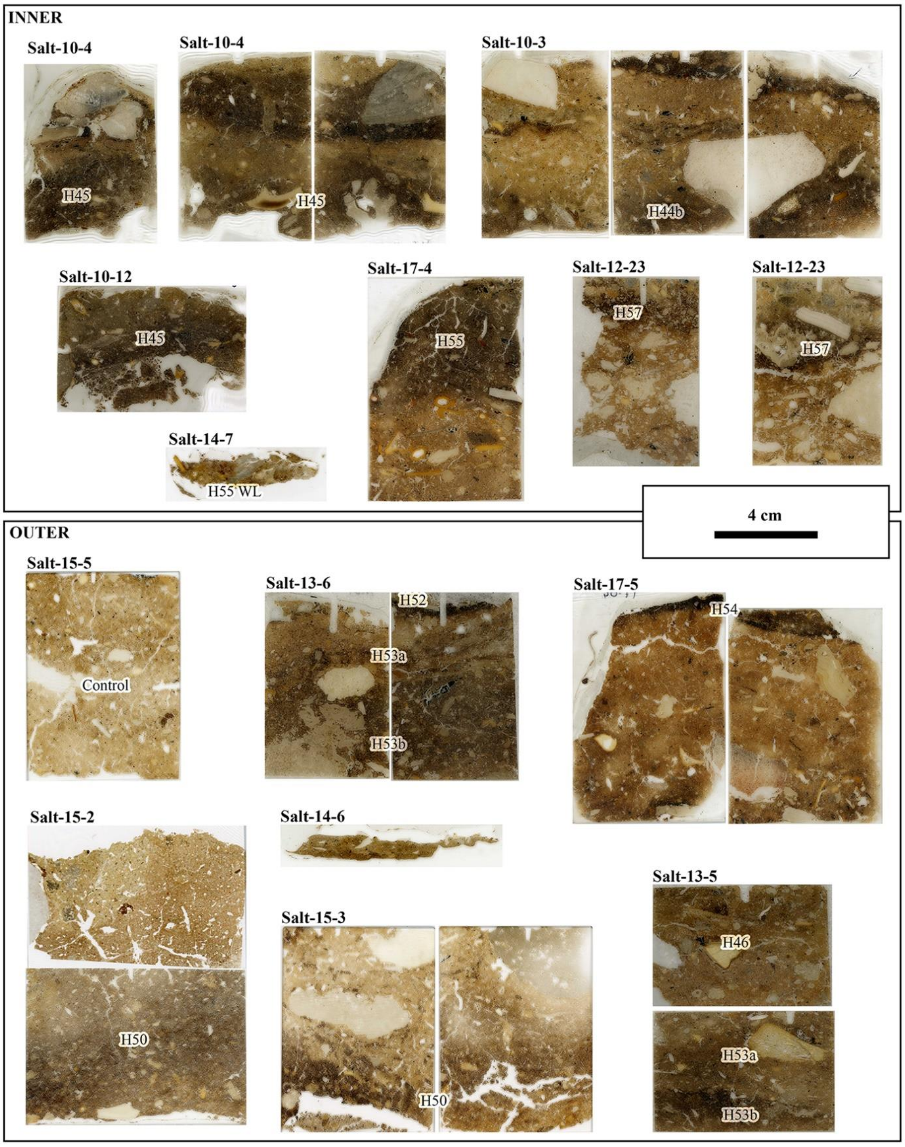

Appendix 2 – Case Study I – Thin section description

Quick explanation of Appendix 2 and 3

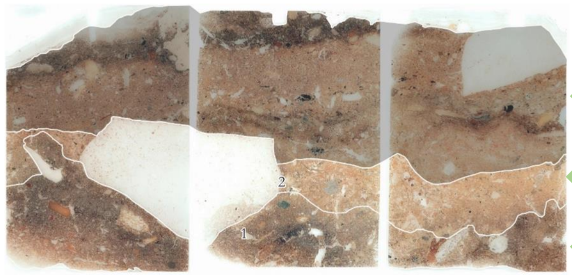

Abbreviations
S: subrounded/subangular
R: rounded
A: angular
1: rare to few
2: common to frequent
3: abundant
fg: fine gravel
vfg: very fine gravel
vcs: very coarse sand
cs: coarse sand
ms: medium sand
fs: fine sand
vfs: very fine sand
s: silt
c: clay

	Lithology Class
L1	Limestone, vcs-fs (2S), Quartz, s-vfs (2S), Tufa, fg-cs (2S), Travertine, mg-vcs (1S)
L2	Limestone, cs-ms (1S) Quartz, s-vfs (1S) Tufa, vfg-cs (1S) Travertine, cs (1S)
L3	burned Limestone, cs-ms (1S) Quartz, s-vfs (1S) burned Tufa, vfg-cs (1S) burned Travertine, fg-cs (1S)
L4	Limestone, ms-fs (2S) Quartz, s-vfs (2S) Tufa, cs (1S)
L5	Limestone, ms-fs (1S) Quartz, s-vfs (1S) Tufa, cs (1S)
L6	burned Limestone, cs-ms (1S) Quartz, s-vfs (1S) burned Tufa, vfg-cs (1S) burned Travertine, cs (1S)

Full name of MFU — Combustion structure/layer — frequency and angularity (see Abbreviations) — Lithology class — Microfacies type

Salt-10-3-MFU-1 **H44b – BL** Lithology class L4 MFT 1

Voids: complex packing voids (... ns (1), channels (1), planes (1)

Microstructure and porosity: weakly developed gr... tergrain microaggregate microstructure, double spaced po... ic c/f $_{20\mu m}$ 1/3

Components: mostly burned bone (1S), charcoal (1S), other carbonized plant (1S), animal fat d... ved char (1S), undetermined carbonized particles (1S), fissured flint (1S), fibrous coprolite (2S), celtis (2S)

Post depositional processes: bioturbation, passage feature

Thin section Salt-10-3

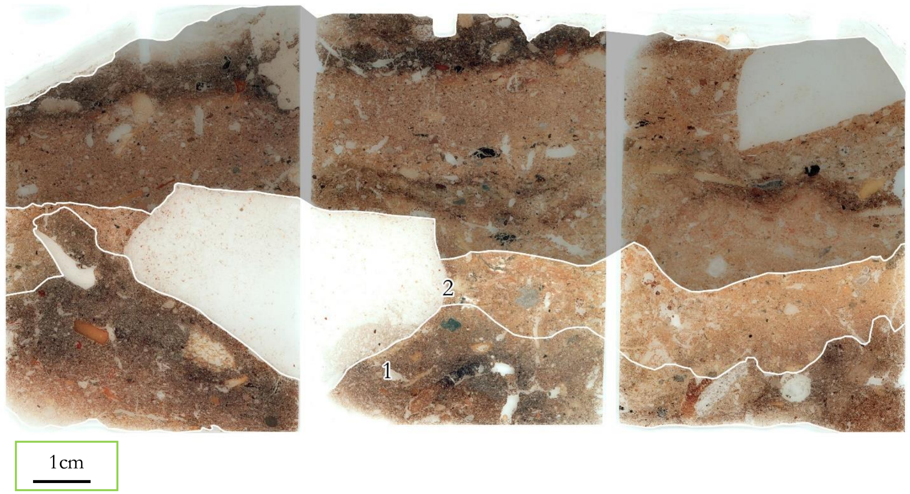

Salt-10-3-MFU-1 **H44b – BL** Lithology class L4 MFT 1

Voids:	complex packing voids (2), vughs (1), channels (1), planes (1)
Microstructure and porosity:	weakly developed granules, intergrain microaggregate microstructure, double spaced porphyric $c/f_{20\mu m}$ 1/3
Components:	mostly burned bone (1S), charcoal (1S), other carbonized plant (1S), animal fat derived char (1S), undetermined carbonized particles (1S), fissured flint (1S), fibrous coprolite (2S), celtis (2S)
Post depositional processes:	bioturbation, passage feature

Salt-10-3-MFU-2 **Xb** Lithology class L4 MFT 3

Voids:	vughs (2), channels (1)
Microstructure and porosity:	massive pedality, vughy microstructure, open porphyric $c/f_{20\mu m}$ 1/4
Components:	unburnt bone (1S), other carbonized plant (1S), fibrous coprolite (1S), celtis (2S)
Post depositional processes:	bioturbation

Thin section Salt-10-4

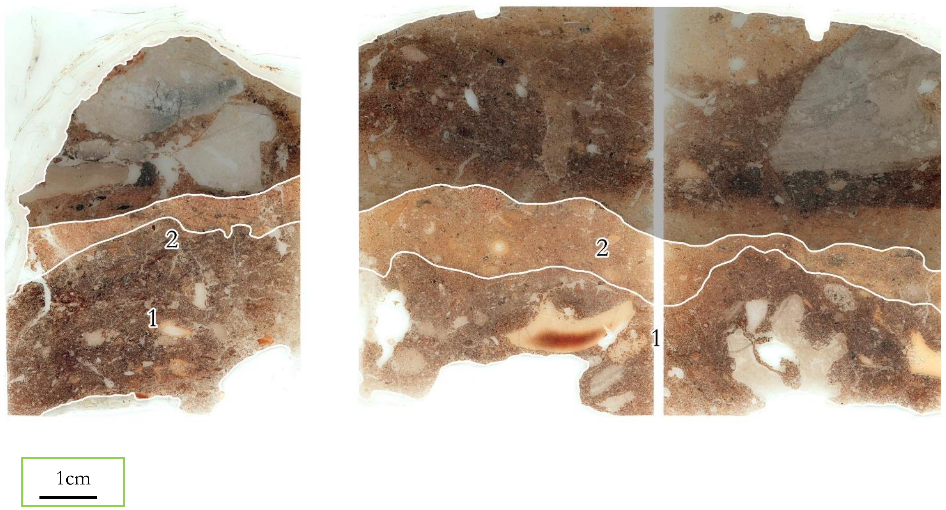

Salt-10-4-MFU-1	**H45 – BL**	Lithology class L3	MFT 1
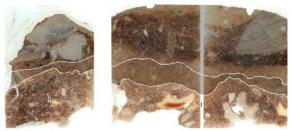	Voids:	planes (1), channels (1), compound packing voids (1), vughs (2)	
	Microstructure and porosity:	no pedality, intergrain microaggregate, double spaced porphyric c/f $_{20\mu m}$ 1/3	
	Components:	burned bone (2S), fibrous coprolites (1S), other carbonized plant (2S), celtis (1S)	
	Post depositional processes:	-	

Salt-10-4-MFU-2	**Xb**	Lithology class L1	MFT 6
	Voids:	channels (1), compound packing voids (1), vughs (2)	
	Microstructure and porosity:	no pedality, intergrain microaggregate, double spaced porphyric c/f $_{20\mu m}$ 1/3	
	Components:	celtis (2S), unburned bone (1S), fibrous coprolite (1S)	
	Post depositional processes:	-	

Appendix 2

Thin section Salt-10-12

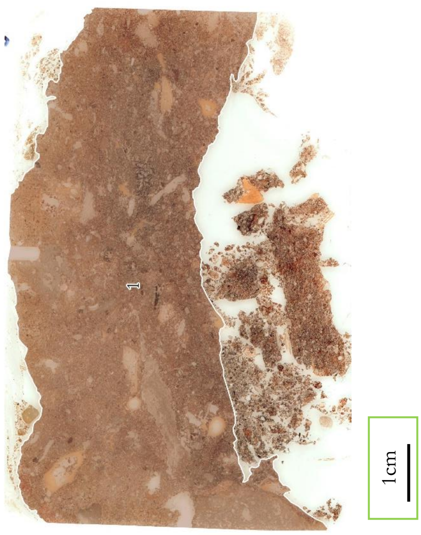

Salt-10-12-MFU-1	H45 – BL		Lithology class L3	MFT 1
	Voids:	vughs (2), channels (1)		
	Microstructure and porosity:	no pedality, vughy microstructure, single spaced porphyric c/f $_{20\mu m}$ 1/2		
	Components:	tooth (1S), burned bone (1S), celtis (1S), fibrous coprolite (1S)		
	Post depositional processes:	-		

Thin section Salt-12-23

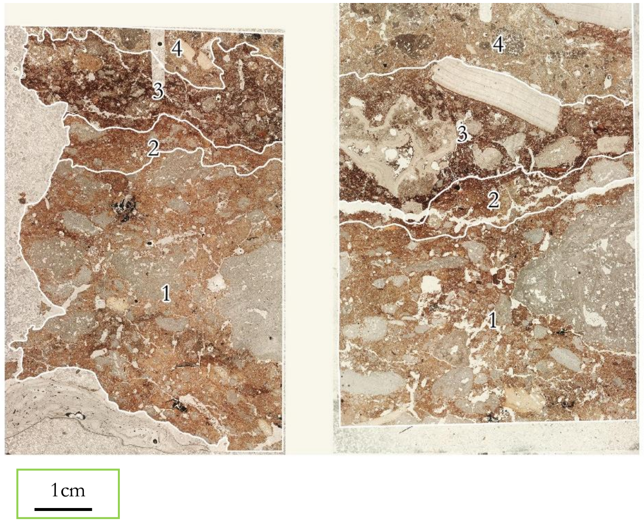

Salt-12-23-MFU-1 **Xb** Lithology class L1 MFT 7

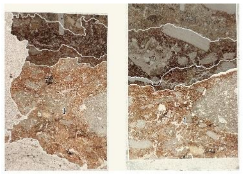

Voids:	planes (2), vesicles (1), channels (1), chambers (1)
Microstructure and porosity:	weakly developed S blocky peds, S blocky microstructure, double spaced porphyric c/f $_{20\mu m}$ 1/2
Components:	unburnt bone (2S), burned bone (1S), rotten charcoal (1S), fibrous coprolite with celtis (1S), square black particle (see picture) (1S), massive black particle (1S), fibrous coprolite with celtis (1S), celtis (1S)
Post depositional processes:	bioturbation (passage feature, infillings from MFU 2 above)

Salt-12-23-MFU-2 **H57 - RL** Lithology class L1 MFT 2

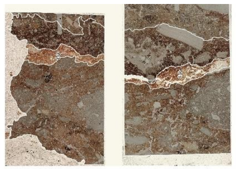

Voids:	vughs (1), complex packing voids (1)
Microstructure and porosity:	weakly developed granules, vughy-granular microstructure, open porphyric/f $_{20\mu m}$ 1/5
Components:	orange unburnt bone (1S), burned bone (2S), square black particle, linear, horizontal (3A), celtis (1S)
Post depositional processes:	-

Salt-12-23-MFU-3 **H57 - BL** Lithology class L2 MFT 5

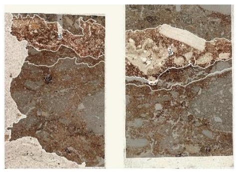

Voids:	planes (2), channels (1), vughs (2)
Microstructure and porosity: 1/3	moderately developed S blocky peds, complex microstructure, single spaced porphyric c/f $_{20\mu m}$
Components:	burnt bone (2S), fibrous long chains of black material without pores (1S), square black particles (3A)
Post depositional processes:	-

Salt-12-23-MFU-4	**H57 - WL**	Lithology class L3	MFT 9
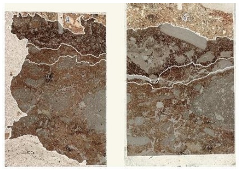	Voids:	vughs (2)	
	Microstructure and porosity:	weakly developed peds, vughy microstructure, close porphyric c/f $_{20\mu m}$ 1/3	
	Components:	calcined bone (3S), burned bone (1S), square black particles (1S), charcoal (1S), other carbonized plant (1S), fibrous coprolite, some burned (1S), massive coprolite (1S)	
	Post depositional processes:	-	

Thin section Salt-13-05

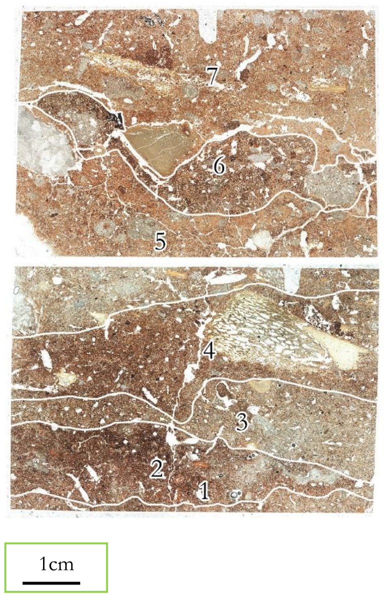

Salt-13-05-MFU-1	**Xb**	Lithology class L4	MFT 3
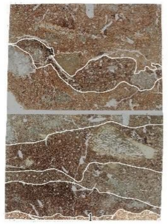	Voids:	vughs (1), channels (2), chambers (3)	
	Microstructure and porosity:	weakly developed granules, chamber microstructure, open porphyric c/f $_{20\mu m}$ 1/5	
	Components:	unburned bone (1S), undetermined carbonized particle (1R), fibrous coprolite with undefined borders, weathered (1S)	
	Post depositional processes:	bioturbation	

Salt-13-05-MFU-2	**H53b - BL**	Lithology class L5	MFT 1
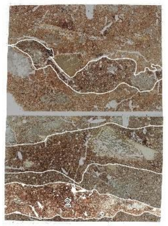	Voids:	vughs (2), vesicles (1)	
	Microstructure and porosity:	no pedality, vughy microstructure, open porphyric c/f $_{20\mu m}$ 1/4	
	Components:	unburned bone (2S), fish bone, some burned (2R), burnt bone (1S), rotten charcoal (1S), other carbonized plant (2S)	
	Post depositional processes:	-	

Salt-13-05-MFU-3	**Xb**	Lithology class L2	MFT 3
	Voids:	vughs (1), vesicles (3), channels (1), chambers (1)	
	Microstructure and porosity:	no pedality, vesicular microstructure, open porphyric c/f $_{20\mu m}$ 1/5	
	Components:	unburnt bone (1S), burnt bone (1S), undetermined carbonized particle (1S)	
	Post depositional processes:	bioturbation, needle fiber calcite	

Salt-13-05-MFU-4	H53a - BL	Lithology class L1	MFT 5
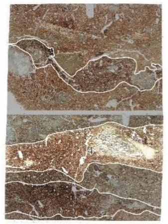	Voids:	vughs (2), vesicles (2), channels (1), chambers (1)	
	Microstructure and porosity:	no pedality, vughy, vesicular microstructure, open porphyric c/f $_{20\mu m}$ 1/5	
	Components:	burnt bone (1S), undetermined carbonized particle (1S)	
	Post depositional processes:	water percolation	

Salt-13-05-MFU-5	Xb	Lithology class L1	MFT 3
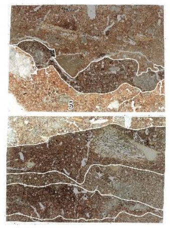	Voids:	vughs (2), vesicles (1), channels (1), chambers (1)	
	Microstructure and porosity:	no pedality, vughy microstructure, no related distribution c/f $_{20\mu m}$ 1/3	
	Components:	unburnt bone (2S), fish bone, some burned (1S), undetermined carbonized particle (1S), flint (1A)	
	Post depositional processes:	bioturbation	

Salt-13-05-MFU-6	H46 - BL	Lithology class L1	MFT 1
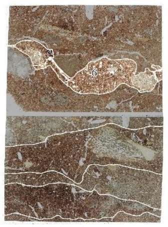	Voids:	vughs (2), vesicles (1), channels (1), chambers (1)	
	Microstructure and porosity:	no pedality, vughy, vesicular microstructure, open porphyric c/f $_{20\mu m}$ ¼	
	Components:	burnt bone (1S), unburnt bone (1S), tooth (1A), other carbonized plant (1S)	
	Post depositional processes:	-	

Salt-13-05-MFU-7	**Xb**	Lithology class L1	MFT 3
	Voids:	vughs (2), vesicles (1), channels (1), chambers (1)	
	Microstructure and porosity:	no pedality, vughy, vesicular microstructure, open porphyric c/f $_{20\mu m}$ 1/7	
	Components:	unburnt bone (3S), burned bone (1S), animal fat derived char (1S)	
	Post depositional processes:	bioturbation	

Thin section Salt-13-06

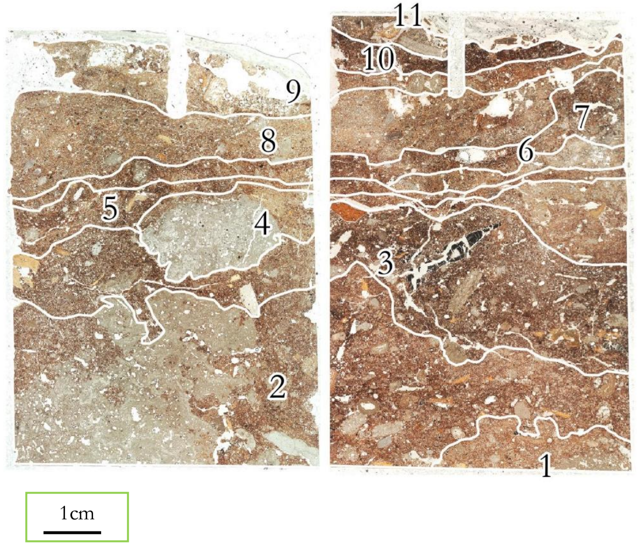

Salt-13-06-MFU-1	Xb	Lithology class L1	MFT 3
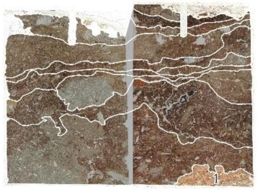	Voids:	channels (2), vughs (2)	
	Microstructure and porosity:	no pedality, vughy microstructure, open porphyric c/f $_{20\mu m}$ 1/6	
	Components:	unburnt bone (2S), fissured charcoal (1R), burned/dark fibrous coprolite (1S)	
	Post depositional processes:	bioturbation	

Salt-13-06-MFU-2	H53b - RL	Lithology class L1	MFT 2
	Voids:	vughs (2)	
	Microstructure and porosity:	no pedality, vughy microstructure, open porphyric c/f $_{20\mu m}$ 1/4	
	Components:	unburnt bone (3S), burned fish bone (1R) fissured charcoal (1R), other carbonized plant (1R)	
	Post depositional processes:	gypsum crystal (1A)	

Salt-13-06-MFU-3	H53b - BL	Lithology class L1	MFT 1
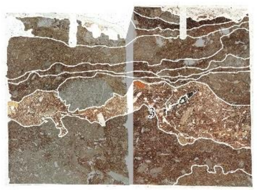	Voids:	vughs (2), channels (1), planes (2)	
	Microstructure and porosity:	no pedality, vughy microstructure, open porphyric c/f $_{20\mu m}$ 1/4	
	Components:	unburnt bone (1S), rotten charcoal (1S), other carbonized plant (1S), fibrous burned coprolite (1S), celtis (2S)	
	Post depositional processes:	gypsum crystal (1A)	

Salt-13-06-MFU-4	H53b - WL		Lithology class L4	MFT 10
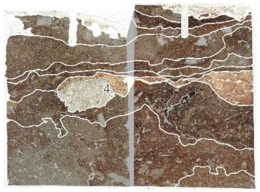	Voids:	vughs (3), channels (1)		
	Microstructure and porosity:	no pedality, vughy microstructure, close porphyric c/f $_{20\mu m}$ 1/2		
	Components:	burnt bone (2S), other carbonized plant (1S), burned celtis (1R)		
	Post depositional processes:	-		

Salt-13-06-MFU-5	H53a - BL		Lithology class L4	MFT 5
	Voids:	vughs (2), planes (1)		
	Microstructure and porosity:	no pedality, vughy microstructure, close porphyric c/f $_{20\mu m}$ 1/4		
	Components:	burnt bone (1S), undetermined carbonized particle (1S)		
	Post depositional processes:	-		

Salt-13-06-MFU-6	H53a - WL		Lithology class L4	MFT 10
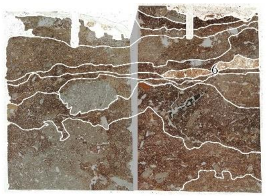	Voids:	vughs (2), vesicles (1)		
	Microstructure and porosity:	no pedality, vughy microstructure, open porphyric c/f $_{20\mu m}$ 1/5		
	Components:	calcined bone (1S), unburnt bone (1S)		
	Post depositional processes:	-		

Salt-13-06-MFU-7	H53a - BL	Lithology class L4	MFT 5
	Voids:	channels (2), planes (1)	
	Microstructure and porosity:	no pedality, channel microstructure, open porphyric c/f $_{20\mu m}$ 1/5	
	Components:	burnt bone (1S), other carbonized plant (1S)	
	Post depositional processes:	bioturbation	

Salt-13-06-MFU-8	H53a - WL	Lithology class L4	MFT 10
	Voids:	planes (1), channels (1), chambers (2), vughs (1)	
	Microstructure and porosity:	weakly developed plates, channel microstructure, open porphyric c/f $_{20\mu m}$ 1/4	
	Components:	calcined bone (1S), unburnt bone (1S)	
	Post depositional processes:	bioturbation	

Salt-13-06-MFU-9	H52 - RL	Lithology class L4	MFT 2
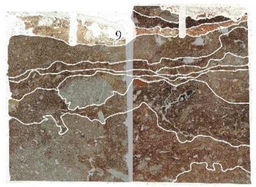	Voids:	planes (1)	
	Microstructure and porosity:	weakly developed plates, platy microstructure, open porphyric c/f $_{20\mu m}$ 1/3	
	Components:	bone (1S)	
	Post depositional processes:	-	

Salt-13-06-MFU-10	H52 - BL	Lithology class L5	MFT 5
	Voids:	planes (2)	
	Microstructure and porosity:	weakly developed plates, platy microstructure, open porphyric c/f $_{20\mu m}$ 1/3	
	Components:	burnt bone (1S), other carbonized plant (2S)	
	Post depositional processes:	-	

Salt-13-06-MFU-11	H52 - WL	Lithology class L1	MFT 9
	Voids:	vughs (3)	
	Microstructure and porosity:	no pedality, vughy microstructure, open porphyric c/f $_{20\mu m}$ 1/5	
	Components:	unburnt bone (1S), fibrous coprolite (3S)	
	Post depositional processes:	-	

Thin section Salt-14-07

Salt-14-06-MFU-1	**H55 – WL**	Lithology class L4	MFT 4
	Voids:	compound packing voids (2)	
	Microstructure and porosity:	moderately developed crumbs, crumb microstructure, enaulic c/f $_{20\mu m}$ 1/2	
	Components:	unburnt bone (1S), undetermined carbonized particle (1S), flint mainly horizontally oriented (3A), fibrous coprolite (1S), shell (1S)	
	Post depositional processes:	-	

Thin section Salt-15-02

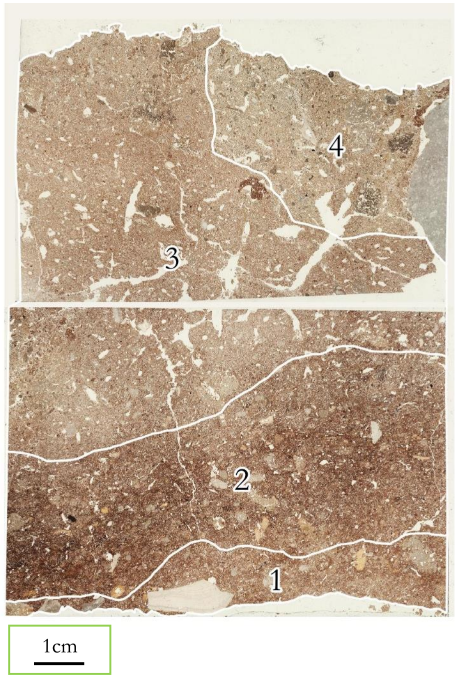

Salt-15-02-MFU-01 **Xb** Lithology class L4 MFT 3

Voids:	vughs (2), channels (1)
Microstructure and porosity:	massive peds, spongy, vughy microstructure, open porphyric c/f $_{20\mu m}$ 1/3
Components:	burnt bone (1S), unburnt bone (2S), other carbonized plant (1S), animal fat derived char (1S), undetermined carbonized particles (1S), flint (1R), fibrous coprolite (1S), weathered celtis (1S), shells (1S)
Post depositional processes:	bioturbation

Salt-15-02-MFU-02 **H50 - BL** Lithology class L2 MFT 1

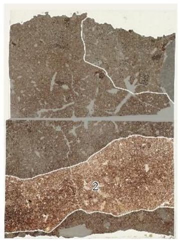

Voids:	planes (1), vughs (2), vesicles (1), channels (1)
Microstructure and porosity:	massive peds, vughy microstructure, open porphyric c/f $_{20\mu m}$ 1/3
Components:	mostly burned bone (2S), rotten, fissured charcoal (1S), other carbonized plant (2S), fragmented accumulated particles (2S), undetermined carbonized particles (2S), fibrous coprolite, some burned (2S)
Post depositional processes:	-

Salt-15-02-MFU-03 | **Xb** | Lithology class L2 | MFT 3

Voids:	channels (1), vughs (2), chambers (1), vesicles (1)
Microstructure and porosity:	massive peds, vughy, channel microstructure, open porphyric c/f $_{20\mu m}$ 1/4
Components:	unburnt bone (1S), burnt bone (1S), undetermined carbonized particle (1S), massive coprolite (1S), vertically oriented celtis (1S)
Post depositional processes:	bioturbation

Salt-15-02-MFU-04 | **H50 - WL** | Lithology class L6 | MFT 4

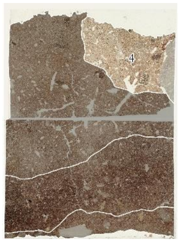

Voids:	channels (2), complex packing voids (1), vughs (1)
Microstructure and porosity:	weakly developed crumbs, crumb microstructure, open porphyric c/f $_{20\mu m}$ 1/4
Components:	unburnt bone (1S), vertically oriented celtis (2S) fibrous calcified organic material (1S)
Post depositional processes:	bioturbation

Thin section Salt-15-03

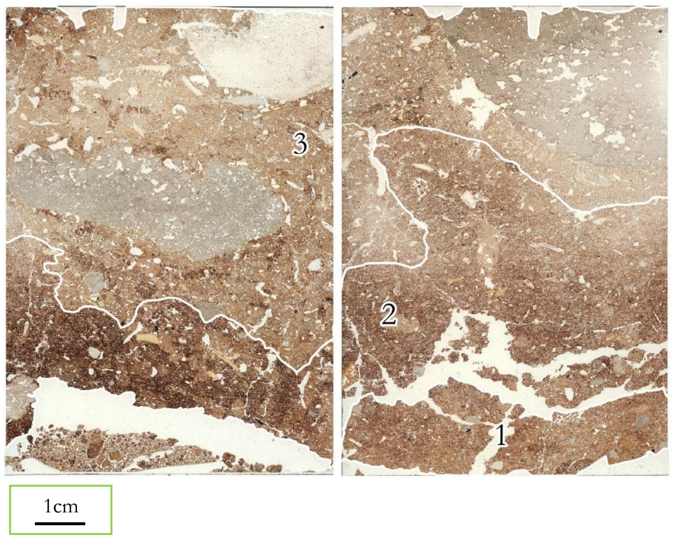

Salt-15-03-MFU-01 **Xb** Lithology class L4 MFT 3

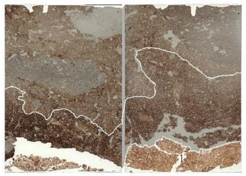

Voids:	vughs (2), planes (1), channels (1)
Microstructure and porosity:	massive peds, vughy microstructure, open porphyric c/f $_{20\mu m}$ 1/4
Components:	apparently burnt bone (1S), charcoal (1S), other carbonized plant (1S), undetermined carbonized particle (1S), massive coprolite with cracks (fissured) (1S), fibrous coprolite incorporated in matrix (1S)
Post depositional processes:	bioturbation

Salt-15-03-MFU-02 **H50 - BL** Lithology class L4 MFT 1

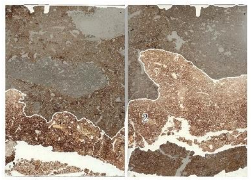

Voids:	vughs (2), planes (1), channels (1)
Microstructure and porosity:	massive peds, vughy microstructure, open porphyric c/f $_{20\mu m}$ 1/3
Components:	apparently burned bone (2S), fissured charcoal (1S), other carbonized plant (1S), undetermined carbonized particles (1S), fibrous coprolite incorporated in matrix (1S)
Post depositional processes:	-

Salt-15-03-MFU-03 **Xb** Lithology class L1 MFT 3

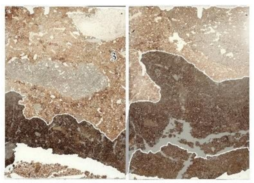

Voids:	vughs (1), channels (1), chambers (1), complex packing voids (1)
Microstructure and porosity:	weakly developed subangular blocky peds, granules, vughy microstructure, loose spaced porphyric c/f $_{20\mu m}$ 1/2
Components:	unburned bone (2S), burnt bone (1S), undetermined carbonized particles (1S), celtis (2S)
Post depositional processes:	bioturbation

Thin section Salt-15-05

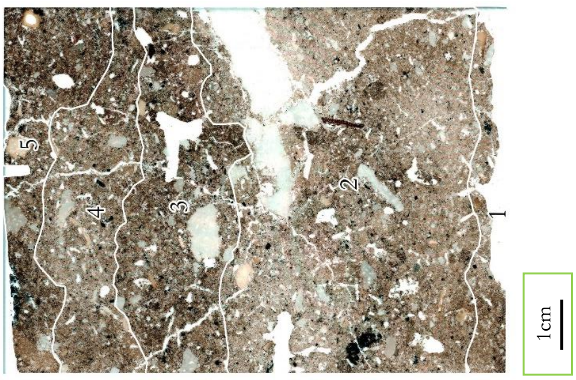

Salt-15-05-MFU-01 **Xb** Lithology class L1 MFT 7

Voids:	vughs (2), chambers (1)
Microstructure and porosity:	massive peds, vughy microstructure, open porphyric c/f $_{20\mu m}$ 1/3
Components:	unburnt bone (1S), charcoal (1S), other carbonized plant (1S), celtis (1S), massive coprolite (1S)
Post depositional processes:	dark staining around chambers, bioturbation

Salt-15-05-MFU-02 **Xb** Lithology class L1 MFT 7

Voids:	vughs (2), chambers (1), channels (1)
Microstructure and porosity:	massive peds, vughy microstructure, open porphyric c/f $_{20\mu m}$ 1/2
Components:	unburned bone (2S), calcined bone (1R), charcoal (1S), other carbonized plant (1S), silicified celtis (1S), massive coprolite (1S)
Post depositional processes:	bioturbation (infilling)

Salt-15-05-MFU-03 **Xb** Lithology class L1 MFT 7

Voids:	channels (2), chambers (1), planes (1), vughs (1)
Microstructure and porosity:	no pedality, channel microstructure, open porphyric c/f $_{20\mu m}$ 1/2
Components:	unburned bone (2S), calcined bone (1S), charcoal (1S), other carbonized plant (1S), fibrous coprolite (1S), massive coprolite (1S)
Post depositional processes:	dark staining around channel, phosphates, bioturbation

Salt-15-05-MFU-04	**Xb**	Lithology class L1	MFT 7
	Voids:	vughs (2), channels (2)	
	Microstructure and porosity:	no pedality, vughy microstructure, open porphyric c/f $_{20\mu m}$ 1/3	
	Components:	unburnt bone (2S), charcoal (1S), other carbonized plant (1S), silicified celtis (1S)	
	Post depositional processes:	dark staining around channel, bioturbation	

Salt-15-05-MFU-05	**Xb**	Lithology class L1	MFT 7
	Voids:	vughs (2), channels (2)	
	Microstructure and porosity:	no pedality, vughy microstructure, open porphyric c/f $_{20\mu m}$ 1/2	
	Components:	unburned bone (2S), burned bone (1S), charcoal (2S), animal fat derived char (2S), fibrous coprolite (1S), massive coprolite (2S)	
	Post depositional processes:	dark staining around channel, bioturbation	

Thin section Salt-17-04

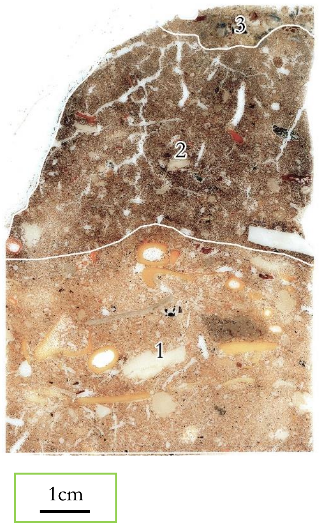

Salt-17-04-MFU-01 | **Xb** | Lithology class L1 | MFT 7

Voids:	channels (2), vughs (3)
Microstructure and porosity:	no pedality, vughy microstructure, double spaced porphyric c/f $_{20\mu m}$ 1/3
Components:	unburnt bone (3S), celtis (2S), other carbonized plant (1S), fibrous coprolite (1S)
Post depositional processes:	gypsum pseudomorph (1A), bioturbation

Salt-17-04-MFU-02 | **H55 - BL** | Lithology class L3 | MFT 7

Voids:	vughs (2), channels (2)
Microstructure and porosity:	no pedality, channel microstructure, open porphyric c/f $_{20\mu m}$ 1/5
Components:	burned bone (2S), charcoal (1R), celtis (1S), other carbonized plant (1S), flint (1S), massive coprolite (1R)
Post depositional processes:	bioturbation

Salt-17-04-MFU-03 | **H55 - WL** | Lithology class L3 | MFT 7

Voids:	vughs (2)
Microstructure and porosity:	no pedality, vughy microstructure, single spaced porphyric c/f $_{20\mu m}$ 1/2
Components:	ashes (3), burned bone (2S), calcined bone (1S)
Post depositional processes:	-

Thin section Salt-17-05

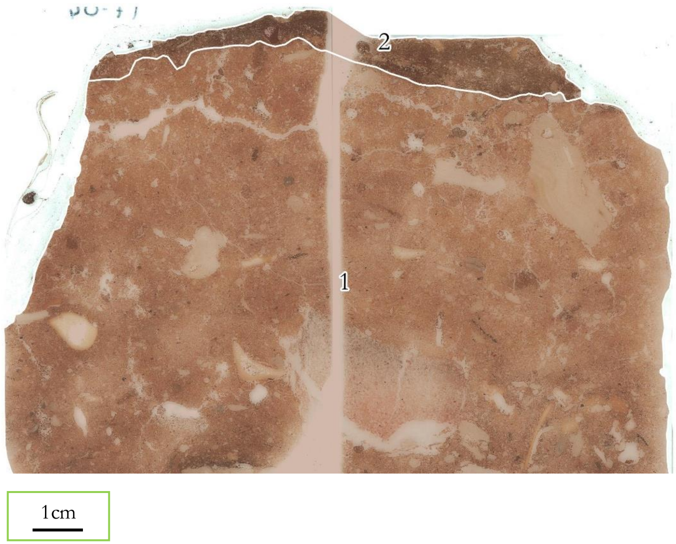

Salt-17-05-MFU-01 **Xb** Lithology class L1 MFT 6

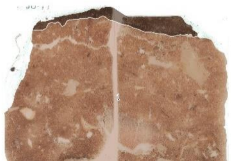

Voids: channels (1), planes (2), vughs (2)

Microstructure and porosity: no pedality, intergrain microaggregate, open porphyric c/f $_{20\mu m}$ 1/5

Components: unburnt bone (3S), burnt bone (1S), celtis (2S), teeth (1S), other carbonized plant (1S)

Post depositional processes: gypsum pseudomorph (2A)

Salt-17-05-MFU-02 **H54 - BL** Lithology class L3 MFT 1

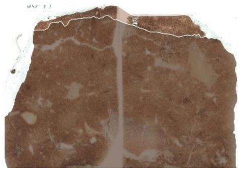

Voids: vughs (1)

Microstructure and porosity: massive pedality, massive microstructure, single spaced porphyric c/f $_{20\mu m}$ 1/1

Components: burned bone (1S), celtis (2S), other carbonized plant (3S)

Post depositional processes: bioturbation

Appendix 3 – Case Study II – Thin section description

Quick explanation of Appendix 3

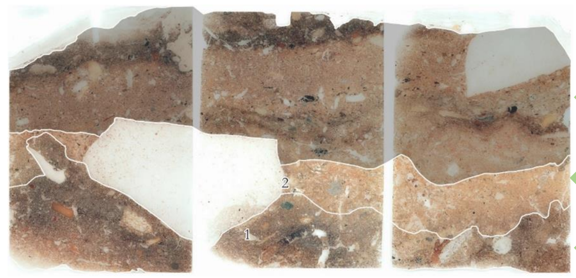

Abbreviations
S: subrounded/subangular
R: rounded
A: angular
1: rare to few
2: common to frequent
3: abundant
fg: fine gravel
vfg: very fine gravel
vcs: very coarse sand
cs: coarse sand
ms: medium sand
fs: fine sand
vfs: very fine sand
s: silt
c: clay

MFT	Corresponding Lithology Class
XI	Limestone, vcs-fs (1S), Quartz, s-vfs (2S), Tufa, mostly weathered fg-cs (2S), Travertine, fg-cs (1S)
RL	Limestone, vcs-fs (1S), Quartz, s-vfs (2S), Tufa, mostly weathered, some burnt, fg-cs (2S), Travertine, fg-cs (1S)
WL	Quartz, s-vfs (2S), Tufa, some burnt, vcs-ms (1S)
Lsg	Limestone, vcs-fs (1S), Quartz, s-vfs (2S), Tufa, fg-cs (2S), Travertine, fg-cs (1S)

Full name of MFU

frequency and angularity (see Abbreviations)

Lithology class

Salt-10-3-MFU-1 Lithology class L4 MFT 1

highlighted layer

Microfacies type

Voids:	complex packing voids ([illegible]ns (1), channels (1), planes (1)
Microstructure and porosity:	weakly developed gr[illegible]intergrain microaggregate microstructure, double spaced po[illegible]ic c/f $_{20\mu m}$ 1/3
Components:	mostly burned bone (1S), charcoal (1S), other carbonized plant (1S), animal fat d[illegible]ved char (1S), undetermined carbonized particles (1S), fissured flint (1S), fibrous coprolite (2S), celtis (2S)
Post depositional processes:	bioturbation, passage feature

Thin section Salt-18-7

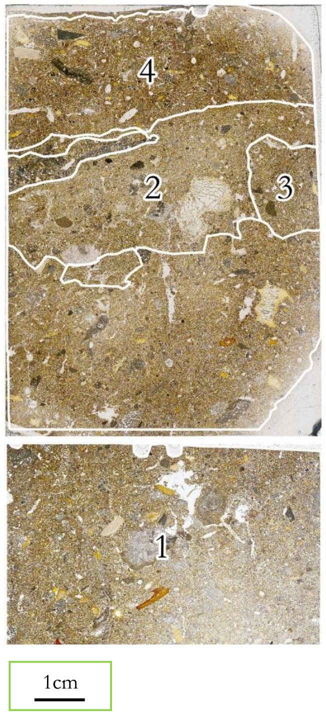

Salt-18-7-MFU-1 Lithology class XI MFT XI

Voids:	complex packing voids (1), channels (1), chambers (1)
Microstructure and porosity:	apedal, vughy microstructure (2), double spaced porphyric c/f $_{20\mu m}$ 1/2
Components:	bone (2S), fibrous coprolites (1S), massive coprolites (1S), celtis australis seed coat (1S), undetermined carbonized particles (2S), fat derived char (1S), charcoal (1S), teeth (1S)
Post depositional processes:	bioturbation (1)

Salt-18-7-MFU-2 Lithology class RL MFT RL

Voids:	complex packing voids (1), channels (1)
Microstructure and porosity:	apedal, vughy microstructure (2), double spaced porphyric c/f $_{20\mu m}$ 1/2
Components:	celtis australis seed coat (1S), bone (1S), fibrous coprolites (1S), massive coprolites (1S), teeth (1A)
Post depositional processes:	bioturbation (1)

Salt-18-7-MFU-3 Lithology class WL MFT WL

Voids:	complex packing voids (1), channels (1), star shaped vughs (1)
Microstructure and porosity:	weakly developed granules, vughy microstructure (2), open porphyric c/f $_{20\mu m}$ 1/5
Components:	celtis australis seed coat (1S)
Post depositional processes:	bioturbation (1)

Salt-18-7-MFU-4 Lithology class Lsg11 MFT Lsg11

Voids:	complex packing voids (1), channels (2)
Microstructure and porosity:	apedal, vughy microstructure (2), double spaced porphyric c/f $_{20\mu m}$ 1/2
Components:	flint (1S), bone (2S), fibrous coprolites (1S), massive coprolites (1S), undetermined carbonized particles (2S), fat derived char (1S), charcoal (1S)
Post depositional processes:	bioturbation (2)

Thin section Salt-18-8a

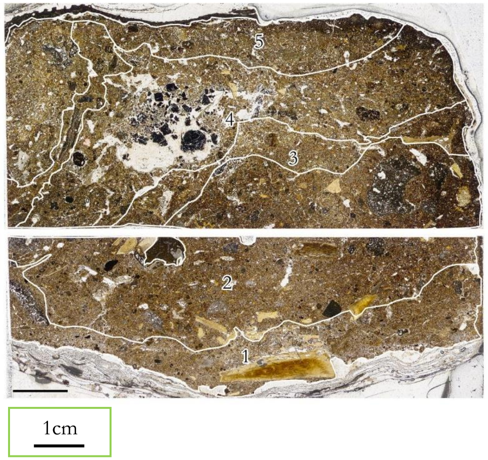

Salt-18-8a-MFU-1 Lithology class WL MFT WL

Voids:	channels (1), planes (1), complex packing voids (1)
Microstructure and porosity:	weakly developed granules, granular microstructure (2), vughy microstructure (1), open porphyric c/f $_{20\mu m}$ 1/4
Components:	mostly heated bone (2S), fibrous coprolites, some charred (1R), undetermined carbonized particles (1S), fat-derived char (1A), celtis australis seed coat (1S), ash (2)
Post depositional processes:	bioturbation (1)

Salt-18-8a-MFU-2 Lithology class XI MFT XI

Voids:	channels (1), planes (1), complex packing voids (1)
Microstructure and porosity:	weakly subangular blocky peds, subangular blocky microstructure (2), double spaced porphyric c/f $_{20\mu m}$ 1/2
Components:	calcined bone (1A), mostly heated bone (2S), massive coprolite (1R), celtis australis seed coat (2S), undetermined carbonized particles (1S), teeth (1S)
Post depositional processes:	bioturbation (1)

Salt-18-8a-MFU-3 Lithology class RL MFT RL

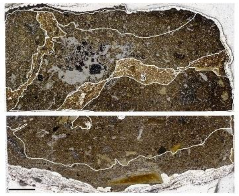

Voids:	planes (2), channels (1), compound packing voids (1)
Microstructure and porosity:	weakly developed plates, vughy microstructure (1), planar microstructure (1), double spaced porphyric c/f $_{20\mu m}$ 1/2
Components:	bone (1S), fibrous coprolites (1S), massive coprolites (1S), celtis (1S), teeth (1S)
Post depositional processes:	bioturbation (1)

Salt-18-8a-MFU-4 Lithology class WL MFT WL

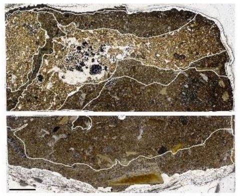

Voids:	channels (2), compound packing voids (2), planes (1)
Microstructure and porosity:	weakly developed granules, granular microstructure (1), channel microstructure (1), open porphyric c/f $_{20\mu m}$ 1/4
Components:	calcined bone (1S), mostly heated bone (1S), fibrous coprolites (2S), massive coprolites (1S), charcoal (2R), undetermined carbonized particles (1S)
Post depositional processes:	bioturbation (2)

Salt-18-8a-MFU-5 Lithology class Lsg11 MFT Lsg11

Voids:	channels (2), compound packing voids (2)
Microstructure and porosity:	apedal, vughy microstructure (1), channel microstructure (1), double spaced porphyric c/f $_{20\mu m}$ 1/3
Components:	mostly heated bone (1S), fibrous coprolite (1S), undetermined carbonized particles (1S), celtis (1S)
Post depositional processes:	bioturbation (2)

Thin section Salt-18-8b

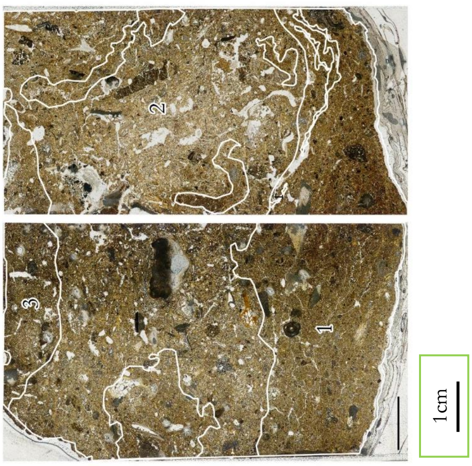

Salt-18-8b-MFU-1 Lithology class RL MFT RL

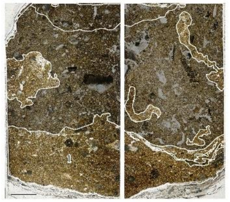

Voids:	channels (1), planes (2)
Microstructure and porosity:	moderately developed subangular blocky peds, subangular blocky microstructure (2), massive microstructure (1), double spaced porphyric c/f $_{20\mu m}$ 1/3
Components:	mostly unheated bone (1S), celtis australis seed coat (1S), flint (1A)
Post depositional processes:	bioturbation (1)

Salt-18-8b-MFU-2 Lithology class WL MFT WL

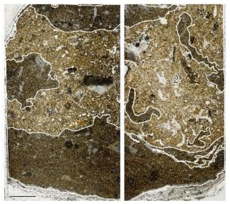

Voids:	channels (2), compound packing voids (2), planes (1)
Microstructure and porosity:	weakly developed granules, granular microstructure (2), channel microstructure (1), open porphyric c/f $_{20\mu m}$ 1/4
Components:	calcined bone (1S), mostly heated bone (1S), tooth (1S), fibrous coprolites (2S), massive coprolites (1S), charcoal (2R), undetermined carbonized particles (1S)
Post depositional processes:	bioturbation (3), passage features (1)

Salt-18-8b-MFU-3 Lithology class Lsg11 MFT Lsg11

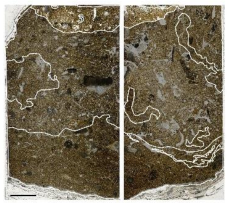

Voids:	complex packing voids (1), channels (2)
Microstructure and porosity:	apedal, vughy microstructure (1), channel microstructure (1), double spaced porphyric c/f $_{20\mu m}$ 1/3
Components:	undetermined carbonized particles (1S), ash inclusions (1S)
Post depositional processes:	bioturbation (2)

Thin section Salt-18-9

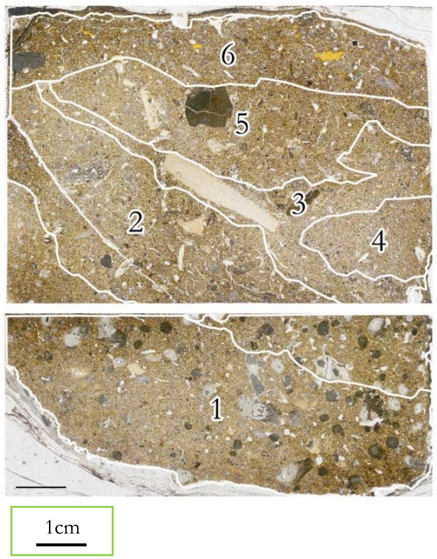

Salt-18-9-MFU-1 Lithology class XI MFT XI

Voids:	complex packing voids (2), channels (2)
Microstructure and porosity:	apedal, vughy microstructure (2), double spaced porphyric c/f $_{20\mu m}$ 1/3
Components:	mostly unheated bone (1S), fibrous coprolites (1S), massive coprolite (1S), fine undetermined carbonized particles (2S), charcoal (1S), celtis australis seed coat (1S)
Post depositional processes:	bioturbation (2)

Salt-18-9-MFU-2 Lithology class RL MFT RL

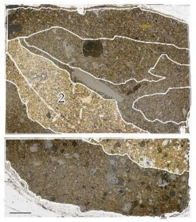

Voids:	planes (2), channels (2), complex packing voids (1)
Microstructure and porosity:	weakly developed plates, planar microstructure (2), vughy microstructure (1), double spaced porphyric c/f $_{20\mu m}$ 1/3
Components:	heated flint (1A), unheated and heated bone (2S), celtis australis seed coat (1S), fibrous coprolites (1S), massive coprolites (1S)
Post depositional processes:	bioturbation (1)

Salt-18-9-MFU-3 Lithology class WL MFT WL

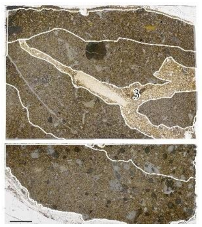

Voids:	complex packing voids (1), star shaped vughs (1), channels (1)
Microstructure and porosity:	weakly developed granules, vughy microstructure (2), granular microstructure (1), open porphyric c/f $_{20\mu m}$ 1/4
Components:	ash (3), celtis australis seed coat (1S), fibrous coprolite (1S), calcined and heated bone (1S)
Post depositional processes:	bioturbation (1)

Salt-18-9-MFU-4 Lithology class RL MFT RL

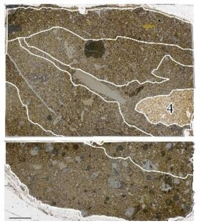

Voids:	complex packing voids (1), channels (1)
Microstructure and porosity:	apedal, vughy microstructure (1), channel microstructure (1), double spaced porphyric c/f $_{20\mu m}$ 1/3
Components:	celtis australis seed coat (1S), bone (2S), fibrous coprolite (1S), ash (1)
Post depositional processes:	bioturbation (1)

Salt-18-9-MFU-5 Lithology class RL MFT RL

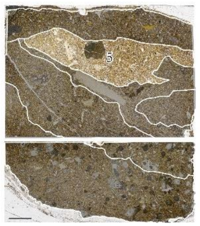

Voids:	complex packing voids (1), channels (1)
Microstructure and porosity:	apedal, vughy microstructure (1), channel microstructure (1), double spaced porphyric c/f $_{20\mu m}$ 1/3
Components:	celtis australis seed coat (1S), bone (2S), fibrous coprolite (1S), ash (1), massive coprolite (1S)
Post depositional processes:	bioturbation (1)

Salt-18-9-MFU-6 Lithology class Lsg11 MFT Lsg11

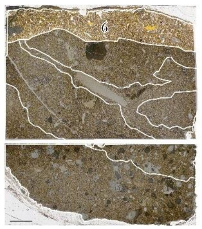

Voids:	complex packing voids (1), channels (1), planes (1)
Microstructure and porosity:	apedal, vughy microstructure (1), channel microstructure (1), double spaced porphyric c/f $_{20\mu m}$ 1/3
Components:	fat derived char (1S), bone mostly heated (3S), charcoal (1S), organic particles (2S), fibrous coprolite (1S), massive coprolite (1S), celtis australis seed coat (1S)
Post depositional processes:	bioturbation (2)

Appendix 4 – Case Study 3 – Other compounds

	unburnt	error	150	error	250	error	350	error	450	error	550	error	m3	error	m4	error
(3β,22E)-acetate-Ergosta-5,22-dien-3-ol			0.012	0.025	0.027	0.008										
(3β,22E)-acetateStigmasta-5,22-dien-3-ol			0.226	0.169												
(3β,22E,24S)-Ergosta-5,22-dien-3-ol			0.084	0.013												
(3β,22Z)-acetate-Stigmasta-5,22-dien-3-ol	0.966	1.119			0.148	0.136										
(3β,24R)-acetate-Ergost-5-en-3-ol	1.349	1.283			0.038	0.020										
(3β,24S)-Stigmast-5-en	0.312	0.023			0.246	0.332										
(5α)-Stigmastane-3,6-dione			0.122	0.065												
2,4-Di-tert-butylphenol	3.435	0.844	1.843	0.273	0.454	0.197	0.260	0.009	0.472	0.182	0.328	0.146	0.031	0.014	0.084	0.462
3,4-diethyl-1,1'-Biphenyl							0.009	0.011								
4,8,12,16-Tetramethylheptadecan-4-olide	0.042	0.080	0.395	0.018	0.079	0.040									0.041	0.018
5-dodecylhydro-2(3H)-Foranone					0.052	0.055										
6,10,14-trimethyl-2-Pentadecanone			0.051	0.019	0.229	0.113									0.047	0.015
6-Hydroxy-4,4,7a-trimethyl-5,6,7,7a-tetrahydrobenzofuran-2(4H)-one			0.008	0.003												
9-Octadecenoic acid			0.012	0.014												
Campesterol	1.220	1.716	2.197	0.612	0.642	0.504							0.018	0.023	0.019	0.000
Cis, cis, cis-8,11,14-Eicosatrienoic acid			0.098	0.071												
Cis, cis-9,12-Octadecadienoic acid			0.373	0.165												
Cis-5,8,11,14,17-Eicosapentaenoic acid			0.041	0.008												
Cycloartenol 3-acetate			0.040	0.002			0.217	1.064								
dimethyl ester of Nonanedioic acid							1.945	9.879								
Docosanoic acid			0.181	0.231											0.009	0.000
Dodecanoic acid			0.023	0.003											0.007	0.000
Eicosanoic acid			0.166	0.085												
Hexacosanoic acid							0.283	0.686								
Hexadecanitrile							0.013	0.014					0.151	0.034	0.159	0.027
Hexadecanoic acid	13.898	4.670	5.537	1.172	5.952	3.691	0.069	0.000	0.161	0.049	0.018	0.021	0.300	0.215	1.843	4.638
Lignoceric acid			0.011	0.017												
Linoelaidic acid					0.319	0.701										
Linoleic acid	0.021	0.005														
Lupeol	0.055	0.089														
Monopalmitin			0.010	0.013	0.088	0.247									0.014	0.000
Neophytadiene	1.253	0.533	1.991	0.205	0.245	0.189									0.065	0.038
Nonanoic acid			0.060	0.014												
Octadecanoic acid	0.268	0.062	0.580	0.169	0.559	0.267	0.571	0.841	0.170	0.071			0.029	0.041	0.325	0.482
Pentadecanoic acid			0.077	0.094	0.108	0.204									0.007	0.000
Phytol	0.400	0.097	1.569	0.204	0.226	0.038										
Stigmast-5-en-3-ol, oleate	0.410	1.187														
Stigmasta-3,5-dien-7-one					0.068	0.071										
Stigmasta-3,5-diene	1.592	1.328			0.485	0.172										
Stigmastan-3,5-diene	0.249	0.008	0.488	0.189	0.053	0.066										
Stigmastan-6.33-dien, 3.5-dedihydro-	0.075	0.107														
Stigmasterol	0.583	1.603	1.266	0.422	0.107	0.358							0.011	0.012	0.011	0.000
Tetracosanoic acid	0.029	0.018	0.210	0.378												
Tetradecanoic acid			0.052	0.025	0.052	0.087							0.005	0.003	0.013	0.000
Uvaol			0.036	0.004												
Vitamin E			0.072	0.190												
γ-Sitostenone			0.201	0.061												
γ-Sitosterol	0.474	3.725	1.718	0.644												
Sum	**26.633**	**18.498**	**19.751**	**5.579**	**10.177**	**7.499**	**3.366**	**12.504**	**0.802**	**0.301**	**0.345**	**0.168**				

	m3	error	m4	error
1-Heptatriacotanol			0.010	0.001
Isodextropimaric acid			0.158	0.413
(5α)-Androstane	0.065	0.096	0.409	2.537
Dehydroabietic acid			0.096	0.000
Hexadecanol	0.117	0.017		
Methyl dehydroabietate			0.100	0.012
Octadecanol	0.051	0.027		
Stigmastenol	0.041	0.027	0.047	0.000
β-Sitosterol			0.040	0.305
Sum	**0.819**	**0.510**	**3.504**	**8.948**

- Aromatic
- Saturated fatty acids
- unsaturated fatty acid
- fatty alcohol
- diterpene-alcohol/sesquiterpenoid/diterpenoid
- triterpenoid
- phenol
- sterol
- steroid
- nitlrile
- ketone
- lactone
- compound derived from stigmastenol, ergostanol
- Other